UNIVERSITY OF PALERMO
PHD JOINT PROGRAM:
UNIVERSITY OF CATANIA - UNIVERSITY OF MESSINA
XXXVI CYCLE

DOCTORAL THESIS

New stability results on parallel shear flows

Author:
Carla PERRONE

Supervisor:
Prof. Maria Carmela LOMBARDO

Co-Supervisors:
Prof. Giuseppe Mulone
Prof. Andrea Giacobbe

A thesis submitted in fulfillment of the requirements for the degree of Doctor of Philosophy

in

Mathematics and Computational Sciences

2024

Signed: Carla Perrone

Date: 19/01/2024

UNIVERSITY OF PALERMO

Abstract

Department of Mathematics and Computer Sciences

Doctor of Philosophy

New stability results on parallel shear flows

by Carla PERRONE

The study of the stability and instability of laminar flows, which has attracted the attention of many authors for more than 150 years, is still studied today both because of its importance in the field of applications and because the transition from laminar fluids to instability, turbulence and chaos is not yet completely clear and there are discrepancies between linear and nonlinear analysis and experiments.
In this thesis this problem is investigated by highlighting the problems that arose and how we tried to solve them.

Acknowledgements

I want to thank Prof. Maria Carmela Lombardo for being my mentor during my PhD and Profs. Giuseppe Mulone and Andrea Giacobbe for their constant support and for what they taught me.

Contents

List of Figures

List of Tables

Physical Constants

Acceleration of gravity $\mathbf{g} = 9.81\,\mathrm{m/s^2}$

List of Symbols

a	wave number	m^{-1}
b	wave number	m^{-1}
t	time	s
p	pressure	Pa
D	characteristic length	m
ρ	density	kg/m^3
γ	dynamic viscosity	$\mathrm{Pa} \cdot \mathrm{s}$
ν	kinematic viscosity	m^2/s
μ	magnetic permeability	N/A^2
ψ	electrical resistivity	$\Omega \cdot \mathrm{m}$
β	angle of channel inclination	rad
θ	angle of tilted perturbation inclination	rad
Re	Reynolds number	
Rm	magnetic Reynolds number	
Ha	Hartmann number	
Pm	Prandtl magnetic number	
N	interaction parameter	

Chapter 1

Introduction

1.1 Description of the problem

In general many dynamical systems with parameters, like the flows studied in this thesis, are structurally unstable, and it is important to search for critical parameter values that identify the transition from stability to instability of the solutions (such basic solutions are often equilibrium points or stationary solutions). Such parameters are called threshold or bifurcation parameters.

Different methods are used for their determination:

1. linear analysis (study of the system of perturbations linearized around such basic solutions)
2. methods of global analysis which are differentiated into:
    - (approximate) perturbative methods (weakly nonlinear analysis): development of the solution of the perturbation as a perturbative series of which the coefficients are to be computed, the perturbative series is summed, if convergent, and information is drawn from an appropriate number of terms in the series, (if it is asymptotic);
    - Lyapunov method (appropriate Lyapunov functions are sought that are decreasing in time along the perturbations).

In particular, we study the stability of base flows using two of the listed approaches: a) *Lyapunov investigation* (also called non-modal) for the *stability*, and b) *spectral investigation* (also called modal) for *instability*. The Reynolds number Re, which is a ratio between a reference velocity times the width of the channel divided by the viscosity of the fluid, is the main parameter on which the stability of the type of flows we investigated depends.
Often the critical parameters (linear and nonlinear) do not coincide, and sometimes they do not coincide with the threshold-parameters obtained in experiments (one of the notable cases is Couette's paradox: linear analysis gives an infinite value for the Reynolds number, nonlinear analysis gives values around 44, while experiments give values in a range [340, 415]).
This fact is illustrated in Fig. 1.1. The nonlinear energy critical number is Re_1, while the linear critical number is Re_2 (here Re_1 refers to the monotonic stability in energy, the other types of energies will be described in SubSec. 3.1).
For Re less than Re_1 the energy (E in figure) is monotonically decreasing, therefore we have sufficient conditions of energy stability. For Re greater than Re_1, we can deduce nothing about stability/instability in energy. Indeed, according to this choice of energy, the system is unstable, but this energy could not be the best choice and

there could exist other energies (Lyapunov functions) such that the corresponding critical number is greater that Re_1.
For Re greater than Re_2, there is at least one eigenvalue in the spectrum that has positive real part therefore we have spectral instability, to be more precise, there exist at least one perturbation that, chosen as initial value, has increasing energy. For Re less than Re_2, all the eigenvalues of the spectrum have negative real parts. In finite spaces this fact implies spectral stability, but, in our case, that is in infinite space, this fact do not necessarily implies monotonic stability.
The critical parameter obtained through experiments Re_{exp} usually does coincide neither with Re_1 nor Re_2, but it is a value between them. Therefore the region between Re_1 and Re_2 is called subcritical region.

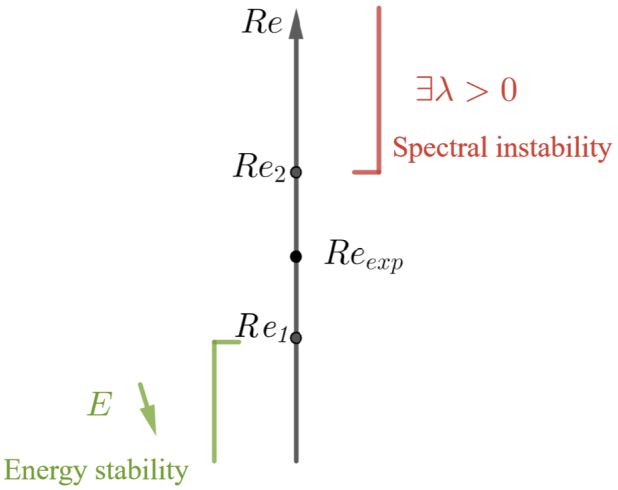

FIGURE 1.1: Critical Reynolds parameters obtained through Lyaponov investigation (Re_1), spectral investigation (Re_2) and experiments (Re_{exp}).

In the next section the structure of the thesis is presented. In particular we describe the starting point of the work, related to the problem explained in this section, and then we describe how the research went on.

1.2 Overview of the thesis

The first aim of the thesis is to study the stability of flows both from a theoretical and an applied point of view, trying to solve the problem described in Fig. 1.1.
The idea to overcome the problem is to looking for, if they exist, classes of perturbations for which suitable energies (possibly weighted) give the same critical parameters for both the linearized and the nonlinear systems and, in particular cases, compare with the critical parameters obtained from the experimental data, if available. The study we carried out is presented in Sec. 8.

The second aim is to prove, at least numerically, that in the nonlinear case the most destabilizing perturbations are the two-dimensional ones. Indeed, in the study of the stability/instability of laminar flows in the linear case it has been proved that the most destabilizing perturbations are the two-dimensional. In the nonlinear case, on the contrary, this has not been proved but, classically, also in this case, sometimes

only two-dimensional perturbations are studied. Most of the research are devoted to this study and the related works are presented in Secs. 9-11. In particular in Sec. 9 we study this problem for the classical laminar flows of Couette and Poiseuille, we run into a contradiction and we solve it through a conjecture. In Sec. 10 we change the boundary conditions, we obtain the same problem and we solve it in a similar way. Finally in Sec. 11 we extend this idea also in magnetohydrodynamic.

The last two works concern with the analysis of a flow between two horizontal planes that occurs when the plates move in opposite directions and the flow is subjected to a pressure with longitudinal and transversal components. The resulting basic motion is a combination of Couette and Poiseuille flows in the streamwise direction and just Poiseuille in the spanwise direction.
In particular in the first of these two works reported in Sec. 12 we simplify the basic motion by imposing that the spanwise component was zero. The principal goal is to study the transient growth of the energy obtaining, as particular cases, the Couette and the Poiseuille flows. Indeed the study of the transient growth in these two particular cases could give a contribution in the understanding of the conjecture of Sec. 9.
In the last work Sec. 13 we study the general basic motion with both streamwise and spanwise components.

Before going deep into all these works, in Sec. 2 we recall the Navier Stokes equations because we need them to describe the evolution of flows. In Secs. 4 and 5 we derive respectively the basic motions for laminar flows between horizontal planes and flows in inclined channels, as they are object of our investigation. In Sec. 3 we explain two approaches (see a) and b) above) we use to study the stability/instability and in Sec. 6 we describe one of the numerical methods that these two approaches require, that is the spectral method. Finally, in Sec. 7 we recall the classical linear and non linear results for Couette and Poiseuille flows and the numerical and experimental results. It is highlighted that the situation described in Fig. 1.1 takes place.

The results of the works presented in this thesis pose the problem of what is the critical parameter of monotonic nonlinear stability. We remember that classically the values proposed by Orr, 1907, Joseph, 1968 and Joseph and Carmi, 1969 give critical values on particular non-3D perturbations. We observe here that both Orr and Joseph in their papers do not prove which are the maximizing perturbations, indeed Joseph assumes that the maximizing perturbations are those which do not depend on x, and Orr assumes that they are the two-dimensional perturbations which do not depend on y. Observing that these parameters give only sufficient stability conditions, a conjecture which corroborates Orr's stability results has been proposed by Falsaperla, Mulone, and Perrone, 2022a. Conversely, numerical analyses would suggest that the results of Joseph and Joseph and Carmi are correct. The question is still open and complex but some recent results proposed by Mulone, 2024 seem to suggest that Orr's solutions are correct. In the final comments I will deepen this possible solution.

Chapter 2

Navier Stokes equations

2.1 Fluid dynamics

In this section we recall how the Navier Stokes equations which govern the motion of a Newtonian, homogeneous and incompressible fluid are derived by Rionero, 2000. Let us first recall how the first and the second indefinite equations of the mechanics of continuous systems are obtained.
We introduce:

$$\mathbf{R} = \int_{C_1(t)} \rho \mathbf{F}(P,t) dC_1, \quad \mathbf{M}_O = \int_{C_1(t)} (P-O)\rho \mathbf{F}(P,t) dC_1, \tag{2.1.1}$$

which are respectively the resultant force and the corresponding resultant moment with respect to the pole O, and ρ is the density of the fluid.
The Cauchy's stress axiom states that:

$$\mathbf{R} = \int_{\sigma} \mathbf{\Phi} d\sigma, \quad \mathbf{M}_O = \int_{\sigma} (Q-O) \times \mathbf{\Phi} d\sigma, \tag{2.1.2}$$

We define the momentum $\mathbf{Q}$ and the moment of momentum $\mathbf{K}_O$ as:

$$\mathbf{Q} = \int_{C_1} \rho \mathbf{v} dC_1, \quad \mathbf{K}_O = \int_{C_1} (P-O) \times \rho \mathbf{v} dC_1. \tag{2.1.3}$$

where $\mathbf{v}$ is the velocity of the fluid.
The following axiom holds:

$$\dot{\mathbf{Q}} = \mathbf{R}^{(e)}, \quad \dot{\mathbf{K}}_O = \mathbf{M}_O{}^{(e)}. \tag{2.1.4}$$

Therefore:

$$\mathbf{R}^{(e)} = \int_{C_1} \rho \mathbf{F} dC_1 + \int_{dC_1} \mathbf{\Phi} d\sigma \tag{2.1.5}$$

$$\mathbf{M}_O{}^{(e)} = \int_{C_1} (P-O) \times \rho \mathbf{F} dC_1 + \int_{dC_1} (Q-O) \times \mathbf{\Phi} d\sigma.$$

Eq. (2.1.4) can be rewritten as:

$$\begin{cases} \int_{C_1} \rho \mathbf{a} dC_1 = \int_{C_1} \rho \mathbf{F} dC_1 + \int_{dC_1} \mathbf{\Phi} d\sigma \\ \int_{C_1} (P-O) \times \rho \mathbf{a} dC_1 = \int_{C_1} (P-O) \times \rho \mathbf{F} dC_1 + \int_{dC_1} (Q-O) \times \mathbf{\Phi} d\sigma, \end{cases} \tag{2.1.6}$$

The Cauchy theorem states that:

$$\Phi(P,n,t) = n_i \Phi(P,e_i,t) = n_i \Phi^i, \tag{2.1.7}$$

as a result of this theorem, if we use the notation T^{ij} to indicate the components of $\mathbf{\Phi}^i$ along the versor $\mathbf{e}_j$, we have:

$$\mathbf{\Phi}^i = T^{ij}\mathbf{e}_j, \tag{2.1.8}$$

and eq. (2.1.7) becomes

$$\Phi(P, n, t) = n_i T_{ij}\mathbf{e}_j = \mathbf{n}\cdot\mathbf{T}. \tag{2.1.9}$$

By replacing eq. (2.1.9) in $(2.1.6)_1$ we obtain:

$$\int_{C_1}\rho\mathbf{a} = \int_{C_1}\rho\mathbf{F}dC_1 + \mathbf{e}_j\int_{dC_1} n_i T_{ij}d\sigma = \int_{C_1}(\rho\mathbf{F} + d_i T^{ij}\mathbf{e}_j)dC_1, \tag{2.1.10}$$

which implies:

$$\rho\mathbf{a} = \rho\mathbf{F} + \nabla\cdot\mathbf{T}. \tag{2.1.11}$$

The latter equation is the local momentum balance equation, also called first indefinite equation of the mechanics of continuous systems. Using, once again, the Cauchy's theorem, and applying the Gauss's lemma, from $(2.1.6)_2$ we obtain

$$\mathbf{T} = \mathbf{T}^T. \tag{2.1.12}$$

The latter equation is the local momentum balance equation, also called second indefinite equation of the mechanics of continuous systems.
Finally, considering the continuity equation, i.e.:

$$\dot{\rho} + \rho\nabla\cdot\mathbf{v} = 0, \tag{2.1.13}$$

we obtain the following system

$$\begin{cases}\dot{\rho} + \rho\nabla\cdot\mathbf{v} = 0\\ \rho\mathbf{a} = \rho\mathbf{F} + \nabla\cdot\mathbf{T}\end{cases} \quad (\mathbf{T} = \mathbf{T}^T). \tag{2.1.14}$$

The acceleration can be written in the Eulerian form as:

$$\mathbf{a} = \mathbf{v}_t + \mathbf{v}\cdot\nabla\mathbf{v}. \tag{2.1.15}$$

If the fluid is Newtonian, the stress tensor $\mathbf{T}$ is

$$\mathbf{T} = (-p + \lambda\nabla\cdot\mathbf{v})\mathbf{I} + 2\gamma\mathbf{D}. \tag{2.1.16}$$

where λ and γ are viscosity coefficients.

By replacing (2.1.15) and (2.1.16) in (2.1.11) we have:

$$\rho(\mathbf{v}_t + \mathbf{v}\cdot\nabla\mathbf{v}) = \rho\mathbf{F} - \nabla p + \nabla(\lambda\nabla\cdot\mathbf{v}) + \nabla\cdot(2\gamma\mathbf{D}). \tag{2.1.17}$$

We observe that for small variations in temperature (of the order of 10^0), the viscosity coefficients λ and γ can be held constant, so under these assumptions we have:

$$\rho(\mathbf{v}_t + \mathbf{v}\cdot\nabla\mathbf{v}) = \rho\mathbf{F} - \nabla p + \lambda\nabla(\nabla\cdot\mathbf{v}) + \gamma\nabla\cdot(2\mathbf{D}). \tag{2.1.18}$$

After having easily proved that

$$\nabla\cdot(2\mathbf{D}) = \Delta\mathbf{v} + \nabla(\nabla\cdot\mathbf{v}), \tag{2.1.19}$$

we obtain

$$\rho(\mathbf{v}_t + \mathbf{v}\cdot\nabla\mathbf{v}) = \rho\mathbf{F} - \nabla p + (\lambda+\gamma)\nabla(\nabla\cdot\mathbf{v}) + \gamma\Delta\mathbf{v}. \tag{2.1.20}$$

In particular, as the fluid is incompressible, that is $\nabla\cdot\mathbf{v} = 0$, we have

$$\mathbf{v}_t + \mathbf{v}\cdot\nabla\mathbf{v} = \mathbf{F} - \nabla(\frac{p}{\rho}) + \nu\Delta\mathbf{v}, \tag{2.1.21}$$

where

$$\nu = \frac{\gamma}{\rho},$$

is the kinematic viscosity coefficient, while γ is called dynamic viscosity coefficient.

Therefore, system (2.1.14) becomes:

$$\begin{cases} \mathbf{v}_t + \mathbf{v}\cdot\nabla\mathbf{v} = \mathbf{F} - \nabla(\frac{p}{\rho}) + \nu\Delta\mathbf{v} \\ \nabla\cdot\mathbf{v} = 0. \end{cases} \tag{2.1.22}$$

Eqs. (2.1.22) are the Navier-Stokes equations for incompressible fluids.

2.2 Magnetohydrodynamics

Let us consider an incompressible fluid and conductor of electricity. It is evident that the equations used to describe its motion will be a combination of the equations governing the motion of a fluid in absence of an electromagnetic field, suitably modified, and the Maxwell's equations.

- **Case 1** First of all let us assume that there is no acceleration of gravity.

  We introduce:

$$\mathbf{R} = \int_{C_1(t)} (\mathbf{j} \times \mathbf{B}) dC_1, \quad \mathbf{M}_O = \int_{C_1(t)} (P - O) \times (\mathbf{j} \times \mathbf{B}) dC_1, \tag{2.2.1}$$

  which are respectively the resultant force and the corresponding resultant moment with respect to the pole O. Indeed the Lorentz force is:

$$\mathbf{F} = q(\mathbf{E} + \mathbf{v} \times \mathbf{B}), \tag{2.2.2}$$

  therefore, dividing by the volume, we obtain the force per unit of volume:

$$\mathbf{F}_{volume} = \rho(\mathbf{E} + \mathbf{v} \times \mathbf{B}) = \rho\mathbf{E} + \mathbf{j} \times \mathbf{B}, \tag{2.2.3}$$

  where $\mathbf{j}$ is the current density. Assuming that there are not free charges in the fluid, eq. (2.2.3) becomes:

$$\mathbf{F}_{volume} = \mathbf{j} \times \mathbf{B}. \tag{2.2.4}$$

  By using eqs. (2.1.2), (2.1.3), (2.1.4) and (2.2.1) we have:

$$\mathbf{R}^{(e)} = \int_{C_1} (\mathbf{j} \times \mathbf{B}) dC_1 + \int_{dC_1} \Phi d\sigma. \tag{2.2.5}$$

$$\mathbf{M}_O{}^{(e)} = \int_{C_1} (P - O) \times (\mathbf{j} \times \mathbf{B}) dC_1 + \int_{dC_1} (Q - O) \times \mathbf{\Phi} d\sigma.$$

  Eq. (2.1.4) can be rewritten as:

$$\begin{cases} \int_{C_1} \rho \mathbf{a} dC_1 = \int_{C_1} (\mathbf{j} \times \mathbf{B}) dC_1 + \int_{dC_1} \mathbf{\Phi} d\sigma \\ \int_{C_1} (P - O) \times \rho \mathbf{a} dC_1 = \int_{C_1} (P - O) \times (\mathbf{j} \times \mathbf{B}) dC_1 + \int_{dC_1} (Q - O) \times \mathbf{\Phi} d\sigma, \end{cases} \tag{2.2.6}$$

  By using the Cauchy's theorem, as we did before, substituting eq. (2.1.9) into $(2.2.6)_1$ we obtain:

$$\int_{C_1} \rho \mathbf{a} = \int_{C_1} (\mathbf{j} \times \mathbf{B}) dC_1 + \mathbf{e}_j \int_{dC_1} n_i T_{ij} d\sigma = \int_{C_1} (\mathbf{j} \times \mathbf{B} + d_i T^{ij} \mathbf{e}_j) dC_1, \tag{2.2.7}$$

  and therefore:

$$\rho \mathbf{a} = \mathbf{j} \times \mathbf{B} + \nabla \cdot \mathbf{T}. \tag{2.2.8}$$

We can write the acceleration in the Eulerian form, as before, and we recall the Maxwell's equations:

$$\begin{cases} \nabla \times \mathbf{B} = \mu \mathbf{j} + \mu\epsilon \dfrac{\partial \mathbf{E}}{\partial t} \\ \nabla \times \mathbf{E} = -\dfrac{\partial \mathbf{B}}{\partial t} \\ \nabla \cdot \mathbf{B} = 0 \\ \nabla \cdot \mathbf{E} = \dfrac{\rho}{\epsilon}, \end{cases} \tag{2.2.9}$$

where μ is the magnetic permeability and ϵ is the dielectric constant.
If we assume that ϵ is small enough to neglect $\dfrac{\partial \mathbf{E}}{\partial t}$, we have

$$\mathbf{j} \times \mathbf{B} = \frac{1}{\mu}(\nabla \times \mathbf{B}) \times \mathbf{B} = \frac{1}{\mu}(\mathbf{B} \cdot \nabla \mathbf{B} - \nabla \mathbf{B}^2). \tag{2.2.10}$$

Substituting eqs. (2.1.15), (2.1.16) and (2.2.10) in eq. (2.2.8) we have:

$$\rho(\mathbf{v}_t + \mathbf{v} \cdot \nabla \mathbf{v}) = \frac{1}{\mu}(\mathbf{B} \cdot \nabla \mathbf{B} - \nabla \mathbf{B}^2) + \nabla \cdot [(-p + \lambda \nabla \cdot \mathbf{v})\mathbf{I} + 2\mu \mathbf{D}]. \tag{2.2.11}$$

By using eq. (2.1.19) and the fact that the fluid is incompressible ($\nabla \cdot \mathbf{v} = 0$), eq. (2.2.11) becomes:

$$\mathbf{v}_t + \mathbf{v} \cdot \nabla \mathbf{v} = \frac{1}{\mu\rho}(\mathbf{B} \cdot \nabla \mathbf{B} - \nabla \mathbf{B}^2) - \nabla(\frac{p}{\rho}) + \frac{\mu}{\rho}\Delta \mathbf{v}. \tag{2.2.12}$$

The dimensional equations obtained are:

$$\begin{cases} \mathbf{v}_t + \mathbf{v} \cdot \nabla \mathbf{v} = \dfrac{1}{\rho\mu} \mathbf{B} \cdot \nabla \mathbf{B} - \nabla \Pi + \nu \Delta \mathbf{v} \\ \nabla \cdot \mathbf{v} = 0 \\ \mathbf{B}_t + \mathbf{v} \cdot \nabla \mathbf{B} - \mathbf{B} \cdot \nabla \mathbf{v} = \psi \, \Delta \mathbf{B} \\ \nabla \cdot \mathbf{B} = 0, \end{cases} \tag{2.2.13}$$

where Π is the pressure (included the magnetic pressure) and ν and ψ are positive physics parameters, respectively the kinematic viscosity and the electrical resistivity.
We observe that the first equation of the system is the first cardinal equation, the second one is the incompressibility condition, the third one is the Faraday's law and the last one is the Gauss's law on the non-existence of the magnetic monopole.

- **Case 2** We suppose to have the gravity acceleration.

  We introduce:

$$\mathbf{R} = \int_{C_1(t)} (\rho \mathbf{g} + \mathbf{j} \times \mathbf{B}) dC_1, \quad \mathbf{M}_O = \int_{C_1(t)} (P - O) \times (\rho \mathbf{g} + \mathbf{j} \times \mathbf{B}) dC_1, \tag{2.2.14}$$

  which are respectively the resultant force and the corresponding resultant moment with respect to the pole O.

We follow the same procedure of **Case 1** and we obtain the dimensional equations:

$$\begin{cases} \mathbf{v}_t + \mathbf{v}\cdot\nabla\mathbf{v} = \dfrac{1}{\rho\mu}\mathbf{B}\cdot\nabla\mathbf{B} - \nabla\Pi + \nu\Delta\mathbf{v} + \mathbf{g} \\ \nabla\cdot\mathbf{v} = 0 \\ \mathbf{B}_t + \mathbf{v}\cdot\nabla\mathbf{B} - \mathbf{B}\cdot\nabla\mathbf{v} = \psi\,\Delta\mathbf{B} \\ \nabla\cdot\mathbf{B} = 0. \end{cases} \tag{2.2.15}$$

Chapter 3

Stability/instability

In this section we recall how to study the problem of stability and instability of a base flow. As mentioned in the introduction, the methods used are usually differentiated into approximate linear methods and strict Lyapunov methods.

We take, as an example, the case of an incompressible viscous fluid which is described, as seen, by the Navier-Stokes equations (2.1.22).
Let Ω be an open limited set of $\mathbb{R}^3$ filled with a Newtonian incompressible fluid. Let $(\mathbf{v}, p)$ be a solution (also called basic flow) of (2.1.22), that describes the motion of the fluid, in $\Omega \times (0, T)$ with the initial conditions

$$\mathbf{v}(P, 0) = \mathbf{v}_0(P), \qquad P \in \Omega, \tag{3.0.1}$$

and at the boundaries

$$\mathbf{v}(P, t) = \mathbf{a_1}(P, t), \qquad \partial\Omega \times [0, T), \tag{3.0.2}$$

where the vector fields $\mathbf{v}_0(P)$, $\mathbf{a_1}$ and $\mathbf{F}(P, t)$ are regular fields such that

$$\nabla \cdot \mathbf{v}_0(P) = 0, \qquad \int_{\partial\Omega} \mathbf{a_1}(P, t) \cdot \mathbf{n} d\sigma = 0. \tag{3.0.3}$$

We perturb the basic motion at the initial instant, in correspondence with the same external force and with the same boundary conditions. Also the perturbed basic motion $(\mathbf{v} + \mathbf{u}, p + p')$ satisfies the system (2.1.22). Therefore, the difference basic motion $(\mathbf{u}, p')$ satisfies the following system

$$\begin{cases} \mathbf{u}_t + (\mathbf{v} + \mathbf{u}) \cdot \nabla \mathbf{u} + \mathbf{u} \cdot \nabla \mathbf{v} = -\nabla \dfrac{p'}{\rho} + \nu \Delta \mathbf{u} \\ \nabla \cdot \mathbf{u} = 0, \end{cases} \tag{3.0.4}$$

for each $(P, t) \in \Omega \times (0, +\infty)$, with initial condition

$$\mathbf{u}(P, 0) = \mathbf{u}_0(P), \qquad P \in \Omega, \tag{3.0.5}$$

and with boundary condition

$$\mathbf{u}(P, t) = 0, \qquad (P, t) \in \partial\Omega \times [0, T). \tag{3.0.6}$$

The study of the stability of the basic motion $m_0 = (\mathbf{v}, p)$ is reduced to the study of the perturbation $(\mathbf{u}, p')$. If $\mathbf{u}_0$ "small", with respect to "some measure", implies that also $\mathbf{u}(P, t)$ is "small" $\forall t > 0$, then m_0 is stable; otherwise, if $\mathbf{u}_0$ can "increase" regardless the smallness of $\mathbf{u}_0$, then m_0 is unstable.

3.1 Nonlinear energy stability

As a measure of the perturbation we choose

$$E(t) = \frac{1}{2}||\mathbf{u}(P,t)||^2, \tag{3.1.1}$$

that is, except for a constant factor, the “kinetic energy" of the perturbation.

Let us recall some definitions of nonlinear energy stability (see Joseph, 1976, Schmid and Henningson, 2001a).

- The basic motion is *monotonically stable in the energy norm*, and Re_E is the critical Reynolds number, if the time orbital derivative of the energy $\dot{E}$ is always less than zero,
$$\dot{E} < 0, \tag{3.1.2}$$
when $\mathrm{Re} < \mathrm{Re}_E$. In particular the stability is monotonic and exponential if there is a positive number α such that $E(t) \leq E(0)\exp\{-\alpha t\}$ for any $t \geq 0$ and $\mathrm{Re} < \mathrm{Re}_E$.
- The basic motion is *globally stable* to perturbations if the perturbation energy E satisfies
$$\lim_{t\to+\infty} \frac{E(t)}{E(0)} = 0, \quad \forall E(0) > 0. \tag{3.1.3}$$

The basic motion is *unstable* if and only if it is not *stable*.
The energy method was introduced by Orr and Reynolds but only in 1959 in an important article Serrin, 1959 showed that the problem of nonlinear stability could be reduced to a variational problem (minimum or maximum) solved by calculating the associated Euler-Lagrange equations. The Euler-Lagrange equations are precisely an eigenvalue problem and they allow to obtain the nonlinear critical parameter.

3.2 Linear instability

From the previous definitions of nonlinear stability it can be deduced that the rigorous study of the stability of a basic motion is reduced to studying, through the Lyapunov function, the evolution of the solutions of the system (3.0.4). However, due to the presence of the nonlinear terms in (3.0.4), for a long time it was difficult to study these solutions, and initially only qualitative results were obtained (Reynolds, 1895a, Orr, 1907, Thomas, 1943, Fériet, 1948).

Therefore, to simplify the problem and obtain significant quantitative and not only qualitative results, the linearized method was used.

According to this method, the perturbation system is first linearized. Then, solutions like e^{st}, with s complex number, are sought. We get a generalized eigenvalue

problem where s is the eigenvalue. The problem of the study of stability is therefore reduced to the solution of this generalized eigenvalue problem and the stability will depend precisely on the eigenvalue s.

In general $re(s)$ depends on a parameter Q, for example the Reynolds number, the Taylor number, the Rayleigh number and, in the case of periodic perturbations also by the wave numbers. Therefore, one would like to find the smallest value Q_c (critical parameter) for which $re(s) = 0$, that is, the one for which instability arises.

Chapter 4

Laminar flows between horizontal planes

In this section we derive first of all the expression of the velocity field of non- electroconductive fluids between horizontal planes, that is the velocity field of Couette and Poiseuille flows.
Then we suppose that the fluid is electroconductive, we find also in this case the expression of the velocity field and in addition the expression of the magnetic field. We will see that the first case can be obtained from the second one as a particular case.

1. **Without magnetic field**

   We consider a fluid in motion and we suppose that the motion occurs in a layer $\mathcal{D} = \mathbb{R}^2 \times [-D, D]$ with depth $2D$.
   The layer may be considered in a reference frame $Oxyz$, with unit vectors $\mathbf{i}, \mathbf{j}, \mathbf{k}$. The sheet (channel) extends to infinity in the x and y directions and has a finite depth $2D$ in the z direction.

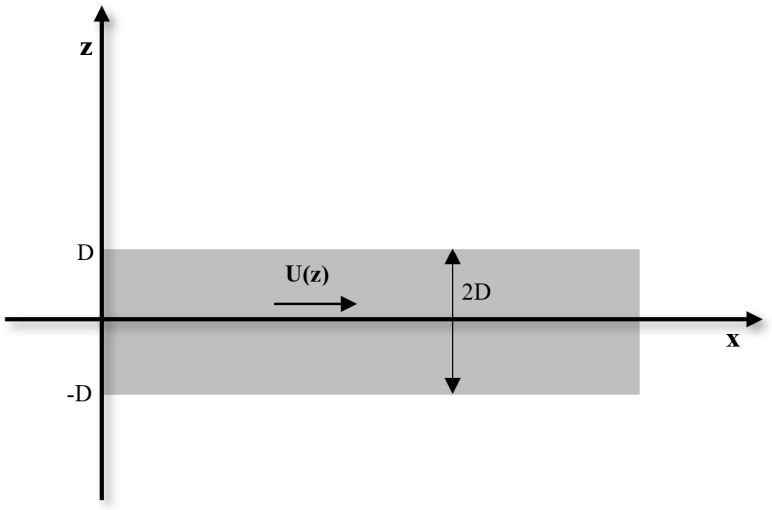

FIGURE 4.1: A layer of width $2D$ filled with a fluid. The direction of x-axis is the direction of the flow.

   Assuming that the fluid is Newtonian, homogeneous and incompressible, the equations governing the motion of the fluid are given by those of the system (2.1.22).
   We suppose that the only body force is that due to gravity, that is $\mathbf{F} = -g\mathbf{k}$.

If we wanted to compare the coefficients that appear in the equations of the system (2.1.22), we would have to calculate the value of each individual term. To avoid this, we can divide each coefficient by a certain homogeneous reference quantity, so the coefficients will be dimensionless and comparing them will be easier. We introduce the non-dimensional variables x^*, y^*, z^*, p^*, t^*, $\mathbf{v}^*$, $\mathbf{F}^*$ defined by

$$x^* = \frac{x}{D}, \quad y^* = \frac{y}{D}, \quad z^* = \frac{z}{D}, \quad p^* = \frac{p}{\rho V_0^2}, \quad t^\star = \frac{V_0 t}{D},$$

$$\mathbf{v}^\star = \frac{\mathbf{v}}{V_0}, \quad \mathbf{F}^* = \frac{D\mathbf{F}}{V_0^2},$$

where V_0 is a scaling factor (note that these definitions imply that $\nabla = \frac{\nabla^*}{D}$, $\nabla^2 = \frac{\nabla^{*2}}{D^2}$). With these new variables, system (2.1.22) becomes:

$$\begin{cases} \frac{V_0^2}{D}\frac{\partial \mathbf{v}^*}{\partial t^*} + \frac{V_0^2}{D}\mathbf{v}^*\cdot(\nabla^* v_x, \nabla^* v_y, \nabla^* v_z) = \frac{V_0^2 \mathbf{F}^*}{D} - \frac{V_0^2}{D}\nabla^* p + \frac{\nu V_0}{D^2}(\nabla^{*2} v_x^*, \nabla^{*2} v_y^*, \nabla^{*2} v_z^*) \\ \frac{V_0}{D}\nabla^*\cdot\mathbf{v}^* = 0, \end{cases} \tag{4.0.1}$$

If we define the following non-dimensional parameter

$$\mathrm{Re} = \frac{V_0 D}{\nu},$$

i.e. the Reynolds number, we multiply $(4.0.1)_1$ by $\frac{D}{V_0^2}$ and $(4.0.1)_2$ by $\frac{D}{V_0}$, and we neglect "*", we obtain the following system (4.0.2) in the domain $\mathbb{R}^2 \times [-1,1] \times (0,+\infty)$ in non-dimensional form:

$$\begin{cases} \mathbf{v}_t + \mathbf{v}\cdot\nabla\mathbf{v} = \mathbf{F} - \nabla p + \mathrm{Re}^{-1}\Delta\mathbf{v} \\ \nabla\cdot\mathbf{v} = 0. \end{cases} \tag{4.0.2}$$

If we restrict the analysis to laminar solutions dependent on z, that is to non-dimensional solutions of the kind

$$\mathbf{v}(z) = (U(z), 0, 0)$$

from eq. $(4.0.2)_3$ we obtain

$$v_i\mathbf{e}_i \cdot \frac{\partial v_j}{\partial x_k}\mathbf{e}_k\mathbf{e}_j = \mathbf{F} - \nabla p + \mathrm{Re}^{-1}\Delta v_i\mathbf{e}_i \Rightarrow \tag{4.0.3}$$

$$v_i\frac{\partial v_j}{\partial x_k}\delta_{ik}\mathbf{e}_j = \mathbf{F} - \nabla p + \mathrm{Re}^{-1}\Delta v_1\mathbf{e}_1 \Rightarrow \tag{4.0.4}$$

$$v_i\frac{\partial v_j}{\partial x_i}\mathbf{e}_j = \mathbf{F} - \nabla p + \mathrm{Re}^{-1}\Delta v_1\mathbf{e}_1 \Rightarrow \tag{4.0.5}$$

$$0 = (0,0,-g) - (p_x, p_y, p_z) + \mathrm{Re}^{-1}(U''(z), 0, 0). \tag{4.0.6}$$

From the last equation we obtain the following system:

$$\begin{cases} -p_x + \mathrm{Re}^{-1} U''(z) = 0 \\ p_y = 0 \\ g + p_z = 0. \end{cases} \tag{4.0.7}$$

Eq. $(4.0.7)_2$ implies that $p(x, y, z)$ does not depend explicitly on y, therefore, by integrating $(4.0.7)_3$, we have:

$$p(x, y, z) = p(x, z) = p_1(x) - gz. \tag{4.0.8}$$

Eq. $(4.0.7)_1$ can be rewritten as:

$$p_{1_x}(x) = \mathrm{Re}^{-1} U''(z). \tag{4.0.9}$$

The first member of the last equation depends only on x and the second one depends only on z, this implies that:

$$p_{1_x}(x) \equiv b_1, \qquad \mathrm{Re}^{-1} U''(z) \equiv b_1, \tag{4.0.10}$$

where b_1 is a constant. Therefore the basic motion $U(z)$ is:

$$U(z) = b_1 \mathrm{Re} \frac{z^2}{2} + c_1 z + d_1$$

where c_1 and d_1 are unknown constants that we can find using the boundary conditions.
• If we fix

$$U(1) = 0, \qquad U(-1) = 0,$$

we find $b_1 = -\dfrac{2d_1}{\mathrm{Re}}$, $c_1 = 0$ and

$$U(z) = d_1(1 - z^2).$$

If we impose that $U(0) = 1$ we have $d_1 = 1$ and we find the velocity profile of the *Poiseuille flow*:

$$U(z) = 1 - z^2.$$

• If we remove the pressure gradient, i.e. $b_1 = 0$, and we suppose that the motion of the fluid occurs just thanks to the motion of the plates along x and $-x$, the boundary conditions we have to fix are:

$$U(-1) = -1, \qquad U(1) = 1$$

and the constants are $c_1 = 0$ and $d_1 = 1$. Therefore we find

$$U(z) = z$$

which is the velocity profile of the *Couette flow*.

2. **With magnetic field**

We now consider an electroconductive fluid in motion. The layer and the reference frame are the same ones described in the **Case 1**.

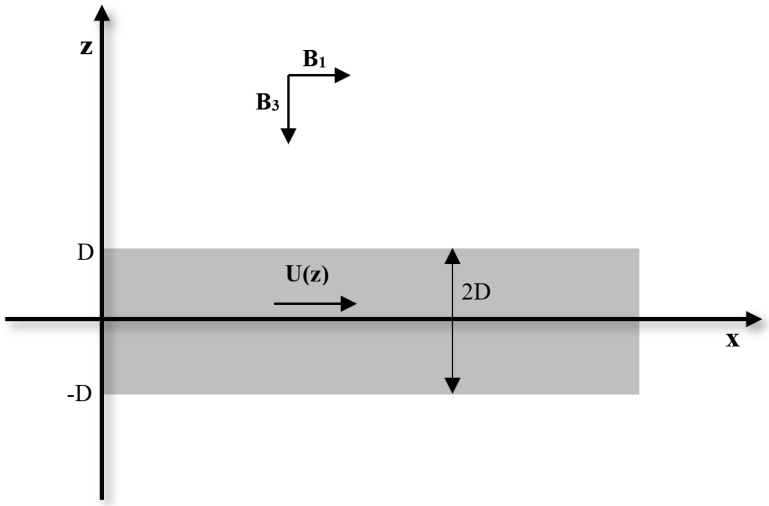

FIGURE 4.2: A layer of width $2D$ filled with an electroconductive fluid. The direction of x-axis is the direction of the flow.

Assuming that the fluid is Newtonian, homogeneous and incompressible, the equations governing the motion of the fluid are given by those of the system (2.2.13).
To non-dimensionalize the equations, as in Takashima, 1996, 1998, we introduce the non-dimensional variables $x^*, y^*, z^*, \Pi^*, t^*, \mathbf{v}^*, \mathbf{B}^*$ defined by

$$x^* = \frac{x}{D}, \quad y^* = \frac{y}{D}, \quad z^* = \frac{z}{D}, \quad t^\star = \frac{V_0 t}{D}, \quad \Pi^* = \frac{\Pi}{V_0^2},$$

$$\mathbf{v}^\star = \frac{\mathbf{v}}{V_0}, \quad \mathbf{B}^* = \frac{\mathbf{B}}{B_0},$$

where V_0 and B_0 are scaling factors (note that these definitions imply that $\nabla = \frac{\nabla^*}{D}$, $\nabla^2 = \frac{\nabla^{*2}}{D^2}$).
With these new variables (2.2.13) becomes:

$$\begin{cases} \frac{V_0^2}{D}\frac{\partial \mathbf{v}^*}{\partial t^*} + \frac{V_0^2}{D}\mathbf{v}^*\cdot(\nabla^* v_x, \nabla^* v_y, \nabla^* v_z) = \frac{1}{\rho\mu}\frac{B_0^2}{D}\mathbf{B}^*\cdot(\nabla^* B_x^*, \nabla^* B_y^*, \nabla^* B_z^*) + \\ -\frac{V_0^2}{D}\nabla^*\Pi + \frac{\nu V_0}{D^2}(\nabla^{*2} v_x^*, \nabla^{*2} v_y^*, \nabla^{*2} v_z^*) \\ \frac{V_0}{D}\nabla^*\cdot\mathbf{v}^* = 0 \\ \frac{V_0 B_0}{D}\frac{\partial \mathbf{B}^*}{\partial t^*} + \frac{V_0 B_0}{D}\mathbf{v}^*\cdot(\nabla^* B_x^*, \nabla^* B_y^*, \nabla^* B_z^*) - \frac{B_0 V_0}{d}\mathbf{B}^*\cdot(\nabla^* v_x^*, \nabla^* v_y^*, \nabla^* v_z^*) = \\ \qquad = \frac{\eta B_0}{D^2}(\nabla^{*2} B_x^*, \nabla^{*2} B_y^*, \nabla^{*2} B_z^*) \\ \frac{B_0}{D}\nabla^*\cdot\mathbf{B}^* = 0, \end{cases} \tag{4.0.11}$$

If we define the following non-dimensional parameters:

- $\mathrm{Re} = V_0 D/\nu$, the Reynolds number,
- $\mathrm{Rm} = V_0 D/\psi$, the magnetic Reynolds number,
- $\mathrm{Ha} = \dfrac{B_0 D}{\sqrt{\rho\nu\mu\psi}}$, the Hartmann number,
- $\mathrm{Pm} = \dfrac{\nu}{\psi} = \dfrac{\mathrm{Rm}}{\mathrm{Re}}$, the Prandtl magnetic number,
- $\mathrm{N} = \mathrm{Ha}^2\mathrm{Re}^{-1}$ the interaction parameter,

multiplying (4.0.11)$_1$ by $\frac{D}{V_0^2}$, (4.0.11)$_2$ by $\frac{D}{V_0}$, (4.0.11)$_3$ by $\frac{D}{V_0 B_0}$, (4.0.11)$_4$ by $\frac{D}{B_0}$ and neglecting "*", we obtain the following system (4.0.12) in the domain $\mathbb{R}^2 \times [-1,1] \times (0,+\infty)$ in non-dimensional form:

$$\begin{cases} \mathbf{v}_t + \mathbf{v}\cdot\nabla\mathbf{v} = \mathrm{Ha}^2\mathrm{Re}^{-1}\mathrm{Rm}^{-1}\,\mathbf{B}\cdot\nabla\mathbf{B} - \nabla\Pi + \mathrm{Re}^{-1}\Delta\mathbf{v} \\ \nabla\cdot\mathbf{v} = 0 \\ \mathbf{B}_t + \mathbf{v}\cdot\nabla\mathbf{B} - \mathbf{B}\cdot\nabla\mathbf{v} = \mathrm{Rm}^{-1}\,\Delta\mathbf{B} \\ \nabla\cdot\mathbf{B} = 0, \end{cases} \tag{4.0.12}$$

If we restrict the analysis to laminar solutions dependent on z, that is to non-dimensional solutions of the kind

$$\mathbf{v}(z) = (U(z),0,0), \quad \mathbf{B}(z) = (B(z),0,1),$$

from eq. (4.0.12)$_3$ we obtain

$$v_i\mathbf{e}_i\cdot\frac{\partial B_j}{\partial x_k}\mathbf{e}_k\mathbf{e}_j - B_i\mathbf{e}_i\cdot\frac{\partial v_j}{\partial x_k}\mathbf{e}_k\mathbf{e}_j = \mathrm{Rm}^{-1}\,\Delta B_i\mathbf{e}_i \Rightarrow \tag{4.0.13}$$

$$\Rightarrow v_i\frac{\partial B_j}{\partial x_k}\delta_{ik}\mathbf{e}_j - B_i\frac{\partial v_j}{\partial x_k}\delta_{ik}\mathbf{e}_j = \mathrm{Rm}^{-1}\,\Delta B_1\mathbf{e}_1 \Rightarrow \tag{4.0.14}$$

$$\Rightarrow v_i\frac{\partial B_j}{\partial x_i}\mathbf{e}_j - B_i\frac{\partial v_j}{\partial x_i}\mathbf{e}_j = \mathrm{Rm}^{-1}\,\Delta B_1\mathbf{e}_1 \Rightarrow \tag{4.0.15}$$

$$\Rightarrow (0,0,0) - (U'(z),0,0) = \mathrm{Rm}^{-1}\,(B''(z),0,0) \tag{4.0.16}$$

and therefore:

$$B''(z) = -\mathrm{Rm}\,U'(z). \tag{4.0.17}$$

Eq. (4.0.17) implies that $B'(z) = -\mathrm{Rm}\,(U(z) + a_1/\mathrm{Ha}^2)$ where a_1 is a constant of integration. From eq. (4.0.12)$_1$ it follows that:

$$v_i\mathbf{e}_i\cdot\frac{\partial v_j}{\partial x_k}\mathbf{e}_k\mathbf{e}_j = \mathrm{Ha}^2\mathrm{Re}^{-1}\mathrm{Rm}^{-1}\,B_i\mathbf{e}_i\cdot\frac{\partial B_j}{\partial x_k}\mathbf{e}_k\mathbf{e}_j - \nabla\Pi + \mathrm{Re}^{-1}\Delta v_i\mathbf{e}_i \Rightarrow \tag{4.0.18}$$

$$v_i\frac{\partial v_j}{\partial x_k}\delta_{ik}\mathbf{e}_j = \mathrm{Ha}^2\mathrm{Re}^{-1}\mathrm{Rm}^{-1}\,B_i\frac{\partial B_j}{\partial x_k}\delta_{ik}\mathbf{e}_j - \nabla\Pi + \mathrm{Re}^{-1}\Delta v_1\mathbf{e}_1 \Rightarrow \tag{4.0.19}$$

$$v_i\frac{\partial v_j}{\partial x_i}\mathbf{e}_j = \mathrm{Ha}^2\mathrm{Re}^{-1}\mathrm{Rm}^{-1}\,B_i\frac{\partial B_j}{\partial x_i}\mathbf{e}_j - \nabla\Pi + \mathrm{Re}^{-1}\Delta v_1\mathbf{e}_1 \Rightarrow \tag{4.0.20}$$

$$0 = \mathrm{Ha}^2\mathrm{Re}^{-1}\mathrm{Rm}^{-1}\,(B'(z),0,0) - (\Pi_x,\Pi_y,\Pi_z) + \mathrm{Re}^{-1}(U''(z),0,0). \tag{4.0.21}$$

From the last equation we obtain the following system:

$$\begin{cases} \mathrm{Ha}^2\mathrm{Re}^{-1}\mathrm{Rm}^{-1}B'(z) - \Pi_x + \mathrm{Re}^{-1}U''(z) = 0 \\ \Pi_y = 0 \\ -\Pi_z = 0. \end{cases} \tag{4.0.22}$$

Eq. $(4.0.22)_2$ implies that $\Pi(x,y,z)$ does not depend explicitly on y, therefore, by integrating $(4.0.22)_3$, we have:

$$\Pi(x,y,z) = \Pi(x,z) = \Pi_1(x). \tag{4.0.23}$$

Eq. $(4.0.22)_1$ can be rewritten as:

$$\mathrm{Ha}^2\mathrm{Re}^{-1}\mathrm{Rm}^{-1}B'(z) - \Pi_{1x}(x) + \mathrm{Re}^{-1}U''(z) = 0 \Rightarrow \tag{4.0.24}$$

$$\Pi_{1x}(x) = \mathrm{Ha}^2\mathrm{Re}^{-1}\mathrm{Rm}^{-1}B'(z) + \mathrm{Re}^{-1}U''(z) \Rightarrow \tag{4.0.25}$$

$$\mathrm{Re}\,\Pi_{1x}(x) = \mathrm{Ha}^2\mathrm{Rm}^{-1}B'(z) + U''(z). \tag{4.0.26}$$

The first member of the last equation depends only on x and the second one depends only on z, this implies that:

$$\mathrm{Re}\,\Pi_{1x}(x) \equiv b_1, \qquad \mathrm{Ha}^2\mathrm{Rm}^{-1}B'(z) + U''(z) \equiv b_1, \tag{4.0.27}$$

and from (4.0.16):

$$\mathrm{Re}\,\Pi_{1x}(x) \equiv b_1, \qquad U''(z) - \mathrm{Ha}^2U(z) \equiv b_1 + a_1. \tag{4.0.28}$$

The solutions of this second-order, non-homogeneous differential equation are

$$U(z) = u_1\cosh(\mathrm{Ha}\,z) + u_2\sinh(\mathrm{Ha}\,z) - \frac{a_1+b_1}{\mathrm{Ha}^2},$$

and therefore

$$B(z) = -\frac{\mathrm{Rm}}{\mathrm{Ha}}\left(u_1\sinh(\mathrm{Ha}\,z) + u_2\cosh(\mathrm{Ha}\,z) - \frac{b_1}{\mathrm{Ha}}z + \frac{c_1}{\mathrm{Ha}}\right).$$

We observe that Re depends on β because

$$\mathrm{Re} = \frac{V_0 D}{\nu} = \frac{U(D)D}{\nu}. \tag{4.0.29}$$

For the Couette and Hartmann flows we choose boundary conditions that correspond to the rigid conditions for the velocity field and to non-conducting boundaries.

• For the *Couette flow* we fix

$$U(1) = 1, \qquad U(-1) = -1, \qquad B(1) = B(-1) = 0 \tag{4.0.30}$$

(cf. Alexakis et al., 2003).
We assume that there is no forcing pressure in the channel, that is $b_1 = 0$. We

obtain the following system:

$$\begin{cases} 0 = -\dfrac{\mathrm{Rm}}{\mathrm{Ha}}\left(u_1\sinh(\mathrm{Ha}) + u_2\cosh(\mathrm{Ha}) + \dfrac{c_1}{\mathrm{Ha}}\right) \\ 0 = -\dfrac{\mathrm{Rm}}{\mathrm{Ha}}\left(-u_1\sinh(\mathrm{Ha}) + u_2\cosh(\mathrm{Ha}) + \dfrac{c_1}{\mathrm{Ha}}\right) \\ 1 = u_1\cosh(\mathrm{Ha}) + u_2\sinh(\mathrm{Ha}) - \dfrac{a_1}{\mathrm{Ha}^2} \\ -1 = u_1\cosh(\mathrm{Ha}) - u_2\sinh(\mathrm{Ha}) - \dfrac{a_1}{\mathrm{Ha}^2}, \end{cases} \tag{4.0.31}$$

which is equivalent to:

$$\begin{cases} 0 = -2\dfrac{\mathrm{Rm}}{\mathrm{Ha}}\left(u_2\cosh(\mathrm{Ha}) + \dfrac{c_1}{\mathrm{Ha}}\right) \\ 0 = -2\dfrac{\mathrm{Rm}}{\mathrm{Ha}}u_1\sinh(\mathrm{Ha}) \\ 1 = u_1\cosh(\mathrm{Ha}) + u_2\sinh(\mathrm{Ha}) - \dfrac{a_1}{\mathrm{Ha}^2} \\ -1 = u_1\cosh(\mathrm{Ha}) - u_2\sinh(\mathrm{Ha}) - \dfrac{a_1}{\mathrm{Ha}^2}, \end{cases} \tag{4.0.32}$$

obtained by adding and subtracting member by member eq. $(4.0.31)_1$ and eq. $(4.0.31)_2$. Eq. $(4.0.32)_1$ implies that $u_1 = 0$ and the system becomes:

$$\begin{cases} 0 = -2\dfrac{\mathrm{Rm}}{\mathrm{Ha}}\left(u_2\cosh(\mathrm{Ha}) + \dfrac{c_1}{\mathrm{Ha}}\right) \\ u_1 = 0 \\ 1 = u_2\sinh(\mathrm{Ha}) - \dfrac{a_1}{\mathrm{Ha}^2} \\ -1 = -u_2\sinh(\mathrm{Ha}) - \dfrac{a_1}{\mathrm{Ha}^2}, \end{cases} \tag{4.0.33}$$

which is equivalent to:

$$\begin{cases} 0 = -2\dfrac{\mathrm{Rm}}{\mathrm{Ha}}\left(u_2\cosh(\mathrm{Ha}) + \dfrac{c_1}{\mathrm{Ha}}\right) \\ u_1 = 0 \\ 1 = u_2\sinh(\mathrm{Ha}) \\ 0 = -2\dfrac{a_1}{\mathrm{Ha}^2}, \end{cases} \tag{4.0.34}$$

obtained by adding and subtracting member by member eq. $(4.0.33)_3$ and eq. $(4.0.33)_4$.

$$\begin{cases} u_1 = 0 \\ a_1 = 0 \\ u_2 = \dfrac{1}{\sinh(\mathrm{Ha})} \\ c_1 = -\mathrm{Ha}\coth(\mathrm{Ha}), \end{cases} \tag{4.0.35}$$

Therefore:

$$U(z) = \frac{\sinh(\mathrm{Ha}\,z)}{\sinh(\mathrm{Ha})}, \qquad B(z) = \frac{\mathrm{Rm}}{\mathrm{Ha}}\frac{[\cosh(\mathrm{Ha}) - \cosh(\mathrm{Ha}\,z)]}{\sinh(\mathrm{Ha})}. \tag{4.0.36}$$

- For the *Hartmann flow* we fix

$$U(-1) = U(1) = 0, \qquad B(-1) = B(1) = 0. \tag{4.0.37}$$

We obtain the following system:

$$\begin{cases} 0 = -\dfrac{\mathrm{Rm}}{\mathrm{Ha}}\left(u_1\sinh(\mathrm{Ha}) + u_2\cosh(\mathrm{Ha}) - \dfrac{b_1}{\mathrm{Ha}} + \dfrac{c_1}{\mathrm{Ha}}\right) \\ 0 = -\dfrac{\mathrm{Rm}}{\mathrm{Ha}}\left(-u_1\sinh(\mathrm{Ha}) + u_2\cosh(\mathrm{Ha}) + \dfrac{b_1}{\mathrm{Ha}} + \dfrac{c_1}{\mathrm{Ha}}\right) \\ u_1\cosh(\mathrm{Ha}) + u_2\sinh(\mathrm{Ha}) - \dfrac{a_1+b_1}{\mathrm{Ha}^2} = 0 \\ u_1\cosh(\mathrm{Ha}) - u_2\sinh(\mathrm{Ha}) - \dfrac{a_1+b_1}{\mathrm{Ha}^2} = 0 \end{cases} \Rightarrow \tag{4.0.38}$$

$$\Rightarrow \begin{cases} 0 = -2\dfrac{\mathrm{Rm}}{\mathrm{Ha}}\left(u_2\cosh(\mathrm{Ha}) + \dfrac{c_1}{\mathrm{Ha}}\right) \\ 0 = -2\dfrac{\mathrm{Rm}}{\mathrm{Ha}}\left(u_1\sinh(\mathrm{Ha}) - \dfrac{b_1}{\mathrm{Ha}}\right) \\ 2(u_1\cosh(\mathrm{Ha}) - \dfrac{a_1+b_1}{\mathrm{Ha}^2}) = 0 \\ 2u_2\sinh(\mathrm{Ha}) = 0 \end{cases} \Rightarrow \tag{4.0.39}$$

$$\Rightarrow \begin{cases} c_1 = 0 \\ b_1 = u_1\mathrm{Ha}\sinh(\mathrm{Ha}) \\ a_1 = \mathrm{Ha}^2u_1\cosh(\mathrm{Ha}) - b_1 \\ \quad = \mathrm{Ha}u_1(\mathrm{Ha}\cosh(\mathrm{Ha}) - \sinh(\mathrm{Ha})) \\ u_2 = 0. \end{cases} \Rightarrow \tag{4.0.40}$$

By imposing $U(0) = 1$, we obtain the following system:

$$\begin{cases} c_1 = 0 \\ b_1 = u_1\mathrm{Ha}\sinh(\mathrm{Ha}) \\ a_1 = \mathrm{Ha}u_1(\mathrm{Ha}\cosh(\mathrm{Ha}) - \sinh(\mathrm{Ha})) \\ u_2 = 0 \\ 1 = u_1 - \dfrac{a_1+b_1}{\mathrm{Ha}^2} \end{cases} \Rightarrow \tag{4.0.41}$$

$$\Rightarrow \begin{cases} c_1 = 0 \\ b_1 = u_1\mathrm{Ha}\sinh(\mathrm{Ha}) \\ a_1 = \mathrm{Ha}u_1(\mathrm{Ha}\cosh(\mathrm{Ha}) - \sinh(\mathrm{Ha})) \\ u_2 = 0 \\ 1 = u_1 - \dfrac{\mathrm{Ha}u_1(\mathrm{Ha}\cosh(\mathrm{Ha}) - \sinh(\mathrm{Ha})) + u_1\mathrm{Ha}\sinh(\mathrm{Ha})}{\mathrm{Ha}^2} \end{cases} \Rightarrow \tag{4.0.42}$$

$$\Rightarrow \begin{cases} c_1 = 0 \\ b_1 = u_1\mathrm{Ha}\sinh(\mathrm{Ha}) \\ a_1 = \mathrm{Ha}u_1(\mathrm{Ha}\cosh(\mathrm{Ha}) - \sinh(\mathrm{Ha})) \\ u_2 = 0 \\ u_1 = \dfrac{1}{1-\cosh(\mathrm{Ha})} \end{cases} \Rightarrow \tag{4.0.43}$$

$$\Rightarrow \begin{cases} c_1 = 0 \\ u_2 = 0 \\ u_1 = \dfrac{1}{1-\cosh(\mathrm{Ha})} \\ b_1 = \dfrac{1}{1-\cosh(\mathrm{Ha})}\mathrm{Ha}\sinh(\mathrm{Ha}) \\ a_1 = \mathrm{Ha}\dfrac{1}{1-\cosh(\mathrm{Ha})}(\mathrm{Ha}\cosh(\mathrm{Ha}) - \sinh(\mathrm{Ha})), \end{cases} \Rightarrow \tag{4.0.44}$$

and the solutions are:

$$U(z) = \frac{\cosh(\mathrm{Ha}) - \cosh(\mathrm{Ha}z)}{\cosh(\mathrm{Ha}) - 1}, \tag{4.0.45}$$

and

$$B(z) = \frac{\sinh(\mathrm{Ha}z) - z\sinh(\mathrm{Ha})}{\mathrm{Ha}(\cosh(\mathrm{Ha}) - 1)}. \tag{4.0.46}$$

If we define $\hat{\mathbf{B}} = \mathrm{Rm}^{-1}\mathbf{B}$, system (4.0.12) becomes

$$\begin{cases} \mathbf{v}_t + \mathbf{v}\cdot\nabla\mathbf{v} = \mathrm{Ha}^2\mathrm{Re}^{-1}\mathrm{Rm}\,\hat{\mathbf{B}}\cdot\nabla\hat{\mathbf{B}} - \nabla\Pi + \mathrm{Re}^{-1}\Delta\mathbf{v} \\ \nabla\cdot\mathbf{v} = 0 \\ \hat{\mathbf{B}}_t + \mathbf{v}\cdot\nabla\hat{\mathbf{B}} - \hat{\mathbf{B}}\cdot\nabla\mathbf{v} = \mathrm{Rm}^{-1}\Delta\hat{\mathbf{B}} \\ \nabla\cdot\hat{\mathbf{B}} = 0. \end{cases} \tag{4.0.47}$$

The basic solution of the system is $(U(z), 0, 0)$, $(\bar{B}(z), 0, \mathrm{Rm}^{-1})$ where

$$U(z) = \frac{\sinh(\mathrm{Ha}\,z)}{\sinh(\mathrm{Ha})}, \qquad \bar{B}(z) = \frac{1}{\mathrm{Ha}}\frac{[\cosh(\mathrm{Ha}) - \cosh(\mathrm{Ha}\,z)]}{\sinh(\mathrm{Ha})}$$

for the Couette flow, and

$$U(z) = \frac{\cosh(\mathrm{Ha}) - \cosh(\mathrm{Ha}z)}{\cosh(\mathrm{Ha}) - 1}, \qquad \bar{B}(z) = \frac{\sinh(\mathrm{Ha}z) - z\sinh(\mathrm{Ha})}{\mathrm{Ha}(\cosh(\mathrm{Ha}) - 1)}$$

for the Hartmann flow.

The basic motions obtained in the Case 1 can be derived from the current one as particular cases. Indeed, in absence of the magnetic field we have:

$$\lim_{\mathrm{Ha}\to 0} U(z) = \frac{\sinh(\mathrm{Ha}\,z)}{\sinh(\mathrm{Ha})} = z$$

which is the Couette flow, and

$$\lim_{\mathrm{Ha}\to 0} U(z) = \frac{\cosh(\mathrm{Ha}) - \cosh(\mathrm{Ha}z)}{\cosh(\mathrm{Ha}) - 1} = 1 - z^2$$

which is the Hartmann flow.

Chapter 5

Laminar flows in inclined channel

In this section we consider first of all a fluid that flows in an inclined channel and that is non-electroconductive. We derive the expressions of the velocity and the magnetic fields.
Then we suppose that the fluid is electroconductive and we find also in this case the expression of the velocity field and in addition the expression of the magnetic field.

1. **Without magnetic field**

   Let D be a positive real number. Consider a layer $\mathcal{D} = \mathbb{R}^2 \times [-D, D]$ of gap $2D$ filled with an electrically conducting fluid. As in Falsaperla et al. 2020b, the layer may be considered, a sheet of fluid down an incline (open inclined channel) with constant slope angle β, $0 < \beta < \pi/2$ in a reference frame $Oxyz$, with unit vectors $\mathbf{i}, \mathbf{j}, \mathbf{k}$. The x-axis is taken along the slope direction while the z-axis is perpendicular to the layer, and the y-axis is orthogonal to the slope direction in the plane xy. The sheet (channel) extends to infinity in the x and y directions and has a finite depth $2D$ in the z direction.

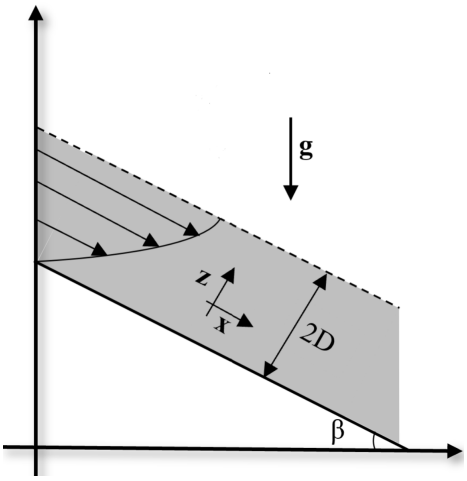

FIGURE 5.1: Inclined parabolic shear flow: the direction of x-axis is the direction of the flow. The layer of depth $2D$ is inclined of an angle β.

The motion is described by the equations (2.1.22) where $\mathbf{F} = g \sin\beta\, \mathbf{i} - g \cos\beta\, \mathbf{k}$:

$$\begin{cases} \mathbf{U}_t + \mathbf{U} \cdot \nabla \mathbf{U} = g \sin\beta\, \mathbf{i} - g \cos\beta\, \mathbf{k} - \nabla p/\rho + \nu \Delta \mathbf{U} \\ \nabla \cdot \mathbf{U} = \mathbf{0}. \end{cases} \quad \Leftrightarrow$$

$$\Leftrightarrow \begin{cases} \mathbf{U}_t + \mathbf{U}\cdot\nabla\mathbf{U} = -\nabla q/\rho + \nu\Delta\mathbf{U} \\ \nabla\cdot\mathbf{U} = \mathbf{0}. \end{cases} \tag{5.0.1}$$

In the second set of equations the function q is a pressure gradient incorporating the linear term coming from gravity (see Chandrasekhar, 1961). This shows that the inclination produces a natural pressure gradient.

We plan to determine the stationary flows $\overline{\mathbf{U}}$ that satisfy the equations above with the addition of rigid conditions on the values of the field $\overline{\mathbf{U}}$ on $z = \pm d$, the upper and lower boundaries of Ω, and assuming that such boundaries are possibly in constant motion, one with respect to the other. Resorting to a uniformly translating reference frame, such requirements can be recast in two conditions $\overline{\mathbf{U}}(x,y,-D) = -\alpha\mathbf{i}$ and $\overline{\mathbf{U}}(x,y,D) = \alpha\mathbf{i}$ for every x, y. This fact creates a inhomogeneity between the direction $\mathbf{i}$, that we call *streamwise* and $\mathbf{j}$, that we call *spanwise*.

We seek for steady laminar solutions, that is solutions of the form $\mathbf{U} = (U(z), V(z), 0)$. Therefore, from (1) we have that:

$$U_i\mathbf{e}_i \cdot \frac{\partial U_j}{\partial x_k}\mathbf{e}_k\mathbf{e}_j = -\nabla q/\rho + \Delta\mathbf{U} \Leftrightarrow$$

$$\Leftrightarrow (\cancel{W\frac{\partial U}{\partial z}}, \cancel{W\frac{\partial V}{\partial z}}, \cancel{W\frac{\partial W}{\partial z}}) = \nu(U_{zz}, V_{zz}, \cancel{W_{zz}}) - \frac{1}{\rho}(q_x, q_y, q_z) \Leftrightarrow \tag{5.0.2}$$

$$\Leftrightarrow \begin{cases} q_x = \rho\nu U_{zz} \\ q_y = \rho\nu V_{zz} \\ q_z = 0 \end{cases} \tag{5.0.3}$$

From the last equation of the system, one has that q does not depend on z, that is, $q = q(x,y)$. Therefore the left sides of the first two equations of the system depend on x and y, but the right sides of them depend only on z. Therefore there must exist two constants a and b such that:

$$\begin{cases} q_x = \rho\nu U_{zz} = a \\ q_y = \rho\nu V_{zz} = b. \end{cases} \tag{5.0.4}$$

This implies that the pressure must be a linear function $q = ax + by$ and the possible steady laminar solutions to eq. (1) that also satisfies the rigid boundary conditions, is quadratic function and has analytic expression

$$\overline{\mathbf{U}} = \left(\frac{\alpha}{d}z + \frac{\gamma}{D^2}(z^2 - D^2)\right)\mathbf{i} + \frac{\delta}{D^2}(z^2 - D^2)\mathbf{j}. \tag{5.0.5}$$

By computing, from the last expression of $\overline{\mathbf{U}}$, the second derivative with respect to z, and by substituting it in (5.0.4), we obtain:

$$\begin{cases} \rho\nu\dfrac{2\gamma}{d^2} = a \\ \rho\nu\dfrac{2\delta}{d^2} = b, \end{cases} \tag{5.0.6}$$

therefore $\gamma = D^2/(2\nu\rho)a, \delta = D^2/(2\nu\rho)b$ and these parameters have dimension of mt/sec, like α (see Joseph, 1976). The parameter α is the relative velocity of the boundaries, and effects the solution because of the rigidity of the boundaries. The parameters γ, δ depend on the particular choice of base pressure, that is possibly due to gravity or to other physical phenomena that create a pressure gradient. We nondimensionalise the system rescaling space with D, time with $D/(\alpha+\gamma)$, denoting $R = 2D(\alpha+\gamma)/\nu$, $\xi = \gamma/(\alpha+\gamma)$, $\eta = \delta/(\alpha+\gamma)$, and calling P the consequent rescaling of q. The system reduces to

$$\begin{cases} \mathbf{U}_t + \mathbf{U}\cdot\nabla\mathbf{U} = \frac{1}{R}\Delta\mathbf{U} - \nabla P \\ \nabla\cdot\mathbf{U} = \mathbf{0}, \end{cases} \tag{5.0.7}$$

where

$$\overline{\mathbf{U}} = \begin{pmatrix} (1-\xi)z + \xi(z^2-1) \\ \eta(z^2-1) \\ 0 \end{pmatrix} = \begin{pmatrix} f(z) \\ g(z) \\ 0 \end{pmatrix}. \tag{5.0.8}$$

This choice of rescaling allows to include Poiseuille and Couette flows as special cases. In fact Couette base flow corresponds to the choice $\xi = 0, \eta = 0$, Poiseuille base flow corresponds to the choice of $\xi = 1, \eta = 0$.

We note that, despite being physically relevant, *the pressure gradient induced by gravity produces effects not different from those induced by a pump*. Therefore we can represent the setup and the basic flow also as illustrated in the figure below: the upper boundary of the layer moves with velocity $\alpha\mathbf{i}$, the lower boundary with velocity $-\alpha\mathbf{i}$ and the base flow is also influenced by a pressure gradient q.

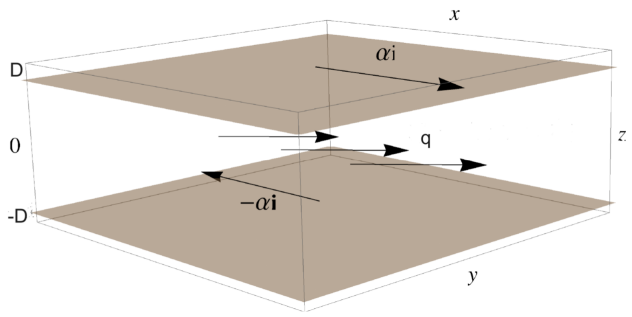

FIGURE 5.2: A layer of width $2D$ filled with a fluid. The upper boundary of the layer moves with velocity $\alpha\mathbf{i}$, the lower boundary with velocity $-\alpha\mathbf{i}$. The base flow is also influenced by a pressure gradient q non parallel to $\mathbf{i}$.

2. **With magnetic field**

We now consider the same setup as in **Case 1** but we suppose that the fluid is electroconductive.

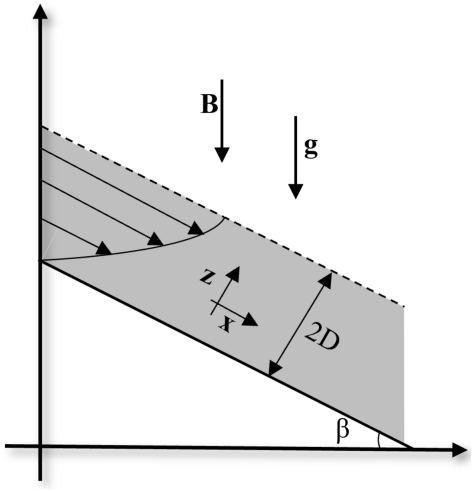

FIGURE 5.3: Electroconductive fluid that flows in a layer of depth $2D$ inclined of an angle β. The direction of x-axis is the direction of the flow.

Assuming that the fluid is Newtonian, homogeneous and incompressible, the equations governing the motion of the fluid are given by those of the system (2.2.15).
As we did before, we nondimensonalize (2.2.15) obtaining the following system:

$$\begin{cases} \frac{V_0^2}{D}\frac{\partial \mathbf{v}^*}{\partial t^*} + \frac{V_0^2}{D}\mathbf{v}^*\cdot(\nabla^* v_x, \nabla^* v_y, \nabla^* v_z) = \frac{1}{\rho\mu}\frac{B_0^2}{D}\mathbf{B}^*\cdot(\nabla^* B_x^*, \nabla^* B_y^*, \nabla^* B_z^*) + \\ -\frac{V_0^2}{D}\nabla^*\Pi + \frac{\nu V_0}{D^2}(\nabla^{*2} v_x^*, \nabla^{*2} v_y^*, \nabla^{*2} v_z^*) + \mathbf{g} \\ \frac{V_0}{D}\nabla^*\cdot\mathbf{v}^* = 0 \\ \frac{V_0 B_0}{D}\frac{\partial \mathbf{B}^*}{\partial t^*} + \frac{V_0 B_0}{D}\mathbf{v}^*\cdot(\nabla^* B_x^*, \nabla^* B_y^*, \nabla^* B_z^*) - \frac{B_0 V_0}{d}\mathbf{B}^*\cdot(\nabla^* v_x^*, \nabla^* v_y^*, \nabla^* v_z^*) = \\ \qquad = \frac{\psi B_0}{D^2}(\nabla^{*2} B_x^*, \nabla^{*2} B_y^*, \nabla^{*2} B_z^*) \\ \frac{B_0}{D}\nabla^*\cdot\mathbf{B}^* = 0. \end{cases} \tag{5.0.9}$$

where $\mathbf{g} = g\sin\beta\mathbf{i} - g\cos\beta\mathbf{k}$.
The parameters that appear in (5.0.9) are the same we introduced in (4.0.11).
Multiplying eq. $(5.0.9)_1$ by $\frac{D}{V_0^2}$, eq. $(5.0.9)_2$ by $\frac{D}{V_0}$, eq. $(5.0.9)_3$ by $\frac{D}{V_0 B_0}$, eq. $(5.0.9)_4$ by $\frac{D}{B_0}$ and dropping "*", we obtain equations (5.0.10) in the domain $\mathbb{R}^2 \times [-1,1] \times (0,+\infty)$ and in nondimensional form

$$\begin{cases} \mathbf{v}_t + \mathbf{v}\cdot\nabla\mathbf{v} = \mathrm{Ha}^2\mathrm{Re}^{-1}\mathrm{Rm}^{-1}\,\mathbf{B}\cdot\nabla\mathbf{B} - \nabla\Pi + \mathrm{Re}^{-1}\Delta\mathbf{v} + \hat{\mathbf{g}} \\ \nabla\cdot\mathbf{v} = 0 \\ \mathbf{B}_t + \mathbf{v}\cdot\nabla\mathbf{B} - \mathbf{B}\cdot\nabla\mathbf{v} = \mathrm{Rm}^{-1}\,\Delta\mathbf{B} \\ \nabla\cdot\mathbf{B} = 0, \end{cases} \tag{5.0.10}$$

where $\hat{\mathbf{g}} = \frac{D}{V_0^2}\mathbf{g}$.
Restricting our analysis to z-dependent laminar solutions, i.e. non-dimensional

solutions of the form

$$\mathbf{v}(z) = (v_1, v_2, v_3) = (U(z), 0, 0), \quad \mathbf{B}(z) = (B_1, B_2, B_3) = (B(z), 0, 1), \tag{5.0.11}$$

we obtain from eq. (5.0.10)$_3$ that

$$v_i \mathbf{e}_i \frac{\partial B_j}{\partial x_k} \mathbf{e}_k \mathbf{e}_j - B_i \mathbf{e}_i \frac{\partial v_j}{\partial x_k} \mathbf{e}_k \mathbf{e}_j = \mathrm{Rm}^{-1} \frac{\partial^2 B_j}{\partial x_k^2} \mathbf{e}_i \Rightarrow \tag{5.0.12}$$

$$\Rightarrow v_i \frac{\partial B_j}{\partial x_k} \delta_{ik} \mathbf{e}_j - B_i \frac{\partial v_j}{\partial x_k} \delta_{ik} \mathbf{e}_j = \mathrm{Rm}^{-1} \frac{\partial^2 B_j}{\partial x_k^2} \mathbf{e}_i \Rightarrow \tag{5.0.13}$$

$$\Rightarrow v_i \frac{\partial B_j}{\partial x_i} \mathbf{e}_j - B_i \frac{\partial v_j}{\partial x_i} \mathbf{e}_j = \mathrm{Rm}^{-1} \frac{\partial^2 B_j}{\partial x_k^2} \mathbf{e}_i \Rightarrow \tag{5.0.14}$$

$$\Rightarrow \begin{array}{l} (v_i \dfrac{\partial B_1}{\partial x_i}, v_i \dfrac{\cancel{\partial B_2}}{\cancel{\partial x_i}}, v_i \dfrac{\cancel{\partial B_3}}{\cancel{\partial x_i}}) - (B_i \dfrac{\partial v_1}{\partial x_i}, B_i \dfrac{\cancel{\partial v_2}}{\cancel{\partial x_i}}, B_i \dfrac{\cancel{\partial v_3}}{\cancel{\partial x_i}}) = \\ = \mathrm{Rm}^{-1} (\Delta B_1, \cancel{\Delta B_2}, \cancel{\Delta B_3}) \end{array} \Rightarrow \tag{5.0.15}$$

$$\Rightarrow \begin{array}{l} (v_1 \dfrac{\cancel{\partial B_1}}{\cancel{\partial x}} + \cancel{v_2} \dfrac{\cancel{\partial B_1}}{\cancel{\partial y}} + \cancel{v_3} \dfrac{\partial B_1}{\partial z}, 0, 0) - (B_1 \dfrac{\cancel{\partial v_1}}{\cancel{\partial x}} + \cancel{B_2} \dfrac{\cancel{\partial v_1}}{\cancel{\partial y}} + B_3 \dfrac{\partial v_1}{\partial z}, 0, 0) = \\ = \mathrm{Rm}^{-1} (B''(z), 0, 0) \Rightarrow \end{array} \tag{5.0.16}$$

$$\Rightarrow (0, 0, 0) - (U'(z), 0, 0) = \mathrm{Rm}^{-1} (B''(z), 0, 0) \Rightarrow \tag{5.0.17}$$

$$\Rightarrow B''(z) = -\mathrm{Rm}\, U'(z). \tag{5.0.18}$$

Integrating, we have $B'(z) = -\mathrm{Rm}\,(U(z) + a_1/\mathrm{Ha}^2)$, with a_1 an integrating constant. Substituting in eq. (5.0.10)$_1$, we obtain that:

$$v_i \mathbf{e}_i \frac{\partial v_j}{\partial x_k} \mathbf{e}_k \mathbf{e}_j = \mathrm{Ha}^2 \mathrm{Re}^{-1} \mathrm{Rm}^{-1} B_i \mathbf{e}_i \frac{\partial B_j}{\partial x_k} \mathbf{e}_k \mathbf{e}_j - \Pi_i \mathbf{e}_i + \mathrm{Re}^{-1} \nabla^2 v_i \mathbf{e}_i + \hat{\mathbf{g}} \Rightarrow \tag{5.0.19}$$

$$\Rightarrow 0 = 0 - (\Pi_x, \Pi_y, \Pi_z) + \mathrm{Re}^{-1} (U''(z), 0, 0) + (\hat{g} \sin\beta, 0, -\hat{g} \cos\beta). \tag{5.0.20}$$

From the second component of the latter equation we deduce that $\Pi(x, y, z) = \Pi(x, z)$, and from the third component we deduce that

$$\Pi(x, z) = -\hat{g} \cos\beta z + \Pi_1(x). \tag{5.0.21}$$

Finally, from the first component we deduce that:

$$\mathrm{Re}\, \Pi_{1_x}(x) = -\mathrm{Ha}^2 U(z) + U''(z) - a_1 + \mathrm{Re}\, \hat{g} \sin\beta. \tag{5.0.22}$$

The left side of eq. (5.0.22) only depends on x, while the right side depends only on z. This means that the two sides of eq. (5.0.22) are equal to a constant, that is, there exists a constant b_1 such that:

$$\begin{cases} \mathrm{Re}\,\Pi_{1_x} \equiv b_1 \\ U''(z) - \mathrm{Ha}^2 U(z) = a_1 + b_1 - \mathrm{Re}\,\hat{g}\sin\beta. \end{cases} \tag{5.0.23}$$

The solutions of this second order, non homogeneous, differential equation are:

$$U(z) = u_1\cosh(\mathrm{Ha}\,z) + u_2\sinh(\mathrm{Ha}\,z) - \frac{a_1 + b_1 - \mathrm{Re}\,\hat{g}\sin\beta}{\mathrm{Ha}^2}, \tag{5.0.24}$$

and hence, as $B'(z) = -\mathrm{Rm}\,(U(z) + a_1/\mathrm{Ha}^2)$,

$$B(z) = -\frac{\mathrm{Rm}}{\mathrm{Ha}}\left(u_1\sinh(\mathrm{Ha}\,z) + u_2\cosh(\mathrm{Ha}\,z) - \frac{b_1 - \mathrm{Re}\,\hat{g}\sin\beta}{\mathrm{Ha}}z + \frac{c_1}{\mathrm{Ha}}\right), \tag{5.0.25}$$

where u_1, u_2 and c_1 are constants of integration.

These solutions are called Hartmann solutions.

Now we choose the reference velocity V_0 and the Reynolds number

$$\mathrm{Re} = \frac{V_0 d}{\nu}, \tag{5.0.26}$$

with

$$V_0 = \frac{2gd^2\sin\beta}{\nu}. \tag{5.0.27}$$

This means that the reference speed V_0 is equal to $\bar{U}(d)$ where $\bar{U}(d)$ is the speed evaluated in d when there is not a magnetic field (cf. Falsaperla et al. 2022c, eq. (5)).

Note that with this choice we have:

$$\mathrm{Re}\,\hat{g}\sin\beta = \frac{1}{2}. \tag{5.0.28}$$

We choose boundary conditions for Hartmann flows which are appropriate to the open channel. They correspond to rigid conditions for the kinetic field at the boundary $z = -1$, stress-free conditions for the kinetic field at the boundary $z = 1$. Moreover we assume that the boundaries are non-conducting. Therefore, we have:

$$\left.\frac{\partial U}{\partial z}\right|_{z=1} = U(-1) = 0, \qquad B(-1) = B(1) = 0. \tag{5.0.29}$$

By assuming that there is no gradient of pressure along the x axis, we have $b_1 = 0$. Substituting (5.0.29) in (5.0.24), (5.0.25), we obtain

$$\Rightarrow \begin{cases} u_1 = -\dfrac{1}{2\mathrm{Ha}\sinh(\mathrm{Ha})} \\ u_2 = -u_1\dfrac{\sinh(\mathrm{Ha})}{\cosh(\mathrm{Ha})} = \dfrac{1}{2\mathrm{Ha}\cosh(\mathrm{Ha})} \\ a_1 = \mathrm{Ha}^2(u_1\cosh(\mathrm{Ha}) - u_2\sinh(\mathrm{Ha})) + \dfrac{1}{2} = \\ \quad = -\mathrm{Ha}\dfrac{1}{2}\Big(\dfrac{\cosh(\mathrm{Ha})}{\sinh(\mathrm{Ha})} + \dfrac{\sinh(\mathrm{Ha})}{\cosh(\mathrm{Ha})}\Big) + \dfrac{1}{2} \\ b_1 = 0, \quad c_1 = -\dfrac{1}{2}. \end{cases} \tag{5.0.30}$$

From this it follows

$$U(z) = \frac{1}{2}\left[\frac{\sinh(\mathrm{Ha}z) + \sinh(\mathrm{Ha})}{\mathrm{Ha}\cosh(\mathrm{Ha})} + \frac{\cosh(\mathrm{Ha}) - \cosh(\mathrm{Ha}z)}{\mathrm{Ha}\sinh(\mathrm{Ha})}\right]$$

and

$$B(z) = \frac{\mathrm{Rm}}{2\mathrm{Ha}}\left[\frac{\sinh(\mathrm{Ha}z)}{\mathrm{Ha}\sinh(\mathrm{Ha})} - \frac{\cosh(\mathrm{Ha}z)}{\mathrm{Ha}\cosh(\mathrm{Ha})} + \frac{1-z}{\mathrm{Ha}}\right].$$

Chapter 6

Spectral methods

Since spectral methods are fundamental both for the study of linearized equations and for the study of Euler-Lagrange equations related to the Lyapunov energy method, in this section we recall spectral methods in general and then we focus on one of them, namely the Chebychev collocation method, the one we adopted.
The term “spectral methods" (see Schlatter, 2009) refers to methods which are based on an expansion of the solution as a finite sum of basis functions that are multiplied by coefficients. The collocation methods are a special case of spectral methods in which collocation nodes are chosen and it is imposed that the differential equation is satisfied exactly on these points. Chebychev collocation methods use Chebychev polynomials as basis functions. The latter will be the ones to which we will refer.
Spectral methods are generally global methods which means, for example, that the derivative in a certain point depends on the solution in all the other points of the space and not only on that in the “nearby points". From this it follows that spectral methods are high-order methods: they have exponential convergence, contrary to finite-difference methods which have polynomial convergence. This makes these methods better than finite difference methods, however they are less flexible than finite difference methods and difficulties may arise in the presence of shocks or discontinuities for example. However, for certain problems, such as those related to fluid dynamics, it has been been proved that they are the best choice because the fact that they have a high order of accuracy implies that an accurate solution can be obtained with a not too large number of basis functions.

6.1 Basic principle

Suppose we want to find the solution $u(x)$ of the partial differential equation:

$$P[u] = 0, \tag{6.1.1}$$

in a domain D and with the boundary conditions $B(u) = 0$. We approximate the solution with a finite sum of functions:

$$u_N(x) = \sum_{k=0}^{N} a_k \cdot \phi_k(x). \tag{6.1.2}$$

The functions $\phi_k(x)$ are called basis functions and a_k are their coefficients.
If we put (6.1.2) in (6.1.1) we obtain the residual, defined as:

$$R(x) := P(u_N(x)). \tag{6.1.3}$$

To determine the $N+1$ coefficients a_k, the method of weighted residuals is used: the residual $R(x)$ multiplied by the $N+1$ test functions $w_j(x)$, which will be described in the next section, and integrated over the domain D must be zero, that is:

$$\int_D w_j(x) \cdot R(x) dx = 0, \qquad j = 0, \ldots, N, \tag{6.1.4}$$

or written using the scalar product $(f, g) = \int_D f \cdot g dx$

$$(R, w_j) = 0, \qquad j = 0, \ldots, N.$$

This means that the residual R is required to be orthogonal to all test functions (weights) w_j.
If there is time dependence, an initial condition is added on $u(x,t)$, the coefficients a_k will be of the type $a_k(t)$ and the residuals $R(x)$ will be of the type $R(x,t)$.

6.2 Choice of the test functions

There are several methods to choose the test functions. The most common approaches are the Galerkin method and the collocation method. There are other methods as well, such as the tau method and the Petrov-Galerkin method.

Galerkin method: after the choice of the basic functions $\phi_k(x)$, one has to require that:

$$\phi_j = w_j, \qquad j = 0, \ldots, N. \tag{6.2.1}$$

Collocation method: a set of $N+1$ collocation nodes in the domain D is chosen such that the residual R is zero on the nodes, that is:

$$R(x_j) = 0, \qquad j = 0, \ldots, N. \tag{6.2.2}$$

The consequence of this is that the PDE is satisfied in the collocation nodes, $P(u_N) = 0$ in $x = x_j$. Therefore the test functions become:

$$w_j = \delta(x - x_j), \qquad j = 0, \ldots, N, \tag{6.2.3}$$

where δ is the Dirac delta function

$$\delta(x) = \begin{cases} +\infty, & \text{for} \quad x = 0 \\ 0, & \text{otherwise.} \end{cases}$$

6.3 Choice of the basis functions

The basis functions are regular functions defined throughout the domain D. Several choices are possible, for example, Fourier functions or Chebychev or Legendre polynomials.
The approach using Fourier functions gives rise to Fourier series which are useful for problems with periodic boundary conditions. For problems with non-periodic boundary conditions, on the other hand, it is preferable to consider orthogonal polynomials such as Chebychev polynomials as basis functions.

Chebychev polynomials: the Chebychev polynomials are defined in the interval $[-1, 1]$ in the following way:

$$T_k(x) = \cos(k \arccos x), \qquad k = 0, 1, 2, \ldots \tag{6.3.1}$$

A function $u(x)$ is approximated with a finite series of Chebychev polynomials such that:

$$u_N(x) = \sum_{k=0}^{N} a_k T_k(x), \tag{6.3.2}$$

where a_k are the Chebychev coefficients.

6.4 Chebychev collocation method

The Chebychev collocation method is, therefore, a spectral method in which the function $u(x)$ is approximated with a finite series of Chebychev polynomials, and a set of nodes in which the PDE is satisfied is considered (collocation). A common distribution of nodes for Chebychev polynomials is the one given by the Gauss-Lobatto points:

$$x_j = \cos(\pi \frac{j}{N}), \qquad j = 0, ..., N. \tag{6.4.1}$$

Chapter 7

Results for classical Couette and Poiseuille flows

The stability and instability of the classical laminar flows of an incompressible fluid have been studied analytically, numerically and with experiments (see Poiseuille, 1843, Reynolds, 1883, Couette, 1890, Orr, 1907, Sommerfeld, 1908, Squire, 1933, Joseph, 1968, Joseph and Carmi, 1969, Busse, 1972, Romanov, 1973, Joseph, 1976, Falsaperla et al. 2019b).

The current problem with the object of study is the transition from laminar flows to instability, turbulence and chaos. It is not completely understood and there are some discrepancies (see Fig. 1.1) between the critical Reynolds numbers of linear and nonlinear analysis and the experiments (also called "paradox" in Galdi and Rionero, 1985, pag. 7).

Firstly we recall the definitions of two particular classes of perturbations, i.e the streamwise and the spanwise perturbations, as we will refear to them in the discussions that follow.

Definition 7.0.1. *We define streamwise (or longitudinal) perturbations the perturbations* $\mathbf{u}, p$ *which do not depend on* x.

Definition 7.0.2. *We define spanwise (or transverse) perturbations the perturbations* $\mathbf{u}, p$ *which do not depend on* y.

Secondly we recall some classical results:
a) For the linear perturbation system, the Squire theorem holds (Squire, 1933): the least stabilizing perturbations are the two-dimensional spanwise perturbations (see Drazin and Reid, 2004, p. 129);

b_1) *plane Poiseuille flow* is *unstable* for $\mathrm{Re} > 5772$ (Orszag, 1971) and the critical Reynolds number is obtained on the spanwise perturbations;

b_2) *plane Couette flow* is *linearly stable for any* Reynolds numbers (Romanov, 1973);

c) in laboratory experiments plane Poiseuille flows undergo transition to three-dimensional turbulence for Reynolds numbers on the order of 1000. In the case of plane Couette flow the lowest Reynolds numbers at which turbulence can be produced and sustained have been shown to be between 300 and 450 both in the numerical simulations and in the experiments (see Barkley and Tuckerman, 2007, Prigent et al., 2003);

d) nonlinear monotonic L_2*-energy stability* has been proved for Reynolds numbers Re below some critical nonlinear value Re_E which is of the order 10^2. In particular Joseph, 1968, 1976 proved that $\mathrm{Re_E} = \mathrm{Re}^y = 20.65$ for plane Couette flow, and Joseph and Carmi, 1969 proved that $\mathrm{Re_E} = \mathrm{Re}^y = 49.55$ for plane Poiseuille flow. Orr proved instead that $\mathrm{Re_E} = \mathrm{Re}^x = 44.3$ for plane Couette flow and $\mathrm{Re_E} = \mathrm{Re}^x = 87.6$

for plane Poiseuille flow.
With the symbol Re^y we mean the critical Reynolds value for streamwise perturbations, and Re^x is the critical Reynolds value for spanwise perturbations.

Therefore for the classical laminar flows of Couette and Poiseuille the situation described in Fig. 1.1 occurs. Falsaperla et al. 2019b partially solved this paradox by studying the tilted perturbations. This idea came from some experiments and from numerical studies.

Prigent et al., 2003 made experiments at the CEA-Sanclay Centre to study, by decreasing the Reynolds number, the reverse transition from the turbulent to the laminar flow. They observed "a continuous transition towards a regular pattern made of periodically spaced, inclined stripes of well-defined width and alternating turbulence strength ...". "For lower Re, a regular pattern is eventually reached after a transient during which domains, separated by wandering fronts, compete. The oblique stripes have a wavelength of the order of 50 times the gap. The pattern is stationary in the plane Couette flow case... The pattern was observed for $340 < \mathrm{Re} < 415$ in the plane Couette flow" (see Fig. 7.1).

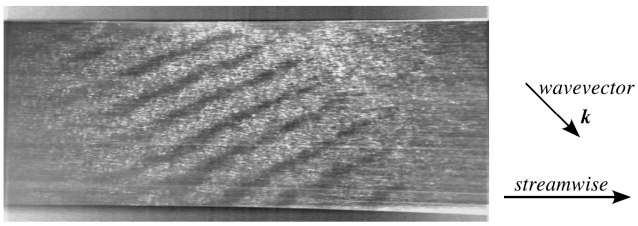

FIGURE 7.1: Photograph of a turbulent-laminar pattern in plane Couette flow from the Saclay experiment. Light regions correspond to turbulent flow and dark regions to laminar flow. The striped pattern of alternating laminar and turbulent flow forms with a wavevector k oblique to the streamwise direction. The wavelength is approximately 40 times the half-gap between the moving walls. The lateral dimensions are 770 by 340 half-gaps and the Reynolds number is Re = 385.

Source: Barkley and Tuckerman Barkley and Tuckerman, 2007

Barkley and Tuckerman, 1999, 2005, 2007, studied numerically a turbulent-laminar banded pattern in plane Couette flow which is statistically steady and is oriented obliquely to the streamwise direction with a very large wavelength relative to the gap. They wrote: "Regimes computed for a full range of angle and Reynolds number in a tilted rectangular periodic computational domain are presented ... The unusual but key feature of our study of turbulent-laminar patterns is the use of simulation domains aligned with the pattern wave vector and thus tilted relative to the streamwise-spanwise directions of the flow." For their numerical simulations they are guided by the experiments of Prigent et al., 2003.

Falsaperla et al. 2019b proved that the plane Couette and Poiseuille flows are nonlinearly stable if the Reynolds number is less then

$$\bar{R}_\theta(\lambda) = \frac{1}{\sin\theta}\mathrm{Re}_{Orr}\left(\frac{2\pi}{\lambda\sin\theta}\right), \tag{7.0.1}$$

when a perturbation is a tilted perturbation which forms an angle $\theta \in (0, \pi/2]$

with the direction of the basic motion. Re_{Orr} is the critical Orr-Reynolds number for spanwise perturbations which is computed for wave number $2\pi/(\lambda \sin\theta)$, λ being any positive wavelength. By taking the minimum with respect to λ they obtained the critical energy Reynolds number for a fixed inclination angle and any wavelength: for plane Couette flow it is $\mathrm{Re}_{Orr} = 44.3/\sin\theta$ and for plane Poiseuille flow it is $\mathrm{Re}_{Orr} = 87.6/\sin\theta$ (in particular, for $\theta = \pi/2$ we have the classical values $\mathrm{Re}_{Orr} = 44.3$ for plane Couette flow and $\mathrm{Re}_{Orr} = 87.6$ for plane Poiseuille flow).
These results improve those obtained by Joseph, who found for streamwise perturbations a critical nonlinear value of 20.65 in the plane Couette case, and those obtained by Joseph and Carmi who found the value 49.55 for plane Poiseuille flow for streamwise perturbations. For fixed wavelengths taken from the experimental data and the numerical simulations, the critical Reynolds numbers obtained are in a very good agreement both with the experiments and the numerical simulations.

For instance, if we consider the case of the experiments of Prigent et al., 2003 (see also Fig. 29 of Barkley and Tuckerman, 2007), we have:

i) $\theta = 25°$, $\lambda = 46$, experimental Reynolds number is about 395, Falsaperla et al. 2019b obtain approximately $\bar{R} = 369$

ii) $\theta = 26°$, $\lambda = 48$, experimental Reynolds number is about 385, Falsaperla et al. 2019b obtain approximately $\bar{R} = 383$

iii) $\theta = 27,5°$, $\lambda = 51$, experimental Reynolds number is about 375, Falsaperla et al. 2019b obtain approximately $\bar{R} = 404$

iv) in the simulation of Barkley and Tuckerman, 2007 $\theta = 24°$, $\lambda = 40$, Reynolds number is about 350, Falsaperla et al. 2019b obtain approximately $\bar{R} = 325$

v) $\theta = 30°$, $\lambda = 57$, experimental Reynolds number is about 350, Falsaperla et al. 2019b obtain approximately $\bar{R} = 450$ and $R = 398$ in Barkley and Tuckerman, 2007.

The study presented by Falsaperla et al. 2019b was then extended by them in 2020b to laminar flows down an open inclined channel (particular case of the flow described in Sec. 5) and in 2020a to laminar flows between horizontal planes subjected to a magnetic field with a component in the direction of the flow and a constant component orthogonal to the layer (see Sec. 4).

The starting point of my phd work was the study of a flow given by the combination of the flows studied by Falsaperla et al. 2020a,b as described in the following Section. In particular the idea was to focus on the analysis of tilted perturbation also in the more general case of an inclined channel where an electroconductive fluid flows.

Chapter 8

Stability of Hartmann shear flows in an open inclined channel

The results presented in this Section have been published by Falsaperla, Mulone, and Perrone, 2022c.

8.1 Summary

We study the stability of laminar flows in a sheet of fluid (open channel) down an incline with constant slope angle $\beta \in (0, \pi/2)$ assuming that the fluid is electrically conducting and subjected to a magnetic field as described in Sec. 5. We study the local (linear) stability and instability, and we obtain critical Reynolds numbers for the onset of instability by solving a generalised Sommerfeld equation. We also study the nonlinear Lyapunov stability by solving the Orr equation for the associated maximum problem of the Reynolds-Orr energy equation. As in Falsaperla et al. 2019b we finally study the nonlinear stability of tilted rolls. The critical Reynolds numbers we obtain allow us to determine, for every inclination angle β, the critical velocity.

8.2 State of the art

Stationary flows of electrically conducting fluids with an imposed magnetic field play an important role in many applications, for instance in geophysics, astrophysics, e.g. when dealing with solar winds, industry, biology, metallurgy, biofilms, and medicine, see Ferraro and Plumpton, 1961, Kakutani, 1964, Takashima, 1996, 1998, Davidson, 2001, Alexakis et al., 2003, Falsaperla et al. 2016, 2017, 2017, 2020a, Falsaperla, Mulone, and Perrone, 2022c.
One of the first applications of laminar flows of a liquid in the presence of a magnetic field was done by Michael Faraday. He tried in 1832 to measure the potential difference between each side of the two river-banks of the Waterloo bridge in London caused by the ebbing salt water flowing that interacts with the Earth's magnetic field (Faraday, 1839, p. 55).
Many research papers have been devoted to the study of stability of an electroconducting fluid at rest confined in a horizontal layer between two parallel planes. If the layer is heated from below, we have the magnetic Bénard problem. This problem has been studied by many authors both in the linear case, see for instance the book of Chandrasekhar, 1981, and in the nonlinear case Rionero, 1967 - Mulone and Rionero, 2003.
When the basic motion is not the rest, like laminar flows, many theoretical and experimental studies have been done after the experiments of Hartmann, see Hartmann,

1937, Alboussière and Lingwood, 2000, Alexakis et al., 2003. Usually, the fluid is confined in a horizontal layer bounded by to rigid parallel boundaries, see Falsaperla et al. 2020a; 2016, 2017; 2017. Some experimental and computational results obtained for flows in pipes, ducts and channels in the presence of a magnetic field are reviewed by Zikanov et al., 2014.
Sometimes, in the applications (geophysical studies, and materials processing), laminar flows in a sheet of fluid (open channel) down an incline with constant slope angle β must be considered. Falsaperla et al., 2016 investigated analytical solutions of stationary laminar flows of an inclined layer filled with a hydromagnetic fluid heated from below and subjected to the gravity field. Falsaperla et al., 2017 studied the linear instability and nonlinear stability of some of the above solutions. The inclined layer is bounded by two rigid non-conducting planes heated from below. An energy norm has been used, the Euler-Lagrange equations have been written but not solved. Only sufficient nonlinear stability conditions have been given. Other stability conditions have been considered by Xu, 2020.
The problem of stability for classical Couette and Poiseuille flows, in a horizontal layer, has been studied for many years. In the previous section we have said that recently, Falsaperla et al. 2019b obtained values for “critical" linear and nonlinear energy Reynolds number (see Reynolds, 1883) which are in good agreement with the experiments of Prigent et al., 2003 and with the numerical simulation of Barkley and Tuckerman, 2007. Falsaperla et al. 2020a have generalised these results for a fluid which is electrically conducting and subjected to a magnetic field. The stability of the stationary magnetic Couette and Hartmann flows has been investigated and it has been proved that such flows are nonlinearly stable if the Reynolds number Re is less then

$$\bar{R}_\theta = \mathrm{Re}_{Orr}^{(m)}(2\pi/(\lambda \sin\theta))/\sin\theta.$$

In the expression above $\mathrm{Re}_{Orr}^{(m)}(\mu)$ is the magnetic Orr-Reynolds number evaluated at the wavenumber $\mu = 2\pi/(\lambda \sin\theta)$, where λ is the wavelength of the perturbation (see Falsaperla et al. Falsaperla, Giacobbe, and Mulone, 2020a).
Here we reconsider the paper by Falsaperla et al., 2017 with the method introduced in 2019b, 2020a, and study the more realistic physical case of Hartmann flow in an open channel down an incline with constant slope angle $\beta \in (0, \pi/2)$.
We investigate local stability and instability of the basic laminar flow (Hartmann flow) with the Chebyshev collocation method, for many different values of the magnetic Prandtl number and Hartmann number, by solving the generalised Sommerfeld equations. The more relevant result we obtain is that, below a critical value of the Hartmann number depending on Pm, the flow is linearly stable for any Reynolds number.
We study nonlinear stability of the Hartmann flow by the Lyapunov energy method. We achieve optimal nonlinear stability conditions by solving the generalised Orr equation obtained with the Euler-Lagrange equations of the related maximum variational problem. We also study stability with respect to tilted perturbations, which are the more appropriate for flows at the onset of turbulence, (see Falsaperla et al. Falsaperla, Giacobbe, and Mulone, 2019b), and generalise to MHD the results by Falsaperla et al. 2020a.
The plan of the paper is the following. In Sec. 8.3 we introduce the basic motion and the perturbation equations.
In Sec. 8.4 we give conditions of local (linear) stability and instability by using the Chebyshev collocation method, in the limit case $\mathrm{Pm} \to 0$ and in the general case

Pm >0. We check, for Pm >0, that the less stabilizing perturbations at the onset of instability are the spanwise perturbations. We show our results in Figs. 8.1-8.4.
In Sec. 8.5, by assuming that the less stabilizing perturbations for the onset of instability are two-dimensional, we study the nonlinear stability of the laminar flow with respect to streamwise perturbations and prove that they are always stabilizing for any Reynolds, Prandtl and Hartmann numbers. Moreover, we study the nonlinear stability with respect to tilted perturbations of an angle θ with the direction of motion and prove that they are nonlinearly exponentially stable for any Reynolds number less than a critical value $\bar{R}_\theta$ which depends on the tilted angle θ.
Sec. 8.6 is dedicated to the discussion of the results.

8.3 Basic motion and perturbation equations

The adimensional equations of the magnetohydrodynamics (MHD) system are those given by (5.0.10).

In Sec. 5 we have proved that:

Theorem 8.3.1. *The basic solution of system* (5.0.10) *for the Hartmann flow down an inclined open channel, with boundary conditions* (5.0.29)*, is given by* $(U(z),0,0)$, $(\bar{B}(z)=\mathrm{Rm}^{-1}B(z),0,\mathrm{Rm}^{-1})$ *where*

$$U(z)=\frac{1}{2}\left[\frac{\sinh(\mathrm{Ha}z)+\sinh(\mathrm{Ha})}{\mathrm{Ha}\cosh(\mathrm{Ha})}+\frac{\cosh(\mathrm{Ha})-\cosh(\mathrm{Ha}z)}{\mathrm{Ha}\sinh(\mathrm{Ha})}\right] \tag{8.3.1}$$

and

$$\bar{B}(z)=\frac{1}{2\mathrm{Ha}}\left[\frac{\sinh(\mathrm{Ha}z)}{\mathrm{Ha}\sinh(\mathrm{Ha})}-\frac{\cosh(\mathrm{Ha}z)}{\mathrm{Ha}\cosh(\mathrm{Ha})}+\frac{1-z}{\mathrm{Ha}}\right], \tag{8.3.2}$$

with $z\in[-1,1]$. *This solution must be completed with the pressure* Π *given by* (5.0.21), (5.0.22), (5.0.23).

Now, we plan to investigate linear and nonlinear stability of the basic solution (8.3.1)-(8.3.2). To this end we consider a perturbation to the stationary solution:

$$\mathbf{v}+\mathbf{u}=(U(z),0,0)+(u,v,w),\quad \bar{\mathbf{B}}+\mathbf{h}=(\bar{B}(z),0,\mathrm{Rm}^{-1})+(h,k,\ell),\quad \Pi+\bar{\pi},$$

with $\mathbf{u}$, $\mathbf{h}$ and $\bar{\pi}$ regular functions depending on x,y,z,t.
Introducing the quantity

$$A=\mathrm{Ha}^2\,\mathrm{Re}^{-1}\mathrm{Rm}=\mathrm{N}\,\mathrm{Rm}=\mathrm{Ha}^2\,\mathrm{Pm},$$

the equations which govern the evolution of the "difference fields" $\mathbf{u}$, $\mathbf{h}$, $\bar{\pi}$ are:

$$\begin{cases}\mathbf{u}_t+U(z)\mathbf{u}_x+U'(z)w\mathbf{i}+\mathbf{u}\cdot\nabla\mathbf{u}=A[\bar{B}(z)\mathbf{h}_x+\mathrm{Rm}^{-1}\mathbf{h}_z+\\ \qquad\qquad +\bar{B}'(z)\ell\mathbf{i}+\mathbf{h}\cdot\nabla\mathbf{h}]-\nabla\bar{\pi}+\mathrm{Re}^{-1}\Delta\mathbf{u}\\ \mathbf{h}_t+\bar{B}'(z)w\mathbf{i}+U(z)\mathbf{h}_x+\mathbf{u}\cdot\nabla\mathbf{h}-\bar{B}(z)\mathbf{u}_x-\mathrm{Rm}^{-1}\mathbf{u}_z-U'(z)\ell\mathbf{i}-\mathbf{h}\cdot\nabla\mathbf{u}=\mathrm{Rm}^{-1}\Delta\mathbf{h}\\ \nabla\cdot\mathbf{u}=0,\qquad \nabla\cdot\mathbf{h}=0\,.\end{cases} \tag{8.3.3}$$

The boundary conditions for $\mathbf{u}, \mathbf{h}$ are rigid conditions, $u = v = w = 0$ and non-conducting conditions $h = k = \ell = 0$ on the bottom of the layer $z = -1$, and stress-free conditions $u_z = v_z = w = 0$ and non-conducting conditions $h = k = \ell = 0$ on the top plane $z = 1$:

$$\begin{cases} u = v = w = 0, & h = k = \ell = 0 \quad \text{on} \quad z = -1, \\ u_z = v_z = w = 0, & h = k = \ell = 0 \quad \text{on} \quad z = 1\,. \end{cases} \tag{8.3.4}$$

8.4 Local (linear) stability and instability

In this section we study the local stability and the instability of the shear Hartmann flow. Linearising eq. (8.3.3), we obtain:

$$\begin{cases} \mathbf{u}_t + U\mathbf{u}_x + U'w\mathbf{i} = A[\bar{B}\mathbf{h}_x + \mathrm{Rm}^{-1}\mathbf{h}_z + \bar{B}'\ell\mathbf{i}] - \nabla\bar{\pi} + \mathrm{Re}^{-1}\Delta\mathbf{u} \\ \mathbf{h}_t + \bar{B}'w\mathbf{i} + U\mathbf{h}_x - \bar{B}\mathbf{u}_x - \mathrm{Rm}^{-1}\mathbf{u}_z - U'\ell\mathbf{i} = \mathrm{Rm}^{-1}\Delta\mathbf{h} \\ \nabla\cdot\mathbf{u} = 0, \quad \nabla\cdot\mathbf{h} = 0\,. \end{cases} \tag{8.4.1}$$

Since the system is autonomous, we consider solutions of the form (cf. Straughan, 2004):

$$f(x, y, z, t) = f(z)e^{i(ax+by)+act}\,, \tag{8.4.2}$$

with $f = u, v, w, h, k, \ell$ or $\bar{\pi}$, in the domain $\mathbb{R}^2 \times (-1, 1) \times (0, +\infty)$, $a \geq 0$, $b \geq 0$, and c is a complex number. By substituting (8.4.2) in (8.4.1), we have the system:

$$\begin{cases} ac\mathbf{u} + iaU\mathbf{u} + U'w\mathbf{i} = A(ia\bar{B}\mathbf{h} + \mathrm{Rm}^{-1}\mathbf{h}_z + \bar{B}'\ell\mathbf{i}) - \nabla\bar{\pi} + \mathrm{Re}^{-1}\Delta\mathbf{u} \\ ac\mathbf{h} + \bar{B}'w\mathbf{i} + iaU\mathbf{h} - ia\bar{B}\mathbf{u} - \mathrm{Rm}^{-1}\mathbf{u}_z - U'\ell\mathbf{i} = \mathrm{Rm}^{-1}\Delta\mathbf{h} \\ \nabla\cdot\mathbf{u} = 0, \quad \nabla\cdot\mathbf{h} = 0. \end{cases} \tag{8.4.3}$$

By writing system (8.4.3) in components, we have:

$$\begin{cases} acu + iaUu + U'w = A(iaBh + \mathrm{Rm}^{-1}Dh + \bar{B}'\ell) + \\ \qquad\qquad + \mathrm{Re}^{-1}(D^2 - (a^2 + b^2))u - ia\bar{\pi} \\ acv + iaUv = A(iaBk + \mathrm{Rm}^{-1}Dk) + Re^{-1}(D^2 - (a^2 + b^2))v - ib\bar{\pi} \\ acw + iaUw = A(iaB\ell + \mathrm{Rm}^{-1}D\ell) + Re^{-1}(D^2 - (a^2 + b^2))w - D\bar{\pi} \\ ach + w\bar{B}' + iaUh - iaBu - \mathrm{Rm}^{-1}Du - \ell U' = \mathrm{Rm}^{-1}(D^2 - (a^2 + b^2))h \\ ack + iaUk - iaBv - \mathrm{Rm}^{-1}Dv = \mathrm{Rm}^{-1}(D^2 - (a^2 + b^2))k \\ ac\ell + iaU\ell - iaBw - \mathrm{Rm}^{-1}Dw = \mathrm{Rm}^{-1}(D^2 - (a^2 + b^2))\ell \\ iau + ibv + Dw = 0, \quad iah + ibk + D\ell = 0\,, \end{cases} \tag{8.4.4}$$

where D and D^2 indicate first and second derivatives with respect to z. The Squire transformation is:

$$\begin{aligned} &\tilde{a} = (a^2 + b^2)^{1/2},\ \tilde{c} = c,\ \tilde{a}\tilde{u} = au + bv,\ \tilde{a}\tilde{h} = ah + bk,\ \tilde{w} = w,\ \tilde{\ell} = \ell, \\ &a\tilde{\bar{\pi}} = \tilde{a}\bar{\pi},\ \tilde{a}\tilde{\mathrm{Re}} = a\mathrm{Re}\,,\ \tilde{\mathrm{Ha}} = \mathrm{Ha},\ \tilde{a}\tilde{\mathrm{Rm}} = a\mathrm{Rm}\,. \end{aligned} \tag{8.4.5}$$

Hunt, 1966 considered coplanar magnetic fields and noted that there is a relation between Re and Rm, and for rigid boundaries and large Hartmann numbers he proved that the Squire theorem (see Squire, 1933) does not hold.
However in our case, as we see below, in the limit case $\mathrm{Pm} \to 0$, it holds (in this case we do not have the last transformation of (8.4.5), cf. also and Takashima, 1996, 1998 and Drazin and Reid, 2004, p. 129). In the limit case $\mathrm{Pm} \to 0$ (that is $\mathrm{Rm} \to 0$) system (8.4.4) becomes:

$$\begin{cases} acu + iaUu + U'w = \mathrm{Ha}^2\mathrm{Re}^{-1}Dh + \mathrm{Re}^{-1}(D^2 - (a^2+b^2))u - ia\bar{\pi} \\ acv + iaUv = \mathrm{Ha}^2\mathrm{Re}^{-1}Dk + Re^{-1}(D^2 - (a^2+b^2))v - ib\bar{\pi} \\ acw + iaUw = \mathrm{Ha}^2\mathrm{Re}^{-1}D\ell + Re^{-1}(D^2 - (a^2+b^2))w - D\bar{\pi} \\ Du = (D^2 - (a^2+b^2))h \\ Dv = (D^2 - (a^2+b^2))k \\ Dw = (D^2 - (a^2+b^2))\ell \\ iau + ibv + Dw = 0, \quad iah + ibk + D\ell = 0\,. \end{cases} \tag{8.4.6}$$

After substituting the Squire transformation into each equation of system (8.4.6), and adding the first and the second equation, and the fourth and the fifth equations, the result is:

$$\begin{cases} \tilde{a}\tilde{c}\tilde{u} + i\tilde{a}U\tilde{u} + U'\tilde{w} = \tilde{\mathrm{H}}\mathrm{a}^2\tilde{\mathrm{R}}\mathrm{e}^{-1}D\tilde{h} + \tilde{\mathrm{R}}\mathrm{e}^{-1}(D^2 - \tilde{a}^2)u - i\tilde{a}\tilde{\bar{\pi}} \\ \tilde{a}\tilde{c}\tilde{w} + i\tilde{a}U\tilde{w} = \tilde{\mathrm{H}}\mathrm{a}^2\tilde{\mathrm{R}}\mathrm{e}^{-1}D\tilde{\ell} + \tilde{\mathrm{R}}\mathrm{e}^{-1}(D^2 - \tilde{a}^2)\tilde{w} - D\tilde{\bar{\pi}} \\ D\tilde{u} = (D^2 - \tilde{a}^2)\tilde{h} \\ D\tilde{w} = (D^2 - \tilde{a}^2)\tilde{\ell} \\ i\tilde{a}\tilde{u} + D\tilde{w} = 0, \quad i\tilde{a}\tilde{h} + D\tilde{\ell} = 0\,. \end{cases} \tag{8.4.7}$$

These equations are the same as (8.4.6) when $b = 0$, $v = 0$ and $\tilde{\mathrm{R}}\mathrm{e}$ replaces Re. "Thus, to each three-dimensional problem there corresponds an equivalent two-dimensional one. Moreover, Squire's transformation shows that the equivalent two-dimensional problem is associate with a *l*ower Reynolds number as $\tilde{a} \geq a$. It follows that, the critical Reynolds number at which the instability starts is reached first by two-dimensional disturbances as Re increases, so we only need to consider a two-dimensional disturbance to determine the minimum Reynolds number for the onset of instability" (Ira M. Cohen, 2007, p. 509). Therefore the following theorem holds:

Theorem 8.4.1. *Assuming that* $\mathrm{Pm} \to 0$, *to obtain the minimum critical linear Reynolds number, for a given Hartmann number* Ha, *it is sufficient to consider only two-dimensional disturbances.*

We note that our numerical calculations show (see Fig. 8.4) that also for $\mathrm{Pm} > 0$ the Squire theorem holds at least for *some values* of the Hartmann number, (cf. also Jédidi et al., 2005.)

We note that for the spanwise perturbations a simple calculation shows that either $v \to 0$ and $k \to 0$ exponentially fast as $t \to \infty$, or $v \equiv 0$ and $k \equiv 0$, see Falsaperla et al. 2020a and Drazin and Reid, 2004.

By taking the third component of the *double-curl* of the first equation in (8.4.3) and the third component of the second equation in (8.4.3), we obtain the system:

$$\begin{cases} (c + i\,a\,U)(D^2 - \alpha^2)w - i\,a\,U''\,w = A[i\,a\,\bar{B}(D^2 - \alpha^2)\ell + \\ +\mathrm{Rm}^{-1}D(D^2 - \alpha^2)\ell) - i\,a\,\bar{B}''\,\ell] + \mathrm{Re}^{-1}(D^4 - 2\alpha^2 D^2 + \alpha^4)w, \\ (c + i\,a\,U)\ell - i\,a\,\bar{B}\,w - \mathrm{Rm}^{-1}Dw = \mathrm{Rm}^{-1}(D^2 - \alpha^2)\ell, \end{cases} \tag{8.4.8}$$

where $\alpha^2 = a^2 + b^2$.
It is not hard to see (cf. Falsaperla, Giacobbe, and Mulone, 2019b and Moffatt, 1990) that the basic motion is always stable with respect to streamwise perturbations. In fact, it is easy to prove (numerically) that the real part of c is always negative, (see also Sec. 8.5 where non linear stability on streamwise perturbations is proved analitically).
In order to obtain the critical linear Reynolds number, as in Falsaperla et al. 2020a, we investigate the stability of the basic solutions with respect to transverse (spanwise) perturbations, that are those corresponding to $b = 0$ and $a \neq 0$ in (8.4.4). From (8.4.8), putting $b = 0$, we obtain the generalised *Sommerfeld equations* (cf. Sommerfeld, 1908, Drazin and Reid, 2004):

$$\begin{cases} (c + i\,a\,U)(D^2 - a^2)w - i\,a\,U''\,w = A[i\,a\,\bar{B}(D^2 - a^2)\ell + \\ +\mathrm{Rm}^{-1}D(D^2 - a^2)\ell - i\,a\,\ell\,\bar{B}''] + \mathrm{Re}^{-1}(D^4 - 2a^2 D^2 + a^4)w, \\ (c + i\,a\,U)\ell - i\,a\,\bar{B}\,w - \mathrm{Rm}^{-1}Dw = \mathrm{Rm}^{-1}(D^2 - a^2)\ell, \end{cases} \tag{8.4.9}$$

with boundary conditions

$$w(-1) = Dw(-1) = \ell(-1) = 0, \quad w(1) = D^2 w(1) = \ell(1) = 0. \tag{8.4.10}$$

We note that these equations are formally equal to those obtained by Falsaperla et al. 2020a, nevertheless the expressions of U and $\bar{B}$ and the boundary conditions are different from those of Falsaperla et al. 2020a, because here we have an open channel.
We recall that $A = \mathrm{Ha}^2\mathrm{Pm}$, this implies that if we fix Ha and Pm we obtain a system which depends only on the parameter Re. We also observe that these equations coincide with those of Takashima, 1996, (2.36)-(2.37), and Takashima, 1998, (2.31)-(2.32) if we put $w = \mathrm{Rm}\,\phi, \quad \ell = \mathrm{Re}\,\psi$.
In order to solve (8.4.9) - (8.4.10), we use the Chebyshev collocation method. We adopt 100 up to 150 Chebyshev polynomials both in the cases $\mathrm{Pm} = 0$ and $\mathrm{Pm} > 0$.
The results we obtain are:
a) In the limit case $\mathrm{Pm} = 0$, from (8.4.9) we have

$$(c + i\,a\,U)(D^2 - a^2)w - i\,a\,U''\,w = \mathrm{Re}^{-1}[(D^2 - a^2)^2 w - \mathrm{Ha}^2 D^2 w]. \tag{8.4.11}$$

In Fig. 8.1, left panel, we show the curve of the critical Reynolds number as a function of the Hartmann number. Each point of the curve corresponds to the real part of c equal to 0, $\mathcal{R}(c) = 0$. We note that below a threshold value of $\mathrm{Ha} = \mathrm{Ha}_0^\star \simeq 3.22890$, the critical Reynolds number diverges and we have always stability (cf. a similar result in Takashima, 1998). The magnetic field is then destabilizing up to Hartmann number $\mathrm{Ha} \simeq 4.106$ ($\mathrm{Re} \simeq 1.24361 \times 10^6$). In the right panel, we show the critical curves in the a$-$Re plane for $\mathrm{Pm} = 0$ and selected values of the Hartmann number. For each value of the Hartmann number the system is unstable inside the

corresponding critical curve. Indeed, by fixing a wavenumber $\bar{a}$, when the vertical line $a = \bar{a}$ intersects the curve in two points $(\bar{a}, \mathrm{Re}_1)$, $(\bar{a}, \mathrm{Re}_2)$, with $\mathrm{Re}_1 < \mathrm{Re}_2$, the perturbation with the wavenumber $\bar{a}$ is destabilizing in the interval $(\mathrm{Re}_1, \mathrm{Re}_2)$.

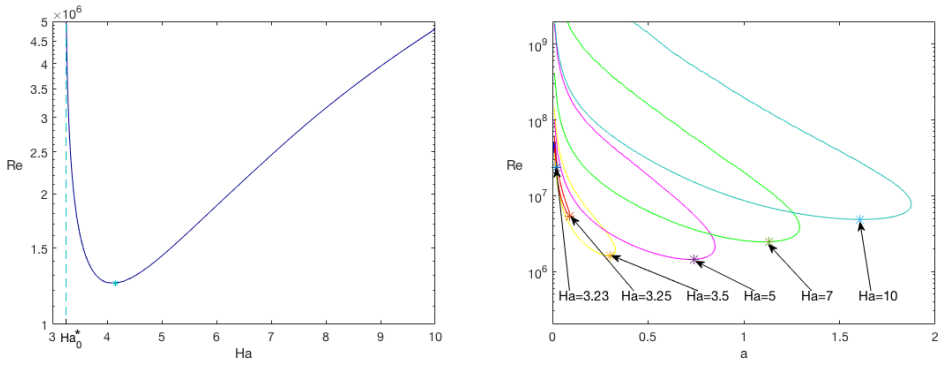

FIGURE 8.1: Left panel: critical Reynolds number versus Hartmann numbers for Pm $= 0$. Right panel: critical curves in the a$-$Re plane for Pm $= 0$ and selected values of the Hartmann number. The arrows point to the minima of each curve.

We note that contrary to the behaviour of other systems, see Falsaperla et al. 2016, 2017, 2019a, where an instability region is bounded and it disappears contracting in a point, here we have instability regions which are unbounded and disappear at infinity (see right panel of Fig. 8.3, for a detail of this phenomenon for Pm > 0).
b) In Fig. 8.2, in the left panel we show the critical Reynolds number versus Hartmann number for different Prandtl numbers. We observe that the curves diverge at some value $\mathrm{Ha}^\star(\mathrm{Pm})$ of the Hartmann number. For very small values of Pm the threshold value $\mathrm{Ha}^\star(\mathrm{Pm})$ decreases, and we find $\mathrm{Ha}^\star(10^{-6}) = 3.22889$, $\mathrm{Ha}^\star(10^{-5}) = 3.22871$, $\mathrm{Ha}^\star(10^{-4}) = 3.22845$ (cf. with $\mathrm{Ha}^\star(0) = \mathrm{Ha}_0^\star = 3.22890$). For larger values of Pm the value $\mathrm{Ha}^\star(\mathrm{Pm})$ increases as shown for the sample values in Fig. 8.2, left panel, where $\mathrm{Ha}^\star(10^{-2}) \simeq 3.30$, $\mathrm{Ha}^\star(10^{-1}) \simeq 3.65$. This result is similar to those obtained by Takashima, 1996 and by Falsaperla et al. 2020a. In the right panel we have plotted the critical curves in the a$-$Re plane for some values of magnetic Prandtl number and Ha $= 4.106$. We choose this last value because it gives the minimum critical Reynolds number in Fig. 8.1, left panel. For other values of Ha we obtain curves which are similar to those shown in this figure.
Fig. 8.2 shows that the minima of the curves increase as Pm increases from 10^{-4} to 10^{-1}, but for small values of Pm we observe instead a slight decrease of the minimum, as shown in Fig. 8.3, left panel.
In Fig. 8.3, right panel, we show a detail of the critical curves for values of Ha close to the threshold value $\mathrm{Ha}^\star$ at Pm $= 10^{-4}$. We observe the same behaviour close to the threshold value $\mathrm{Ha}^\star$ for all Pm.
c) We checked numerically the three-dimensional case ($a > 0$ and $b > 0$) for Pm $= 0$ and several values Pm > 0 and Ha ≤ 10. Our results show that the critical Reynolds number is always obtained, in the range of values of parameters considered in the present paper, for two-dimensional spanwise perturbations ($b = 0$). Fig. 8.4 shows the dependency of the critical Reynolds number on the wavenumber b for a sample value of Ha $= 4.106$ and different values of Pm. For each value of b we show the minimum of Re with respect to the wavenumber a.

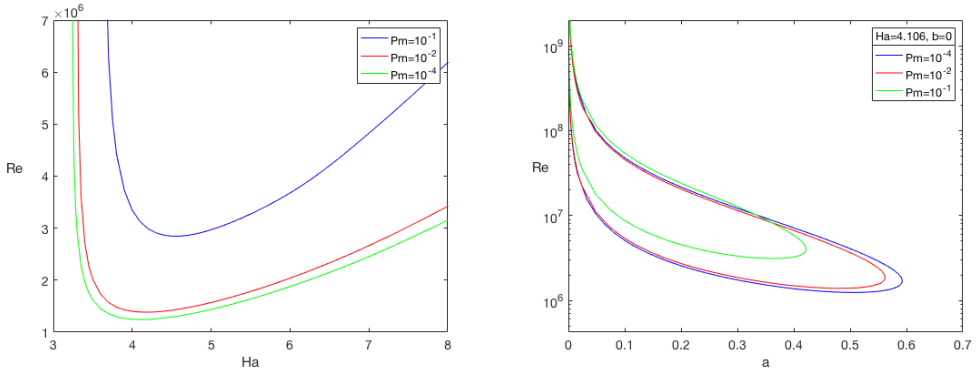

FIGURE 8.2: Left panel: Critical Reynolds number versus Hartmann number for some Prandtl numbers. Note that the critical curves diverge at some thresholds depending on Pm. Right panel: Critical curves in the a−Re plane for some values of magnetic Prandtl number, and Ha = 4.106 (minimum of the curve in Fig. 8.1, left panel).

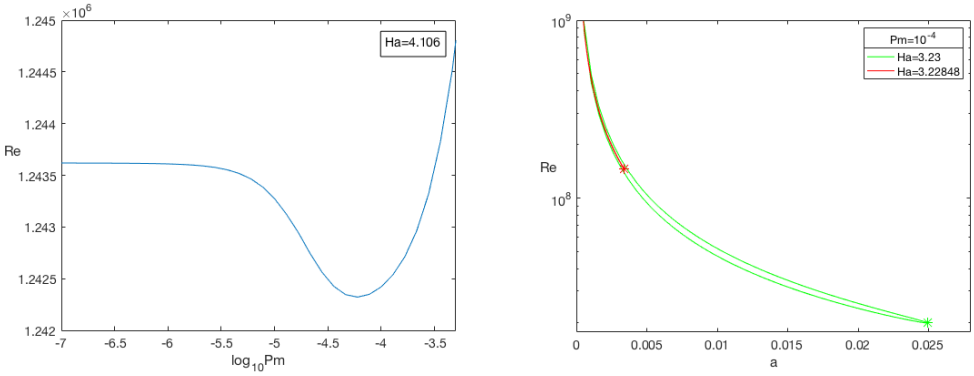

FIGURE 8.3: Left panel: Critical Reynolds number Re for Ha = 4.106 and small values of Pm. Right panel: Critical curves in the a−Re plane for Pm $= 10^{-4}$ and values of Ha close to the threshold value $\mathrm{Ha}^{\star}(10^{-4}) = 3.22845$. We note how the curves diverge towards infinity.

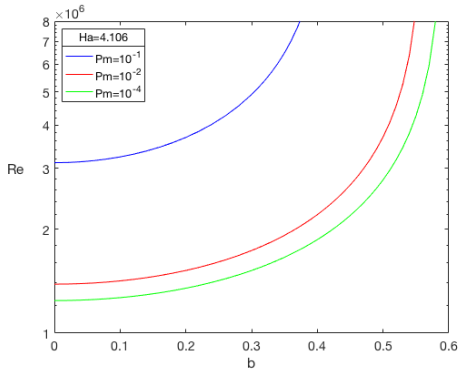

FIGURE 8.4: Critical Reynolds number as function of the wavenumber b for Ha = 4.106 and different values of Pm. For each value of Pm the minimum of is achieved at $b = 0$.

8.5 Nonlinear stability

In this section we study the nonlinear energy stability of the Hartmann shear flow by using the Lyapunov second method with the classical energy.
We assume that $\mathbf{u}$, $\mathbf{h}$ and ∇p are x, y-periodic with periods a and b in the x and y directions, respectively, with wave numbers $(a, b) \in \mathbb{R}^2_+$. In the following it suffices therefore to consider functions over the periodicity cell

$$\Omega = [0, \frac{2\pi}{a}] \times [0, \frac{2\pi}{b}] \times [-1, 1]. \tag{8.5.1}$$

As the basic function space, we take $L_2(\Omega)$, which is the space of square-summable functions in Ω with the scalar product denoted by

$$(g, h) = \int_0^{\frac{2\pi}{a}} \int_0^{\frac{2\pi}{b}} \int_{-1}^{1} g(x, y, z) h(x, y, z) dx dy dz,$$

and the norm given by

$$\|g\| = \Big[\int_0^{\frac{2\pi}{a}} \int_0^{\frac{2\pi}{b}} \int_{-1}^{1} g^2(x, y, z) dx dy dz\Big]^{\frac{1}{2}}.$$

We introduce the classical energy:

$$V(t) = \frac{1}{2}(\|\mathbf{u}\|^2 + A\|\mathbf{h}\|^2), \tag{8.5.2}$$

and coupling parameter $A = \mathrm{Ha}^2\mathrm{Pm}$.

Firstly we note that, following Falsaperla et al. 2020a, it is easy to see that the *streamwise* perturbations are stabilizing for any Prandtl, Hartmann, and Reynolds numbers.

From (8.3.3) and (8.3.4), we obtain the Reynolds energy equation for $V(t)$:

$$\dot{V} = I - \mathrm{Re}^{-1}[\|\nabla \mathbf{u}\|^2 - A\mathrm{Rm}^{-1}\|\nabla \mathbf{h}\|^2], \tag{8.5.3}$$

where

$$I = -(U'w, u) + A(\bar{B}'\ell, u) - A(\bar{B}'w, h) + A(U'\ell, h). \tag{8.5.4}$$

From (8.5.3), it follows

$$\dot{V} = \quad I - \mathrm{Re}^{-1}[\|\nabla \mathbf{u}\|^2 + \mathrm{Ha}^2\|\nabla \mathbf{h}\|^2] \leq \tag{8.5.5}$$

$$\leq \quad (\bar{R}^{-1} - \mathrm{Re}^{-1})[\|\nabla \mathbf{u}\|^2 + \mathrm{Ha}^2\|\nabla \mathbf{h}\|^2], \tag{8.5.6}$$

with

$$\bar{R}^{-1} = \max_{\mathcal{S}} \frac{I}{\|\nabla \mathbf{u}\|^2 + \mathrm{Ha}^2\|\nabla \mathbf{h}\|^2}, \tag{8.5.7}$$

and $\mathcal{S}$ is the space of the admissible perturbations: $\mathcal{S}$ is the space of solenoidal fields $\mathbf{u}, \mathbf{h}$ in the Sobolev space $W^{1,2}(\Omega)$, satisfying the boundary conditions (8.3.4) and $\|\nabla \mathbf{u}\| + \|\nabla \mathbf{h}\| > 0$.
From the previous inequality and the Poincaré's inequality, it follows

Theorem 8.5.1. *Let $U(z)$ and $B(z)$ be given by (8.3.1) and (8.3.2) (the basic Hartmann shear flow). If* $\mathrm{Re} < \bar{R}$, *where $\bar{R}$ is given by (8.5.7), then the Hartmann flow is exponentially nonlinearly stable in the energy norm (8.5.3): $V(t) \leq V(0)e^{C_0(\bar{R}^{-1}-\mathrm{Re}^{-1})t}$, with C_0 a positive constant.*

In order to compute $\bar{R}$, we have to solve the Euler-Lagrange equations of the maximum problem (8.5.7). They are given by equations:

$$\begin{cases} \bar{R}[U'w\mathbf{i} + U'u\mathbf{k} - A\ell\bar{B}'\mathbf{i} + A\bar{B}'h\mathbf{k}] - 2\Delta\mathbf{u} = \nabla\lambda_1 \\ A\bar{R}[\bar{B}'u\mathbf{k} - w\bar{B}'\mathbf{i} + U'\ell\mathbf{i} + U'h\mathbf{k}] + 2\mathrm{Ha}^2\Delta\mathbf{h} = \nabla\lambda_2, \end{cases} \tag{8.5.8}$$

where λ_1 and λ_2 are Lagrange multipliers, and boundary conditions (8.3.4). Following Orr, 1907 (p. 125), we consider here two-dimensional perturbations and prove below that the less stable perturbations are the *spanwise*.
By taking the *double curl* of (8.5.8) and applying the solenoidality of $\mathbf{u}$ and $\mathbf{h}$, i.e. $u_x + w_z = 0$ and $h_x + \ell_z = 0$, we have the *magnetic Orr-Reynolds equations*, see Falsaperla et al. 2020a,

$$\begin{cases} \dfrac{\bar{R}}{2}[U''w_x + 2U'w_{xz} - A\bar{B}''\ell_x] + \Delta\Delta w = 0 \\ \dfrac{A\bar{R}}{2}[\bar{B}''w_x - 2U'\ell_{xz} - U''\ell_x] + \mathrm{Ha}^2\Delta\Delta\ell = 0, \end{cases} \tag{8.5.9}$$

with the boundary conditions $w = Dw = \ell = D\ell = 0$ on the bottom and $w = D^2w = \ell = D\ell = 0$ on the top.
By assuming, as in the linear case,

$$f(x,y,z) = f(z)e^{iax}, \tag{8.5.10}$$

with $f = w, \ell$, we have

$$\begin{cases} \dfrac{\bar{R}}{2}[U''iaw + 2U'iaDw - A\bar{B}''ia\ell] + (D^2 - a^2)^2w = 0 \\ \dfrac{A\bar{R}}{2}[\bar{B}''iaw - 2U'iaD\ell - U''ia\ell] + \mathrm{Ha}^2(D^2 - a^2)^2\ell = 0. \end{cases} \tag{8.5.11}$$

These equations are the generalized *Orr-Reynolds equations* for the magnetic Orr-Reynold number $\bar{R} = \max_a \mathrm{Re}^{(m)}_{Orr}(a)$, a being the wave number. $\mathrm{Re}^{(m)}_{Orr}(a)$ is the the Orr-Reynolds number for a fixed wave number a. The critical magnetic Orr-Reynolds number is given by $\bar{R} = \mathrm{Re}_c = \mathrm{Re}^{(m)}_{Orr}(a_c)$ with a_c the value of wave number that minimizes $\mathrm{Re}^{(m)}_{Orr}(a)$. We note that if $\mathrm{Ha} \to 0$, then $A \to 0$ and this system reduces to the classical *Orr equation* for an open channel in hydrodynamics.
This system with the boundary conditions $w = Dw = \ell = D\ell = 0$ on the bottom and $w = D^2w = \ell = D\ell = 0$ on the top has been solved with the Chebyshev collocation method. In Fig. 8.5, left panel, we use 120 polynomials and show the critical Orr-Reynolds number Re_c as a function of the Hartmann number. The magnetic Prandtl number Pm is fixed to 10^{-4}. In the right panel we use 100 polynomials and plot the Orr-Reynolds number $\mathrm{Re} = Re^{(m)}_{Orr}(a)$ for wave numbers $a \in [0, 10]$, and $\mathrm{Pm} = 10^{-4}$.

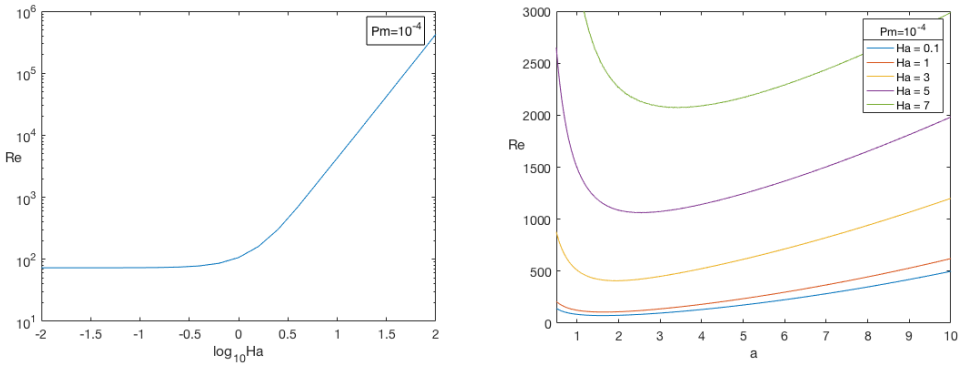

FIGURE 8.5: Left panel: Orr-Reynolds critical number Re as a function of Hartmann number. The magnetic Prandtl number Pm is fixed to 10^{-4}. Right panel: Orr-Reynolds number $\mathrm{Re} = Re^{(m)}_{Orr}(a)$ for wave numbers $a \in [0, 10]$, and $\mathrm{Pm} = 10^{-4}$.

8.5.1 Nonlinear stability with respect to tilted perturbations

Now we prove that, for 2-D perturbations, the less stabilizing perturbations, as in Falsaperla et al. 2019b, are the spanwise, and the best stability results, in the energy norm, are those obtained by the generalized Orr equations (8.5.9), (8.5.11).
For this, we consider an arbitrary tilted perturbation which forms an angle θ with the direction of motion $\mathbf{i}$ (the x-direction).
We easily have:

$$\mathbf{u} = u\mathbf{i} + v\mathbf{j} + w\mathbf{k} = u'\mathbf{i}' + v'\mathbf{j}' + w\mathbf{k}, \quad \mathbf{b} = h\mathbf{i} + k\mathbf{j} + \ell\mathbf{k} = h'\mathbf{i}' + k'\mathbf{j}' + \ell\mathbf{k},$$

with

$$\begin{cases} u' = \cos\theta\, u + \sin\theta\, v \\ v' = -\sin\theta\, u + \cos\theta\, v, \end{cases} \qquad \begin{cases} h' = \cos\theta\, h + \sin\theta\, k \\ k' = -\sin\theta\, h + \cos\theta\, k, \end{cases} \tag{8.5.12}$$

$$\mathbf{i}' = \cos\theta\mathbf{i} + \sin\theta\mathbf{j}, \quad \mathbf{j}' = -\sin\theta\mathbf{i} + \cos\theta\mathbf{j}, \tag{8.5.13}$$

and

$$\begin{cases} x = \cos\theta\, x' - \sin\theta\, y' \\ y = \sin\theta\, x' + \cos\theta\, y'. \end{cases} \tag{8.5.14}$$

Following the same procedure of Falsaperla et al. 2020a, we obtain the system in the new fields u', v', w, h', k', ℓ:

$$\begin{cases} u'_t = -\mathbf{u}\cdot\nabla u' + \mathrm{Re}^{-1}\Delta u' - (Uu'_x + U'\cos\theta\, w) - \dfrac{\partial\bar{\pi}}{\partial x'} + \\ \quad + A(\bar{B}h'_x + \mathrm{Rm}^{-1}h'_z + \bar{B}'\cos\theta\ell + \mathbf{h}\cdot\nabla h') \\ v'_t = -\mathbf{u}\cdot\nabla v' + \mathrm{Re}^{-1}\Delta v' - Uv'_x + U'\sin\theta\, w - \dfrac{\partial\bar{\pi}}{\partial y'} + \\ \quad + A(\bar{B}k'_x + \mathrm{Rm}^{-1}k'_z - \bar{B}'\sin\theta\ell + \mathbf{h}\cdot\nabla k') \\ w_t = -\mathbf{u}\cdot\nabla w + \mathrm{Re}^{-1}\Delta w - Uw_x - \dfrac{\partial\bar{\pi}}{\partial z} + \\ \quad + A(\bar{B}\ell_x + \mathrm{Rm}^{-1}\ell_z + \mathbf{h}\cdot\nabla\ell) \\ h'_t = -\mathbf{u}\cdot\nabla h' + \mathrm{Rm}^{-1}\Delta h' - (Uh'_x + \bar{B}'\cos\theta\, w) + \bar{B}u'_x + \\ \quad + \mathrm{Rm}^{-1}u'_z + U'\cos\theta\ell + \mathbf{h}\cdot\nabla u' \\ k'_t = -\mathbf{u}\cdot\nabla k' + \mathrm{Rm}^{-1}\Delta k' - Uk'_x + \bar{B}'\sin\theta w + \bar{B}v'_x + \\ \quad + \mathrm{Rm}^{-1}v'_z - U'\sin\theta\,\ell + \mathbf{h}\cdot\nabla v' \\ \ell_t = -\mathbf{u}\cdot\nabla\ell - U\ell_x + \mathrm{Rm}^{-1}\Delta\ell + \bar{B}w_x + \mathrm{Rm}^{-1}w_z + \mathbf{h}\cdot\nabla w \\ \dfrac{\partial u'}{\partial x'} + \dfrac{\partial v'}{\partial y'} + \dfrac{\partial w}{\partial z} = 0, \quad \dfrac{\partial h'}{\partial x'} + \dfrac{\partial k'}{\partial y'} + \dfrac{\partial \ell}{\partial z} = 0. \end{cases} \tag{8.5.15}$$

Now we consider *tilted-stream perturbations in the x'-direction*, i.e, those with $\dfrac{\partial}{\partial x'} \equiv 0$ (they physically are *rolls* in the x'-direction).

For these perturbations we easily have the energy equations:

$$\frac{d}{dt}\left[\frac{\|u'\|^2 + A\|h'\|^2}{2}\right] = -(U'\cos\theta u', w) - \mathrm{Re}^{-1}\|\nabla u'\|^2 - A\mathrm{Rm}^{-1}\|\nabla h'\|^2 + \\ + A\cos\theta[(\bar{B}'\ell, u') + (-\bar{B}'w + U'\ell, h')], \tag{8.5.16}$$

and

$$\frac{d}{dt}\left[\frac{\|v'\|^2 + \|w\|^2}{2} + A\frac{\|k'\|^2 + \|\ell\|^2}{2}\right] = -\mathrm{Re}^{-1}(\|\nabla v'\|^2 + \|\nabla w\|^2) - A\mathrm{Rm}^{-1}(\|\nabla k'\|^2 \\ + \|\nabla\ell\|^2) + \sin\theta[(U'v', w) - A((\bar{B}'v', \ell) - (\bar{B}'k', w) + (U'k', \ell))]. \tag{8.5.17}$$

We note that equation (8.5.17) does not contain the fields u' and h'. Moreover the solenoidality conditions for $\mathbf{u}$ and $\mathbf{h}$ are now given by

$$\frac{\partial v'}{\partial y'} + \frac{\partial w}{\partial z} = 0, \quad \frac{\partial k'}{\partial y'} + \frac{\partial \ell}{\partial z} = 0. \tag{8.5.18}$$

So, we first study the energy equation (8.5.17).
Denoting by

$$E_2 = \left[\frac{\|v'\|^2 + \|w\|^2}{2} + A\frac{\|k'\|^2 + \|\ell\|^2}{2}\right], \tag{8.5.19}$$

from (8.5.17), taking into account that $A\mathrm{Rm}^{-1} = \mathrm{Ha}^2\mathrm{Re}^{-1}$, we have the estimate

$$\dot{E}_2 \le -(\mathrm{Re}^{-1} - \bar{R}_\theta^{-1})[(\|\nabla v'\|^2 + \|\nabla w\|^2) + \mathrm{Ha}^2(\|\nabla k'\|^2 + \|\nabla\ell\|^2)], \tag{8.5.20}$$

where

$$\frac{1}{\bar{R}_\theta} = \max_{\mathcal{S}} \frac{I_\theta}{\|\nabla v'\|^2 + \|\nabla w\|^2 + \mathrm{Ha}^2(\|\nabla k'\|^2 + \|\nabla \ell\|^2)}, \tag{8.5.21}$$

$$I_\theta = \sin\theta\Big[(U'v', w) - A\Big((\bar{B}'v', \ell) - (\bar{B}'k', w) + (U'k', \ell)\Big)\Big], \tag{8.5.22}$$

and $\mathcal{S}$ is the space of the *kinematically admissible fields*: $\mathcal{S}$ is the space of fields v', w, k', ℓ in the Sobolev space $W^{1,2}(\Omega_{xz})$, $\Omega_{xz} = [0, 2\pi/a] \times [-1, 1]$, satisfying $v'_{y'} + w_z = 0$, $k'_{y'} + \ell_z = 0$, $\|\nabla v'\| + \|\nabla w\| + \|\nabla k'\| + \|\nabla \ell\| > 0$ and the boundary conditions $v' = w = k' = \ell = 0$ at $z = -1$ and $v'_z = w = k' = \ell = 0$ at $z = 1$.
In order to find $\bar{R}_\theta$ we have to solve the maximum problem (8.5.21).
As before, we write the Euler-Lagrange equations for this maximum problem. As in Falsaperla et al. 2020a, p. 6, we obtain the system:

$$\begin{cases} \bar{R}_\theta\,[U''w_x + 2U'w_{xz} - A\bar{B}''\ell_x] + 2\left(\dfrac{w_{xxxx}}{\sin^4\theta} + 2\dfrac{w_{xx}}{\sin^2\theta} + w_{zzzz}\right) = 0, \\ A\bar{R}_\theta\,[\bar{B}''w_x - U''\ell_x - 2U'\ell_{xz}] + 2\mathrm{Ha}^2\left[(\dfrac{\ell_{xxxx}}{\sin^4\theta} + 2\dfrac{\ell_{xx}}{\sin^2\theta} + \ell_{zzzz})\right] = 0, \end{cases} \tag{8.5.23}$$

with boundary conditions $w = w' = \ell = \ell' = 0$ at $z = -1$ and $w = w'' = \ell = \ell' = 0$ at $z = 1$.
These equations coincide with the magnetic Orr-Reynolds equations (8.5.9) if we substitute the critical Reynolds number $\bar{R}$ in (8.5.9) with $\bar{R}_\theta \sin\theta$ and x with $\dfrac{x}{\sin\theta}$.
Thus we obtain as critical nonlinear Reynolds number for x'-independent perturbations, $\bar{R}_\theta$, the critical number

$$\bar{R}_\theta = \min_{a>0} \mathrm{Re}^{(m)}_{Orr}(a/\sin\theta)/\sin\theta, \tag{8.5.24}$$

where $\mathrm{Re}^{(m)}_{Orr}(a/\sin\theta)$ is the Orr-Reynolds number for a given wave number $\bar{a}$ evaluated at the wave number $a/\sin\theta = 2\pi/(\lambda\sin\theta)$ and λ is the wavelength of the perturbation. From (8.5.24), we easily have that

$$\bar{R}_\theta = \bar{R}/\sin\theta, \tag{8.5.25}$$

with $\bar{R}$ given by (8.5.7). This, in particular gives $\bar{R}_\theta \to +\infty$ if $\theta \to 0$ (streamwise perturbations), and $\bar{R}_\theta \to \bar{R}$ as $\theta \to \pi/2$ (spanwise perturbations).
We now introduce the energy:

$$E(t) = \frac{\beta(\|u'\|^2 + A\|h'\|^2)}{2} + E_2(t), \quad \beta > 0 \tag{8.5.26}$$

where β is an arbitrary positive number to be chosen. The energy equation is

$$\begin{aligned} \dot{E} = &-\beta[(U'\cos\theta u', w) + \mathrm{Re}^{-1}\|\nabla u'\|^2 + A\mathrm{Rm}^{-1}\|\nabla h'\|^2 + A\cos\theta((\bar{B}'\ell, u') + \\ &+ (-\bar{B}'w + U'\ell, h'))] - \mathrm{Re}^{-1}(\|\nabla v'\|^2 + \|\nabla w\|^2) - A\mathrm{Rm}^{-1}(\|\nabla k'\|^2 + \\ &+ \|\nabla \ell\|^2) + \sin\theta[(U'v', w) - A((\bar{B}'v', \ell) - (\bar{B}'k', w) + (U'k', \ell))]. \end{aligned} \tag{8.5.27}$$

Taking into account that $\mathrm{Rm} = \mathrm{Re}\,\mathrm{Pm}$, $A = \mathrm{Ha}^2\mathrm{Re}^{-1}\mathrm{Rm}$, the previous equation becomes:

$$\begin{aligned}\dot{E} = &-\beta\mathrm{Re}^{-1}\|\nabla u'\|^2 - \beta(U'\cos\theta u', w) - \mathrm{Re}^{-1}(\|\nabla v'\|^2 + \|\nabla w\|^2) + \\ &+ (U'\sin\theta v', w) + A[-\beta\mathrm{Pm}^{-1}\mathrm{Re}^{-1}\|\nabla h'\|^2 - \beta(\bar{B}'\cos\theta\ell, u') + \\ &- \beta\cos\theta(-\bar{B}'w + U'\ell, h'))] - \mathrm{Ha}^2\mathrm{Re}^{-1}(\|\nabla k'\|^2 + \|\nabla\ell\|^2) + \\ &+ A\sin\theta(-(\bar{B}'v', \ell) + (\bar{B}'k', w) - (U'k', \ell)).\end{aligned} \tag{8.5.28}$$

Remembering (8.5.21) and (8.5.22), the sum of the fourth term and the last three terms of 8.5.28 is less or equal than $\bar{R}_\theta^{-1}[\|\nabla v'\|^2 + \|\nabla w\|^2 + \mathrm{Ha}^2(\|\nabla k'\|^2 + \|\nabla\ell\|^2)]$, and we have the following estimate:

$$\begin{aligned}\dot{E} \le &-\beta\mathrm{Re}^{-1}\|\nabla u'\|^2 - \beta(U'\cos\theta u', w) - \mathrm{Re}^{-1}(\|\nabla v'\|^2 + \|\nabla w\|^2) + \\ &+ A[-\beta\mathrm{Pm}^{-1}\mathrm{Re}^{-1}\|\nabla h'\|^2 - \beta(\bar{B}'\cos\theta\ell, u') - \beta\cos\theta(-\bar{B}'w + \\ &+ U'\ell, h')] - \mathrm{Ha}^2\mathrm{Re}^{-1}(\|\nabla k'\|^2 + \|\nabla\ell\|^2) + \bar{R}_\theta^{-1}[\|\nabla v'\|^2 + \|\nabla w\|^2 + \\ &+ \mathrm{Ha}^2(\|\nabla k'\|^2 + \|\nabla\ell\|^2)].\end{aligned} \tag{8.5.29}$$

Now define

$$r = \frac{1}{\mathrm{Re}} - \frac{1}{\bar{R}_\theta},$$

and suppose $r > 0$, i.e., $\mathrm{Re} < \bar{R}_\theta$. Since for functions f of the Sobolev space $W^{1,2}(-1,1)$ which vanish at the boundaries $z = \pm 1$, or that vanish at $z = -1$ and whose first derivative vanishes at $z = 1$ the Poincaré inequality $\frac{\pi^2}{4}\|f\|^2 \le \|\nabla f\|^2$ holds, we have the following estimate:

$$\begin{aligned}\dot{E} \le &-\frac{\pi^2}{4}\beta\mathrm{Re}^{-1}\|u'\|^2 - \beta(U'\cos\theta u', w) - \frac{\pi^2}{4}\mathrm{Re}^{-1}(\|v'\|^2 + \|w\|^2) + \\ &+ A[-\frac{\pi^2}{4}\beta\mathrm{Pm}^{-1}\mathrm{Re}^{-1}\|h'\|^2 - \beta(\bar{B}'\cos\theta\ell, u') - \beta\cos\theta(-\bar{B}'w + \\ &+ U'\ell, h'))] - \frac{\pi^2}{4}\mathrm{Ha}^2\mathrm{Re}^{-1}(\|k'\|^2 + \|\ell\|^2) + \frac{\pi^2}{4}\bar{R}_\theta^{-1}[\|v'\|^2 + \|w\|^2 + \\ &+ \mathrm{Ha}^2(\|k'\|^2 + \|\ell\|^2)] \le -\frac{\pi^2}{4}\beta\mathrm{Re}^{-1}\|u'\|^2 + M\beta\|u'\|\|w\| + \\ &- \frac{\pi^2}{4}\mathrm{Re}^{-1}(\|v'\|^2 + \|w\|^2) + A[-\frac{\pi^2}{4}\beta\mathrm{Pm}^{-1}\mathrm{Re}^{-1}\|h'\|^2 + \\ &+ M\beta\|\ell\|\|u'\| + M\beta\|w\|\|h'\| + M\|\ell\|\|h'\|] - \frac{\pi^2}{4}\mathrm{Ha}^2\mathrm{Re}^{-1}(\|k'\|^2 + \\ &+ \|\ell\|^2) + \frac{\pi^2}{4}\bar{R}_\theta^{-1}[\|v'\|^2 + \|w\|^2 + \mathrm{Ha}^2(\|k'\|^2 + \|\ell\|^2)],\end{aligned} \tag{8.5.30}$$

where

$$M = \max(\max_{[-1,1]}|U'|, \max_{[-1,1]}|B'|, \max_{[-1,1]}|AU'|, \max_{[-1,1]}|AB'|).$$

Moreover

$$\begin{aligned}\dot{E} \leq & -r\frac{\pi^2}{4}[\|v'\|^2+\|w\|^2+\mathrm{Ha}^2(\|k'\|^2+\|\ell\|^2)]+\beta M(\|w\|\|u'\|+\\ & +\|\ell\|\|u'\|+\|w\|\|h'\|+\|l\|\|h'\|)-\beta\mathrm{Re}^{-1}\frac{\pi^2}{4}(\|u'\|^2+\mathrm{Ha}^2\|h'\|)\leq\\ & \leq -r\frac{\pi^2}{4}[\|v'\|^2+\|w\|^2+\beta\|u'\|^2+\mathrm{Ha}^2(\|k'\|^2+\|\ell\|^2)]+\\ & +\beta M(\|w\|\|u'\|+\|\ell\|\|u'\|+\|w\|\|h'\|+\|\ell\|\|h'\|)-\beta r\frac{\pi^2}{4}\mathrm{Ha}^2\|h'\|.\end{aligned} \tag{8.5.31}$$

By arithmetic-geometric mean inequality, we have

$$M\beta\|u'\|\|w\| \leq \frac{\beta M^2}{2\epsilon_1}\|w\|^2+\frac{\beta\epsilon_1}{2}\|u'\|^2, \tag{8.5.32}$$

$$M\beta\|l\|\|u'\| \leq \frac{\beta M^2}{2\epsilon_2}\|l\|^2+\frac{\beta\epsilon_2}{2}\|u'\|^2, \tag{8.5.33}$$

$$M\beta\|w\|\|h'\| \leq \frac{\beta M^2}{2\epsilon_3}\|w\|^2+\frac{\beta\epsilon_3}{2}\|h'\|^2, \tag{8.5.34}$$

$$M\beta\|l\|\|h'\| \leq \frac{\beta M^2}{2\epsilon_4}\|l\|^2+\frac{\beta\epsilon_4}{2}\|h'\|^2, \tag{8.5.35}$$

where $\epsilon_1,\epsilon_2,\epsilon_3,\epsilon_4$, are arbitrary positive numbers to be chosen.
Therefore,

$$\begin{aligned}\dot{E} \leq & -r\frac{\pi^2}{4}(\|v'\|^2+\mathrm{Ha}^2\|k'\|^2)+(\frac{\beta M^2}{2\epsilon_1}+\frac{\beta M^2}{2\epsilon_3}-r\frac{\pi^2}{4})\|w\|^2+\\ & +(\frac{\beta M^2}{2\epsilon_2}+\frac{\beta M^2}{2\epsilon_4}-\mathrm{Ha}^2r\frac{\pi^2}{4})\|\ell\|^2+\beta(\frac{\epsilon_1}{2}+\frac{\epsilon_2}{2}-r\frac{\pi^2}{4})\|u'\|^2+\\ & +\beta(\frac{\epsilon_3}{2}+\frac{\epsilon_4}{2}-\mathrm{Ha}^2r\frac{\pi^2}{4})\|h'\|^2.\end{aligned} \tag{8.5.36}$$

By choosing $\epsilon_1=\epsilon_2=r\frac{\pi^2}{8}$ and $\epsilon_3=\epsilon_4=r\frac{\pi^2\mathrm{Ha}^2}{8}$, we obtain

$$\begin{aligned}\dot{E} \leq & -r\frac{\pi^2}{4}(\|v'\|^2+\mathrm{Ha}^2\|k'\|^2)-\beta r\frac{\pi^2}{8}\|u'\|^2-\beta r\frac{\pi^2\mathrm{Ha}^2}{8}\|h'\|^2+\\ & +[\frac{4\beta M^2}{r\pi^2}(1+\frac{1}{\mathrm{Ha}^2})-r\frac{\pi^2}{4}]\|w\|^2+[\frac{4\beta M^2}{r\pi^2}(1+\frac{1}{\mathrm{Ha}^2})+\\ & -\mathrm{Ha}^2r\frac{\pi^2}{4}]\|l\|^2.\end{aligned} \tag{8.5.37}$$

If we choose $\frac{4\beta M^2}{r\pi^2}(1+\frac{1}{\mathrm{Ha}^2})\leq\min\frac{r\pi^2}{8}(1,\mathrm{Ha}^2)$, we have

$$\dot{E} < -r\frac{\pi^2}{4}E, \tag{8.5.38}$$

and finally we obtain

$$E(t) < E(0)e^{-\frac{\pi^2}{4}rt}, \quad t\geq 0. \tag{8.5.39}$$

Taking into account that Re $< \bar{R}$, i.e., $r > 0$, we have that the energy $E(t)$ goes exponentially to zero. In particular all the components, $\|u'\|$, $\|h'\|$, $\|v'\|$, $\|w\|$, $\|k'\|$, $\|\ell\|$ of the energy go to zero as $t \to +\infty$.
From (8.5.39) the following theorem and corollary hold

Theorem 8.5.2. *Let $U(z)$ and $B(z)$ be given by* (8.3.1) *and* (8.3.2) *(the basic Hartmann shear flow). If* Re $< \bar{R}_\theta$, *where $\bar{R}_\theta$ is given by* (8.5.24), *then the Hartmann flow is exponentially nonlinearly stable with respect to tilted perturbations according to inequality* (8.5.39).

Corollary 8.5.1. *The critical nonlinear Orr-Reynolds number with respect to two-dimensional perturbations is achieved with spanwise perturbations.*

8.6 Discussion of the results

We study stability and instability of the Hartmann laminar flow (8.3.1) - (8.3.2) of an electrically conducting liquid in an inclined open channel. We assume that the upper plane is stress-free and the lower plane is rigid. We also adopt electrically insulating boundaries.
We generalise here the results of Falsaperla et al. for laminar flows in fluid-dynamics 2019b and for a laminar flow in MHD for a horizontal layer with rigid boundaries 2020a to laminar flows in an inclined open channel in MHD. We use the method they introduced in 2019b and in 2020a and consider the more realistic physical case of Hartmann flow in an open channel down an incline. We study the local stability and the instability with the spectral method and the nonlinear stability with the Lyapunov second method.
As in Takashima, 1996, 1998, we obtain critical linear Reynolds numbers in two cases, the limit case Pm $= 0$ and the case Pm > 0. In particular, for Pm $= 0$ we prove a Squire theorem: the critical Reynolds number is obtained with two-dimensional perturbations. For Pm > 0 our calculations show that, in a range of the Hartmann number, the critical Reynolds number is also obtained with two-dimensional perturbations.
Our linear results show that, for any given Pm the basic flow remains stable up to a threshold $\mathrm{Ha}^\star(\mathrm{Pm})$. For larger values of Ha the magnetic field destabilizes the flow up to a minimum of Re and then is always stabilizing (see Fig. 8.1 and Fig. 8.2). Moreover, we observe that we obtain an instability region which is unbounded for any fixed Prandtl number. We have studied also the stabilizing effect of Pm for a fixed Ha as it is shown in Fig. 8.3. We note an initial destabilizing character of Pm and then a stabilizing effect.
In the nonlinear case, we define as Lyapunov function an energy (sum of the kinetic and magnetic energy) with a coupling parameter A and study the variational problem which arises from the Reynolds-Orr equation. We then study the variational maximum problem and solve the Euler-Lagrange equations with the Chebyshev collocation method by using 100 and 120 Chebyshev polynomials. We conjecture and assume that, as in the fluid-dynamics case (see Orr, 1907), the less stabilizing perturbations are two-dimensional (cf. also Kaiser and Mulone, 2005 where conditional nonlinear stability has been studied and the critical Reynolds number has been reached with two-dimensional perturbations). Moreover we prove that the critical nonlinear Reynolds number is obtained with spanwise perturbations.
We observe that the Reynolds number we have introduced in (5.0.26) - (5.0.27) depends on the inclination angle β. Thus, the critical Reynolds number we obtain, in the linear and nonlinear cases, allows us to determine, for any inclination angle

β, the characteristic velocity at criticality. The velocity increases when the angle β increases, according to the relation

$$V_{0crit} = \mathrm{Re}_{crit} \sin \beta.$$

Chapter 9

Energy stability of plane Couette and Poiseuille flows: A conjecture

The results presented in this Section have been published by Falsaperla, Mulone, and Perrone, 2022a.

9.1 Summary

With this article we start the study of the stability on three dimensional perturbations in the nonlinear case. In particular we study the nonlinear stability of Couette and Poiseuille flows with the Lyapunov second method by using the classical L_2-energy. First of all we prove that the streamwise perturbations are L_2-energy stable for any Reynolds number. This contradicts the results of Joseph, 1968, Joseph and Carmi, 1969 and Busse, 1972. Then we study the three-dimensional perturbations and we run into a contradiction. Indeed, by using the results of Joseph and Busse, we obtain that the critical Reynolds number is reached on the streamwise perturbations. We suggest how to solve this contradiction through a conjecture. In this way we are able to prove that the critical nonlinear Reynolds numbers are obtained along two-dimensional perturbations, the spanwise perturbations, as Orr Orr, 1907 had supposed. This conclusion combined with the results by Falsaperla et al. 2019b on the stability with respect to tilted rolls, provides a possible solution to the "mismatch" between the critical values of linear stability, nonlinear monotonic energy stability and the experiments.

9.2 State of the art

Here we recall the most important results of stability in the nonlinear case.
As we have highlighted in Sec. 1.2, in the nonlinear case it is often *assumed* that the least stabilizing perturbations, as in the linear case, are the two-dimensional spanwise perturbations, see Orr, 1907. However, Joseph in his paper on Couette flow, see Joseph, 1968, proved that the least stabilizing perturbations are the streamwise perturbations and concluded that the Orr result was wrong. Joseph and Carmi, 1969 and Busse, 1972 obtained a similar result of Joseph, 1968 for Poiseuille flow. We have already reported all these results more in detail in Sec. 7.
Moffatt, 1990 studied the stability of classical laminar flows with respect to streamwise perturbations. For the case of inhomogeneous perturbation flow of a particular type (see Moffatt, 1990, pp. 250-252), in the case of a semi-space, $y \in [0, +\infty)$, with a hypothesis about pressure that vanishes at infinity, he proved stability for any Reynolds number. Even if he doesn't say so explicitly, he used a weighted energy argument.

The nonlinear stability results have been also obtained with some weighted energies (see Straughan, 2004). Rionero and Mulone, 1991, Kaiser, Tilgner, and Wahl, 2005, Kaiser and Mulone, 2005 studied the nonlinear stability by introducing weighted energies. Kaiser and Mulone, 2005 and Kaiser, Tilgner, and Wahl, 2005 obtained conditional nonlinear stability up to the critical Reynolds numbers for spanwise perturbations Re^x. The velocity field has been represented in terms of poloidal, toroidal and the mean field components, and an explicit calculation of so-called stability balls in the $\mathcal{E}$-norm has been done.
The problem of finding the best conditions for monotonic nonlinear energy stability with respect to three-dimensional perturbations is still an open problem. This problem is equivalent to finding the maximum of a functional ratio that arises from the Reynolds energy equation, see Reynolds, 1895a.
We note that the critical values of Re yielded by monotonic energy stability methods do not correspond to any growing eigenmode of the dynamics. Above such a critical value we only know that there exists at least one perturbation vector whose evolution might be "non-monotonic" in the chosen energy norm. By no means does it ensure transition to a turbulent state, nor even the existence of such a state (see e.g. Schmid and Henningson, 2001a, Eckhardt et al., 2007). This perturbation eventually decays after a long time.
The plan of this paper is the following.
In Sec. 9.3 we write the non-dimensional perturbation equations of laminar flows between two horizontal rigid planes, and we recall the classical linear stability/instability results.
In Sec. 9.4 we prove analytically that the basic motions are *nonlinear monotonic stable in the energy norm*, with respect to the streamwise perturbations, for any Reynolds number (i.e. $\mathrm{Re}^y = +\infty$) in three ways: we first use a weighted energy with a positive coupling parameter, then we use the classical L_2-energy norm to prove global and monotonic stability. As far as we know, in the literature there is no precise mathematical proof of this theorem apart from Moffatt's proof in a semi-space, see Moffatt, 1990.
However our numerical calculations obtained from the maximum problem (see Sec. 9.4) and done with the Chebyshev polynomials method (see Fig. 9.2), show that the minimum Reynolds number for the energy method is obtained with respect to streamwise perturbations. In particular we obtain the same numerical results of Joseph for Couette case, Joseph and Carmi and Busse for Poiseuille case ($\mathrm{Re}_E = \mathrm{Re}^y = 20.6$ in Couette case, and $\mathrm{Re}_E = \mathrm{Re}^y = 49.55$ in Poiseuille case). These results contradict the previous one $\mathrm{Re}^y = +\infty$.
Therefore, for the first time in the literature, we *suggest how to solve this contradiction through a conjecture*: the maximum must be sought in a *subspace* of the space of kinematically admissible perturbations, the space of *physically admissible perturbations* competing for the maximum. In this way, we are able to prove that the maximum is reached on two-dimensional perturbations, the spanwise perturbations, as Orr, 1907 had supposed and that the results of Joseph, 1968, 1976, Joseph and Carmi, 1969, and Busse, 1972, and our numerical results *are not correct*.
Sec. 9.5 is dedicated to the discussion of the results.

9.3 Laminar flows between two parallel planes

Given a reference frame $Oxyz$, with unit vectors $\mathbf{i}, \mathbf{j}, \mathbf{k}$, consider the layer $\mathcal{D} = \mathbb{R}^2 \times [-1, 1]$ of thickness 2 with horizontal coordinates x, y and vertical coordinate z.

Plane parallel shear flows are solutions of the stationary Navier-Stokes eqs. (4.0.2). The velocity field $\mathbf{U}$ has the form $\mathbf{U} = f(z)\mathbf{i}$. In particular, for fixed velocity at the boundaries $z = \pm 1$, we have the well known profiles already computed in Sec. 4 (Case 1):
a) Couette $f(z) = z$,
b) Poiseuille $f(z) = 1 - z^2$.

9.3.1 Perturbation equations

The perturbation equations to the plane parallel shear flows, in non-dimensional form, are

$$\begin{cases} u_t = -\mathbf{u}\cdot\nabla u + \mathrm{Re}^{-1}\Delta u - (f u_x + f' w) - \dfrac{\partial p}{\partial x} \\ v_t = -\mathbf{u}\cdot\nabla v + \mathrm{Re}^{-1}\Delta v - f v_x - \dfrac{\partial p}{\partial y} \\ w_t = -\mathbf{u}\cdot\nabla w + \mathrm{Re}^{-1}\Delta w - f w_x - \dfrac{\partial p}{\partial z} \\ \nabla\cdot\mathbf{u} = 0. \end{cases} \tag{9.3.1}$$

In (9.3.1) $\mathbf{u}$ is the perturbation velocity field. It has components (u, v, w) in the directions x, y, z, respectively. p denotes the perturbation to the pressure field.
Here we use the symbols g_x as $\frac{\partial g}{\partial x}$, g_t as $\frac{\partial g}{\partial t}$, etc., for any function g.
To system (9.3.1) we append the *rigid* boundary conditions

$$\mathbf{u}(x, y, \pm 1, t) = 0, \quad (x, y, t) \in \mathbb{R}^2 \times (0, +\infty),$$

and the initial condition

$$\mathbf{u}(x, y, z, 0) = \mathbf{u_0}(x, y, z), \quad \text{in} \quad \mathcal{D},$$

with $\mathbf{u_0}(x, y, z)$ solenoidal vector which vanishes at the boundaries.

9.3.2 Linear stability/instability

As we did in the previous work (see 8.5), we assume that both $\mathbf{u}$ and ∇p are x, y-periodic with periods a and b in the x and y directions, respectively, with wave numbers $(a, b) \in \mathbb{R}^2_+$. Therefore we consider functions over the periodicity cell Ω (see 8.5.1).
With the symbols $(\cdot,\cdot)$ and $\|\cdot\|$we denote the scalar product and the norm in $L_2(\Omega)$.

Linear stability/instability is obtained by studying the linearised system neglecting the nonlinear terms in (9.3.1).
We recall that the classical results of Romanov, 1973 prove that Couette flow is *linearly stable* for *any Reynolds* number.
Instead, Poiseuille flow is unstable for any Reynolds number bigger than 5772 (Orszag, 1971). However, if we restrict the linearized equations to streamwise perturbations, considering eigen-solutions of the form $e^{st}\mathbf{u}(y, z)$ for some complex number $s = \sigma + i\omega$, we find that all eigenvalues have negative real part, and hence the system is always spectrally stable.
Moreover, the Squire theorem (see Squire, 1933) holds for the linearised system: the most destabilizing perturbations are two-dimensional spanwise perturbations. The

critical Reynolds numbers for Poiseuille flows Re_L can be obtained by solving the Orr-Sommerfeld equation (Drazin and Reid, 2004, p. 155).

9.4 Nonlinear energy stability

In SubSec. 3.1 we have recalled some definitions of nonlinear energy stability.

Here we study *the nonlinear energy stability with the Lyapunov method*, by using the classical energy

$$E(t) = \frac{1}{2}[\|u\|^2 + \|v\|^2 + \|w\|^2].$$

We obtain *sufficient conditions of monotonic nonlinear energy stability*.
Taking into account the solenoidality of $\mathbf{u}$ and the boundary condition, we write the energy equation (see Reynolds, 1895a)

$$\dot{E} = -(f'w, u) - \mathrm{Re}^{-1}[\|\nabla u\|^2 + \|\nabla v\|^2 + \|\nabla w\|^2], \tag{9.4.1}$$

and we have

$$\begin{aligned} &\dot{E} = -(f'w, u) - \mathrm{Re}^{-1}[\|\nabla u\|^2 + \|\nabla v\|^2 + \|\nabla w\|^2] = \\ &= \left(\frac{-(f'w, u)}{\|\nabla u\|^2 + \|\nabla v\|^2 + \|\nabla w\|^2} - \frac{1}{\mathrm{Re}}\right)\|\nabla \mathbf{u}\|^2 \leq \\ &\leq \left(\frac{1}{\mathrm{Re}_E} - \frac{1}{\mathrm{Re}}\right)\|\nabla \mathbf{u}\|^2, \end{aligned} \tag{9.4.2}$$

where

$$\frac{1}{\mathrm{Re}_E} = m = \max_{\mathcal{S}} \frac{-(f'w, u)}{\|\nabla u\|^2 + \|\nabla v\|^2 + \|\nabla w\|^2}, \tag{9.4.3}$$

and $\mathcal{S}$ is the space of the *kinematically admissible fields*

$$\begin{aligned} &\mathcal{S} = \{u, v, w \in H^1(\Omega),\ u = v = w = w_z = 0 \text{ on the boundaries,} \\ &\text{periodic in } x, \text{ and } y, \quad u_x + v_y + w_z = 0, \quad \|\nabla \mathbf{u}\| > 0\}. \end{aligned} \tag{9.4.4}$$

$H^1(\Omega)$ is the Sobolev space of the functions which are in $L_2(\Omega)$ together with their first generalized derivatives.
To solve this problem, we assume that the components of the velocity field are of the form

$$u = \tilde{u} + \epsilon\eta_1 \quad v = \tilde{v} + \epsilon\eta_2 \quad w = \tilde{w} + \epsilon\eta_3$$

where $\tilde{\mathbf{u}} = (\tilde{u}, \tilde{v}, \tilde{w})$ maximizes the quotient (9.4.3) and $\epsilon\boldsymbol{\eta} = \epsilon(\eta_1, \eta_2, \eta_3)$ denotes a small deviation from the velocity field $\mathbf{u}$, $0 < \epsilon \ll 1$. We impose that the first variation of the quotient (9.4.3) is zero, that is

$$\frac{\partial}{\partial \epsilon}\left(\frac{1}{\mathrm{Re}}\right)\Big|_{\epsilon=0} = 0.$$

This leads to the Euler-Lagrange equations (see Schmid and Henningson, 2001a pp.189-192)

$$(f'w\mathbf{i} + f'u\mathbf{k}) - 2m\Delta\mathbf{u} = \nabla\lambda, \tag{9.4.5}$$

where $\lambda(x, y, z)$ is a Lagrange multiplier. Assuming as Orr, 1907 that the maximum is achieved for spanwise perturbations, $\frac{\partial}{\partial y} \equiv 0$, by taking the third component of the *double-curl* of (9.4.5) and by using the solenoidality condition $u_x + w_z = 0$ and the boundary conditions, we obtain the *Orr equation* (see Orr, 1907)

$$\frac{\mathrm{Re}_E}{2}(f''w_x + 2f'w_{xz}) + \Delta\Delta w = 0. \tag{9.4.6}$$

By solving this equation we obtain the Orr results: for Couette and Poiseuille flows, we have $\mathrm{Re}_{Orr} = \mathrm{Re}_E = 44.3$ (see Orr, 1907 p. 128) and $\mathrm{Re}_{Orr} = \mathrm{Re}_E = 87.6$ (see Drazin and Reid, 2004 p. 163), respectively (the critical values are converted to the dimensionless form we have used here).
These nonlinear stability conditions have been obtained by Orr, 1907 in a celebrated paper, by using the Reynolds, 1895a energy equation (9.4.1) (see Orr, 1907 p. 122).
In his paper Orr, 1907 writes: "*Analogy with other problems leads us to assume that disturbances in two dimensions will be less stable than those in three; this view is confirmed by the corresponding result in case viscosity is neglected*". He also says: "*The three-dimensioned case was attempted, but it proved too difficult*".
Orr considers two-dimensional spanwise perturbations: $v \equiv 0$ *and* $\frac{\partial}{\partial y} \equiv 0$ (see also Squire, 1933, Drazin and Reid, 2004). The critical value he finds, in the Couette case, $\mathrm{Re}^x = 44.3$, *is the critical Reynolds number with respect to spanwise perturbations* (see Orr, 1907 p. 128, Joseph, 1976 p. 181).
Joseph in his monograph, see Joseph, 1976, p. 181, says: "*Orr's assumption about the form of the disturbance which increases at the smallest* Re *is not correct since we shall see that the energy of an x-independent disturbance (streamwise perturbations) can increase when* $\mathrm{Re} > 2\sqrt{1708} \simeq 82.65$" (in our dimensionless form Re^y=20.6).
Busse, 1972 in his paper (p. 29) writes "*Numerical computations suggest that the eigenvalue R_E is attained for x-independent solutions. Since this result has contradicted the physical intuition of earlier investigators in this field, it is desirable to find a rigorous proof for this property*". However he remarks in a note on p. 29: "*Joseph first found that the minimizing solution in the case of Couette flow was independent of x. He also gave a proof of this fact. A gap of his proof has been found, however, recently by J. Serrin (private communication by D. D. Joseph) who pointed out that Joseph did not account for the possibility that the required minimum could appear at the end point $k_x = k$*". (Note that according to the notations adopted by Joseph $k^2 = k_x^2 + k_y^2$ where k_x and k_y are respectively a and b we use throughout the thesis.)

Drazin and Reid, 2004, p. 430, note: "*The determination of the least eigenvalue of equations (53.21)* (in our case, $\mathrm{Re}_c = 1/m$ in equation (9.4.5)) *is clearly a formidable problem in general and results are known for only a few cases*". They cite the results of Joseph, 1968 for Couette flow, Joseph and Carmi, 1969 and Busse, 1972 for Poiseuille flow. They also say: "*the least eigenvalue ... is still associated with a two dimensional disturbance but one which varies only in the yz-plane, i.e. the perturbed flow consists of rolls whose axes are in the directions of the basic flow*" (streamwise perturbations).

We note that our numerical calculations, with the Chebyshev polynomials method (see Fig. 9.2), also show that the minimum Reynolds number for the energy method is obtained with respect to streamwise perturbations. Therefore, we obtain the same numerical results of Joseph for Couette case, Joseph and Carmi and Busse for Poiseuille case ($\mathrm{Re}_E = \mathrm{Re}^y = 20.6$ in Couette case, and $\mathrm{Re}_E = \mathrm{Re}^y = 49.5$ in Poiseuille case). Despite the results of Joseph, 1968, 1976, Joseph and Carmi, 1969, Busse, 1972 and the observations of Drazin and Reid, 2004, we shall prove below that the numerical calculations of Joseph are correct, however *the conclusion of* Joseph, 1976 *is not correct*. In fact, in the classical L_2-energy, the *streamwise perturbations are always stabilizing*. This result for the first time has been proved by Moffatt, 1990 for the case of inhomogeneous perturbation flow of a particular type (see Moffatt, 1990, pp. 250-252) and $y \in [0, +\infty)$, with a hypothesis about pressure that vanishes at infinity.
In the next subsection we prove that the streamwise perturbations are stable (monotonic stability in the energy norm E) for all Reynolds numbers. Moreover, in what follows, we make a conjecture and we prove that the least stabilizing *physical perturbations* competing for maximum are two-dimensional, and they are the spanwise. This means that the result of Orr is correct (see Falsaperla et al. 2019b and Falsaperla, Mulone, and Perrone, 2022a) as Serrin had also observed (see Busse, 1972).

9.4.1 Stability of streamwise perturbations for any Reynolds number

We assume that the perturbations are *streamwise*, i.e. they *do not depend on* x ($\frac{\partial}{\partial x} \equiv 0$). Therefore the perturbation equations (9.3.1) become

$$\begin{cases} u_t = -\mathbf{u}\cdot\nabla u + \mathrm{Re}^{-1}\Delta u - f'w \\ v_t = -\mathbf{u}\cdot\nabla v + \mathrm{Re}^{-1}\Delta v - \dfrac{\partial p}{\partial y} \\ w_t = -\mathbf{u}\cdot\nabla w + \mathrm{Re}^{-1}\Delta w - \dfrac{\partial p}{\partial z} \\ v_y + w_z = 0. \end{cases} \tag{9.4.7}$$

We introduce two energy norms: a weighted norm E_β and the classical energy E both evaluated in the streamwise perturbations.

i) **Weighted energy**
We define a *weighted energy* E_β (Lyapunov function) equivalent to the classical energy norm E, and show that the streamwise perturbations cannot destabilize the basic Couette or Poiseuille flows in the energy E_β.
First we introduce an arbitrary positive number β. Then, we multiply $(9.4.7)_1$ by βu and integrate over Ω. Besides, we multiply $(9.4.7)_2$ and $(9.4.7)_3$ by v and w and integrate over Ω. By taking into account the solenoidality of $\mathbf{u}$, the boundary conditions and the periodicity, we have

$$\frac{d}{dt}\left[\frac{\beta\|u\|^2}{2}\right] = -\beta(f'w, u) - \beta\mathrm{Re}^{-1}\|\nabla u\|^2$$

$$\frac{d}{dt}\left[\frac{\|v\|^2 + \|w\|^2}{2}\right] = -\mathrm{Re}^{-1}(\|\nabla v\|^2 + \|\nabla w)\|^2.$$

By using the arithmetic-geometric mean inequality, we have

$$-\beta(f'w,u) \leq \beta\frac{M^2}{2\epsilon}\|w\|^2 + \beta\frac{\epsilon}{2}\|u\|^2,$$

where $M = \max_{[-1,1]}|f'(z)|$ and ϵ is an arbitrary positive number to be chosen.
Now we define the Lyapunov function (weighted energy norm)

$$E_\beta(t) = \frac{1}{2}[\beta\|u\|^2 + \|v\|^2 + \|w\|^2], \tag{9.4.8}$$

and choose $\epsilon = \dfrac{\pi^2}{4\mathrm{Re}}$. From the above inequality and the use of the Poincaré inequality $\dfrac{\pi^2}{4}\|g\|^2 \leq \|\nabla g\|^2$ ($g = u$, $g = v$, $g = w$), we have

$$\dot{E}_\beta \leq \frac{1}{2}[(\beta\frac{4M^2\mathrm{Re}}{\pi^2} - \frac{\pi^2}{2\mathrm{Re}})\|w\|^2 - \frac{\pi^2}{2\mathrm{Re}}\|v\|^2 - \beta\frac{\pi^2}{4\mathrm{Re}}\|u\|^2].$$

By choosing $\beta = \dfrac{\pi^4}{16M^2\mathrm{Re}^2}$, we finally have

$$\dot{E}_\beta \leq -\frac{\pi^2}{4\mathrm{Re}}E_\beta.$$

Integrating this inequality, we have the exponential decay

$$E_\beta(t) \leq E_\beta(0)\exp\{-\frac{\pi^2}{4\mathrm{Re}}t\}. \tag{9.4.9}$$

This inequality implies *monotonic nonlinear exponential stability*, in the E_β-norm, of the basic Couette or Poiseuille flows, with respect to the streamwise perturbations, for any Reynolds number.
This result does not rule out that there might be a eigenmode in which the energy E initially grows.

ii) **Classical L_2-energy (global stability)**

Now we use the *classical energy norm* E and we show that the streamwise perturbations cannot destabilize the basic Couette or Poiseuille flows.
We multiply $(9.4.7)_1$ by u and integrate over Ω. Besides, we multiply $(9.4.7)_2$ and $(9.4.7)_3$ by v and w and integrate over Ω. By taking into account of the solenoidality of $\mathbf{u}$, the boundary conditions and the periodicity, as before we have

$$\begin{aligned} \frac{d}{dt}\frac{\|u\|^2}{2} &= -(f'u,w) - \mathrm{Re}^{-1}\|\nabla u\|^2 \\ \frac{d}{dt}(\frac{\|v\|^2}{2} + \frac{\|w\|^2}{2}) &= -\mathrm{Re}^{-1}[\|\nabla v\|^2 + \|\nabla w\|^2]. \end{aligned} \tag{9.4.10}$$

By using the Poincaré inequality and integrating last equation, we have:

$$\begin{aligned}&\frac{d}{dt}(\frac{\|v\|^2}{2}+\frac{\|w\|^2}{2})=-\mathrm{Re}^{-1}[\|\nabla v\|^2+\|\nabla w\|^2]\le -C(\|v\|^2+\|w\|^2)\\&\Rightarrow \|v\|^2+\|w\|^2\le H_0e^{-2Ct},\quad C=\frac{\pi^2}{4\mathrm{Re}},\quad H_0=\|v_0\|^2+\|w_0\|^2.\end{aligned}\tag{9.4.11}$$

Now we consider the equation depending on u and define $M=\max_{[-1,1]}|f'(z)|$. We have the following inequalities:

$$\begin{aligned}\frac{d}{dt}\frac{\|u\|^2}{2}&=-(f'u,w)-\mathrm{Re}^{-1}\|\nabla u\|^2\le M\|u\|\|w\|-\mathrm{Re}^{-1}\|\nabla u\|^2\le\\&\le M(\frac{\|u\|^2}{2\epsilon}+\frac{\epsilon}{2}\|w\|^2)-\mathrm{Re}^{-1}\|\nabla u\|^2\le M(\frac{\|u\|^2}{2\epsilon}+\frac{\epsilon}{2}\|w\|^2)-\\&-C\|u\|^2=(\frac{M}{2\epsilon}-C)\|u\|^2+\frac{\epsilon}{2}M\|w\|^2=-\frac{C}{2}\|u\|^2+\frac{M^2}{C}\frac{\|w\|^2}{2}\end{aligned}\tag{9.4.12}$$

where $\epsilon=\dfrac{M}{C}$, and $C=\dfrac{\pi^2}{4\mathrm{Re}}$.

We use this inequality and (9.4.11) to obtain

$$\begin{aligned}\frac{d}{dt}\|u\|^2&\le -C\|u\|^2+\frac{M^2}{C}\|w\|^2\le -C\|u\|^2+\frac{M^2}{C}(\|v\|^2+\|w\|^2)\le\\&\le -C\|u\|^2+\frac{M^2}{C}H_0e^{-2Ct}.\end{aligned}\tag{9.4.13}$$

Integrating last inequality, we have

$$\|u\|^2\le e^{-Ct}[k-\frac{M^2}{C^2}H_0e^{-Ct}]=ke^{-Ct}-\frac{M^2}{C^2}H_0e^{-2Ct},\tag{9.4.14}$$

with $k=K_0+\dfrac{M^2}{C^2}H_0,\quad K_0=\|u_0\|^2$.

We introduce the classical energy

$$L(t)=\frac{1}{2}[\|u\|^2+\|v\|^2+\|w\|^2],\tag{9.4.15}$$

and observe that the initial energy is given by $L_0=\dfrac{H_0+K_0}{2}$. Adding the (9.4.11) and the (9.4.14) we finally have:

$$\begin{aligned}L(t)&\le H_0e^{-2Ct}+(K_0+\frac{M^2}{C^2}H_0)e^{-Ct}-\frac{M^2}{C^2}H_0e^{-2Ct}\le\\&\le L_0e^{-2Ct}+(L_0+\frac{M^2}{C^2}L_0)e^{-Ct}=\\&=L_0(e^{-2Ct}+e^{-Ct}+\frac{M^2}{C^2}e^{-Ct}).\end{aligned}\tag{9.4.16}$$

This inequality implies global nonlinear exponential stability of the basic Couette or Poiseuille flows with respect to the streamwise perturbations for any Reynolds

number.

Also this result does not rule out that there might be a eigenmode in which the energy E initially grows. Indeed Eq. (9.4.16) implies that $L(t) \leq L_0(2 + \frac{M^2}{C^2})$ and not that $L(t) \leq L_0$. Therefore a situation like the one illustrated in Fig. 9.1 could arise.

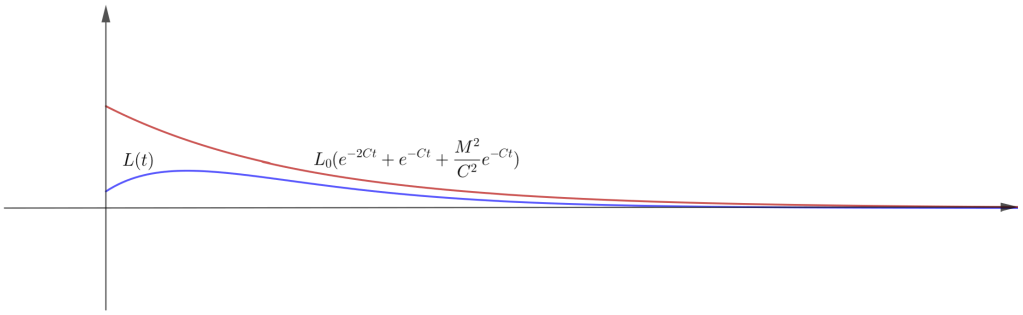

FIGURE 9.1: The red line represents the function of Eq. (9.4.16) that majorates $L(t)$ which is represented by the blue line. The schematic representation shows that Eq. (9.4.16) does not exclude the possibility that the energy $L(t)$ grows initially and then decays.

iii) **Classical L_2-energy (monotonic stability)**

Consider eqs. (9.4.10)

$$\begin{aligned} \frac{d}{dt}\frac{\|u\|^2}{2} &= -(f'u, w) - \mathrm{Re}^{-1}[\|u_y\|^2 + \|u_z\|^2], \\ \frac{d}{dt}\left(\frac{\|v\|^2}{2} + \frac{\|w\|^2}{2}\right) &= -\mathrm{Re}^{-1}[\|v_y\|^2 + \|v_z\|^2 + \|w_y\|^2 + \|w_z\|^2]. \end{aligned} \tag{9.4.17}$$

Summing these two equations and rearranging, we have

$$\dot{E} = -(f'u, w) - \mathrm{Re}^{-1}[\|u_z\|^2 + \|v_y\|^2 + \|w_z\|^2] - \mathrm{Re}^{-1}[\|u_y\|^2 + \|v_z\|^2 + \|w_y\|^2]. \tag{9.4.18}$$

Define the new maximum problem

$$m_1 = \frac{1}{\mathrm{Re}^y} = \max_{\mathcal{S}} \frac{-(f'w, u)}{\|u_z\|^2 + \|v_y\|^2 + \|w_z\|^2}, \tag{9.4.19}$$

and $\mathcal{S}$ is the space of the *kinematically admissible fields* (9.4.4). From (9.4.18) we get

$$\dot{E} \leq (m_1 - \mathrm{Re}^{-1})[\|u_z\|^2 + \|v_y\|^2 + \|w_z\|^2] - \mathrm{Re}^{-1}[\|u_y\|^2 + \|v_z\|^2 + \|w_y\|^2]. \tag{9.4.20}$$

The Euler-Lagrange equations of this maximum problem are given by

$$\begin{cases} -f'w + 2m_1 u_{zz} &= 0 \\ 2m_1 v_{yy} &= \lambda_y \\ -f'u + 2m_1 w_{zz} &= \lambda_z, \end{cases} \tag{9.4.21}$$

where λ is a Lagrange multiplier $\lambda(y,z)$. These equations must be solved with boundary conditions $u = v = w = w_z = 0$ on the planes $z = \pm 1$.
We take the partial derivative of $(9.4.21)_2$ with respect to z and the partial derivative of $(9.4.21)_3$ with respect to y, subtract and use the solenoidality $v_y + w_z = 0$, to obtain

$$\begin{cases} -f'w + 2m_1 u_{zz} & = 0 \\ -f'u_y + 4m_1 w_{yzz} & = 0. \end{cases} \tag{9.4.22}$$

Multiplying the first equation by f' and differentiating with respect to y, substituting in the second equation, we finally obtain

$$8m_1^2[\phi_{zzzz} - 2\frac{f''}{f'}\phi_{zzz} + 2(\frac{f''}{f'})^2\phi_{zz}] - (f')^2\phi = 0, \tag{9.4.23}$$

with $\phi = w_y$, and the boundary conditions $\phi = \phi_z = \phi_{zz} = 0$ on the planes $z = \pm 1$. By solving this equation we get $w_y = 0$ (in the case of Couette flow the equation with boundary conditions is very simple to solve, for Poiseuille flow one can use a software like Mathematica or MatLab). As in Joseph, 1976 (see Schmid and Henningson, 2001a, Drazin and Reid, 2004) we expand the variables in (9.4.21) as $f = \hat{f}(z)e^{i\beta y}$. From $w_y = 0$ we deduce that $\beta = 0$. Therefore we have also $v_y = 0$ and the solenoidality of $\mathbf{u}$ implies $w_z = 0$. Recalling the boundary conditions $w(x,y,\pm 1) = 0$, we conclude $w = 0$ and so $m_1 = 0$, $\mathrm{Re}^y = +\infty$.
From (9.4.20) we get the monotonic energy stability for all Reynolds number on the streamwise perturbations

$$\dot{E} \leq -\mathrm{Re}^{-1}[\|u_z\|^2 + \|v_y\|^2 + \|w_z\|^2 + \|u_y\|^2 + \|v_z\|^2 + \|w_y\|^2], \tag{9.4.24}$$

$$E(t) \leq E(0)\exp\{-\frac{\pi^2}{2\mathrm{Re}}t\}. \tag{9.4.25}$$

Theorem 9.4.1. *Assuming the perturbations to the basic shear flows* $\mathbf{U} = f(z)\mathbf{i}$ *are streamwise, then we have nonlinear monotonic stability according to (9.4.25).*

9.4.2 Nonlinear stability with respect to three-dimensional perturbations

Here consider three-dimensional perturbations. We study the nonlinear stability by using the energy of disturbances E,

$$E(t) = \frac{1}{2}[\|u\|^2 + \|v\|^2 + \|w\|^2].$$

By writing the Reynolds-Orr energy equation

$$\dot{E} = -(f'w, u) - \mathrm{Re}^{-1}[\|\nabla u\|^2 + \|\nabla v\|^2 + \|\nabla w\|^2], \tag{9.4.26}$$

we have

$$\begin{aligned}\dot{E} &= -(f'w,u) - \mathrm{Re}^{-1}[\|\nabla u\|^2 + \|\nabla v\|^2 + \|\nabla w\|^2] = \\ &= \left(\frac{-(f'w,u)}{\|\nabla u\|^2 + \|\nabla v\|^2 + \|\nabla w\|^2} - \frac{1}{\mathrm{Re}}\right)\|\nabla \mathbf{u}\|^2 \leq \\ &\leq \left(m - \frac{1}{\mathrm{Re}}\right)\|\nabla \mathbf{u}\|^2,\end{aligned} \tag{9.4.27}$$

where

$$\frac{1}{\mathrm{Re}_E} = m = \max_{\mathcal{S}} \frac{-(f'w,u)}{\|\nabla u\|^2 + \|\nabla v\|^2 + \|\nabla w\|^2}, \tag{9.4.28}$$

and $\mathcal{S}$ is the space of the *kinematically admissible fields* (9.4.4).
The Euler-Lagrange equations are

$$-f'w\mathbf{i} - f'u\mathbf{k} + 2m\Delta\mathbf{u} = \nabla\lambda, \tag{9.4.29}$$

where λ is a Lagrange multiplier.
We define the third component of the vorticity of velocity field,

$$\zeta = v_x - u_y$$

(it is linked to the toroidal part of the decomposition of the velocity vector $\mathbf{u}$ in the poloidal, toroidal and the mean flow, see Kaiser and Mulone, 2005, Kaiser, Tilgner, and Wahl, 2005) and take the third component of the *double curl* of (9.4.29) and the third component of the *curl* of (9.4.29). We obtain the system of the Euler-Lagrange equations written in terms of ζ and w:

$$\begin{cases} f'(\zeta_y + 2w_{xz}) + f''w_x + 2m\Delta\Delta w = 0 \\ f'w_y + 2m\Delta\zeta = 0, \end{cases} \tag{9.4.30}$$

with the boundary conditions

$$w = w_z = 0,\ \zeta = 0. \tag{9.4.31}$$

The eigenvalue problem (9.4.30) - (9.4.31) is solved with the Chebyshev method by using 80 polynomials. The maximum we obtain corresponds exactly to the critical Reynolds numbers obtained by Joseph, 1968 and Joseph and Carmi, 1969 and Busse, 1972 (i.e. the minimum Reynolds number is reached for the streamwise perturbations). In the Couette case, we report these results in Fig. 9.2.
This conclusion and the results we have obtained in SubSec. 9.4.1 for streamwise perturbations are in an *obvious contradiction*. Most likely this contradiction is due to the choice of the space of *kinematically admissible* perturbations where we look for the maximum. This space is too large and likely contains perturbations which are not admissible as *physical perturbations* competing for the maximum.

How can we solve this contradiction?

We first observe that the *streamwise perturbations* (now $w_x = 0$ and $\zeta_x = 0$) are stable for any Reynolds number. Then $m = 0$ and this implies, from $(9.4.30)_1$, that $\zeta_y = 0$. Eq. $(9.4.30)_2$ implies that also $w_y = 0$. If now we consider plan-form perturbations

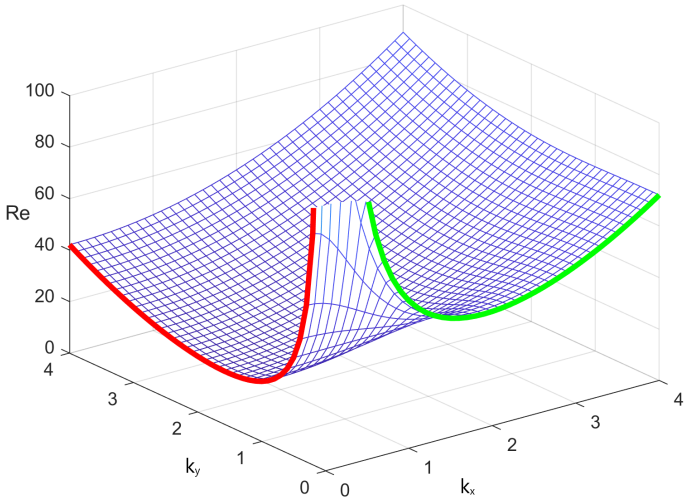

FIGURE 9.2: Plane Couette energy Orr-Reynolds number $\mathrm{Re} = \mathrm{Re}_c$ as function of the wave numbers k_x (i.e. a) and k_y (i.e. b), for system (9.4.30) with rigid boundary conditions. The absolute minimum is $\mathrm{R_c} = 20.6$ and it is achieved for wavenumbers a $= 0$, b $= 1.6$. For Poiseuille flow a similar picture can be drawn.

(see Chandrasekhar, 1961, p.24 formula (111)) we have $v = \dfrac{1}{a^2+b^2}[w_{yz} - \zeta_x] = 0$. For three-dimensional disturbances, we see that, in the numerator of the maximum (9.4.28), the second component v of the vector $\mathbf{u}$ does not appear explicitly (it appears implicitly from the divergence free constraint). Furthermore, the presence of a positive term $\|\nabla v\|^2$ in the denominator reduces the value of the fraction.

So we are led to speculate:

Conjecture

A *possible answer* to the contradiction is this: we introduce the *subspace $\mathcal{S}_0$ of the physical admissible perturbations* which is the subspace of $\mathcal{S}$ consisting of maximizing functions $u, v, w \in \mathcal{S}$ such that $v = 0$ and we *conjecture* that the maximum m is assumed among the functions of this subspace.

With this conjecture, we prove that the maximum is achieved on the spanwise perturbations.
In fact, we have

$$m = \max_{\mathcal{S}_0} \frac{-(f'w, u)}{\|\nabla u\|^2 + \|\nabla w\|^2}, \tag{9.4.32}$$

where $\mathcal{S}_0$ is the space of the *"physically" admissible fields*

$$\begin{aligned} \mathcal{S}_0 = \{u, 0, w \in H^1(\Omega),\ u = w = w_z = 0 \text{ on the boundaries,} \\ \text{periodic in } x, \text{ and } y, \quad u_x + w_z = 0, \quad \|\nabla u\| + \|\nabla w\| > 0\}. \end{aligned} \tag{9.4.33}$$

The Euler-Lagrange equations of this maximum problem are given by

$$-f'w\mathbf{i} - f'u\mathbf{k} + 2m\Delta\mathbf{u} = \nabla\lambda, \tag{9.4.34}$$

where λ is a Lagrange multiplier, $\nabla\lambda = (\lambda_x, 0, \lambda_z)^T$. We take the third component of the double curl of (9.4.34) and the third component of the curl of (9.4.34). We obtain the system of the Euler-Lagrange equations written in terms of ζ and w:

$$\begin{cases} f'(\zeta_y + 2w_{xz}) + f''w_x + 2m\Delta\Delta w = 0 \\ f'w_y + 2m\Delta\zeta = 0, \end{cases} \tag{9.4.35}$$

with the boundary conditions

$$w = w_z = \zeta = 0, \tag{9.4.36}$$

where now $\zeta = -u_y$.
We take the second component of the double curl of (9.4.34) to get

$$f'\zeta_z + f''\zeta - f'w_{xy} = 0. \tag{9.4.37}$$

From this equation and $(9.4.35)_2$ we have that ζ and all its derivatives with respect to z are zero on the boundaries. Let's prove this in a particular case: Couette between rigid planes. The proof in the case of Poiseuille is done in a similar way.
In the case of *RR* Couette, from (9.4.35) and (9.4.37), we have:

$$\begin{cases} \zeta_y + 2w_{xz} + 2m\Delta\Delta w = 0 \\ w_y + 2m\Delta\zeta = 0 \\ \zeta_z - w_{xy} = 0. \end{cases} \tag{9.4.38}$$

On the boundaries $z = \pm 1$ we have $\zeta = 0$, from $(9.4.38)_3$ evaluated on $z = \pm 1$, we have $\zeta' = 0$ ($\zeta' = \dfrac{d\zeta}{dz}$). From $(9.4.38)_2$, evaluated on $z = \pm 1$, we have $\zeta'' = 0$. Now if we differentiate $(9.4.38)_2$ with respect to z and evaluate the result on the boundaries we have $\zeta''' = 0$. From this, if we differentiate twice $(9.4.38)_3$ with respect to z we have that the second derivative of w with respect to z is zero on the boundaries. And so, from $(9.4.38)_2$ differentiated twice with respect to z we have $\zeta'''' = 0$, ad so on.

This implies that $\zeta \equiv 0$, hence $u_y = 0$ and from $(9.4.35)_2$ also $w_y = 0$. Therefore, $u = u(x,z), v = 0, w = w(x,z)$ and the less stabilizing perturbations which satisfy the equation

$$2f'w_{xz} + f''w_x + 2m\Delta\Delta w = 0, \tag{9.4.39}$$

with boundary conditions $w = w_z = 0$ on $z = \pm 1$, are the spanwise perturbations, as Orr, 1907 had assumed.
We report these results in Fig. 9.3 where the critical Reynolds number versus wave numbers for spanwise perturbations are shown.

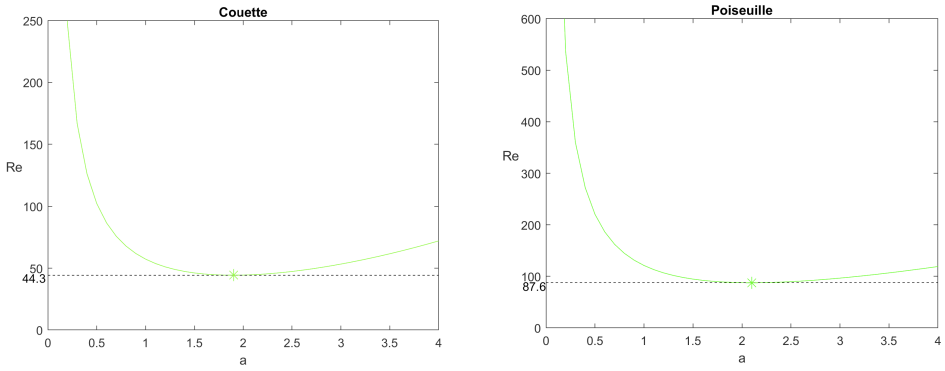

FIGURE 9.3: Reynolds number versus wave number for spanwise perturbations for plane Couette (left) and Poiseuille (right) flows.

9.5 Discussion of the results

We have proved sufficient conditions of nonlinear monotonic energy stability of plane Couette and Poiseuille flows for any Reynolds number less than the ordinary limit of spanwise perturbations, Re_{Orr}. For streamwise perturbations, we have rigorously proved monotonic nonlinear L_2-energy stability results for any Reynolds number and we have suggested a way to overcome an obvious contradiction with classical numerical results. We have introduced a space of "physical" admissible perturbations competing for the maximum problem and *we have proved* that the least stabilizing perturbations are two-dimensional (spanwise perturbations). In the past this result has been only assumed (see Orr, 1907). This conclusion justifies the previous study by Falsaperla et al. 2019b on the stability of two-dimensional tilted rolls with axes in the Oxy-plane. They proved that, for a fixed wavelength $\lambda = \dfrac{2\pi}{a}$ and a given tilted angle θ, one has

$$\mathrm{Re}_c = \mathrm{Re}_{Orr}\left(\frac{2\pi}{\lambda \sin\theta}\right)/\sin\theta, \tag{9.5.1}$$

where $\mathrm{Re}_{Orr}\left(\frac{2\pi}{\lambda \sin\theta}\right)$ is the critical Reynolds number for given wavelength λ and angle $\theta \in (0, \dfrac{\pi}{2}]$. Formula (9.5.1) gives the critical value for a fixed positive wavelength λ. The minimum with respect to λ in $(0, +\infty)$ is the nonlinear critical Reynolds number for tilted perturbations of an angle θ:

$$\mathrm{Re}_c = \min_{\lambda>0} \mathrm{Re}_{Orr}\left(\frac{2\pi}{\lambda \sin\theta}\right)/\sin\theta = \mathrm{Re}_{Orr}/\sin\theta, \tag{9.5.2}$$

where $\mathrm{Re}_{Orr} = 44.3$ for plane Couette flow and $\mathrm{Re}_{Orr} = 87.6$ for plane Poiseuille flow.
These results are in a very good agreement with the experiments done by Prigent et al., 2003 and the numerical simulations carried out by Barkley and Tuckerman, 2007.

Chapter 10

Nonlinear energy stability of magnetohydrodynamics Couette and Hartmann shear flows: A contradiction and a conjecture

The results presented in this Section have been published by Falsaperla, Mulone, and Perrone, 2022b.

10.1 Summary

Here we extend the results presented in the previous section 9 to *magnetohydrodynamics plane Couette and Hartmann* shear flows.
In particular we study the nonlinear stability. We prove that the streamwise perturbations are stable for any Reynolds number. This result is in a contradiction with the numerical solutions of the Euler-Lagrange equations for a maximum energy problem. We solve this contradiction with a conjecture. Then, we rigorous prove that the least stabilizing perturbations, in the energy norm, are the spanwise perturbations and give some critical Reynolds numbers for some selected Prandtl and Hartmann numbers.

10.2 State of the art

In SubSec. 8.2 we have already underlined that laminar flows of electrically conducting fluids have many applications.
The study of the stability of magnetohydrodynamics laminar fluid motions in a channel between parallel planes, the magnetic Couette and Hartmann flows, was done with different boundary conditions for the velocity field (rigid conditions and stress-free conditions) and for the magnetic field (conducting and non-conducting planes) both in the linear case, see Kakutani, 1964, Takashima, 1996, and in the nonlinear case Alexakis et al., 2003, Falsaperla et al. 2016, 2017; 2017, Moresco and Alboussiere, 2004. Furthermore, both the cases of a horizontal and an inclined channel have been studied, see Falsaperla et al. 2016, 2017; 2017 and Falsaperla, Mulone, and Perrone, 2022c .
As for laminar motions in fluid dynamics (Couette and Poiseuille), also in the magnetohydrodynamics case (see Falsaperla et al. Falsaperla, Giacobbe, and Mulone, 2020a) the critical linear (obtained with the spectral analysis) and nonlinear (obtained with the Lyapunov method) Reynolds numbers for the onset of instability

are very different from each other and they do not coincide with the experimental values.
There are still some unsolved mathematical problems: in both linear and nonlinear cases it is not clear whether a Squire theorem holds (even if in the linear case its validity is assumed by Takashima, 1996, 1998): the most destabilizing perturbations are two-dimensional; in the nonlinear case, the critical Reynolds number is determined by looking for the maximum or a minimum of appropriate functional ratios and it is assumed (without any proof) that this maximum or minimum is obtained on spanwise perturbations, see Alexakis et al., 2003, Falsaperla et al. 2020a.
For nonlinear system, Falsaperla et al. 2020a the authors recall that Alexakis et al., 2003 studied shear flows with an applied cross-stream magnetic field using dissipative incompressible magnetohydrodynamics, using the energy $\mathcal{E} = 1/2(u^2 + h^2)$ (sum of kinetic and magnetic energy of perturbations). In Alexakis et al., 2003 the associated minimum problem (of a suitable functional ratio) is solved and they say that "... It is believed, and assumed here, that the global minima of interest also have $k_x = 0$)" (i.e. they *suppose* that the minimum is achieved on the streamwise perturbations). However, in Falsaperla et al. 2020a, it is proved that the streamwise perturbations, for any fixed Hartmann and Prandtl numbers, are nonlinear energy stable *for any* Reynolds number. Moreover, as we recalled in SubSec. 8.2, in Falsaperla et al. 2020a the authors investigated the stability with respect to two-dimensional perturbations that are rolls inclined by an angle θ with respect to the direction of the fluid motion and found that such flows are nonlinearly stable if the Reynolds number Re is less then $\bar{R}_\theta = \mathrm{Re}^{(m)}_{Orr}(2\pi/(\lambda \sin\theta))/\sin\theta$ (see SubSec. 8.2).
In Sec. 8 we have reported the principal results we obtained in 2022a where we study the stability of laminar flows in a sheet of fluid (open channel) down an incline with constant slope angle $\beta \in (0, \frac{\pi}{2})$ assuming that the fluid is electrically conducting and subjected to a magnetic field. In particular in Falsaperla, Mulone, and Perrone, 2022a we study the nonlinear Lyapunov energy stability by solving the Orr equation for the associated maximum problem of the Reynolds-Orr energy equation. We write "following Orr, we consider here two-dimensional perturbations and prove below that the stable perturbations are the spanwise" despite the fact that it is still an open problem to analytically prove that the critical nonlinear Reynolds number $\bar{R}$ is achieved with two-dimensional perturbations.

Therefore the main purpose of this paper is to study the nonlinear energy stability of Couette and Hartmann basic motions with respect to three-dimensional perturbations. For this purpose in Sec. 10.3 we introduce the basic motions and the perturbation equations.
In Sec. 10.4 we study the nonlinear energy stability with respect to three-dimensional perturbations and find that the critical Reynolds numbers are obtained, with the Chebyshev collocation method, with respect to two-dimensional perturbations: the streamwise perturbations. This gives a contradiction that we solve making a conjecture as in the case of fluid dynamics, see 2022a.
With this conjecture we are able to analytically prove that the maximum is reached on two-dimensional perturbations, the spanwise perturbations. Therefore a Squire theorem holds: the least stabilizing perturbations in energy are two-dimensional perturbations. We also give some critical Reynolds numbers for selected Prandtl and Hartmann numbers.
In Sec. 10.5 we report some graphs of the critical Reynolds numbers obtained with

the Chebyshev collocation method for fixed Prandtl and Hartmann numbers.
Sec. 10.6 is dedicated to the discussion of the results.

10.3 Basic motions and perturbation equations

Consider a layer $\mathcal{D} = \mathbb{R}^2 \times [-1, 1]$ filled with an electrically conducting fluid, Davidson, 2001. The magnetohydrodynamics system in the non-dimensional form is the one given by (4.0.12) (see Davidson, 2001; Falsaperla, Mulone, and Perrone, 2022a; Takashima, 1996):
In Sec.4 we have proved that:

Theorem 10.3.1. *The basic solution of system* (4.0.12) *satisfying the boundary conditions* (4.0.30) *is the magnetic Couette flow*

$$U(z) = \frac{\sinh(\mathrm{Ha}\, z)}{\sinh(\mathrm{Ha})}, \qquad \bar{B}(z) = \frac{\cosh(\mathrm{Ha}) - \cosh(\mathrm{Ha}\, z)}{\mathrm{Ha}\sinh(\mathrm{Ha})}$$

Theorem 10.3.2. *The basic solution of system* (4.0.12) *satisfying the boundary conditions* 4.0.37 *is the Hartmann flow*

$$U(z) = \frac{\cosh(\mathrm{Ha}) - \cosh(\mathrm{Ha}\, z)}{\cosh(\mathrm{Ha}) - 1}, \quad \bar{B}(z) = \frac{\sinh(\mathrm{Ha}\, z) - z\sinh(\mathrm{Ha})}{\mathrm{Ha}(\cosh(\mathrm{Ha}) - 1)}.$$

We want to investigate the nonlinear stability of these basic solutions. To this end we consider a regular (at least C^2) perturbation of the stationary solution

$$\mathbf{v} + \mathbf{u} = (U(z), 0, 0) + (u, v, w), \quad \hat{\mathbf{B}} + \mathbf{h} = (\bar{B}(z), 0, \mathrm{Rm}^{-1}) + (h, k, \ell), \quad \Pi + \bar{\pi}.$$

Denoting with

$$A = \mathrm{Ha}^2 \mathrm{Re}^{-1} \mathrm{Rm} = \mathrm{Ha}^2 \mathrm{Pm}, \tag{10.3.1}$$

the equations which govern the evolution of the *difference fields* $\mathbf{u}, \mathbf{h}, \bar{\pi}$ (often such difference fields are improperly called perturbations) are:

$$\begin{cases} \mathbf{u}_t + U(z)\mathbf{u}_x + wU'(z)\mathbf{i} + \mathbf{u}\cdot\nabla\mathbf{u} = A[\bar{B}(z)\mathbf{h}_x + \dfrac{\mathbf{h}_z}{\mathrm{Rm}} + \ell\bar{B}'(z)\mathbf{i} + \mathbf{h}\cdot\nabla\mathbf{h}] - \nabla\bar{\pi} + \dfrac{\Delta\mathbf{u}}{\mathrm{Re}} \\ \mathbf{h}_t + w\bar{B}'(z)\mathbf{i} + U(z)\mathbf{h}_x + \mathbf{u}\cdot\nabla\mathbf{h} - \bar{B}(z)\mathbf{u}_x - \dfrac{\mathbf{u}_z}{\mathrm{Rm}} - \ell U'(z)\mathbf{i} - \mathbf{h}\cdot\nabla\mathbf{u} = \dfrac{\Delta\mathbf{h}}{\mathrm{Rm}} \\ \nabla\cdot\mathbf{u} = 0, \qquad \nabla\cdot\mathbf{h} = 0\,, \end{cases} \tag{10.3.2}$$

where the suffixes x and z denote derivatives with respect to the corresponding variables, the superscript denotes first derivative with respect to z.
We assume that the perturbations are periodic in the variables x and y and denote with $L_2(\Omega)$ the space of real square-integrable functions in Ω, where Ω is the periodicity cell (see (8.5.1)). We denote with the symbols $(\cdot,\cdot)$ and $\|\cdot\|$ the usual scalar product and the norm in $L_2(\Omega)$.
The most common boundary conditions for $\mathbf{u}, \mathbf{h}$ on the planes $z = \pm 1$ are

1. rigid (r), $u = v = w = 0$
2. stress-free (sf), $u_z = v_z = w = 0$
3. non-conducting (n), $h = k = \ell = 0$

4. conducting (c), $h_z = k_z = \ell = 0$

Here we consider only the rigid and non-conducting case. Similar results to the ones we will show also hold true with the other boundary conditions.

10.4 Nonlinear stability

In this section we study (and recall some results presented in Falsaperla et al. 2020a) the nonlinear stability of the shear flows by using the Lyapunov second method with the classical energy

$$V(t) = \frac{1}{2}(\|\mathbf{u}\|^2 + A\|\mathbf{h}\|^2),$$

with the coupling parameter A given by (10.3.1).
Taking the orbital derivative of $V(t)$, taking into account eqs. (10.3.2), the periodicity, the boundary conditions and the solenoidality of $\mathbf{u}$ and $\mathbf{h}$, we obtain the Reynolds-Orr (Orr, 1907, Reynolds, 1883) equation (see Falsaperla et al. 2020a)

$$\dot{V} = -(wU', u) + A((\ell\bar{B}', u) - (w\bar{B}', h) + (\ell U', h)) - \mathrm{Re}^{-1}\|\nabla\mathbf{u}\|^2 - A\,\mathrm{Rm}^{-1}\|\nabla\mathbf{h}\|^2. \tag{10.4.1}$$

10.4.1 Nonlinear stability with respect to three-dimensional perturbations

Applying classical methods, see Joseph, 1976; Rionero, 1968b; Straughan, 2004, we define

$$I = -(U'w, u) + A(\bar{B}'\ell, u) - A(\bar{B}'w, h) + A(U'\ell, h), \tag{10.4.2}$$

and assume that the perturbations $\mathbf{u}$ and $\mathbf{b}$ satisfy the condition $\|\nabla\mathbf{u}\| + \|\nabla\mathbf{h}\| > 0$. We can write the energy equality in this way

$$\begin{aligned} \dot{V} &= I - \mathrm{Re}^{-1}\|\nabla\mathbf{u}\|^2 - A\mathrm{Rm}^{-1}\|\nabla\mathbf{h}\|^2 = \\ &= \left[\frac{I}{\|\nabla\mathbf{u}\|^2 + \mathrm{Ha}^2\|\nabla\mathbf{h}\|^2} - \frac{1}{\mathrm{Re}}\right][\|\nabla\mathbf{u}\|^2 + \mathrm{Ha}^2\|\nabla\mathbf{h}\|^2] \end{aligned} \tag{10.4.3}$$

Introducing the space $\mathcal{S}$ of the kinematically admissible perturbations periodic in x and y,

$$\mathcal{S} = \{\mathbf{u}, \mathbf{h} \in W^{1,2}(\Omega),\ \mathbf{u} = \mathbf{h} = 0 \text{ when } z = \pm 1, \nabla\cdot\mathbf{u} = \nabla\cdot\mathbf{h} = 0,\ \|\nabla\mathbf{u}\| + \|\nabla\mathbf{h}\| > 0\}, \tag{10.4.4}$$

where $W^{1,2}(\Omega)$ is the Sobolev space defined as the subspace of the space of vector fields with their components f_i $(i = 1, 2, 3)$ in $L_2(\Omega)$ such that f_i and its weak derivatives up to order 1 have a finite L_2-norm.
A theorem due to Rionero, 1968b proves that the functional ratio

$$\mathcal{F} = \frac{I}{\|\nabla\mathbf{u}\|^2 + \mathrm{Ha}^2\|\nabla\mathbf{h}\|^2}$$

admits maximum in $\mathcal{S}$. Denoting this maximum with

$$\bar{R}^{-1} = m = \max_{\mathcal{S}} \frac{I}{\|\nabla\mathbf{u}\|^2 + \mathrm{Ha}^2\|\nabla\mathbf{h}\|^2}, \tag{10.4.5}$$

we have the inequality

$$\dot{V} \leq (\bar{R}^{-1} - \mathrm{Re}^{-1})[\|\nabla \mathbf{u}\|^2 + \mathrm{Ha}^2 \|\nabla \mathbf{h}\|^2]. \tag{10.4.6}$$

From this inequality and the Poincaré's inequalities

$$\frac{\pi^2}{4}\|\mathbf{u}\|^2 \leq \|\nabla \mathbf{u}\|^2, \quad \frac{\pi^2}{4}\|\mathbf{h}\|^2 \leq \|\nabla \mathbf{h}\|^2,$$

it follows that the condition

$$\mathrm{Re} < \bar{R}$$

implies nonlinear asymptotical stability of magnetic Couette and Hartmann motions:

Theorem 10.4.1. *Assuming that the Reynolds number satisfies the condition*

$$\mathrm{Re} < \bar{R},$$

the basic magnetic Couette and Hartmann motions are globally asymptotically stable in the energy norm V according to the inequality

$$V(t) \leq V(0) e^{c_0(\mathrm{Re} - \bar{R})t},$$

with a positive constant c_0 depending on Ha *and* Pm.

In order to compute the critical Reynolds number for nonlinear energy stability, we have to compute $\bar{R}$ or $m = 1/\bar{R}$. For this purpose we must calculate the Euler-Lagrange equations of the functional $\mathcal{F}$.
The Euler-Lagrange equations of the maximum problem (10.4.5) are (see Joseph, 1976, Falsaperla et al. 2020a)

$$\begin{cases} [-U'w\mathbf{i} - U'u\mathbf{k} + A\bar{B}'\ell\mathbf{i} - A\bar{B}'h\mathbf{k}] + 2m\Delta\mathbf{u} = \nabla\lambda_1 \\ A[\bar{B}'u\mathbf{k} - w\bar{B}'\mathbf{i} + U'\ell\mathbf{i} + U'h\mathbf{k}] + 2m\mathrm{Ha}^2\Delta\mathbf{h} = \nabla\lambda_2, \end{cases} \tag{10.4.7}$$

where λ_1 and λ_2 are Lagrange multipliers.
We define

$$\zeta = v_x - u_y, \quad \zeta_M = k_x - h_y,$$

where ζ is the third component of the *curl* of velocity field and ζ_M is the third component of *curl* the magnetic field. The eqs. (10.4.7) are linear and we may assume that the fields are sufficiently smooth, see Chandrasekhar, 1961; G. Galdi and Padula, 1990; Mulone and Rionero, 2003. Therefore we take the third component of the *double curl* of (10.4.7) and the third component of the *curl* of (10.4.7). With simple calculations we obtain the system of the Euler-Lagrange equations written in terms of ζ, w, ζ_M and ℓ:

$$\begin{cases} U'w_y - A\bar{B}'\ell_y + 2m\Delta\zeta = 0 \\ A\bar{B}'w_y - AU'\ell_y + 2m\mathrm{Ha}^2\Delta\zeta_M = 0 \\ U'(\zeta_y + 2w_{xz}) + U''w_x - A\bar{B}''\ell_x + A\bar{B}'\zeta_{My} + 2m\Delta\Delta w = 0 \\ -U'A(\zeta_{My} + 2\ell_{xz}) - U''A\ell_x + A\bar{B}''w_x - A\bar{B}'\zeta_y + 2m\mathrm{Ha}^2\Delta\Delta\ell = 0, \end{cases} \tag{10.4.8}$$

with the boundary conditions

$$w = w_z = \ell = \ell_z = 0, \quad \zeta = \zeta_M = 0. \tag{10.4.9}$$

We observe that the boundary conditions for w_z and for ℓ_z are obtained from the solenoidality of $\mathbf{u}$ and $\mathbf{b}$ and from the boundary conditions for u, v, h and k.
Since system (10.4.8) is linear, we seek solution of the form (see Chandrasekhar, 1961; Drazin and Reid, 2004; Straughan, 2004):

$$F(x, y, z) = f(z)e^{i(ax+by)}, \tag{10.4.10}$$

with $F = w, \ell, \zeta, \zeta_M$ in the domain $\mathbb{R}^2 \times [-1, 1]$, $a \geq 0, b \geq 0$, $a^2 + b^2 > 0$ (we note that the two-dimensional streamwise and spanwise perturbations are obtained by taking the limit for a or b which tends to zero). By substituting (10.4.10) in (10.4.8), we have the system

$$\begin{cases} ibU'w - ibA\bar{B}'\ell + 2m(D^2 - (a^2+b^2))\zeta = 0, \\ ibA\bar{B}'w - ibAU'\ell + 2m\mathrm{Ha}^2(D^2 - (a^2+b^2))\zeta_M = 0, \\ U'(ib\zeta + 2iaDw) + iaU''w - iaA\bar{B}''\ell + ibA\bar{B}'\zeta_M + \\ +2m(D^4 - 2(a^2+b^2)D^2 + (a^2+b^2)^2)w = 0, \\ -U'A(ib\zeta_M + 2iaD\ell) - iaU''A\ell + iaA\bar{B}''w - ibA\bar{B}'\zeta + \\ +2m\mathrm{Ha}^2(D^4 - 2(a^2+b^2)D^2 + (a^2+b^2)^2)\ell = 0, \end{cases} \tag{10.4.11}$$

where D and D^2, D^4 indicate first, second and fourth derivatives with respect to z.
The boundary condition are

$$w = Dw = \ell = D\ell = 0, \quad \zeta = \zeta_M = 0, \tag{10.4.12}$$

on $z = \pm 1$.
This ordinary linear differential system with coefficients that depend on z is an eigenvalue problem for m (or Re).
The critical Reynolds numbers we obtain from this system correspond exactly to the critical Reynolds numbers obtained by Joseph, 1968, Joseph and Carmi, 1969, Busse, 1972 and Falsaperla, Mulone, and Perrone, 2022a in fluid dynamics (i.e. the critical Reynolds number is reached for the streamwise perturbations, $\bar{R} = \mathrm{Re}^y$). We report some of these results in Sec. 10.5.

10.4.2 Stability for streamwise perturbations and a contradiction

Now we prove that this result contradicts what was proved in Falsaperla et al. 2020a. In fact it has been proved that the following theorem holds:

Theorem 10.4.2. *For any fixed Hartmann* Ha *and Prandtl* Pm *numbers, the Couette and Hartmann motions are energy-stable, with respect to streamwise perturbations, for any Reynolds number, that is* $\mathrm{Re}^y = +\infty$

Here for completeness we recall the proof made in Falsaperla et al. 2020a in more detail.

Taking into account that for streamwise perturbations the derivatives with respect to x are zero, system (10.3.2) for *streamwise perturbations* becomes

$$\begin{cases} \mathbf{u}_t + wU'(z)\mathbf{i} + \mathbf{u}\cdot\nabla\mathbf{u} = A(\mathrm{Rm}^{-1}\mathbf{h}_z + \ell\bar{B}'(z)\mathbf{i} + \mathbf{h}\cdot\nabla\mathbf{h}) - \nabla\bar{\pi} + \mathrm{Re}^{-1}\Delta\mathbf{u} \\ \mathbf{h}_t + w\bar{B}'(z)\mathbf{i} + \mathbf{u}\cdot\nabla\mathbf{h} - \mathrm{Rm}^{-1}\mathbf{u}_z - \ell U'(z)\mathbf{i} - \mathbf{h}\cdot\nabla\mathbf{u} = \mathrm{Rm}^{-1}\Delta\mathbf{h} \\ \nabla\cdot\mathbf{u} = 0, \qquad \nabla\cdot\mathbf{h} = 0\,. \end{cases} \tag{10.4.13}$$

Introducing

$$V_1 = \frac{1}{2}\left[\|v\|^2 + \|w\|^2 + A(\|k\|^2 + \|\ell\|^2)\right],$$

and taking into account the boundary conditions and the divergence-free conditions $v_y + w_z = 0$, $k_y + \ell_z = 0$, we easily have

$$\dot{V}_1(t) = -\mathrm{Re}^{-1}(\|\nabla v\|^2 + \|\nabla w\|^2) - A\mathrm{Rm}^{-1}(\|\nabla k\|^2) + \|\nabla\ell\|^2)). \tag{10.4.14}$$

From this equation, and the Poincaré's inequality, we have the exponential decay

$$V_1(t) \le V_1(0)e^{-\frac{\pi^2}{2}\mathrm{Re}^{-1}\max(1,\mathrm{Pm}^{-1})t}. \tag{10.4.15}$$

Now we consider the perturbation equations for u and h:

$$\begin{cases} u_t + wU'(z) + \mathbf{u}\cdot\nabla u = A(\mathrm{Rm}^{-1}h_z + \ell\bar{B}'(z) + \mathbf{h}\cdot\nabla h) + \mathrm{Re}^{-1}\Delta u \\ h_t + w\bar{B}'(z) + \mathbf{u}\cdot\nabla h - \mathrm{Rm}^{-1}u_z - \ell U'(z) - \mathbf{h}\cdot\nabla u = \mathrm{Rm}^{-1}\Delta h. \end{cases} \tag{10.4.16}$$

From this it follows that

$$\frac{1}{2}\frac{d}{dt}(\|u\|^2 + A\|h\|^2) = I_1 - \mathrm{Re}^{-1}\|\nabla u\|^2 - A\mathrm{Rm}^{-1}\|\nabla h\|^2, \tag{10.4.17}$$

where

$$I_1 = -(U'w, u) + A(\bar{B}'\ell, u) - A(\bar{B}'w, h) + A(U'\ell, h). \tag{10.4.18}$$

Now we estimate each term of I_1.
Applying the Cauchy-Schwarz and the arithmetic-geometric mean inequality, we have

$$\begin{aligned} I_1 \le M(\frac{1}{2\epsilon_1} + \frac{A}{2\epsilon_2})\|u\|^2 + MA(\frac{1}{2\epsilon_3} + \frac{1}{2\epsilon_4})\|h\|^2 + \\ + M(\frac{\epsilon_1}{2} + \frac{A\epsilon_3}{2})\|w\|^2 + MA(\frac{\epsilon_2}{2} + \frac{\epsilon_4}{2})\|\ell\|^2, \end{aligned} \tag{10.4.19}$$

where $M = \max(\max_{[-1,1]}|U'(z)|, \max_{[-1,1]}|\bar{B}'(z)|)$ and $\epsilon_1, \epsilon_2, \epsilon_3, \epsilon_4$ are positive numbers to be chosen.
Denoting with

$$V_2(t) = \frac{1}{2}(\|u\|^2 + A\|h\|^2), \tag{10.4.20}$$

applying the Poincaré's inequality, we have

$$\begin{aligned} \dot{V}_2(t) \le [M(\frac{1}{2\epsilon_1} + \frac{A}{2\epsilon_2}) - \mathrm{Re}^{-1}\frac{\pi^2}{4}]\|u\|^2 + A[M(\frac{1}{2\epsilon_3} + \frac{1}{2\epsilon_4}) + \\ - \mathrm{Rm}^{-1}\frac{\pi^2}{4}]\|h\|^2 + M(\frac{\epsilon_1}{2} + \frac{A\epsilon_3}{2})\|w\|^2 + MA(\frac{\epsilon_2}{2} + \frac{\epsilon_4}{2})\|\ell\|^2. \end{aligned} \tag{10.4.21}$$

Now we choose ϵ_i, $(i = 1, 2, 3, 4)$, in such a way that the coefficients of $\|u\|^2$ and $\|h\|^2$ are negative. For instance, $\epsilon_1 = \frac{8M\mathrm{Re}}{\pi^2}$, $\epsilon_2 = \frac{8AM\mathrm{Re}}{\pi^2}$, $\epsilon_3 = \epsilon_4 = \frac{8M\mathrm{Rm}}{\pi^2}$, we have

$$\dot{V}_2(t) \leq -\frac{\pi^2}{8\mathrm{Re}}\|u\|^2 - \frac{\pi^2}{8\mathrm{Rm}}\|h\|^2 + h_1\|w\|^2 + h_2 A\|\ell\|^2 \tag{10.4.22}$$

where h_1 and h_2 are the coefficients of $\|w\|^2$ and $\|\ell\|^2$ in (10.4.21) and we have now replaced the values of ϵ_i. Since, by (10.4.15), we have that $\|w\|^2 + A\|\ell\|^2 \leq C_1 e^{-\alpha_0 t}$, with C_1 a positive constant and $\alpha_0 = \frac{\pi^2}{2}\mathrm{Re}^{-1}\max(1, \mathrm{Pm}^{-1})$, we have

$$\dot{V}_2(t) \leq -\max\left(\frac{\pi^2}{8\mathrm{Re}}, \frac{\pi^2}{8A\mathrm{Rm}}\right)V_2 + C_1 e^{-\alpha_0 t}. \tag{10.4.23}$$

Integrating this last inequality and taking into account(10.4.15), the exponential decay of $V(t) = V_1 + V_2$ for *any Reynolds* number is easily obtained.
This means that the streamwise perturbations are always nonlinearly (and linearly) stable, i.e. $\mathrm{Re}^y = +\infty$.

This conclusion and the results we have obtained in SubSec. 10.4.1 for streamwise perturbations are in an *obvious contradiction*. As in the fluid dynamics case (see Falsaperla, Mulone, and Perrone, 2022a) probably this contradiction is due to the choice of the space of *kinematically admissible* perturbations where we look for the maximum. This space is too large and likely contains perturbations which are not admissible as *physical perturbations* competing for the maximum.
In the next subsection, we propose a conjecture to overcome this contradiction.

10.4.3 Conjecture and rigorous proof that spanwise perturbations are the least stabilizing perturbations

We observe that in the numerator of (10.4.5) do not appear explicitly the fields v and k. Therefore we are led to make the following conjecture:

Conjecture 10.4.1. *Let $\mathcal{S}_0$ the subspace of $\mathcal{S}$ consisting of functions $u, v, w, h, k, \ell \in \mathcal{S}$ such that $v = k = 0$. We call this space the space of the physical admissible perturbations competing for the maximum of the functional $\mathcal{F}$. We conjecture that the maximum m is assumed among the functions of this subspace.*

With this conjecture, we see immediately that the perturbations least stabilizing are two-dimensional and that they are the spanwise perturbations.
Indeed, from (10.4.5), we now have

$$m = \max_{\mathcal{S}_0} \frac{I}{\|\nabla u\|^2 + \|\nabla w\|^2 + \mathrm{Ha}^2(\|\nabla h\| + \|\nabla \ell\|)}. \tag{10.4.24}$$

The Euler-Lagrange equations of this maximum problem are given by

$$\begin{cases} [-U'(w\mathbf{i} + u\mathbf{k}) + A\bar{B}'(\ell\mathbf{i} - h\mathbf{k})] + 2m\Delta\mathbf{u} = \nabla\lambda_1 \\ A[\bar{B}'(u\mathbf{k} - w\mathbf{i}) + U'(\ell\mathbf{i} + h\mathbf{k})] + 2m\mathrm{Ha}^2\Delta\mathbf{h} = \nabla\lambda_2, \end{cases} \tag{10.4.25}$$

where now the Lagrange multipliers λ_1 and λ_2 are such that $\nabla\lambda_1 = (\lambda_{1x}, 0, \lambda_{1z})^T$, $\nabla\lambda_2 = (\lambda_{2x}, 0, \lambda_{2z})^T$ (this is because $v = k = 0$).
We take the third component of the double curl of (10.4.25) and the third component of the curl of (10.4.25). We obtain the system of the Euler-Lagrange equations written

in terms of ζ, w, ζ_M and ℓ:

$$\begin{cases} U'w_y - A\bar{B}'\ell_y + 2m\Delta\zeta = 0 \\ A\bar{B}'w_y - AU'\ell_y + 2m\mathrm{Ha}^2\Delta\zeta_M = 0 \\ U'(\zeta_y + 2w_{xz}) + U''w_x - A\bar{B}''\ell_x + A\bar{B}'\zeta_{M_y} + 2m\Delta\Delta w = 0 \\ -U'A(\zeta_{M_y} + 2\ell_{xz}) - U''A\ell_x + A\bar{B}''w_x - A\bar{B}'\zeta_y + 2m\mathrm{Ha}^2\Delta\Delta\ell = 0, \end{cases} \tag{10.4.26}$$

with the boundary conditions

$$w = w_z = \ell = \ell_z = 0, \quad \zeta = \zeta_M = 0. \tag{10.4.27}$$

where now $\zeta = -u_y$ and $\zeta_M = -h_y$.
We take the *second component* of the double curl of (10.4.25) to get

$$\begin{cases} U'\zeta_z + A\bar{B}'\zeta_{M_z} + U''\zeta + A\bar{B}''\zeta_M - U'w_{xy} + A\bar{B}'\ell_{xy} = 0 \\ \bar{B}'\zeta_z + U'\zeta_{M_z} + \bar{B}''\zeta + U''\zeta_M + \bar{B}'w_{xy} - U'\ell_{xy} = 0. \end{cases} \tag{10.4.28}$$

From $w = 0$ when $z = \pm 1$ we have that $w_{xy} = 0$ when $z = \pm 1$. Similarly, we have that $\ell = 0$ when $z = \pm 1$. Furthermore, taking into account, that also $w_z = \zeta = \ell_z = \zeta_M = 0$ when $z = \pm 1$, (10.4.28) evaluated in $z = \pm 1$ becomes

$$\begin{cases} U'\zeta_z + A\bar{B}'\zeta_{M_z} = 0, \quad z = \pm 1 \\ \bar{B}'\zeta_z + U'\zeta_{M_z} = 0, \quad z = \pm 1, \end{cases} \tag{10.4.29}$$

This system implies that $\zeta_z = \zeta_{M_z} = 0$ when $z = \pm 1$, if the determinant of the system, that is $det = U'^2 - A\bar{B}'^2 \neq 0$.
In the case of Couette flow

$$det = U'^2 - A\bar{B}'^2 = \frac{\mathrm{Ha}^2}{\sinh^2(\mathrm{Ha})}(\cosh^2(\mathrm{Ha}) - \mathrm{Pm}\sinh^2(\mathrm{Ha}))$$

which is nonzero at least if $\mathrm{Pm} \leq 1$.

In the case of Hartmann flow

$$det = U'^2 - A\bar{B}'^2 = \frac{\mathrm{Ha}^2}{(\cosh(\mathrm{Ha}) - 1)^2}(\sinh^2(\mathrm{Ha}) - \mathrm{Pm}(\cosh(\mathrm{Ha}) - \frac{\sinh(\mathrm{Ha})}{\mathrm{Ha}})^2)$$

which is nonzero at least if $\mathrm{Pm} \leq 1$ (this is a simple calculation that can also be checked with a math software).
From $(10.4.26)_{1-2}$ we have $\zeta_{zz} = \zeta_{M_{zz}} = 0$ when $z = \pm 1$.
Evaluating the derivative of $(10.4.26)_{1-2}$ with respect to z in $z = \pm 1$, we have that $\zeta_{zzz} = \zeta_{M_{zzz}} = 0$ when $z = \pm 1$.
In order to prove that also the fourth derivative of ζ and ζ_{M_z} is zero when $z = \pm 1$, we compute the second derivative of (10.4.28) with respect to z and evaluate it in $z = \pm 1$.
We obtain:

$$\begin{cases} -U'w_{xyzz} + A\bar{B}'\ell_{xyzz} = 0, \quad z = \pm 1 \\ \bar{B}'w_{xyzz} - U'\ell_{xyzz} = 0, \quad z = \pm 1. \end{cases} \tag{10.4.30}$$

As the determinant of this system is the same as before, that is $det = U'^2 - A\bar{B}'^2 \neq 0$, we have that $w_{xyzz} = \ell_{xyzz} = 0$ when $z = \pm 1$.
Therefore, evaluating the second derivative of $(10.4.26)_{1-2}$ with respect to z on $z = \pm 1$, we have that $\zeta_{zzzz} = \zeta_{M_{zzzz}} = 0$ when $z = \pm 1$.
Iterating this procedure we find that ζ and all its derivatives with respect to z are zero on the boundaries. The same for ζ_M and all its derivatives with respect to z. This implies that $\zeta = \zeta_M \equiv 0$, hence $u_y = h_y = 0$ and from $(10.4.26)_{1-2}$ also $w_y = \ell_y = 0$.
Therefore, $u = u(x,z), v = 0, w = w(x,z), h = h(x,z), k = 0, l = l(x,z)$ and the least stabilizing perturbations which satisfy the system

$$\begin{cases} 2U'w_{xz} + U''w_x - A\bar{B}''\ell_x + 2m\Delta\Delta w = 0 \\ -2U'\ell_{xz} - U''\ell_x + \bar{B}''w_x + 2m\mathrm{Pm}^{-1}\Delta\Delta\ell = 0, \end{cases} \tag{10.4.31}$$

with the boundary conditions $w = w_z = \ell = \ell_z = 0$ on $z = \pm 1$, are the spanwise perturbations. We note that (10.4.31) is the generalized Orr-Reynolds system for the maximum of $\mathcal{F}$.
Moreover, if we consider streamwise perturbations, from the system (10.4.31) we have:

$$\begin{cases} 2m\|\Delta w\|^2 = 0 \\ 2m\mathrm{Pm}^{-1}\|\Delta\ell\|^2 = 0, \end{cases} \tag{10.4.32}$$

which implies $m = 0$, i.e. $\mathrm{Re}^y = +\infty$.
Therefore we have proved:

Theorem 10.4.3. *Supposing that $U'^2 - A\bar{B}'^2 \neq 0$, then ζ, ζ_M and all their derivatives with respect to z are zero.*

Corollary 10.4.1. *In the hypothesis of the previous theorem, then $u_y = w_y = h_y = l_y = 0$ and a Squire theorem holds (see Squire, 1933): the least stabilizing perturbations in the energy norm $V(t)$ are two-dimensional and they are the spanwise perturbations.*

10.5 Some numerical results

We show here some numerical results. These results are obtained solving system (10.4.11) with boundary condition (10.4.12), where we fix respectively $a = 0$ for streamwise perturbations and $b = 0$ for spanwise perturbations. The generalized eigenvalue problem (10.4.11)-(10.4.12) is then solved with a Chebyshev collocation method, using between 50 and 70 base polynomials.

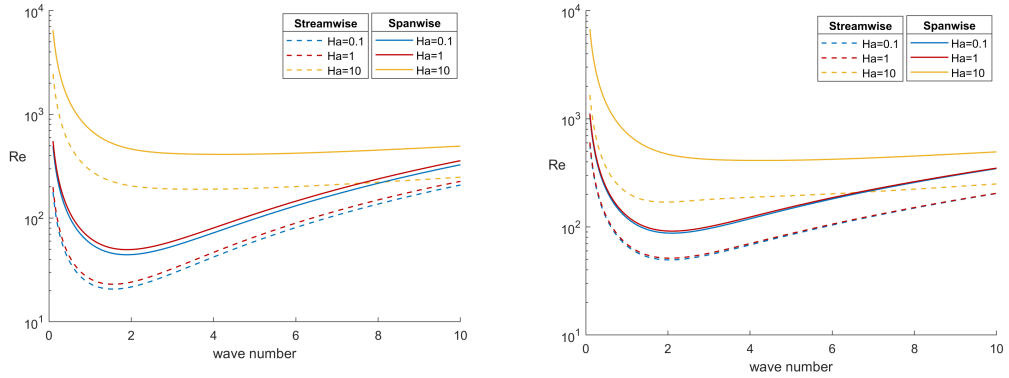

FIGURE 10.1: Orr-Reynolds critical number Re for magnetic Couette flow (left panel) and Hartmann flow (right panel) as a function of the wave numbers and magnetic Prandtl number Pm $= 0.1$. The wave numbers are respectively a and b for the spanwise and streamwise perturbations.

In Fig. 10.1 we fix Pm $= 0.1$ and Ha $= 0.1, 1, 10$ and we obtain the critical Reynolds number Re $= 1/m$ as a function of either a or b. We note from Fig. 10.1 that in all the cases the minima on streamwise curves are lower than the minima on the corresponding (same Ha) spanwise curves.

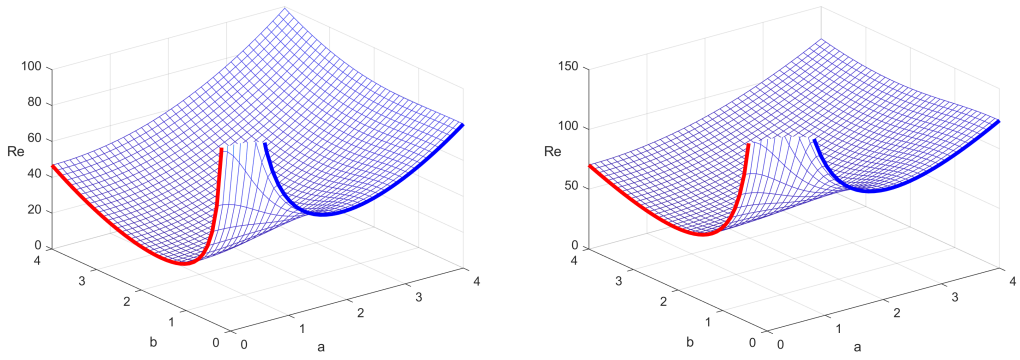

FIGURE 10.2: Orr-Reynolds critical number Re for magnetic Couette flow (left panel) and Hartmann flow (right panel) as a function of both wave numbers, magnetic Prandtl number Pm $= 0.1$ and Ha $= 1$.

In Fig. 10.2 we fix Pm $= 0.1$ and Ha $= 1$ and show Re as a function of *both* a and b. In this way we can check (at least for these sample values of Pm, Ha) that the global minimum with respect to a, b is achieved on streamwise perturbations. In both panels of Fig. 10.2 the streamwise and spanwise curves are highlighted by bolder curves (on the $a = 0$ or $b = 0$ planes), and they are a portions of the curves showed in Fig. 10.1 (for Ha $= 1$).

10.6 Discussion of the results

In this paper we study the nonlinear stability of *magnetohydrodynamics plane Couette and Hartmann* shear flows. We prove that the streamwise perturbations are always

stable. However our numerical calculations for the solutions of the Euler-Lagrange equations for the maximum of the functional ratio (10.4.5) give critical Reynolds numbers on the streamwise perturbations.
To resolve this contradiction, we propose a conjecture relating to the choice of physically admissible perturbations competing for the maximum (10.4.24) that gives the critical Reynolds number on the spanwise perturbations.
With this conjecture here we rigorously prove that the least stabilizing perturbations, in the energy norm, are the spanwise perturbations (we recall that in the fluid dynamics case the critical Reynolds number for spanwise perturbations was only supposed by Orr, 1907). This results implies a Squire theorem for nonlinear stability.

Chapter 11

Stability of plane shear flows in a layer with rigid and stress-free boundary conditions

The results presented in this Section have been published by Falsaperla, Mulone, and Perrone, 2022d.

11.1 Summary

We study the stability of shear flows of an incompressible fluid contained in a horizontal layer. We consider rigid - rigid, rigid - stress-free and stress-free - stress-free boundary conditions. We study (and recall some known results) linear stability/instability of the basic Couette, Poiseuille and a laminar parabolic flow with the spectral analysis by using the Chebyshev collocation method. We then use an L_2-energy with Lyapunov second method to obtain nonlinear critical Reynolds numbers, by solving a maximum problem arising from the Reynolds energy equation. We obtain this maximum (which gives the minimum Reynolds number) for streamwise perturbations $\mathrm{Re}_c = \mathrm{Re}^y$. However, this contradicts a theorem which proves that streamwise perturbations are always stabilizing, $\mathrm{Re}^y = +\infty$. Following Falsaperla, Mulone, and Perrone, 2022a (see Sec. 9) we solve this contradiction with a conjecture and prove that the critical nonlinear Reynolds numbers are obtained for two-dimensional perturbations, the spanwise perturbations, $\mathrm{Re}_c = \mathrm{Re}^x$, as Orr had supposed in the classic case of Couette flow between rigid planes.

11.2 State of the art

In Sec. 9 we presented the results of Falsaperla, Mulone, and Perrone, 2022a where we have studied the nonlinear stability of plane Couette and Poiseuille flows with rigid (and periodic) boundary conditions.
Here we investigate the stability for the classical shear flows, Couette and Poiseuille, in the cases of one rigid an the other stress-free (also called slip-free) boundaries, RF, and both stress-free FF boundaries, for completeness we also add the results for rigid RR boundaries. We also consider a case of a parabolic laminar flow where we assign the velocity at the bottom and the third component of the velocity and the tangential stress at top boundary, this problem is more appropriate for studying the flow of water in a river, see Falsaperla, Mulone, and Perrone, 2022c.
Although the case of stress-free planes is an ideal case (which is more appropriate in astrophysics and meteorology) in some applications it is useful to consider such boundary conditions. For example at the interface of a multiphase flow FF boundary

conditions can occur in situations including micro-and nano-fluid flow, flow over hydrophobic surfaces, rising bubbles in quiescent liquid, and polymer extrusion processes, see Tan, 2018 where the free-slip boundary condition with an adaptive Cartesian grid method has been implemented. In numerical applications, the possibility of using free-slip conditions within the context of the particle finite element method (PFEM) has been investigated Cerquaglia et al., 2017 "for high Reynolds number engineering applications in which tangential effects at the fluid-solid boundaries are not of primary interest, the use of free-slip conditions can alleviate the need for very fine boundary layer meshes".
In Rao and Rajagopal, 1999 a history of slip and no-slip boundary conditions and a list of references can be found. The authors in particular observe that "it has been found that a large class of polymeric materials slip or stick-slip on solid boundaries. For instance, when polymeric melts flow due to an applied pressure gradient, there is a sudden increase in the throughput at a critical", see Rf. Rao and Rajagopal, 1999 p. 113.
The existence of slip between the velocity of the fluid at the wall and the speed of the wall sometimes is considered, see Khaled and Vafai, 2004, the relative velocity is assumed to be proportional to the shear rate at the wall with a suitable slip coefficient (here we do not consider this interesting case that will be object of future study).
In Sec. 7 we have already recalled the classical results for Couette and Poiseuille for RR boundary conditions.
Rionero and Mulone, 1991 studied the nonlinear stability of Couette and Poiseuille flows with the Lyapunov second method in the case of stress-free boundary conditions. By using a weighted energy they proved that plane Couette flows and plane Poiseuille flows are conditionally asymptotically nonlinear stable for any Reynolds numbers. They observed that, by applying the classical L_2-energy method, it is possible to obtain global nonlinear stability. However, they have not studied the maximum problem obtained from the Reynolds-Orr equation, and by introducing a suitable kinematically admissible velocity field, they proved that the nonlinear critical Reynolds numbers are less than 80 and 40 in the FF case of Couette and Poiseuille flows, respectively.
In Falsaperla, Mulone, and Perrone, 2022a we have pointed out that the problem of finding the best conditions for global nonlinear energy stability with respect to three-dimensional perturbations is a complex problem. This problem is equivalent to finding the maximum of a functional ratio that arises from the Reynolds-Orr energy equation, see Reynolds, 1883. In particular in Falsaperla, Mulone, and Perrone, 2022a, using the RR boundary conditions, we run into a contradiction. Also here, using RF and FF boundary conditions, a similar problem arises.
The plan of the paper is the following.
In Sec. 11.3 we write the non-dimensional perturbation equations of laminar flows: plane Couette, plane Poiseuille and "parabolic" flow, and we recall the classical linear stability/instability results.
In Sec. 11.4 we prove nonlinear exponential stability of streamwise perturbations for any Reynolds number and any boundary conditions, i.e. $\mathrm{Re}^y = +\infty$ with respect to the L_2-energy norm. Furthermore, we study the maximum problem arising from the Reynolds energy, we arrive at a contradiction and make a conjecture to solve it by introducing the space of physical admissible perturbations competing for the maximum problem. In this space we find the optimal perturbations which give the critical Reynolds number: the spanwise perturbations, as Orr, 1907 had supposed in the case RR.
Sec. 11.5 is dedicated to the discussion of the results.

11.3 Laminar flows between two parallel planes

Given a reference frame $Oxyz$, with unit vectors $\mathbf{i}, \mathbf{j}, \mathbf{k}$, consider the layer $\mathcal{D} = \mathbb{R}^2 \times [-1, 1]$ of thickness 2 with horizontal coordinates x, y and vertical coordinate z.
Plane parallel shear flows are solutions of the stationary Navier-Stokes eqs. (4.0.2). The velocity field $\mathbf{U}$ has the form $\mathbf{U} = f(z)\mathbf{i}$. In particular, for fixed velocity at the boundaries $z = \pm 1$, we have the well known profiles:
a) *Couette* $f(z) = z$,
b) *Poiseuille* $f(z) = 1 - z^2$.
If the velocity vanishes at $z = -1$ and its derivative with respect to z vanishes at $z = 1$, we have the
c) *laminar parabolic flow* $f(z) = \frac{1}{4}[-z^2 + 2z + 3]$ (see eq. (6) in Falsaperla et al. 2020b).

11.3.1 Perturbation equations

The perturbation equations to the plane parallel shear flows, in non-dimensional form, are

$$\begin{cases} u_t = -\mathbf{u}\cdot\nabla u + \mathrm{Re}^{-1}\Delta u - (f u_x + f' w) - \dfrac{\partial p}{\partial x} \\ v_t = -\mathbf{u}\cdot\nabla v + \mathrm{Re}^{-1}\Delta v - f v_x - \dfrac{\partial p}{\partial y} \\ w_t = -\mathbf{u}\cdot\nabla w + \mathrm{Re}^{-1}\Delta w - f w_x - \dfrac{\partial p}{\partial z} \\ \nabla\cdot\mathbf{u} = 0, \end{cases} \tag{11.3.1}$$

where $\mathbf{u} = u\mathbf{i} + v\mathbf{j} + w\mathbf{k}$ is the perturbation to the velocity field, p is the perturbation to the pressure field.
Throughout the paper, we use the symbol h_x as $\frac{\partial h}{\partial x}$, h_t as $\frac{\partial h}{\partial t}$, etc., for any function h, $f' = \dfrac{df}{dz}$.
To system (11.3.1) we append the
rigid (R) boundary conditions

$$\mathbf{u}(x, y, \pm 1, t) = 0, \quad (x, y, t) \in \mathbb{R}^2 \times (0, +\infty),$$

stress-free (F) boundary conditions

$$u_z(x, y, \pm 1, t) = v_z(x, y, \pm 1, t) = w(x, y, \pm 1, t) = 0,$$

$(x, y, t) \in \mathbb{R}^2 \times (0, +\infty)$,
in this case, in order to guarantee the uniqueness we must add the average conditions

$$\int_\Omega u \, dz\, dy\, dz = \int_\Omega v \, dz\, dy\, dz = 0$$

Kloeden and Wells, 1983 (Ω is the cell of periodicity, see eq. (8.5.1)),
or *mixed (RF, rigid - stress-free)* boundary conditions

$$\mathbf{u}(x, y, -1, t) = 0, \quad (x, y, t) \in \mathbb{R}^2 \times (0, +\infty),$$

$$u_z(x, y, 1, t) = v_z(x, y, 1, t) = w(x, y, 1, t) = 0,$$

$(x, y, t) \in \mathbb{R}^2 \times (0, +\infty)$.

We also give the initial condition

$$\mathbf{u}(x,y,z,0) = \mathbf{u_0}(x,y,z), \quad \text{in} \quad \mathcal{D},$$

with $\mathbf{u_0}(x,y,z)$ solenoidal vector which vanishes at the boundaries.

11.3.2 Linear stability/instability

The linear stability/instability is obtained by studying the linearised system by neglecting the terms $\mathbf{u}\cdot\nabla u$, $\mathbf{u}\cdot\nabla v$, $\mathbf{u}\cdot\nabla w$ in (11.3.1).
The linear perturbation equations become

$$\begin{cases} u_t = \mathrm{Re}^{-1}\Delta u - (fu_x + f'w) - \dfrac{\partial p}{\partial x} \\ v_t = \mathrm{Re}^{-1}\Delta v - fv_x - \dfrac{\partial p}{\partial y} \\ w_t = \mathrm{Re}^{-1}\Delta w - fw_x - \dfrac{\partial p}{\partial z} \\ \nabla\cdot\mathbf{u} = 0. \end{cases} \tag{11.3.2}$$

Since the system is autonomous, we consider solutions of the form (cf. Drazin and Reid, 2004; Straughan, 2004):

$$f(x,y,z,t) = f(z)e^{i(ax+by)+ct}, \tag{11.3.3}$$

with $f = u, v, w$ or p, in the domain $\mathbb{R}^2 \times (-1,1) \times (0,+\infty)$, $a \geq 0$, $b \geq 0$, $a^2+b^2 > 0$, and c is a complex number. By substituting (11.3.3) in (11.3.2), we have the system

$$\begin{cases} cu + iafu + f'w = \mathrm{Re}^{-1}(D^2 - (a^2+b^2))u - iap \\ cv + iafv = \mathrm{Re}^{-1}(D^2 - (a^2+b^2))v - ibp \\ cw + iafw = \mathrm{Re}^{-1}(D^2 - (a^2+b^2))w - Dp \\ iau + ibv + Dw = 0, \end{cases} \tag{11.3.4}$$

where D and D^2 indicate first and second derivatives with respect to z.
We recall that, for rigid boundary conditions, the classical result of Romanov, 1973 proves that Couette flow is *linearly stable* for *any Reynolds* number. Instead, Poiseuille flow is unstable for any Reynolds number bigger that 5772 (Orszag, 1971).
We observe that, in the linear case, the Squire theorem (see Squire, 1933) holds, and the most destabilizing perturbations are two-dimensional, in particular the spanwise perturbations (see Drazin and Reid, 2004, p. 155). The critical Reynolds value, for Poiseuille flow, can be obtained by solving the celebrated Orr-Sommerfeld equation (see Drazin and Reid, 2004).
Applying the Squire transformation, we are led to study the system of the spanwise perturbations:

$$\begin{cases} cu + iafu + f'w = \mathrm{Re}^{-1}(D^2 - a^2)u - iap \\ cw + iafw = \mathrm{Re}^{-1}(D^2 - a^2)w - Dp \\ iau + Dw = 0, \end{cases} \tag{11.3.5}$$

We differentiate the first and second member of $(11.3.5)_1$ with respect to z, then multiply by ia; multiply both sides of $(11.3.5)_1$ by a^2. Taking into account $(11.3.5)_3$, adding term to term the equations so obtained, we get the *Orr-Sommerfeld equation*, Sommerfeld, 1908 (cf. Drazin and Reid, 2004, p. 156)

$$c(D^2 - a^2)w + iaf(D^2 - a^2)w - f''iaw = \mathrm{Re}^{-1}(D^2 - a^2)^2 w. \tag{11.3.6}$$

This equation can also be obtained by taking the third component of the double curl of the equation

$$c\mathbf{u} + f\mathbf{u}_x + f'w\mathbf{i} = \mathrm{Re}^{-1}\Delta\mathbf{u} - \nabla p \tag{11.3.7}$$

and applying the solenoidality of the velocity field and the Squire transformation.
It is easy to see that both Couette and Poiseuille flows under stress-free boundary conditions are *linearly stable* for any Reynolds number. This is in agreement with the result of Rionero and Mulone, 1991. Moreover, plane Couette flow, with rigid boundary conditions is *linearly stable for any* Reynolds numbers (Romanov, 1973).
By solving this equation with the Chebyshev collocation method, we obtain the following results for linear stability/instability:

Couette

1. In the stress-free - stress-free case we have stability for any Reynolds number, see Rionero and Mulone, 1991 (Fig. 11.1).

2. In the rigid - stress-free case we have stability for any Reynolds number (in this case we obtain a graph very similar to the FF case).

3. In the rigid - rigid case we have stability for any Reynolds number, see Romanov, 1973 (in this case we obtain a graph very similar to the FF case).

Poiseuille

1. In the stress-free - stress-free case we have stability for any Reynolds number, see Rionero and Mulone, 1991, (Fig. 11.2).

2. In the rigid - stress-free case we have instability for $\mathrm{Re} > 169785$ (see Fig. 11.3, left panel).

3. In the rigid - rigid case we have instability for $\mathrm{Re} > 5772$ (Orszag, 1971), (see Fig. 11.4, right panel).

Laminar parabolic flow

1. In the stress-free - stress-free case we have stability for any Reynolds number (see Fig. 11.5, top panel)

2. In the rigid - stress-free case we have stability of any Reynolds number, see Falsaperla, Mulone, and Perrone, 2022c (Fig. 11.5, middle panel).

3. In the rigid - rigid case we have stability for any Reynolds number (see Fig. 11.5, bottom panel).

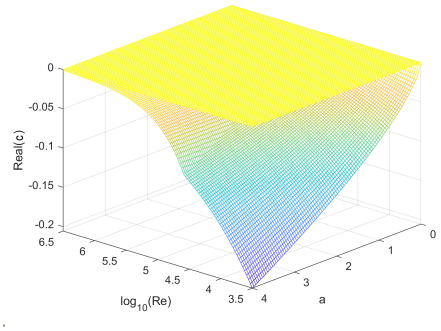

FIGURE 11.1: Plane Couette (linear) stability. The surface gives the maximum real part of the time decay coefficient $Real(c)$, when a runs from 0 to 4, and the Reynolds number Re is in the interval $[10^{3.5}, 10^{6.5}]$ for Orr-Sommerfeld equation (11.3.6) with FF boundary conditions (for RF and RR boundaries the graphics are very similar). The horizontal plane corresponds to $Real(c) = 0$. Other computations in larger ranges of Re and a confirm these stability results.

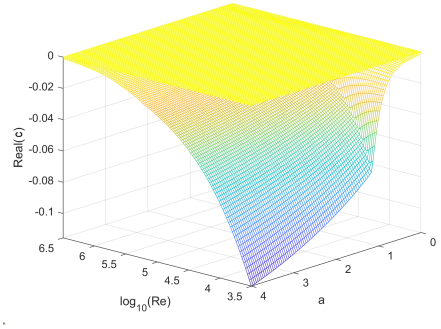

FIGURE 11.2: Plane Poiseuille (linear) stability. The surface gives the maximum real part of the time decay coefficient $Real(c)$, when a runs from 0 to 4, and the Reynolds number Re is in the interval $[10^{3.5}, 10^{6.5}]$ for Orr-Sommerfeld equation (11.3.6) with FF boundary conditions. The horizontal planes correspond to $Real(c) = 0$.

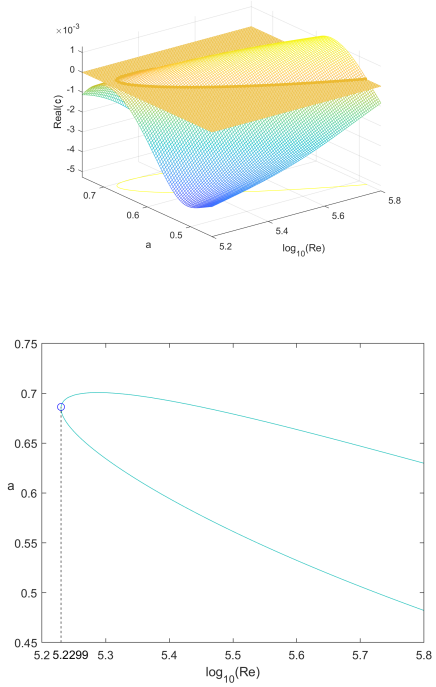

FIGURE 11.3: On the top: the surface gives the real part of the time decay coefficient $Real(\sigma)$ for Orr-Sommerfeld equation (11.3.6) with *RF* boundary conditions, a runs from 0.45 to 0.75, and the Reynolds number Re is in the interval $[10^{5.2}, 10^{5.8}]$. The meshed plane corresponds to $Real(c) = 0$, the surface corresponds to the set of points $(a, log_{10}(\mathrm{Re}), Real(c))$. On the bottom: the correspondent critical curve in the a-Re plane is plotted; the minimum is highlighted by a circle and its numerical value is marked on the horizontal axis. The minimum is equal to $\mathrm{Re} = 169785$.

11.4 Nonlinear energy stability

Assume that both $\mathbf{u}$ and ∇p are x, y-periodic with periods a and b in the x and y directions, respectively, with wave numbers $(a, b) \in \mathbb{R}^2_+$. In the following it suffices therefore to consider functions over the periodicity cell Ω (see 8.5.1).
As the basic function space, we take $L_2(\Omega)$, which is the space of square-summable functions in Ω.
Here we study *the nonlinear energy stability with the Lyapunov method*, by using the classical energy

$$V(t) = \frac{1}{2}[\|u\|^2 + \|v\|^2 + \|w\|^2].$$

We obtain *sufficient conditions of global nonlinear stability*.
Taking into account the solenoidality of $\mathbf{u}$ and the boundary condition, we write the Reynolds-Orr energy identity, see Reynolds, 1883,

$$\dot{V} = -(f'w, u) - \mathrm{Re}^{-1}[\|\nabla u\|^2 + \|\nabla v\|^2 + \|\nabla w\|^2], \tag{11.4.1}$$

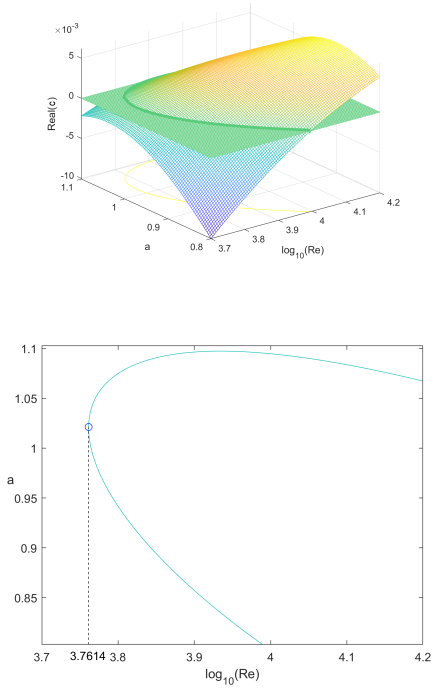

FIGURE 11.4: On the top: the surface gives the real part of the time decay coefficient $Real(\sigma)$ for Orr-Sommerfeld equation (11.3.6) with RR boundary conditions, a runs from 0.45 to 0.75, and the Reynolds number Re is in the interval $[10^{3.7}, 10^{4.2}]$. The meshed plane corresponds to $Real(c) = 0$, the surface corresponds to the set of points $(a, log_{10}(\mathrm{Re}), Real(c))$. On the bottom: the correspondent critical curves in the a-Re plane are plotted; the minimum is highlighted by a circle and its numerical value is marked on the horizontal axis. The minimum is equal to $\mathrm{Re} = 5772$, the Orszag, 1971 result.

and we have

$$\begin{aligned}
&\dot{V} = -(f'w, u) - \mathrm{Re}^{-1}[\|\nabla u\|^2 + \|\nabla v\|^2 + \|\nabla w\|^2] = \\
&= \left(\frac{-(f'w, u)}{\|\nabla u\|^2 + \|\nabla v\|^2 + \|\nabla w\|^2} - \frac{1}{\mathrm{Re}} \right) \|\nabla \mathbf{u}\|^2 \leq \\
&\leq \left(\frac{1}{\mathrm{Re}_c} - \frac{1}{\mathrm{Re}} \right) \|\nabla \mathbf{u}\|^2,
\end{aligned} \tag{11.4.2}$$

where

$$\frac{1}{\mathrm{Re}_c} = m = \max_{\mathcal{S}} \frac{-(f'w, u)}{\|\nabla u\|^2 + \|\nabla v\|^2 + \|\nabla w\|^2}, \tag{11.4.3}$$

$\mathcal{S}$ is the space of the *kinematically admissible fields*

$$\begin{aligned}
&\mathcal{S} = \{u, v, w \in H^2(\Omega), \text{ satisfying the boundary} \\
&\text{conditions } RR, RF, FF, \text{ periodic in } x, \text{ and } y, \\
&u_x + v_y + w_z = 0, \quad \|\nabla \mathbf{u}\| > 0\},
\end{aligned} \tag{11.4.4}$$

and $H^2(\Omega)$ is the Sobolev space of the functions which are in $L_2(\Omega)$ together with their first and second generalized derivatives.

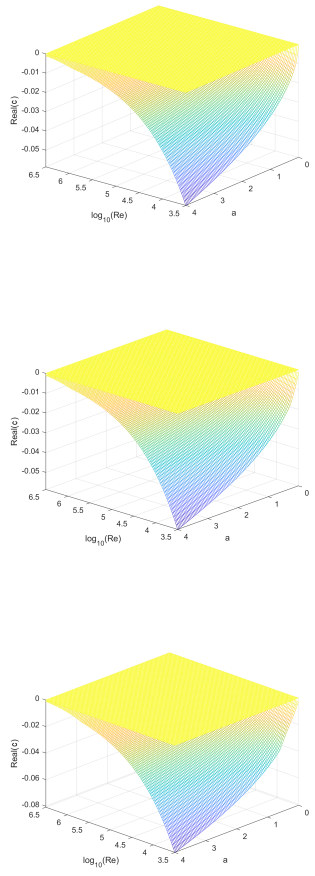

FIGURE 11.5: Plane parabolic (linear) stability. Each surface gives the real part of the time decay coefficient $Real(c)$, when a runs from 0 to 4, and the Reynolds number Re is in the interval $[10^{3.5}, 10^{6.5}]$ for Orr-Sommerfeld equation (11.3.6) with FF, RF and RR boundary conditions (from top to bottom). Each meshed plane corresponds to $\mathrm{Re}\,(c) = 0$, the surface corresponds to the set of points $(a, log_{10}(\mathrm{Re}\,), Real(c))$.

The Euler-Lagrange equations of this maximum problem are given by

$$-f'w\mathbf{i} - f'u\mathbf{k} + 2m\Delta\mathbf{u} = \nabla\lambda, \tag{11.4.5}$$

where λ is a Lagrange multiplier in the cases RR and RF.
In the case FF, the Euler-Lagrange equations of this maximum problem are given by

$$-f'w\mathbf{i} - f'u\mathbf{k} + 2m\Delta\mathbf{u} = \nabla\lambda + \mathbf{h}, \tag{11.4.6}$$

where the function λ and the constant vector $\mathbf{h} = (h_1, h_2, 0)^T$ are Lagrange multipliers which come from the zero divergence of the velocity vector $\mathbf{u}$, and the zero mean conditions of u and v, respectively.
It is easy to prove that $\mathbf{h} = 0$. For this we write equation (11.4.6) in components

$$\begin{cases} -f'w + 2m\Delta u = \lambda_x + h_1 \\ 2m\Delta v = \lambda_y + h_2 \\ -f'u + 2m\Delta w = \lambda_z \,. \end{cases} \tag{11.4.7}$$

Integrating $(11.4.7)_2$ over Ω we have

$$2m \int_\Omega \Delta v d\,\Omega = \int_\Omega \lambda_y d\,\Omega + \int_\Omega h_2 d\,\Omega.$$

Due to the boundary conditions and the periodicity it follows

$$h_2(meas(\Omega)) = 0$$

and so $h_2 = 0$. Integrating $(11.4.7)_1$ over Ω we have

$$-\int_\Omega f'w d\,\Omega + 2m \int_\Omega \Delta u d\,\Omega = \int_\Omega \lambda_x d\,\Omega + \int_\Omega h_1 d\,\Omega.$$

As before we deduce

$$-\int_\Omega f'w d\,\Omega = h_1(meas(\Omega)).$$

Computing this integral and using the boundary conditions and the divergence-free equation, we have

$$-\int_\Omega f'w d\,\Omega = \int_\Omega f w_z d\,\Omega = -\int_\Omega [(fu)_x + (fv)_y] d\,\Omega = 0,$$

and so also $h_1 = 0$. Therefore the Euler-Lagrange equations are given by (11.4.5) for any boundary condition.
We define

$$\zeta = v_x - u_y$$

(it is linked to the toroidal part of the decomposition of the velocity vector $\mathbf{u}$ in the poloidal, toroidal and the mean flow, see Kaiser and Mulone, 2005; Kaiser, Tilgner, and Wahl, 2005) and take the third component of the *double curl* of (11.4.5) and the third component of the *curl* of (11.4.5). We obtain the system of the Euler-Lagrange equations written in terms of ζ and w:

$$\begin{cases} f'(\zeta_y + 2w_{xz}) + f''w_x + 2m\Delta\Delta w = 0 \\ f'w_y + 2m\Delta\zeta = 0, \end{cases} \tag{11.4.8}$$

with the boundary conditions

$$w = w_z = 0,\ \zeta = 0 \tag{11.4.9}$$

on $z = \pm 1$ in the RR case,

$$w = w_z = 0,\ \zeta = 0 \text{ on } z = -1 \text{ and } w = w_{zz} = 0,\ \zeta_z = 0 \text{ on } z = 1 \tag{11.4.10}$$

in the RF case,
and

$$w = w_{zz} = 0,\ \zeta_z = 0, \tag{11.4.11}$$

on $z = \pm 1$ in the FF case.

By solving this system with the Chebyshev collocation method, and using 80 polynomials, we obtain that the critical Reynolds numbers are reached for streamwise perturbations, $\mathrm{Re}_c = \mathrm{Re}^y$.

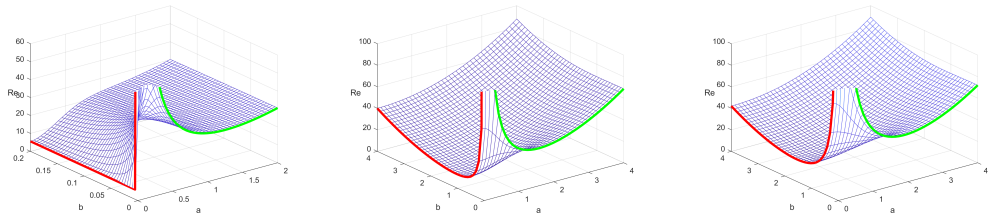

FIGURE 11.6: Plane Couette energy Orr-Reynolds number $\mathrm{Re} = \mathrm{Re}_c$ as function of the wave numbers a and b, for system (11.4.8) with FF, RF and RR boundary conditions (from top to bottom). The absolute minimum of each surface is achieved on the streamwise perturbations ($a = 0$).

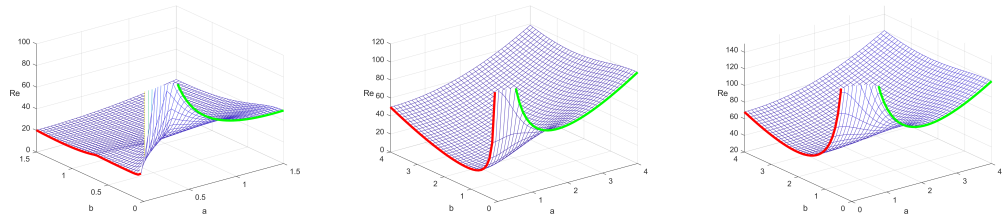

FIGURE 11.7: Plane Poiseuille energy Orr-Reynolds number $\mathrm{Re} = \mathrm{Re}_c$ as function of the wave numbers a and b, for system (11.4.8) with FF, RF and RR boundary conditions (from top to bottom). The absolute minimum of each surface is achieved on the streamwise perturbations ($a = 0$).

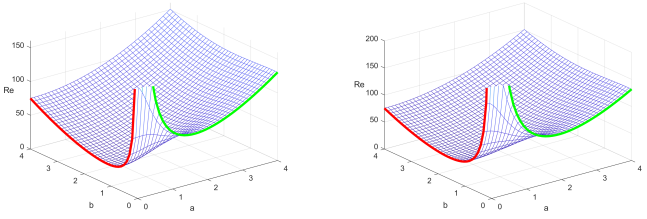

FIGURE 11.8: Plane parabolic energy Orr-Reynolds number $\mathrm{Re} = \mathrm{Re}_c$ as function of the wave numbers a and b, for system (11.4.8) with RF and RR boundary conditions (from top to bottom). The absolute minimum of each surface is achieved on the streamwise perturbations ($a = 0$).

In Table 11.1 we report the critical energy Orr-Reynolds numbers obtained for streamwise Re^y, and for spanwise perturbations Re^x, corresponding to the solutions of system (11.4.8).
In the next subsection we prove that the streamwise perturbations are stable for any Reynolds number. This means that the previous results, even if numerically correct

	Couette		Poiseuille		Parabolic	
RR	$\mathrm{Re}^x = 44.30$	$a = 1.89$	$\mathrm{Re}^x = 87.59$	$a = 2.09$	$\mathrm{Re}^x = 84.95$	$a = 1.92$
	$\mathrm{Re}^y = 20.66$	$b = 1.55$	$\mathrm{Re}^y = 49.59$	$b = 2.05$	$\mathrm{Re}^y = 39.86$	$b = 1.58$
RF	$\mathrm{Re}^x = 34.88$	$a = 1.57$	$\mathrm{Re}^x = 62.64$	$a = 1.70$	$\mathrm{Re}^x = 72.98$	$a = 1.62$
	$\mathrm{Re}^y = 12.93$	$b = 1.04$	$\mathrm{Re}^y = 22.25$	$b = 1.15$	$\mathrm{Re}^y = 30.63$	$b = 1.13$
FF	$\mathrm{Re}^x = 26.34$	$a = 1.21$	$\mathrm{Re}^x = 48.89$	$a = 1.39$	$\mathrm{Re}^x = 50.51$	$a = 1.27$
			$\mathrm{Re}^y = 19.22$	$b = 1.14$		
FR	$\mathrm{Re}^x = 34.88$	$a = 1.57$	$\mathrm{Re}^x = 62.64$	$a = 1.70$	$\mathrm{Re}^x = 61.73$	$a = 1.57$
	$\mathrm{Re}^y = 12.93$	$b = 1.04$	$\mathrm{Re}^y = 22.25$	$b = 1.15$	$\mathrm{Re}^y = 21.19$	$b = 1.02$

TABLE 11.1: We report the Reynolds numbers and wave numbers for spanwise (Re^x, a) and streamwise (Re^y, b) perturbations, obtained from system (11.4.8) for different basic laminar flows and boundary conditions. The case *FR* corresponds to consider stress-free perturbations at the bottom plane.

(see for example the case of the Couette flow with rigid boundary conditions studied by Joseph, 1968) do not match the physics of the problem, see Falsaperla, Mulone, and Perrone, 2022a. This is due to a possible wrong choice of the space of the fields competing for a maximum problem (see below).

11.4.1 Stability of streamwise perturbations for any Reynolds number

We assume that the perturbations are *streamwise*, i.e. they *do not depend on* x ($\frac{\partial}{\partial x} \equiv 0$). Therefore the perturbation equations (11.3.1) become

$$\begin{cases} u_t = -\mathbf{u}\cdot\nabla u + \mathrm{Re}^{-1}\Delta u - f'w \\ v_t = -\mathbf{u}\cdot\nabla v + \mathrm{Re}^{-1}\Delta v - \dfrac{\partial p}{\partial y} \\ w_t = -\mathbf{u}\cdot\nabla w + \mathrm{Re}^{-1}\Delta w - \dfrac{\partial p}{\partial z} \\ v_y + w_z = 0. \end{cases} \tag{11.4.12}$$

We use the *classical energy norm* and show that the streamwise perturbations cannot destabilize the basic laminar flows: Couette, Poiseuille and laminar parabolic flow (see Falsaperla, Mulone, and Perrone, 2022a).
We multiply $(11.4.12)_1$ by u and integrate over Ω (now $\Omega = \Omega_{yz} = [0, \frac{2\pi}{b}] \times [-1, 1]$). Besides, we multiply $(11.4.12)_2$ and $(11.4.12)_3$ by v and w and integrate over Ω. By taking into account of the solenoidality of $\mathbf{u}$, the boundary conditions and the periodicity, we have

$$\frac{d}{dt}\frac{\|u\|^2}{2} = -(f'u, w) - \mathrm{Re}^{-1}\|\nabla u\|^2,$$

$$\frac{d}{dt}\left(\frac{\|v\|^2}{2} + \frac{\|w\|^2}{2}\right) = -\mathrm{Re}^{-1}[\|\nabla v\|^2 + \|\nabla w\|^2].$$

By using the Wirtinger inequality, see Kaiser and Mulone, 2005; Kaiser and Xu, 1998,

$$\frac{d}{dt}(\frac{\|v\|^2}{2}+\frac{\|w\|^2}{2}) = -\mathrm{Re}^{-1}[\|\nabla v\|^2+\|\nabla w\|^2] \leq \\ \leq -C(\|v\|^2+\|w\|^2). \tag{11.4.13}$$

and integrating we have

$$\|v\|^2+\|w\|^2 \leq H_0 e^{-2Ct}, \quad H_0 = \|v_0\|^2+\|w_0\|^2, \tag{11.4.14}$$

where C is a positive constant which depends on the domain and the boundary conditions: $C = \frac{1}{\mathrm{Re}}\min\{\frac{\pi^2}{4}, b^2\}$ for FF boundaries, $C = \frac{\pi^2}{16\mathrm{Re}}$ for RF boundaries, and $C = \frac{\pi^2}{4\mathrm{Re}}$ for RR boundaries. v_0 and w_0 are the initial values of v and w.
Now we consider the equation depending on u and define $M = \max_{[-1,1]}|f'(z)|$. We have the following inequalities:

$$\begin{aligned}\frac{d}{dt}\frac{\|u\|^2}{2} &= -(f'u,w) - \mathrm{Re}^{-1}\|\nabla u\|^2 \leq M\|u\|\|w\|+ \\ &- \mathrm{Re}^{-1}\|\nabla u\|^2 \leq M(\frac{\|u\|^2}{2\epsilon}+\frac{\epsilon}{2}\|w\|^2)+ \\ &- \mathrm{Re}^{-1}\|\nabla u\|^2 \leq M(\frac{\|u\|^2}{2\epsilon}+\frac{\epsilon}{2}\|w\|^2)+ \\ &- C\|u\|^2 = (\frac{M}{2\epsilon}-C)\|u\|^2+\frac{\epsilon}{2}M\|w\|^2 = \\ &= -\frac{C}{2}\|u\|^2+\frac{M^2}{C}\frac{\|w\|^2}{2}.\end{aligned} \tag{11.4.15}$$

where $\epsilon = \frac{M}{C}$.
We use this inequality and (11.4.14) to obtain

$$\begin{aligned}\frac{d}{dt}\|u\|^2 &\leq -C\|u\|^2+\frac{M^2}{C}\|w\|^2 \leq -C\|u\|^2+ \\ &+\frac{M^2}{C}(\|v\|^2+\|w\|^2) \leq -C\|u\|^2+\frac{M^2}{C}H_0e^{-2Ct}.\end{aligned} \tag{11.4.16}$$

Integrating last inequality, we have

$$\|u\|^2 \leq e^{-Ct}[k-\frac{M^2}{C^2}H_0e^{-Ct}] = ke^{-Ct}-\frac{M^2}{C^2}H_0e^{-2Ct}, \tag{11.4.17}$$

with $k = K_0+\frac{M^2}{C^2}H_0$, $\quad K_0 = \|u_0\|^2$, and u_0 are the initial value of u.
We introduce the classical energy

$$L(t) = \frac{1}{2}[\|u\|^2+\|v\|^2+\|w\|^2], \tag{11.4.18}$$

and observe that the initial energy is given by $L_0 = \frac{H_0+K_0}{2}$. Adding the (11.4.14) and the (11.4.17) we finally have:

$$
\begin{aligned}
L(t) &\leq H_0 e^{-2Ct} + (K_0 + \frac{M^2}{C^2} H_0) e^{-Ct} - \frac{M^2}{C^2} H_0 e^{-2Ct} \leq \\
&\leq L_0 e^{-2Ct} + (L_0 + \frac{M^2}{C^2} L_0) e^{-Ct} = \\
&= L_0 (e^{-2Ct} + e^{-Ct} + \frac{M^2}{C^2} e^{-Ct}).
\end{aligned} \tag{11.4.19}
$$

This inequality implies nonlinear exponential stability of the basic laminar flows (Couette, Poiseuille and parabolic) with respect to the streamwise perturbations *for any* Reynolds number.

Therefore, we have proved:

Theorem 11.4.1. *Assuming the perturbations to the basic shear flows* $\mathbf{U} = f(z)\mathbf{i}$ *are streamwise, then we have nonlinear stability according to* (11.4.19) *for any Reynolds number.*

From this Theorem we have $\mathrm{Re}^y = +\infty$, i.e., *the streamwise perturbations cannot destabilize the basic flows.* This contradicts the numerical results we have reached (cf. Joseph, 1968, Joseph and Carmi, 1969 and Busse, 1972, in the *RR* case).

11.4.2 Possible solution of the contradiction

To solve this contradicton we suppose, as in Falsaperla, Mulone, and Perrone, 2022a, whose principal results are reported in Sec. 9, that this space is too large and likely contains perturbations which are not admissible as *physical perturbations* competing for the maximum.

With this conjecture, we see immediately that the streamwise perturbations are always stable and the maximum is achieved on the spanwise perturbations.
In fact, from the Reynolds-Orr equation, we obtain the Euler-Lagrange equations (see eq. (9.4.34) for more details) :

$$
-f' w \mathbf{i} - f' u \mathbf{k} + 2m\Delta \mathbf{u} = \nabla \lambda, \tag{11.4.20}
$$

The system of the Euler-Lagrange equations written in terms of ζ and w:

$$
\begin{cases}
f'(\zeta_y + 2w_{xz}) + f'' w_x + 2m\Delta\Delta w = 0 \\
f' w_y + 2m\Delta\zeta = 0,
\end{cases} \tag{11.4.21}
$$

with the boundary conditions (11.4.11), (11.4.10), (11.4.9), where now $\zeta = -u_y$.
We take the second component of the double curl of (11.4.20) to get

$$
f'\zeta_z + f''\zeta - f' w_{xy} = 0. \tag{11.4.22}
$$

From this equation and $(11.4.21)_2$ we have that ζ and all its derivative with respect to z are zero on the boundaries. We have already proved this in the particular case of Couette between rigid planes in SubSec. 9.4.2.
Let's prove now this in another particular case of Couette with *FF* boundary conditions. The proof in the case of the other laminar flows and different boundary conditions is done in a similar way.

In the case of RR Couette, from (11.4.21) and (11.4.22), we have:

$$\begin{cases} \zeta_y + 2w_{xz} + 2m\Delta\Delta w = 0 \\ w_y + 2m\Delta\zeta = 0 \\ \zeta_z - w_{xy} = 0. \end{cases} \tag{11.4.23}$$

On the boundaries $z = \pm 1$ we have $\zeta = 0$, from $(11.4.23)_3$ evaluated on $z = \pm 1$, we have $\zeta' = 0$ ($\zeta' = \dfrac{d\zeta}{dz}$). From $(11.4.23)_2$, evaluated on $z = \pm 1$, we have $\zeta'' = 0$. Now if we differentiate $(11.4.23)_2$ with respect to z and evaluate the result on the boundaries we have $\zeta''' = 0$. From this, if we differentiate twice $(11.4.23)_3$ with respect to z we have that the second derivative of w with respect to z is zero on the boundaries. And so, from $(11.4.23)_2$ differentiated twice with respect to z we have $\zeta'''' = 0$, ad so on.
In the case of FF Couette we have $\zeta' = 0$ on the boundaries. From $\zeta = -u_y$ and the solenoidality of velocity field, we have $\zeta_x = -u_{xy} = w_{zy}$. Moreover, by taking the Laplacian of $(11.4.23)_3$ we have $\Delta\zeta_z = \Delta w_{xy}$. Evaluating this on $z = \pm 1$, we have $\Delta\zeta_z = 0$ on the boundaries. From $(11.4.23)_2$ we now have $w_{yz} = \zeta_x = 0$. This implies that $\zeta = 0$ on the boundaries. $(11.4.23)_2$, evaluated on $z = \pm 1$, implies that $\zeta'' = 0$ on $z = \pm 1$. From this and $\Delta\zeta_z = 0$ on the boundaries, we also have $\zeta''' = 0$ on the boundaries. Now we take the Laplacian of $(11.4.23)_2$ and we get also $\zeta'''' = 0$ on $z = \pm 1$. And so on.
This implies that $\zeta \equiv 0$, hence $u_y = 0$ and from $(11.4.21)_2$ also $w_y = 0$. Therefore, $u = u(x,z), v = 0, w = w(x,z)$ and the less stabilizing perturbations which satisfy the equation

$$2f'w_{xz} + f''w_x + 2m\Delta\Delta w = 0, \tag{11.4.24}$$

with boundary conditions (11.4.11), (11.4.10), (11.4.9), are the spanwise perturbations, as Orr, 1907 had supposed for RR Couette case. Moreover, if we consider streamwise perturbations, from the equation

$$m\|\Delta w\|^2 = 0,$$

we immediately find $m = 0$, i.e. $\mathrm{Re}^y = +\infty$. We report these results in Figs. 11.9, 11.10, 11.11 (similar graphs can be done in the case FR), where the critical Reynolds number versus wave numbers for spanwise perturbations are shown.

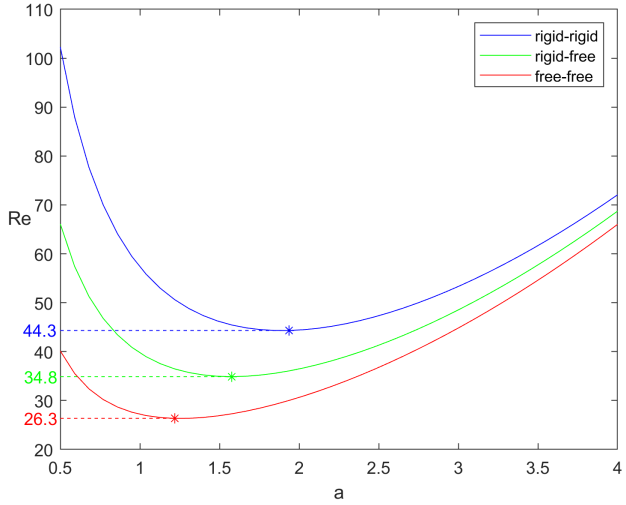

FIGURE 11.9: The energy Orr-Reynolds number, for *Couette* shear flow, as function of the wavenumber a, for eq. (11.4.24) with rigid-rigid, rigid-free, free-free boundary conditions (from the top to the bottom curve). For each curve, the minimum is highlighted by an asterisk and its numerical value is marked on the y-axis. Note that the minimum of the curve corresponding to the rigid-free boundary conditions is greater than the one corresponding to the free-free boundary conditions and lower than the one corresponding to the rigid-rigid boundary conditions.

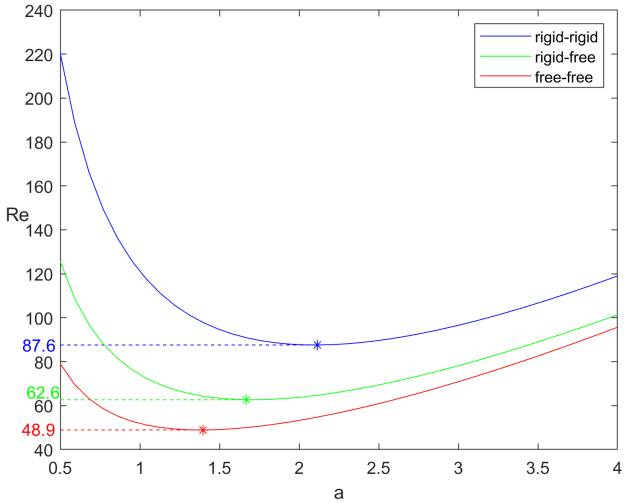

FIGURE 11.10: The energy Orr-Reynolds number, for *Poiseuille* shear flow, as function of the wavenumber a, for eq. (11.4.24) with rigid-rigid, rigid-free, free-free boundary conditions (from the top to the bottom curve). For each curve, the minimum is highlighted by an asterisk and its numerical value is marked on the y-axis. Note that the minimum of the curve corresponding to the rigid-free boundary conditions is greater than the one corresponding to the free-free boundary conditions and lower than the one corresponding to the rigid-rigid boundary conditions.

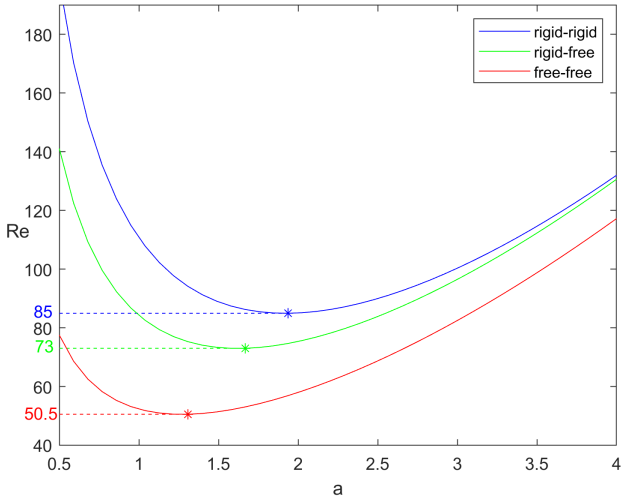

FIGURE 11.11: The energy Orr-Reynolds number, for *parabolic shear flow*, as function of the wavenumber a, for eq. (11.4.24) with rigid-rigid, rigid-free, free-free boundary conditions (from the top to the bottom curve). For each curve, the minimum is highlighted by an asterisk and its numerical value is marked on the y-axis. Note that the minimum of the curve corresponding to the rigid-free boundary conditions is greater than the one corresponding to the free-free boundary conditions and lower than the one corresponding to the rigid-rigid boundary conditions.

11.5 Discussion of the results

We study linear instability and nonlinear stability in the L_2-energy norm for laminar Couette, Poiseuille and parabolic flows when at least one of the planes bounding the layer is stress-free. We also recall the classic case of rigid boundaries for Couette and Poiseuille flows.
We observe that the classical Couette and Poiseuille basic motions are obtained with RR boundary conditions, however it is possible to study the stability also with respect to stress-free perturbations. In fact, as can be verified, such basic motions can be obtained when one of the two planes has an assigned tangential stress (stress-free perturbations), for example in the case of the Couette motion $U(z) = z$, the value of $U(z)$ can be assigned in the lower plane - rigid plane - and its first derivative in the upper plane, or both have a fixed tangential stress (in this case, for the purpose of uniqueness of the motion, an assigned average condition must be requested).
By using the energy norm, we prove nonlinear stability conditions with respect to streamwise perturbations for any Reynolds number, and for any boundary condition RR, RF and FF i.e. we have $\mathrm{Re}^y = +\infty$. On the other hand, the numerical calculations made with the Chebyshev collocation method give critical Reynolds numbers $\mathrm{Re}^y < +\infty$ for nonlinear energy stability on streamwise perturbations. This, as seen in the work of Falsaperla, Mulone, and Perrone, 2022a, gives rise to a contradiction. We make a conjecture to overcome this contradiction: we introduce a space of physical perturbations competing for the maximum problem and we prove that

the least stabilizing perturbations are two-dimensional (spanwise perturbations), for any boundary conditions RR, RF, FF.
We note that the critical Reynolds numbers we obtain for each basic flow Couette, Poiseuille and parabolic, show the stabilizing effect of the *no slip* boundaries as Figs. 11.9 - 11.11 also indicate. This happens also in the Bénard problem, see Chandrasekhar, 1961 for a fluid in a layer between rigid or stress-free boundaries. Moreover, we observe that the least critical Reynolds numbers (on the spanwise perturbations) are given for Couette case (for any boundary conditions).
We observe that in Table 11.1, in the FF case, we left two empty lines because our calculations, for streamwise perturbations, give some problems of convergence and numerical instability for $b \to 0$.

Chapter 12

Monotonic energy stability for inclined laminar flows

In the previous sections we have analysed the perturbations of a basic laminar motion (e.g. Couette, Poiseuille) without being interested in the study of the transient, i.e. for a finite time interval $[0, T]$, and which can give information on the possible development of turbulence (only a mention of the transient was made in SubSec. 9.4.1, see Case ii)). Therefore in Giacobbe, Mulone, and Perrone, 2022 the transient growth has been investigated in the wake of Henningson's works. In this section the main results of this work are presented.

12.1 Summary

In this article we consider the family of basic flows introduced in Sec. 5 (see eq. (5.0.8) and Fig. 5.2). We simplify the basic motion by considering that the plates of the layer where the fluid flows are in relative motion and the fluid is subjected to a gradient of pressure with only a non zero component in direction of the boundaries' relative motion. In this setup the possible laminar steady state solutions becomes a combination of Couette-Poiseuille flow in the direction parallel to the boundaries' relative motion (the transverse component is equal to zero). We use analytical methods and a Chebyshev collocation method with many different approaches to investigate the monotonic behaviour of the energy along perturbations. One of these approaches is related to the transient growth. We obtain in different ways an extension of known results for general shear flows, and we confirm the validity of some approaches that can be found in the literature. The basic motion includes the Poiseuille flow and the Couette flow as special cases. Therefore the results obtained may give a contribution to the conjecture.

12.2 State of the art

There are many physical applications of laminar flows in the real world. For example, to geophysics (sea, rivers and water flows in channels), astrophysics, biology (blood flow), industry, etc. Many articles are devoted to the study of these flows, also in the magnetic case, and to their stability/instability regimes, see for example Reynolds, 1895b, Orr, 1907, Joseph, 1976, Schmid and Henningson, 2001b, Drazin and Reid, 2004, Blasio, 2011, Falsaperla et al. 2019b, Falsaperla, Mulone, and Perrone, 2022a. The stability of inclined flows has received also attention due to its applications to rivers flows and to geophysical applications such as the evolution of landslides (see Blasio, 2011). Finally, the stability of Couette flows or Poiseuille flows has been studied separately for each of these flows. Sometimes

the combination of Poiseuille-Couette flows has been examined (see Potter, 1966, Cowley and Smith, 1985, Balakumar, 1997, Höink and Lenardic, 2010).

In this work we consider the monotonic stability of an inclined Poiseuille-Couette flows. The basic motion is given by (5.0.8) which depends only on the parameter ξ, because $\eta = 0$, In particular we investigate the monotone behaviour of energy along perturbations and the nonlinear Reynolds critical parameters for monotonic stability. We compute with two different methods some critical stability surfaces for a-few values of the coupling parameter ξ, which is a parameter in $[0, 1]$ that interpolates from Couette ($\xi = 0$) to Poiseuille ($\xi = 1$), and we show how these surfaces change as ξ varies. We finally compare our results with those obtained in the literature. In the limit cases of Couette flows and Poiseuille flows we find results in agreement with previous studies (see, e.g., Reddy and Henningson, 1993).
In Sec. 12.4 we introduce the Reynolds-Orr energy equations, in Sec. 12.5 we compute the critical threshold using an Euler-Lagrange equation approach, in Sec. 12.6 we compute the same critical threshold using a maximal initial growth rate approach, in Sec. 12.7 we make comparisons with the maximal total growth and draw some conclusions.

12.3 Basic flow and perturbations equations

Consider the setup described in Sec. 5 **Case 1**.
Let us for now assume that $\eta = 0$ (the case $\eta \neq 0$ is intestigated in the next section 13). The linear equations for the perturbations $u\,\mathbf{i} + v\,\mathbf{j} + w\,\mathbf{k}$, p to the steady state are

$$\begin{cases} u_t = \frac{1}{R}\Delta u - f u_x - f' w - p_x \\ v_t = \frac{1}{R}\Delta v - f v_x - p_y \\ w_t = \frac{1}{R}\Delta w - f w_x - p_z \\ u_x + v_y + w_z = 0 \\ u = v = w = 0 \quad \text{on the boundary.} \end{cases} \tag{12.3.1}$$

Considering w and $\zeta = v_x - u_y$, the vorticity of (u, v, w), one can reduce the equations to

$$\begin{cases} \Delta w_t = \frac{1}{R}\Delta^2 w - f\Delta w_x + f'' w_x \\ \zeta_t = \frac{1}{R}\Delta\zeta - f\zeta_x + f' w_y \\ w = w_z = \zeta = 0 \quad \text{on the boundary.} \end{cases} \tag{12.3.2}$$

The first equation of (12.3.2) can be obtained considering the third component of the double curl of equations (12.3.1). The system of equations (12.3.2) is deduced from (12.3.1) but there are means of reconstructing solutions of (12.3.1) starting from solutions of (12.3.2). In fact if u, v, w is a divergence-free vector field satisfying (12.3.1) then w, ζ are two functions satisfying (12.3.2). Vice versa, if w, ζ satisfy (12.3.2), by the divergence-free condition one has that u and v can be obtained using equations

$$\begin{cases} \Delta' u = -\zeta_y - w_{xz} \\ \Delta' v = \zeta_x - w_{yz} \\ u = v = 0 \quad \text{on the boundary,} \end{cases} \tag{12.3.3}$$

where $\Delta' = \partial_x^2 + \partial_y^2$ (see Chandrasekhar, 1961).

Indeed

$$\begin{cases} u_x + v_y + w_z = 0 \\ \zeta = v_x - u_y \end{cases} \Leftrightarrow \begin{cases} w_{zx} = u_{xx} - v_{xy} \\ \zeta_y = v_{xy} - u_{yy}. \end{cases} \tag{12.3.4}$$

The sum of these two equations gives $\zeta_y + w_{zx} = -\Delta' u$. Similarly, one can obtain the equation for $\Delta' v$ of (12.3.3). As we can see the complete equivalence of these two sets of equations is, in our understanding, not settled. In fact in the literature authors (see Schmitt and Wahl, 1992) seem to resort to the poloidal, toroidal, and mean field decomposition, but that is only a partial solution to the problem. The projection $\Pi : (u, v, w) \mapsto (v_x - u_y, w) = (\zeta, w)$ is linear from the space of divergence-free vector fields to 2-dimensional fields that we call *stream-fields*. The kernel of such map are the velocity fields of the type $(F_x, F_y, 0)$ where F is a function of (x, y, z), periodic on x and y like the perturbation, zero on the boundaries, and such that $\Delta' F = 0$ (harmonic function).
It might seem that from (ζ, w) we are not able to reconstruct (u, v, w) because from eq. (12.3.3) we have that if there exist $F(x, y, z)$ with $\Delta' F = 0$, which means that there are non zero functions in the kernel of the map, if $\Delta' u = -(\zeta_y + w_{zx})$, also $\Delta'(u + F) = -(\zeta_y + w_{zx})$ (similarly for v) and we do not have a bijection. Therefore the solutions of (12.3.3) would not be uniquely defined. However Liouville's theorem asserts that every bounded harmonic function is constant. Our function F is bounded and is zero on the boundaries. This implies that it must be zero everywhere. Therefore there are not non zero functions in the kernel of the map and equations (12.3.3) really define a bijection between incompressible velocity fields and stream functions.

12.4 The Orr-Reynolds energy equations

Eqs. (12.3.1) can be thought as *constrained* equations in the space

$$\mathcal{S} = \{(u, v, w) \,|\, u_x + v_y + w_z = 0,\, u(x, y, \pm 1) = v(x, y, \pm 1) = w(x, y, \pm 1) = 0\},$$

where u, v, w are sufficiently regular. The space $\mathcal{S}$ can be decomposed into Fourier components $\mathcal{S} = \oplus_{a,b} \mathcal{S}_{a,b}$ where $a, b \in \mathbb{R}$, $a, b \geq 0$ and $k^2 = a^2 + b^2 > 0$.

$$\mathcal{S}_{a,b} = \left\{ \left(u(z)e^{i(ax+by)}, v(z)e^{i(ax+by)}, w(z)e^{i(ax+by)}\right) \,\middle|\, iau + ibv + w_z = 0,\, u(\pm 1) = v(\pm 1) = w(\pm 1) = 0 \right\}.$$

The same can be done for $\mathcal{R} = \oplus_{a,b} \mathcal{R}_{a,b}$, where

$$\mathcal{R}_{a,b} = \left\{ \left(w(z)e^{i(ax+by)}, \zeta(z)e^{i(ax+by)}\right) \,\middle|\, \zeta(\pm 1) = w(\pm 1) = w_z(\pm 1) = 0 \right\}.$$

Behind this technique lays the common extension to complex-valued velocity fields and the understanding that, given a complex component of the velocity field e.g. $we^{i(ax+by)}$ there corresponds a real-valued physical component of the velocity field $\mathrm{Re}\,(w)\cos(ax + by) - \Im(w)\sin(ax + by)$. This fact is particularly important to understand the expression of $(\bar{u}, \bar{v}, \bar{w})$ in (12.5.6) which, with appropriate choices of wave numbers a, b, becomes Joseph's (when $a = 0$) or Orr's (when $b = 0$) extremal velocity field perturbations (see Falsaperla, Mulone, and Perrone, 2022a).

In each $\mathcal{S}_{a,b}$ one can define an energy

$$\mathcal{E}_{a,b} = \frac{1}{2}\iiint_\Omega \left(|u|^2+|v|^2+|w|^2\right)dxdydz = \frac{1}{2k^2}\iiint_\Omega \left(|\nabla w|^2+|\zeta|^2\right)dxdydz \tag{12.4.1}$$

where Ω is the periodicity cell (see eq. 8.5.1). The second expression of the energy is easily obtained from the first one by using the Fourier modes. Indeed $|u|^2 = u\cdot\bar{u}$. $\zeta = v_x - u_y$. We plan to investigate the growth of the energy function along the solutions. In particular we would like to determine which, among all solutions, is the one whose energy grows the fastest at $t = 0$ (or decreases the slowest), and which, among all solutions, at a given time t attains the maximal value.
The first question can be stated more directly: on which perturbation velocity field the orbital derivative of the energy has its maximum? To do so let us compute the orbital derivative of $\mathcal{E}_{a,b}$. Indicating $(f,g) = \iiint_\mathcal{C} f\bar{g}\,dxdydz$ one has that for every $(u,v,w)\neq(0,0,0)$, (i.e. $\mathcal{E}(u,v,w)\neq 0$).

$$\begin{aligned}\dot{\mathcal{E}}_{a,b} &= \left[\frac{-(f'u,w)}{|\nabla u|^2+|\nabla v|^2+|\nabla w|^2}-\frac{1}{R}\right]\left(|\nabla u|^2+|\nabla v|^2+|\nabla w|^2\right) = \\ &= \frac{1}{k^2}\left[\frac{(f'\zeta,w_y)+(fw,\Delta w_x)}{(\Delta w)^2+|\nabla\zeta|^2}-\frac{1}{R}\right]\left((\Delta w)^2+|\nabla\zeta|^2\right).\end{aligned} \tag{12.4.2}$$

Denoting

$$\mathcal{F}_{a,b}(u,v,w) = \frac{-(f'u,w)}{|\nabla u|^2+|\nabla v|^2+|\nabla w|^2}, \qquad \mathcal{G}_{a,b}(w,\zeta) = \frac{(f'\zeta,w_y)+(fw,\Delta w_x)}{(\Delta w)^2+|\nabla\zeta|^2}. \tag{12.4.3}$$

one has that $\mathcal{E}_{a,b}$ is strictly decreasing if and only if $1/R > m$ where m is the maximum of either of the two functionals. A very special case is that $a = b = 0$, that we do not consider, and in which the energy is always decreasing.

12.5 The general and the particular solutions of Joseph and Orr

The stationary solutions for the functional $\mathcal{F}_{a,b}(u,v,w)$, i.e. the solutions to the Euler-Lagrange equations are the perturbation vector fields (u,v,w) such that

$$\begin{cases} 2m\Delta u - f'w = \lambda_x \\ 2m\Delta v = \lambda_y \\ 2m\Delta w - f'u = \lambda_z \\ u_x + v_y + w_z = 0, \\ u = v = w = 0 \quad \text{on the boundary.}\end{cases} \tag{12.5.1}$$

Denoting $\zeta = v_x - u_y$, the above equations are equivalent, in every space $\mathcal{S}_{a,b}$, to the system of equations 12.5.1 we are solving the last system

$$\begin{cases} 2m\Delta\zeta + f'w_y = 0 \\ f'\zeta_y + 2m\Delta^2 w + f''w_x + 2f'w_{xz} = 0 \\ w = w_z = \zeta = 0 \quad \text{on the boundary.}\end{cases} \tag{12.5.2}$$

These are the stationary solutions of the functional $\mathcal{G}_{a,b}(w,\zeta)$. Both systems can be recast as a linear equation of order 6 in w only with three boundary conditions in $z=-1$ and three in $z=1$, more precisely, by deriving $(12.5.2)_1$ with respect to y, by computing the Δ of $(12.5.2)_2$, if one get $\Delta\zeta_y$ from $(12.5.2)_2$ and substitute it in $(12.5.2)_1$, obtain

$$4m^2\Delta\tfrac{\Delta^2 w}{f'}+4m\Delta w_{xz}+2mf''\Delta\tfrac{w_x}{f'}-f'w_{yy}=0,\quad w=w_z=(w_{zz}+2\Delta' w)_{zz}=0, \tag{12.5.3}$$

where the last boundary condition has been obtained from $(12.5.2)_2$. Indeed, by taking into account the boundary conditions of (12.5.2), $(12.5.2)_2$ computed on the boundaries, becomes $2m\Delta(w_{xx}+w_{yy}+w_{zz})=0 \Leftrightarrow w_{xxxx}+2w_{xxyy}+w_{yyyy}+2w_{xxzz}+2w_{yyzz}+w_{zzzz}=0 \Leftrightarrow 2w_{xxzz}+2w_{yyzz}+w_{zzzz}=0 \Leftrightarrow (w_{zz}+2\Delta' w)_{zz}=0$. Eqs. (12.5.3) are linear but, except for Couette case, with non-constant coefficients, and when $\xi\geq 1/3$ there is a point $z_\xi\in[-1,0]$ in which some denominator becomes zero, and hence the differential equation becomes singular (the computation has been done with the software Mathematica). This poses interesting questions, but we can analytically solve the problem only when $\xi=0$ (Couette) in which the equation has constant coefficients and becomes

$$\begin{cases} -w_{yy}+4m\Delta w_{xz}+4m^2\Delta^3 w=0\\ w=w_z=(w_{zz}+2\Delta' w)_{zz}=0. \end{cases} \tag{12.5.4}$$

We note that when w is independent of x the equations depend on m^2 only, but a solution $\bar{w}$ corresponds only to one possible choice, the positive m or the negative m whose square is m^2. In Sec. 14 will be explained how to overcome this problem.
In each space $\mathcal{S}_{a,b}$, if we seek for solution of the type $w=H(z)e^{i(k_x x+k_y y)}$, from (12.5.4) we obtain:

$$\begin{cases} b^2H(z)+4iam\left(D^2-k^2\right)H'(z)+4m^2\left(D^2-k^2\right)^3H(z)=0\\ H(\pm1)=H'(\pm1)=H''''(\pm1)-2k^2H''(\pm1)=0. \end{cases} \tag{12.5.5}$$

Where $H(z)=F(z)+iG(z)$ is a non zero solution of (12.5.5).
It can be shown (the computation has been done with the software Mathematica) that the stationary solutions of (12.5.4) have physical, real form

$$\begin{aligned} \bar{u}&=\left(-4a^2mG''(z)+aF'(z)-4b^2mG''(z)+2mG^{(4)}(z)+2k^4mG(z)\right)\sin(ax+by)+\\ &+\left(4a^2mF''(z)+aG'(z)+4b^2mF''(z)-2mF^{(4)}(z)-2k^4mF(z)\right)\cos(ax+by)\\ \bar{v}&=\frac{\sin(ax+by)}{b}\left(-2a^2F'(z)-2amG^{(4)}(z)+4amk^2G''(z)-2ak^4mG(z)-b^2F'(z)\right)+\\ &+\frac{\cos(ax+by)}{b}\left(-2a^2G'(z)+2amF^{(4)}(z)-4amk^2F''(z)+2ak^4mF(z)-b^2G'(z)\right)\\ \bar{w}&=\cos(ax+by)k^2F(z)-k^2G(z)\sin(ax+by). \end{aligned} \tag{12.5.6}$$

The idea is that first one has to solve (12.5.5). The solution $H(z)$ gives $F(z)$ and $G(z)$ that allow to find $\bar{w}$. Indeed $\bar{w}$ is obtained by taking the real part of $H(z)e^{i(k_x x+k_y y)}$, which is $\cos(ax+by)F(z)-G(z)\sin(ax+by)$. Then from (12.5.2) ζ can be computed and finally this value and $\bar{w}$ are used to find $\bar{u}$ and $\bar{v}$ through (12.3.3). We observe that in order to obtain $\bar{u}$ and $\bar{v}$ we have to divide the two sides of the equations in (12.3.3) by $k^2=a^2+b^2$. If we want to avoid to have a fraction in the vector $(\bar{u},\bar{v},\bar{w})$,

we can multiply all the components by k^2 obtaining (12.5.6).

The existence of a non-zero complex valued function H satisfying (12.5.5) is equivalent to the question of finding, given $a, b, m = 1/R$, a non-zero solution satisfying the boundary conditions on which $\mathcal{F}$ has a critical value. Such non-zero solutions exists for every $a, b, m = 1/R$ at which vanish the determinant of the matrix

$$\begin{pmatrix} B \\ Be^{2A} \end{pmatrix} \qquad \text{with} \qquad B = \begin{pmatrix} 1 & 0 & 0 & 0 & 0 & 0 \\ 0 & 1 & 0 & 0 & 0 & 0 \\ 0 & 0 & -2k^2 & 0 & 1 & 0 \end{pmatrix}$$

and

$$A = \begin{pmatrix} 0 & 1 & 0 & 0 & 0 & 0 \\ 0 & 0 & 1 & 0 & 0 & 0 \\ 0 & 0 & 0 & 1 & 0 & 0 \\ 0 & 0 & 0 & 0 & 1 & 0 \\ 0 & 0 & 0 & 0 & 0 & 1 \\ k^6 - \frac{b^2}{4m^2} & \frac{a}{m}k^2 i & -3k^4 & -\frac{a}{m}i & 3k^2 & 0 \end{pmatrix} =$$

$$= \begin{pmatrix} 0 & 1 & 0 & 0 & 0 & 0 \\ 0 & 0 & 1 & 0 & 0 & 0 \\ 0 & 0 & 0 & 1 & 0 & 0 \\ 0 & 0 & 0 & 0 & 1 & 0 \\ 0 & 0 & 0 & 0 & 0 & 1 \\ k^6 - \frac{b^2}{4}R^2 & iaRk^2 & -3k^4 & iaR & 3k^2 & 0 \end{pmatrix}$$

Indeed if we define

$$\bar{H} = \begin{pmatrix} H \\ H' \\ H'' \\ H''' \\ H'^{\text{v}} \\ H^{\text{v}} \end{pmatrix},$$

(12.5.5) can be rewritten as a system of six differential equations such that:

$$\bar{H}' = A\bar{H} \Leftrightarrow \bar{H}(t) = e^{tA}\bar{H}_0.$$

The boundaries conditions can be written as:

$$\begin{pmatrix}1 & 0 & 0 & 0 & 0 & 0\end{pmatrix} e^{\pm A}\bar{H}_0 = 0, \quad \begin{pmatrix}0 & 1 & 0 & 0 & 0 & 0\end{pmatrix} e^{\pm A}\bar{H}_0 = 0,$$
$$\begin{pmatrix}0 & 0 & -2k^2 & 0 & 1 & 0\end{pmatrix} e^{\pm A}\bar{H}_0 = 0.$$

which means that $Be^{A}\bar{H}_0 = 0$ and $Be^{-A}\bar{H}_0 = 0$.
If we define $\bar{K}_0 = e^{-A}H_0$, we have that the two last conditions become $Be^{2A}\bar{K}_0 = 0, \quad B\bar{K}_0 = 0$. Therefore $\bar{K}_0$ is in the kernel of

$$\begin{pmatrix} B \\ Be^{2A} \end{pmatrix}$$

and then we seek for a, b, m such that the determinant of the latter matrix is zero.

The level set of $\det(a, b, R) = 0$ in a, b, R space is represented in Fig. 12.1. Particularly important is the limiting case $a = 0$, where the solutions and the equations become

$$\begin{cases} b^2 H(z) + 4m^2 \left(D^2 - b^2\right)^3 H(z) = 0 \\ H(\pm 1) = H'(\pm 1) = H''''(\pm 1) - 2b^2 H''(\pm 1) = 0 \end{cases}$$

which are Joseph's equations, and $b = 0$, where the equation becomes

$$\begin{cases} \left(D^2 - a^2\right)\left(4iamH'(z) + 4m^2\left(D^2 - a^2\right)^2 H(z)\right) = 0 \\ H(\pm 1) = H'(\pm 1) = H''''(\pm 1) - 2a^2 H''(\pm 1) = 0, \end{cases} \Leftrightarrow$$

$$\Leftrightarrow \begin{cases} 4iamH'(z) + 4m^2\left(D^2 - a^2\right)^2 H(z) = 0 \\ H(\pm 1) = H'(\pm 1) = 0, \end{cases} \tag{12.5.7}$$

which are Orr's equations. The equivalence of the two systems of equations is easily proven by observing that in the equation to the left the two last boundary conditions and the equation imply that the argument of $\left(D^2 - a^2\right)$ must be zero. This allows to neglect the differential operator $\left(D^2 - a^2\right)$ and to drop the last two boundary conditions. The eqs. (12.5.7)-right can also be deduced directly from (12.5.2).
For all other cases $\xi \neq 0$ (non-Couette) we can make a spectral numerical investigation of equations (12.5.2), using $m = 1/R$ as spectral parameter. In each space $\mathcal{S}_{a,b}$ we use a Chebyshev collocation algorithm with $N+1$ nodes, considering w, ζ functions of z in the interval $[-1, 1]$. Chebyshev collocation method, see Wright, 1964, Boor and Swartz, 1973, Trefethen, 2000, consists of a discretization of functions in an interval by means of their values on $N+1$ Gaussian points in the interval. This identifies the function w, ζ with $N+1$-dimensional vectors w_N, ζ_N. The derivation operator $\partial_z = D$ becomes a (matrix) linear operator D_N on $N+1$ vectors. In this way a differential equation becomes a linear system, and a differential equation depending on parameters becomes a generalized eigenvalue problem. We thus reduce eq. (12.5.2) into a finite dimensional spectral equation

$$\left[\begin{pmatrix} D_N^4 - 2k^2 D_N^2 + k^4 & 0 \\ 0 & D_N^2 - k^2 \end{pmatrix} + R\begin{pmatrix} 0 & \frac{ibf'}{2} \\ \frac{ibf'}{2} & \frac{iaf''}{2} + iaf' D_N \end{pmatrix}\right]\begin{pmatrix} w_N \\ \zeta_N \end{pmatrix} = \begin{pmatrix} 0 \\ 0 \end{pmatrix}, \tag{12.5.8}$$

where these apparently 2×2 matrices are $2(N+1) \times 2(N+1)$ matrices, and D_N is a $(N+1) \times (N+1)$ matrix which approximates the derivative with respect to z. The results are extremely stable with the increase of nodes, and we use $N = 100$. The lowest eigenvalue $1/R$ gives the threshold for monotonic stability. In Fig. 12.1 (right pane) we plot the threshold curve of minimal values for R as a function of a, b for the choices of $\xi = 0, 0.2, 0.5, 0.8, 1$.

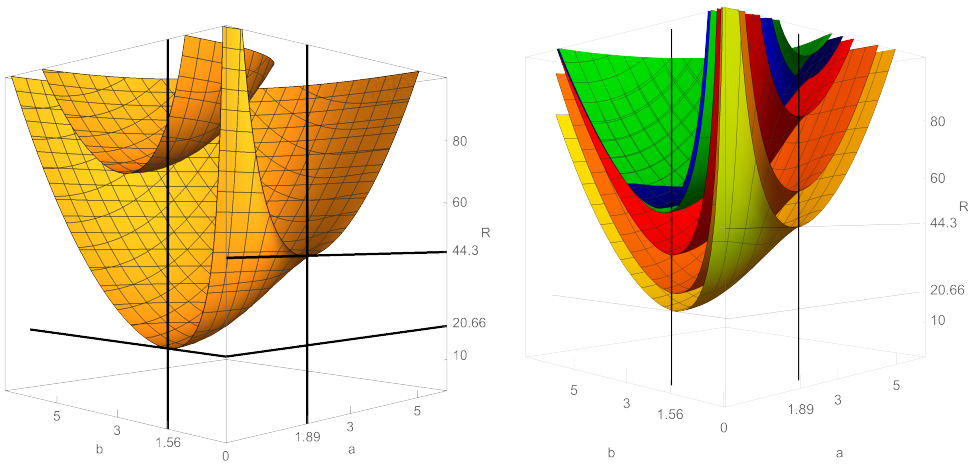

FIGURE 12.1: In the left pane, for every wave number pair a, b, the values of R at which there exists an analytical critical vector field (u, v, w) critical for $\mathcal{F}_{a,b}$ with $f = z$ (Couette). In the left pane, the component of the below surface corresponds to minima critical values while the component of the above surface corresponds to saddle critical values. In the right pane the same problem solved numerically using a Chebyshev collocation algorithm. We plot in different colours only the minima for each steady state solution with $\xi = 0$ (yellow), $\xi = 0.2$ (orange) $\xi = 0.5$ (red) $\xi = 0.8$ (green) and $\xi = 1$ (blue). (5.0.7). A feature to be observed is the change of monotonicity as the parameter moves close to 1.

12.6 Maximal initial growth rate of the energy

In this section we always fix ξ, and then we use a spectral method to compute, for every choice of wave numbers a, b and Reynolds number R, the initial velocity field $(w_{a,b,R}, \zeta_{a,b,R})$ at which $\dot{\mathcal{E}}$ attains its maximum. We also compute such maximal value of the derivative that we denote $\mathrm{maxd}(a, b, R)$. The computation is numerical and it is performed writing independently in Mathematica and Matlab an algorithm that implements a Chebyshev collocation method.
The energy is a quadratic functional, that is $\mathcal{E}(\lambda v) = \lambda^2 \mathcal{E}(v)$ for every λ real, and therefore the investigation must be restricted to initial values of the velocity field that have with energy 1.
In Trefethen et al., 1992 this type investigation is called *maximal initial growth rate*. The maximal initial growth rate differs from the investigation performed in Reddy and Henningson, 1993 in which, for every (a, b, R, t), the authors find the velocity field $(w_{a,b,R,t}, \zeta_{a,b,R,t})$ on which, at time t, the energy attains the highest value $\mathrm{maxe}(a, b, R, t)$. This investigation has been given the name of *maximal total growth*

in Trefethen et al., 1992. Explicitly, we denote

$$\mathrm{maxd}(a,b,R) = \sup_{\substack{(\zeta_0,w_0)\\ \mathcal{E}(\zeta_0,w_0)=1}} \dot{\mathcal{E}}(\zeta_0,w_0), \qquad \mathrm{maxe}(a,b,R,t) = \sup_{\substack{(\zeta_0,w_0)\\ \mathcal{E}(\zeta_0,w_0)=1}} \mathcal{E}(\zeta_t,w_t),$$

where (ζ_0, w_0) is a generic velocity field and (ζ_t, w_t) is, at frozen time t, the solution to eqs. (12.3.2) that at $t = 0$ is (ζ_0, w_0).
The maximal initial growth rate has not been, to our knowledge, thoroughly investigated in the literature. This because most authors are interested in computing the highest value of the energy, and consider such maximal value as possibly responsible of the onset of instability. In fact K.M. Butler, 1992; Reddy and Henningson, 1993 are devoted to the second type of investigation, and there the authors compute the graph of the maximal total growth for particular cases of a, b and R far above the threshold that we investigate in this work. In the next section we will explicitly compare maximal initial growth with maximal total growth.
The computation of the maximal initial growth allows to define a surface. For every fixed ξ let $\mathcal{T}_\xi = \{(a,b,R) \,|\, \mathrm{maxd}(a,b,R) = 0\}$. This surface is the threshold which separates the region in parameter space where the energy is always decreasing from the region in parameter space where the energy does increase at least along a solution. In this section we investigate the coincidence of the surfaces $\mathcal{T}_\xi$ computed using the maximal initial growth rate with those computed in the previous section (see Fig. 12.1) computed using Euler-Lagrange equation for the functional $\mathcal{F}_{a,b}$. The surfaces $\mathcal{T}_\xi$ are drawn in Fig. 12.2 (left pane) for choices of $\xi = 0$ (yellow), $\xi = 0.2$ (orange), $\xi = 0.5$ (red), $\xi = 0.8$ (green) and $\xi = 1$ (blue). This manifold should be compared with the manifolds obtained in the previous section.
Our computation is based on the following facts: the eigenfunctions $(e^{\lambda t}w, e^{\lambda t}\zeta)$ of system (12.3.2) are associated to the eigenvalue problem

$$\begin{cases} \lambda \Delta w = \frac{1}{R}\Delta^2 w - f\Delta w_x + f'' w_x \\ \lambda \zeta = \frac{1}{R}\Delta\zeta - f\zeta_x + f' w_y \\ w = w_z = \zeta = 0 \quad \text{on the boundary.} \end{cases} \tag{12.6.1}$$

with λ a complex spectral parameter. When the system is linearly stable, i.e. when all eigenvalues λ have negative real part, it is reasonable to assume that the most important modes are those associated to eigenfunctions whose eigenvalue λ have real part negative but close to zero, we call such eigenvalues and eigenfunctions *dominating*. We thus discretise eq. (12.6.1) using a Chebyshev approximation with $N + 1$ nodes, and then consider only the first $n < N$ dominating eigenvalues and eigenvectors of the discretised operator.
Indeed if we consider the generic initial field $\mathbf{v}_0 = (\mathbf{v}_1, ..., \mathbf{v}_N)\mathbf{k} = \mathbf{v}_1 k_1 + \cdots + \mathbf{v}_N k_N$, $(k \in \mathbb{C}^N)$, where N is the number of eigenvectors of (12.6.1), we have that it evolves according to

$$\mathbf{v}(t) = (\mathbf{v}_1, ..., \mathbf{v}_N) e^{\Lambda_N t}\mathbf{k} = \sum_{i=1}^{N} \mathbf{v}_i e^{\lambda_i t} k_i$$

The last expression is due to the fact that if we want to find the solution of $\dot{\mathbf{x}} = A\mathbf{x}$, which is analogous to our system (12.3.2), we have that $\mathbf{x}(t) = e^{At}\mathbf{x}_0$. Therefore, in our case, each eigenvector $\mathbf{v}_i$ evolves according to $\mathbf{v}_i(t) = e^{At}\mathbf{v}_i k_i$, where $e^{At} = 1 + tA + t^2/2A + t^3/3A + \ldots$. This implies that $e^{At}\mathbf{v}_i = \mathbf{v}_i + tA\mathbf{v}_i + t^2/2A\mathbf{v}_i + t^3/3A\mathbf{v}_i + \cdots + t^N/NA\mathbf{v}_n$. As $\mathbf{v}_i$ is an eigenvector, $A\mathbf{v}_i = \lambda_i \mathbf{v}_i$. Therefore $e^{At}\mathbf{v}_i = \mathbf{v}_i + t\lambda_i\mathbf{v}_i + t^2/2\lambda_i\mathbf{v}_i + t^3/3\lambda_i\mathbf{v}_i + \cdots + t^N/N\lambda_i\mathbf{v}_N = e^{\lambda_i t}\mathbf{v}_i$.

If $l \leq N$ and $m \leq N$ are two indices such that $\text{Real}(e^{\lambda_l t}) \approx 0$ while $\text{Real}(e^{\lambda_m t}) \ll 0$, then the first exponential dominates the second one.
Furthermore it is not restrictive to assume that the eigenvalues are ordered by increasing real part.

Therefore we denote by λ_i, $i = 1, ..., n$ the dominating eigenvalues, v_i the corresponding eigenvectors, and $\Lambda = \text{diag}(\lambda_1, ..., \lambda_n)$ the diagonal matrix of the eigenvalues. Using the common symbols to indicate conjugate, transpose, and adjoint of a matrix, it follows that the generic initial velocity field $\mathbf{v}_0 = (\mathbf{v}_1, ..., \mathbf{v}_n)\mathbf{k}$, ($\mathbf{k} \in \mathbb{C}^n$), evolves according to

$$\mathbf{v}(t) = (\mathbf{v}_1, ..., \mathbf{v}_n)e^{\Lambda t}\mathbf{k} \Rightarrow \frac{\mathcal{E}(\mathbf{v}(t))}{\mathcal{E}(\mathbf{v}_0)} = \frac{\mathbf{k}^* e^{\overline{\Lambda} t} A e^{\Lambda t}\mathbf{k}}{\mathbf{k}^* A \mathbf{k}},$$

$$\mathcal{E}(\mathbf{v}(t)) = \frac{1}{2}|\mathbf{v}(t)|^2 = \frac{1}{2}\mathbf{v}(t)^*\mathbf{v}(t) = \frac{1}{2}\mathbf{k}^* e^{\overline{\Lambda} t} \begin{pmatrix} \bar{\mathbf{v}}_1^T \\ \dots \\ \bar{\mathbf{v}}_n^T \end{pmatrix} (\mathbf{v}_1, ..., \mathbf{v}_n)e^{\Lambda t}\mathbf{k} = \frac{1}{2}\mathbf{k}^* e^{\overline{\Lambda} t} A e^{\Lambda t}\mathbf{k}$$

and hence

$$\text{maxd}(a, b, R) = \sup_{\mathcal{E}(v_0)=1} \dot{\mathcal{E}}(v_0) = \sup_{v_0} \frac{\dot{\mathcal{E}}(v_0)}{\mathcal{E}(v_0)} = \sup_{\mathbf{k}} \frac{\mathbf{k}^* \left(\overline{\Lambda} A + A\Lambda\right) \mathbf{k}}{\mathbf{k}^* A \mathbf{k}},$$

where $A = (A_{i,j})$ with $A_{i,j} = \mathbf{v}_i{}^* \mathbf{v}_j$ a positive definite Hermitian matrix (remember that $*$ indicates the Hermitian conjugate, that is the transpose conjugate, also called adjoint). Denoting $H = \overline{\Lambda} A + A\Lambda$ and recalling that every positive-definite Hermitian matrix admits a square-root, we have that $A = F^* F$, where $F := \sqrt{\Sigma} U^*$, Σ is the diagonal matrix of positive real eigenvalues of A, and the columns of U are the corresponding right eigenvectors.

Indeed $A\mathbf{v_i} = \breve{}_\mathbf{i}\mathbf{v_i}, \mathbf{i} = \mathbf{1}, \dots, \mathbf{n}$, therefore

$$A(\mathbf{v_1}, \cdots, \mathbf{v_n}) = (\mathbf{v_1}, \cdots, \mathbf{v_n}) \begin{pmatrix} \lambda_1 & \dots & \dots & 0 \\ 0 & \lambda_2 & \dots & 0 \\ \vdots & \vdots & \vdots & \vdots \\ 0 & \dots & \dots & \lambda_n \end{pmatrix} \Rightarrow$$

$$\Rightarrow (\mathbf{v_1}, \cdots, \mathbf{v_n})^* \mathbf{A} (\mathbf{v_1}, \cdots, \mathbf{v_n}) = \begin{pmatrix} \lambda_1 & \dots & \dots & 0 \\ 0 & \lambda_2 & \dots & 0 \\ \vdots & \vdots & \vdots & \vdots \\ 0 & \dots & \dots & \lambda_n \end{pmatrix},$$

if we define $U := (\mathbf{v_1}, \cdots, \mathbf{v_n})$ and $\Sigma = diag(\lambda_1, \cdots, \lambda_n)$, we obtain $U^* A U = \Sigma$, which implies that $A = U\Sigma U^* = (U\sqrt{\Sigma})(\sqrt{\Sigma}U^*) = F^* F$. Note that the square

root of Σ can be computed because A is a positive definite Hermitian matrix, which implies that its eigenvalues are real positive.

Following fact Reddy and Henningson, 1993 one has that

$$\begin{aligned}\operatorname{maxd}(a,b,R) &= \sup_{\substack{\mathbf{k}\in\mathbb{C}^n\\ \mathbf{k}\neq 0}} \frac{\mathbf{k}^* H\mathbf{k}}{\mathbf{k}^* A\mathbf{k}} = \sup_{\substack{\mathbf{k}\in\mathbb{C}^n\\ \mathbf{k}\neq 0}} \frac{\mathbf{k}^* H\mathbf{k}}{\mathbf{k}^* F^* F\mathbf{k}} = \sup_{\substack{\mathbf{h}\in\mathbb{C}^n\\ \mathbf{h}\neq 0}} \frac{\mathbf{h}^*(F^*)^{-1}HF^{-1}\mathbf{h}}{\mathbf{h}^*\mathbf{h}} = \\ &= \sup_{\substack{\mathbf{h}\in\mathbb{C}^n\\ \mathbf{h}\neq 0}} \frac{\mathbf{h}^*\left(F^*\right)^{-1}HF^{-1}\mathbf{h}}{|\mathbf{h}|^2} = \sup_{\substack{h\in\mathbb{C}^n\\ \mathbf{h}\neq 0}} \frac{\mathbf{h}^*}{|\mathbf{h}|}\left(F^*\right)^{-1}HF^{-1}\frac{\mathbf{h}^*}{|\mathbf{h}|} = \\ &= \sup_{|\mathbf{h}|^2=1} \mathbf{h}^*\left(F^*\right)^{-1}HF^{-1}\mathbf{h},\end{aligned} \tag{12.6.2}$$

where the third equality is obtained defining $k := F^{-1}h$.

It follows that the maximal value of the derivative $\operatorname{maxd}(a,b,R)$ is the maximal eigenvalue of the Hermitian matrix $\left(F^*\right)^{-1}HF^{-1}$. Indeed computing $\sup_{|h|^2=1} h^*\left(F^*\right)^{-1}HF^{-1}h$ means to find the critical values of $h^*\left(F^*\right)^{-1}HF^{-1}h$, with the constraint $|h|^2 = 1$, and then to select the greatest one. If we define $\tilde{H} := \left(F^*\right)^{-1}HF^{-1}$, first we have to solve $\nabla h^*\tilde{H}h = 0$, that is

$$\nabla(\bar{h}_1,\cdots,\bar{h}_n)\tilde{H}\begin{pmatrix}h_1\\ \vdots\\ h_n\end{pmatrix} = 0.$$

If $h_i = x_i + iy_i$, then the partial derivatives of this function with respect to x_i an y_i are respectively equal to

$$\begin{cases}\mathbf{e}_i^T\tilde{H}\begin{pmatrix}h_1\\ \vdots\\ h_n\end{pmatrix} + (\bar{h}_1,\cdots,\bar{h}_n)\tilde{H}\mathbf{e}_i\\ -i\mathbf{e}_i^T\tilde{H}\begin{pmatrix}h_1\\ \vdots\\ h_n\end{pmatrix} + i(\bar{h}_1,\cdots,\bar{h}_n)\tilde{H}\mathbf{e}_i.\end{cases} \tag{12.6.3}$$

We recall that we have to find the maximum of a function subjected to the constraint $|\mathbf{h}|^2 = 1$. The derivatives of the constraint with respect to x_i and y_i are respectively $2x_i$ and $2y_i$. Therefore, according to the method of Lagrange multipliers, one has that $(12.6.3)_1$ and $(12.6.3)_2$ are parallel respectively to $2x_i$ and $2y_i$:

$$\begin{cases} \mathbf{e}_i^T \tilde{H} \begin{pmatrix} h_1 \\ \vdots \\ h_n \end{pmatrix} + (\bar{h}_1, \cdots, \bar{h}_n) \tilde{H} \mathbf{e}_i \parallel 2x_i \\ -i\mathbf{e}_i^T \tilde{H} \begin{pmatrix} h_1 \\ \vdots \\ h_n \end{pmatrix} + i(\bar{h}_1, \cdots, \bar{h}_n) \tilde{H} \mathbf{e}_i \parallel 2y_i. \end{cases} \tag{12.6.4}$$

From (12.6.4) follows that

$$\begin{cases} \text{Real}(\mathbf{e}_i^T \tilde{H} \begin{pmatrix} h_1 \\ \vdots \\ h_n \end{pmatrix} + (\bar{h}_1, \cdots, \bar{h}_n) \tilde{H} \mathbf{e}_i) \parallel \text{Real}(2x_i) \\ \text{Real}(-i\mathbf{e}_i^T \tilde{H} \begin{pmatrix} h_1 \\ \vdots \\ h_n \end{pmatrix} + i(\bar{h}_1, \cdots, \bar{h}_n) \tilde{H} \mathbf{e}_i) \parallel \text{Real}(2y_i). \end{cases} \Leftrightarrow \tag{12.6.5}$$

that is:

$$\Leftrightarrow \begin{cases} \text{Real}(\mathbf{e}_i^T \tilde{H} \begin{pmatrix} h_1 \\ \vdots \\ h_n \end{pmatrix}) + \text{Real}((\bar{h}_1, \cdots, \bar{h}_n) \tilde{H} \mathbf{e}_i)) \parallel 2x_i \\ \text{Imag}(\mathbf{e}_i^T \tilde{H} \begin{pmatrix} h_1 \\ \vdots \\ h_n \end{pmatrix}) - \text{Imag}((\bar{h}_1, \cdots, \bar{h}_n) \tilde{H} \mathbf{e}_i)) \parallel 2y_i, \end{cases} \Leftrightarrow \tag{12.6.6}$$

$$\Leftrightarrow \begin{cases} \text{Real}(\mathbf{e}_i^T \tilde{H} \begin{pmatrix} h_1 \\ \vdots \\ h_n \end{pmatrix}) + \text{Real}(\mathbf{e}_i^T \tilde{H}^* \begin{pmatrix} h_1 \\ \vdots \\ h_n \end{pmatrix})) \parallel 2x_i \\ \text{Imag}(\mathbf{e}_i^T \tilde{H} \begin{pmatrix} h_1 \\ \vdots \\ h_n \end{pmatrix}) + \text{Imag}(\mathbf{e}_i^T \tilde{H}^* \begin{pmatrix} h_1 \\ \vdots \\ h_n \end{pmatrix})) \parallel 2y_i, \end{cases} \Leftrightarrow \tag{12.6.7}$$

$$\Leftrightarrow \begin{cases} 2\text{Real}(\mathbf{e}_i^T \tilde{H} \begin{pmatrix} h_1 \\ \vdots \\ h_n \end{pmatrix}) \parallel 2x_i \\ 2\text{Imag}(\mathbf{e}_i^T \tilde{H} \begin{pmatrix} h_1 \\ \vdots \\ h_n \end{pmatrix}) \parallel 2y_i \end{cases} \Leftrightarrow \mathbf{e}_i^T \tilde{H} \begin{pmatrix} h_1 \\ \vdots \\ h_n \end{pmatrix} \parallel x_i + iy_i = h_i. \tag{12.6.8}$$

Therefore:

$$\tilde{H}\begin{pmatrix} h_1 \\ \vdots \\ h_n \end{pmatrix} \parallel \begin{pmatrix} h_1 \\ \vdots \\ h_n \end{pmatrix} \Rightarrow \tilde{H}\begin{pmatrix} h_1 \\ \vdots \\ h_n \end{pmatrix} = \mu \begin{pmatrix} h_1 \\ \vdots \\ h_n \end{pmatrix}$$

This means that the critical vectors are the eigenvectors of the matrix $\tilde{H}$ and from the last equality we have that

$$(h_1, \cdots, h_n)\tilde{H}\begin{pmatrix} h_1 \\ \vdots \\ h_n \end{pmatrix} = \mu.$$

Therefore the value that the function $h^*\tilde{H}h$ assumes in correspondence to each eigenvector is equal to the related eigenvalue. Therefore $\sup_{|h|^2=1} h^*(F^*)^{-1}\tilde{H}F^{-1}h$ is equal to the maximum eigenvalue of $\tilde{H}$, which is the same as the maximal eigenvalue of the matrix $A^{-1}H$, because these two matrices are similar.
We have hence, fixing a, b, a function from R to the real numbers, $R \mapsto \text{maxd}(a, b, R)$. Such a function is monotonically increasing, and hence a bisection algorithm allows us to determine the particular value of R at which $\text{maxd}(a, b, R) = 0$, which is what is needed to obtain sample points of the surfaces $\mathcal{T}_\xi$ and then produce Fig. 12.2 (left pane). In our computations we use $N = 100$ and $n = 50$. We have also used $N = 150$ and $n = 60$, with no change in the results.

12.7 Comparison between maximal initial growth and maximal total growth, and conclusions

To compare the graph of the energy of the solution with maximal initial growth with the graph of maximal total growth we need to find the eigenvector of $(F^*)^{-1}HF^{-1}$ associated to the maximal eigenvalue $\text{maxd}(a, b, R)$. Indeed, as we have observed, the matrices $(F^*)^{-1}HF^{-1}$ and $A^{-1}H$ are similar, which implies that they have the same eigenvalues but not the same eigenvectors. To be more precise, if $\lambda_m := \text{maxd}(a, b, R)$ is the maximum eigenvalue of the matrix $A^{-1}H$, and h_m the correspondent eigenvector, we have that $A^{-1}Hh_m = \lambda_m h_m$, but h_m does not coincide with the eigenvector of $(F^*)^{-1}HF^{-1}$. In order to find it we recall that, as the two matrices are similar, we have that

$$F^{-1}((F^*)^{-1}HF^{-1})F = A^{-1}H \Leftrightarrow ((F^*)^{-1}HF^{-1})F = FA^{-1}H \Leftrightarrow$$

$$\Leftrightarrow ((F^*)^{-1}HF^{-1})Fh_m = F\lambda_m h_m \Leftrightarrow ((F^*)^{-1}HF^{-1})Fh_m = \lambda_m Fh_m,$$

and the last equality implies that Fh_m is the eigenvector of the matrix $(F^*)^{-1}HF^{-1}$ associated to λ_m.
We note that in (12.6.2) we made a change of variable from k to h such that $Fk = h$. In our case h is Fh_m, therefore $Fk_m = Fh_m$, that implies $k = h_m$. We conclude that, in this particular case, the eigenvector h_m we had found coincides with the one associated to the matrix $(F^*)^{-1}HF^{-1}$.

This eigenvector k_m is such that $(v_1, ..., v_n)k_m$ is the initial data of a solution

with maximal initial growth. The graph of the energy at time t of such solution must lay below the graph of maximal total growth at time t, that is the function $t \mapsto \text{maxe}(a, b, R, t)$. The two graphs must have identical first derivative at $t = 0$. In Reddy and Henningson, 1993 the authors compute $\text{maxe}(a, b, R, t)$.

The procedure to find the maximal total growth, described in Reddy and Henningson, 1993, is the following:

$$maxe(a,b,R,t) = \sup_{\substack{k\in\mathbb{C}^n \\ k\neq 0}} \frac{\mathcal{E}(\mathbf{v}(t))}{\mathcal{E}(\mathbf{v}_0)} = \frac{k^* e^{\overline{\Lambda}t} A e^{\Lambda t} k}{k^* A k} = \sup_{\substack{k\in\mathbb{C}^n \\ k\neq 0}} \frac{k^* e^{\overline{\Lambda}t} F^* F e^{\Lambda t} k}{k^* F^* F k} =$$

$$= \sup_{\substack{k\in\mathbb{C}^n \\ k\neq 0}} \frac{||Fe^{\Lambda t}k||_2^2}{||Fk||_2^2} = \sup_{|h|^2=1} ||Fe^{\Lambda t}F^{-1}h||_2^2.$$

We define $\tilde{F} := Fe^{\Lambda t}F^{-1}$ and we rewrite $||Fe^{\Lambda t}F^{-1}h||_2^2$ as $(\tilde{F}h)^*(\tilde{F}h) = h^*\tilde{F}^*Fh$. As in (12.6.2) we compute the gradient of $h^*\tilde{F}^*Fh$ that is equal to $\tilde{F}^*\tilde{F}h$ and we impose that it is parallel to h, i. e. the gradient of the constraint. The solutions h we are seeking for are the eigenvectors of $\tilde{F}^*\tilde{F}$ which means that $\tilde{F}^*\tilde{F}h = \lambda h$. This implies that $h^*\tilde{F}^*\tilde{F}h = \lambda$. Therefore the function whose maximum we are seeking for, in correspondance to the eigenvectors, assumes a value which is equal to the related eigenvalues. λ is the eigenvalue of $\tilde{F}^*\tilde{F}$ which means the eigenvalue of $(Fe^{\Lambda t}F^{-1})^*(Fe^{\Lambda t}F^{-1})$. Therefore:

$$maxe(a,b,R,t) = ||Fe^{\Lambda t}F^{-1}||_2^2.$$

In Fig. 12.2 (right pane) we show four graphs of maximal total energy growth and energy evolution of the solution with maximal initial energy growth. The computations are done for Poiseuille flow ($\xi = 1$) and $a = 2.1$, $b = 0$, and $R = 50, 87.55, 110$ and 1000. The results are in line with what is expected because the energy starts to grow for Reynolds number greater than 87.55 which is the Orr's critical Reynolds number. Computations can be done for any choice of ξ, a, b, R. We remark that Fig. 12.1 right and Fig. 12.2 (left pane) are computed with completely different methods and, taking into account that the second one is much more computationally heavy and hence has less sampling points, are identical. Both these figure are consistent with classical results for the flows of Couette $\xi = 0$ and of Poiseuille $\xi = 1$. Moreover, the surfaces are monotonically staked when ξ grows up to about 0.8. Above that value the surfaces intersect (this fact could be interesting to investigate).

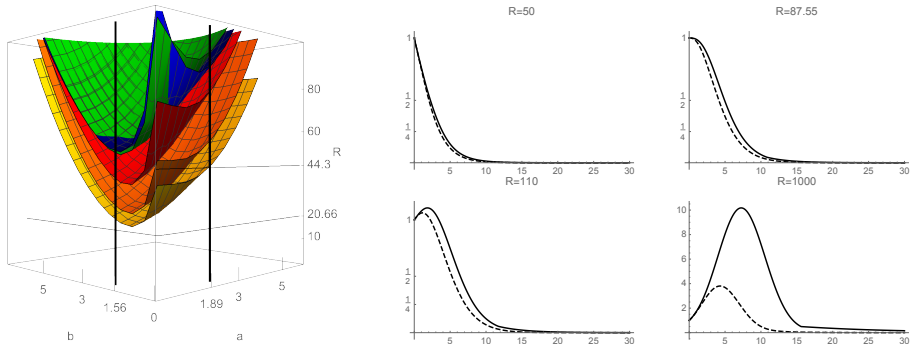

FIGURE 12.2: On the left pane, the threshold values $R_{a,b}$ for some choices of $\xi = 0$ (yellow), $\xi = 0.2$ (orange) $\xi = 0.5$ (red) $\xi = 0.8$ (green) and $\xi = 1$ (blue). The surfaces are computed determining, for sampling choices of a, b, the value of R at which the maximal initial growth rate is zero. This graph is identical to that of Fig. 12.1 right, it only contains fewer sampling points and doesn't diverge as clearly when $a = b = 0$ because the algorithm is less effective. On the right pane, four plots of maximal energy growth (solid) and energy growth along the solution with maximal initial growth (dashed). In the four pictures $\xi = 1$ (Poiseuille), $a = 2.1$, $b = 0$, and the value of R is declared in the figure.

Similar computations done for Poiseuille flow by fixing the Orr's critical wave numbers and that produce Fig. 12.2 (right pane), can be done for the same flow but by fixing the Joseph's critical wave number $a = 0$, $b = 2.05$.
The results are showed in Fig. 12.3 and they are obtained in correspondence to $R = 35, 49.55, 80$ and $R = 100$. They are in agreement with Joseph's results because the energy starts to grow for Reynolds numbers greater than 49.55 which is the Joseph's critical Reynolds number, but they are in contradiction with the proof that the streamwise perturbation are always stabilizing (see SubSec. 9.4.1). Indeed, according to such proof (see case iii) in SubSec. 9.4.1), the energy was expected to be always decreasing, for each value of Reynolds number.
A possible explanation of this contradiction between the proof and the results reported in Fig. 12.3 will be given at the end of the next section.

Finally we observe that in inclined channel the boundary conditions are typically stress free at the above boundary and temperature is often taken into account. In this work for simplicity we imposed rigid boundary conditions at both boundaries and isothermal fluid, this allows to disregard inclination.

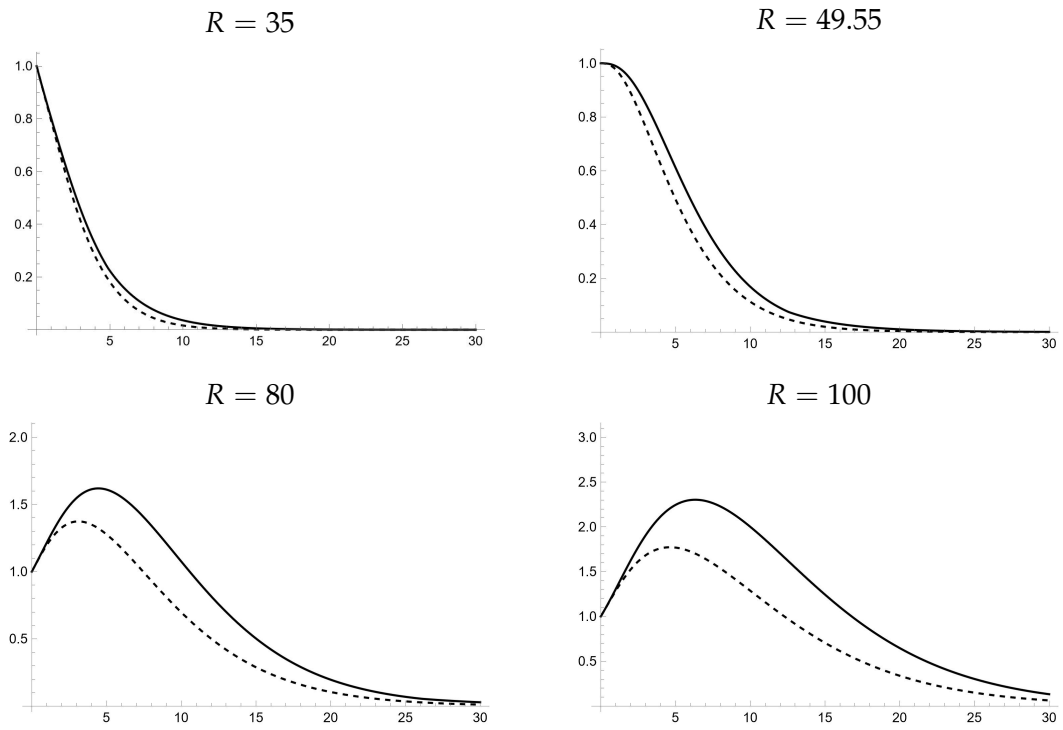

FIGURE 12.3: Four plots of maximal energy growth (solid) and energy growth along the solution with maximal initial growth (dashed). In the four pictures $\xi = 1$ (Poiseuille), $a = 0$, $b = 2.05$, and the value of R is declared in the figure.

Chapter 13

Spectral and Energy–Lyapunov stability of streamwise Couette–Poiseuille and spanwise Poiseuille base flows

In this last work we extend the study reported in Sec. 12. The setup is the one we introduced in Sec. 5 (**Case 1**). In Sec. 12 we simplified the basic motion by putting $\eta = 0$. Here we consider the more general case $\eta \neq 0$. Therefore we assume that the pressure gradient can have also a component transverse to the relative velocity of the moving plates. This adds to the Couette-Poiseuille base flow a Poiseuille component along the transverse direction (see eq. (5.0.8)). The results presented in this section have been published in a work carried out by Giacobbe and Perrone, 2023.

13.1 Summary

When a fluid fills an infinite layer between two rigid plates in relative motion, and it is simultaneously subject to a gradient of pressure not parallel to the motion, the base flow is a combination of Couette–Poiseuille in the direction along the boundaries' relative motion, but it also it possesses a Poiseuille component in the transverse direction. For this reason the linearised equations include all variables x, y, z, and not only explicitly two variables x, z as it typically happens in the literature. For convenience, we indicate as streamwise the direction of the relative motions of the plates, and spanwise the orthogonal direction. We use Chebyshev collocation method to investigate the monotonic behaviour of the energy along perturbations of general streamwise Couette–Poiseuille plus spanwise Poiseuille base flow, thus obtaining energy-critical Reynolds numbers depending on two parameters. We finally compute the spectrum of the linearisation at such base flows, and hence determine spectrum-critical Reynolds numbers depending on the two parameters. The choice of convex combinations of Couette and Poiseuille flows along the streamwise direction, and spanwise Poiseuille flow, affects the value of the energy-critical Reynolds and wave numbers in interesting ways. Also the spectrum-critical Reynolds and wave numbers depend on the type of base flow in peculiar ways. These dependencies are not described in the literature.

13.2 State of the art

Laminar steady state solutions for a fluid layer with rigid moving boundaries and a non-zero pressure gradient can be a combination of Couette and Poiseuille flows, see for example Drazin and Reid, 2004, pag. 223. The first investigation of linear stability of a base flow that is a combination of Couette and Poiseuille motions has been performed by Potter, 1966 and Hains, 1967. The first theoretical investigation in the same setup using Lyapunov's functions is a much more recent study of the evolution of energy (see Bergström, 2005). Experiments of such theoretical results have been performed by Klotz and Wesfreid, 2017. Such experiments lead to subcritical transition to turbulence, which is a debated argument in the field of stability of fluid flows Klotz et al., 2017.
The articles of Potter and Hains, and that of Bergstrom as well, are particular cases of our analysis for base flows that have vanishing spanwise Poiseuille component. The presence of cross-flow is particularly important in filtration, where the medium is porous and the Poiseuille type flow, due to a pressure gradient, is transversal with respect to a Poiseuille-Couette flow due to the motion of the filtrating substrate, see Lilley, 1959, Hains, 1971, Guha and Frigaard, 2010, Samanta, 2020. Most modern investigations deal with this type of flows in presence of porous media, few recent articles deal with the stability of Couette-Poiseuille flow, some in relation with Sommerfeld paradox (see for example Barkley and Tuckerman, 2005 or Falsaperla et al. 2019b), some with the addition of a magnetic field, see Ghosh and Das, 2019. None, to our knowledge, deal with base flows having two non-zero components.
Our setup generates base flows that depend on two parameters, that we call ξ and η (see eq. (5.0.8)). The first parameter ξ indicates the type of combination of Couette and Poiseuille flows along the streamwise direction, the second parameter η indicates the relative strength of the Poiseuille flow along the spanwise component. To every choice of parameters ξ, η there corresponds a threshold value of the Reynolds number above which there exist perturbations which correspond to eigenvectors whose eigenvalue has positive real part. We call this critical value *spectral-critical Reynolds number*. The spectral analysis requires heavy numerical computations, for this reason we plot graphs of the energy-critical Reynolds number and its corresponding critical wave number as functions of ξ with η fixed to zero (retracing Potter and Hains results) and as functions of η with ξ fixed to zero (Couette plus a spanwise increasingly strong Poiseuille flow) and to one (Poiseuille flow of given strength along the streamwise direction plus a spanwise increasingly strong Poiseuille flow). On the other hand, for every choice of parameters ξ, η there corresponds a threshold value of the Reynolds number above which there exist perturbations that have increasing energy. We call this critical value *energy-critical Reynolds number*. We compute both critical Reynolds numbers as functions of ξ, η. Together with the energy-critical Reynolds number we determine the associated critical perturbation and, in particular, its energy-critical wave numbers. We will make considerations on the 3D graph of energy-critical Reynolds numbers as function of ξ, η, and we will observe interesting features of energy-critical wave numbers.
The layout of the paper is the following: in Sec. 13.3 we write the equations for perturbations to the base flow in the original velocity fields and also in the stream fields, we conclude the section computing the orbital derivative of the energy. In Sec. 13.4 we compute the Euler-Lagrange equations for the critical values of the orbital derivative of the energy, we make an investigation of the energy-critical Reynolds number, and we compute the energy-critical wave numbers. In Sec. 13.5 we make a spectral investigation. Sec. 13.6 is dedicated to the discussion of the results and conclusions.

13.3 Base motions, perturbation equations, and Orr-Reynold's energy equations

We consider the setup we introduced in Sec. 5 (**Case 1**). The basic motion is given by eq. (5.0.8).
Observe that the choices $\xi = 1$ and $\eta \in \mathbb{R}$ do not allow the definition of spanwise and streamwise directions, and they all correspond to Poiseuille flow along a well defined direction, depending on η, parallel to $\mathbf{i}$ only when $\eta = 0$, but inclined with respect to our choice of $\mathbf{i}, \mathbf{j}$ when $\eta \neq 0$ (we will return to this observation when describing Fig. 13.4). This observation can be done in any case, and the base flow is always a combination of Couette in the streamwise direction and Poiseuille along any other direction, not necessarily streamwise.
The linear equations for the perturbations $u\,\mathbf{i} + v\,\mathbf{j} + w\,\mathbf{k}$, p to the base flow are

$$\begin{cases} u_t = \frac{1}{R}\Delta u - f u_x - g u_y - f' w - p_x \\ v_t = \frac{1}{R}\Delta v - f v_x - g v_y - g' w - p_y \\ w_t = \frac{1}{R}\Delta w - f w_x - g w_y - p_z \\ u_x + v_y + w_z = 0 \\ u = v = w = 0 \quad \text{on the boundary.} \end{cases} \tag{13.3.1}$$

Considering w and $\zeta = v_x - u_y$, the vorticity of (u, v, w) and performing the common reduction by means of the double curl of eqs. (13.3.1), one reduces the equations above to

$$\begin{cases} \Delta w_t = \frac{1}{R}\Delta^2 w - f\Delta w_x - g\Delta w_y + f'' w_x + g'' w_y \\ \zeta_t = \frac{1}{R}\Delta\zeta - f\zeta_x - g\zeta_y + f' w_y - g' w_x \\ w = w_z = \zeta = 0 \quad \text{on the boundary.} \end{cases} \tag{13.3.2}$$

As we have observed in Giacobbe, Mulone, and Perrone, 2022 (SubSec. 12.3), eqs. (12.3.3) define a bijection between incompressible velocity fields and stream functions (w and ζ).
Following Giacobbe, Mulone, and Perrone, 2022 (see SubSec. 12.4), eqs. (13.3.1) can be thought as *constrained* equations in the space $\mathcal{S}$ and eqs. (13.3.2) can be thought as *unconstrained* equations in the space $\mathcal{R}$. The space $\mathcal{S}$ can be decomposed in Fourier components $\mathcal{S} = \oplus_{a,b}\mathcal{S}_{a,b}$. The same can be done for $\mathcal{R} = \oplus_{a,b}\mathcal{R}_{a,b}$.
In each $\mathcal{S}_{a,b}$ and $\mathcal{R}_{a,b}$ one can define an energy $\mathcal{E}_{a,b}$.
We plan to investigate, depending on ξ, η, the *energy-critical Reynolds number* $\overline{R}_{\xi,\eta}$ of R at which the energy stops being a Lyapunov function, and the *energy-critical wave numbers* $(\overline{a}_{\xi,\eta}, \overline{b}_{\xi,\eta})$ of the perturbation $(\overline{u}_{\xi,\eta}, \overline{v}_{\xi,\eta}, \overline{w}_{\xi,\eta})$ that first violates strict monotonic decrease of the energy.
The problem we posed can be stated in analytic terms: on which perturbation of the velocity field the orbital derivative of the energy has its maximum, and for which R this maximum is zero? To solve this problem we numerically compute, for every ξ, η the maximum $\overline{m}_{\xi,\eta}$ of the functional

$$\mathcal{G}_{a,b}(w, \zeta) = \frac{(f' w_x, w_z) + (g' w_y, w_z) + (f' w_y, \zeta) - (g' w_x, \zeta)}{(\Delta w)^2 + |\nabla\zeta|^2}, \tag{13.3.3}$$

together with the associated wave numbers $(\overline{a}_{\xi,\eta}, \overline{b}_{\xi,\eta})$ (and the functions $(\overline{w}_{\xi,\eta}(z), \overline{\zeta}_{\xi,\eta}(z))$ that realise such maximum). The functional $\mathcal{G}$ is deduced from the

orbital derivative of $\mathcal{E}_{a,b}$ in its stream functions form. In fact

$$\dot{\mathcal{E}}_{a,b} = \left[\mathcal{G}_{a,b}(w,\zeta) - \frac{1}{R}\right]\left((\Delta w)^2 + |\nabla\zeta|^2\right), \tag{13.3.4}$$

and hence $\mathcal{E}_{a,b}$ is strictly decreasing if and only if $1/R > \overline{m}_{\xi,\eta}$, from which it follows that the energy-critical Reynolds number $\overline{R}_{\xi,\eta} = 1/\overline{m}_{\xi,\eta}$, and the energy-critical wave numbers are the wave numbers $(\overline{a}_{\xi,\eta}, \overline{b}_{\xi,\eta})$ computed above.

13.4 Energy (non-modal) investigation of the system

The critical stream fields for the functional $\mathcal{G}_{a,b}(w,\zeta)$ are the solutions to the Euler-Lagrange equations

$$\begin{cases} 2m\Delta^2 w = -f''w_x - g''w_y - 2f'w_{xz} - 2g'w_{yz} - f'\zeta_y + g'\zeta_x \\ 2m\Delta\zeta = -f'w_y + g'w_x \\ w = w_z = \zeta = 0 \quad \text{on the boundary.} \end{cases} \tag{13.4.1}$$

We stress the often disregarded fact that if there exists an m such that eqs. (13.4.1) admit a non-zero solution $(\overline{w}_m, \overline{\zeta}_m)$, then m is a critical value for $\mathcal{G}$ and $(\overline{w}_m, \overline{\zeta}_m)$ is a critical point only if *in addition* $\mathcal{G}(\overline{w}_m, \overline{\zeta}_m) = m$.
Starting from eqs. (13.4.1), we use a spectral method to compute the critical values m of $\mathcal{G}$. We can in fact consider eqs. (13.4.1) as a generalised eigenvalue problem

$$\left[m\begin{pmatrix} D^4 - 2k^2D^2 + k^4 & 0 \\ 0 & D^2 - k^2 \end{pmatrix} - \begin{pmatrix} -i\frac{af''+bg''}{2} - iaf'D - ibg'D & -i\frac{bf'-ag'}{2} \\ -i\frac{bf'-ag'}{2} & 0 \end{pmatrix}\right]\begin{pmatrix} w(z) \\ \zeta(z) \end{pmatrix} = 0, \tag{13.4.2}$$

where D represents the derivative with respect to z. We use a standard Chebyshev collocation algorithm to compute the values m that admit a non-zero solution, in other words we write

$$\left[m\begin{pmatrix} (D_N^2 - k^2\mathbb{I})^2 & 0 \\ 0 & D_N^2 - k^2\mathbb{I} \end{pmatrix} + i\begin{pmatrix} \frac{af_N'' + bg_N''}{2} + af_N'D_N + bg_N'D_N & \frac{bf_N' - ag_N'}{2} \\ \frac{bf_N' - ag_N'}{2} & 0 \end{pmatrix}\right]\begin{pmatrix} w_N \\ \zeta_N \end{pmatrix} = 0, \tag{13.4.3}$$

where D_N is a $(N+1)\times(N+1)$ matrix f_N is a diagonal matrix that on the diagonal has the values of f on the $N+1$ Chebyshev nodes (same for g and their derivatives), $\mathbb{I}$ is the $(N+1)\times(N+1)$ identity matrix, and w_N, ζ_N are $n+1$ vectors whose components are the values of w, ζ along the Chebyshev nodes. This approach allows to compute, for every ξ, η, the maximum $\overline{m}_{\xi,\eta}$, its associated energy-critical Reynolds numbers $\overline{R}_{\xi,\eta} = 1/\overline{m}_{\xi,\eta}$, and the associated energy-critical wave numbers $(\overline{a}_{\xi,\eta}, \overline{b}_{\xi,\eta})$.
An idea of the critical wave numbers $\overline{a}_{\xi,\eta}$ and $\overline{b}_{\xi,\eta}$ can be given with a density plot in the plane ξ, η. In Fig. 13.1 left we indicate in dark gray the region in which $\overline{a}_{\xi,\eta} = 0$, in light gray the region in which $\overline{b}_{\xi,\eta} = 0$, and in white the region in which both $\overline{a}_{\xi,\eta}$ and $\overline{b}_{\xi,\eta}$ are not zero.
In absence of spanwise component in the base flow ($\eta = 0$) the energy-critical solution is independent of x. In the literature, see Reddy et al., 1998, Falsaperla et al. 2019b, this event is defined as streamwise, but this name is misleading, since it does not mean that the energy-critical solution has only streamwise component (i.e.

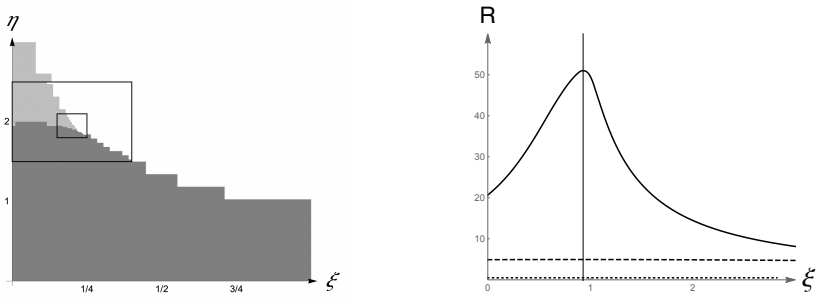

FIGURE 13.1: In the left pane, a density plot of energy-critical wave numbers: the energy-critical perturbation is only streamwise, that is $a = 0$, when (ξ, η) belongs to the dark gray region, it is only spanwise, that is $b = 0$, when (ξ, η) belongs to the light gray region, it is mixed, that is $a, b \neq 0$, when (ξ, η) belongs to the white region. In the rectangular frames an investigation on a finer grid has been performed to give a better understanding around the meeting point of the three regions. The main plot is computed on a grid with steps of approximately 0.15 in η, 0.05 in ξ. In the two rectangles the steps have been reduced to 0.05 in η, 0.02 in ξ and 0.005 in η, 0.01 in ξ respectively. In the right pane, three slices of $\overline{R}_{\xi,\eta}$, as ξ ranges from 0 to 3, for fixed values of $\eta = 0$ (continuous black) $\eta = 10$ (dashed) and $\eta = 100$ (dotted).

$v = 0$), but it only means that the solution is independent on x and hence its flow can be translated along the x-component, which typically produces rolls whose axis is along the stream direction.
When the streamwise component is Couette ($\xi = 0$) and in presence of increasingly strong Poiseuille spanwise component of the base flow, the energy-critical solution turns suddenly from streamwise to spanwise, this is not unreasonable, and it has a possible realisation with an appropriate deformation of Figure 1 right in Giacobbe, Mulone, and Perrone, 2022. For every $\xi \neq 0$ and η large enough, the most energy-critical perturbation will have both wave numbers non-zero (we call such perturbation "mixed"). If the Couette component is dominating (that is ξ is close enough to zero) then an increase of η changes the energy-critical perturbation from streamwise to spanwise and finally to mixed.
The peculiar meeting point of the three regions required a finer investigation to check the presence of a chaotic interface, which does not seem to appear. The step-size of the coarse and finer grids are specified in the caption of Fig. 13.1.
The representation of the energy-critical Reynolds numbers is given in Fig. 13.2 as a function of ξ, η and in Fig. 13.1 right for three slices with $\eta = 0, 10, 100$. Observe that in the case of zero spanwise component in the base flow, the energy-critical Reynolds numbers have a maximum on a base flow that is not Poiseuille only, but it has a small Couette component, and hence it corresponds to slowly moving plates. The consequence of this fact is visible in the crossing of the surfaces computed by Giacobbe, Mulone, and Perrone, 2022 and plotted in their Figure 1 and 2. The energy-critical Reynolds number decreases when η increases, and it can be numerically proven to converge to zero (see Fig. 13.1 right). This indicates a destabilising effect of the transverse flow.
The energy-critical values $\overline{R}_{\xi,\eta}$ plotted in Fig. 13.2 are a continuous function of ξ, η, but at the boundaries of the regions shaded in Fig. 13.1 left such function appears to have crests that indicate discontinuous derivative.

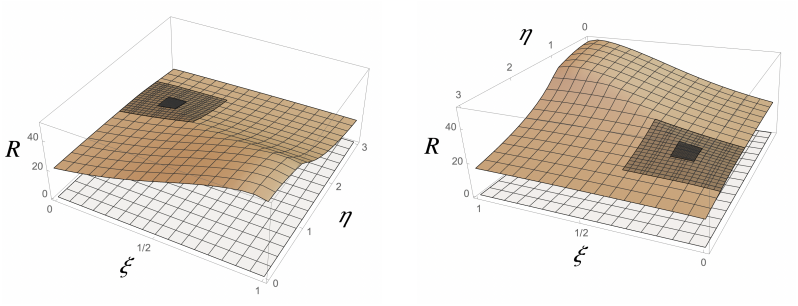

FIGURE 13.2: Two views of the graph of $\overline{R}_{\xi,\eta}$, the function that to every ξ, η associates the smallest value of R at which the energy stops being a Lyapunov function. The two rectangular patches correspond to the two rectangles where a finer grid has been used to produce Fig. 13.1 left.

13.5 Spectral (modal) investigation of the system

Eqs. (13.3.2) can be used to compute the spectrum of this system for any given base flow, that is for every choice of ξ, η, and for any choice of wave numbers a, b and Reynolds numbers R.
The computation of the spectrum leads to the determination of the critical wave numbers and the critical Reynolds number that are, for every ξ, η, the triplet $(\widetilde{a}_{\xi,\eta}, \widetilde{b}_{\xi,\eta}, \widetilde{R}_{\xi,\eta})$ at which one eigenvalue of the spectrum has zero real part and for which $\widetilde{R}_{\xi,\eta}$ is the smallest possible Reynolds number at which this happens.

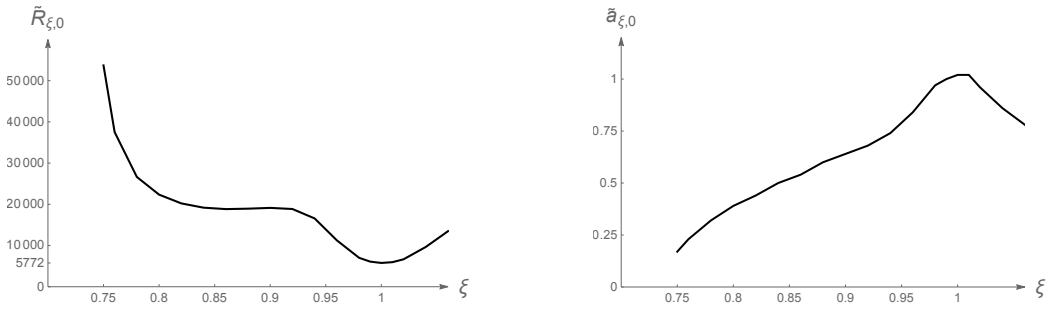

FIGURE 13.3: In the left pane the plot of $\widetilde{R}_{\xi,0}$ with ξ from 0.76 to 1.06. In the right pane the plot of $\widetilde{a}_{\xi,0}$ in the same range for ξ.

For $\eta = 0$ these critical values have been computed implicitly in Potter, 1966 and explicitly in Hains, 1967, where a plot similar to our Fig. 13.3 left can be found. For Couette base flow, which corresponds to our case $\xi = 0$ and $\eta = 0$, it is known that $\widetilde{R}_{0,0} = +\infty$ and hence there are no critical wave numbers. For Poiseuille base flow, which corresponds to our case $\xi = 1$ and $\eta = 0$, it is known that $\widetilde{R}_{1,0} = 5772$ and the critical wave numbers are $\widetilde{a}_{1,0} = 1.02$ and $\widetilde{b}_{1,0} = 0$.
We make our computations using a Chebyshev collocation method. For every chosen ξ, η, we numerically define the function $EVmax(a, b, R)$ that, given two wave numbers a, b and a Reynolds number R computes the maximum of the real part of the eigenvalues. The determination of $\widetilde{a}_{\xi,\eta}, \widetilde{b}_{\xi,\eta}, \widetilde{R}_{\xi,\eta}$ requires to find the Reynolds number that makes this maximum equal to zero, one has then to minimise with respect to a, b. For this reason a simple bisection method on R

cannot be used, we hence defined a function $EVmaxab(a_0, b_0, \delta)(R)$ that seeks, for a given R, the values $(a_w, b_w) \in [a_0 - \delta, a_0 + \delta] \times [b_0 - \delta, b_0 + \delta]$ on which $EVmax(a_w, b_w, R)$ is maximal. A modified bisection method on R can hence be set up: for every couple $((a_-, b_-, R_-), (a_+, b_+, R_+))$ such that $EVmax(a_-, b_-, R_-) < 0$ and $EVmax(a_+, b_+, R_+) > 0$, we compute the minimising wave numbers

$$(a_w, b_w) \in [(a_- + a_+)/2 - \delta, (a_- + a_+)/2 + \delta] \times [(b_- + b_+)/2 - \delta, (b_- + b_+)/2 - \delta]$$

for $R_m = (R_- + R_+)/2$. If $EVmax(a_w, b_w, R_m) < 0$ then the first element of the initial couple can be replaced by (a_w, b_w, R_m), otherwise $EVmax(a_w, b_w, R_m) > 0$ and hence the second element of the initial couple can be replaced with (a_w, b_w, R_m). Iterating this process, the convergence of R is granted, but some care has to be used to make sure that also the wave numbers do converge to the real critical wave numbers.
In our computations we made various choices for δ, but mainly we chose $\delta = 0.1$. For every choice of ξ, η we used the critical values computed for neighbouring ξ, η, with small variations in the wave numbers and variation of the order 10^2 for R.
In Fig. 13.3 we fix $\eta = 0$ and plot the critical Reynolds number $\widetilde{R}_{\xi,0}$ and the critical wave number $\widetilde{a}_{\xi,0}$ for varying values of $\xi \in [0.76, 1.06]$. A plot equivalent to this can be found in Hains, 1967, Figure 2. In this case, the critical wave number $\widetilde{b}_{\xi,0}$ is always zero. A few peculiar facts are that:

- In this case the critical perturbations, where instability must occur, are perturbations independent from y. This is in opposition with what happens for the energy-critical perturbations, where “instability" first occurs on perturbations independent from x;
- Poiseuille flow realises the minimal critical Reynolds number;
- when ξ decreases from 1, the increase of $\widetilde{R}_{\xi,0}$ flattens and slightly changes monotonicity in the region $[0.8, 0.9]$;
- the critical Reynolds number does eventually tend to infinity as ξ diminishes. In our computation we have not been able to compute a critical Reynolds number for $\xi = 0.75$, the last value of ξ for which we found a critical Reynolds number is $\xi = 0.76$.

The first point is reasonable, the second is a known result due to Joseph, the third is unexpected, and a monotonic behaviour would appear more natural. As for the last point, an asymptote is expected, because it is well known that Couette is always spectrally stable, but it would be interesting to compute the position of the vertical asymptote (possibly $\xi = 3/4$) and understand if there is a reason for this.
In Fig. 13.4 we fix $\xi = 1$, and we plot the critical Reynolds number and the critical wave numbers as η moves in $[0, 1.05]$. These plots are precisely as expected, since when $\xi = 1$, for every η, the base flow is a Poiseuille flow along the direction $\mathbf{i} + \jmath\,\mathbf{j}$ with the nondimensionalisation done so that the maximal velocity of the fluid is $\sqrt{1+\eta^2}$. This implies that the Reynolds number must be $\widetilde{R}_{1,\eta} = 5772/\sqrt{1+\eta^2}$ and the two wave numbers must be $\widetilde{a}_{1,\eta} = 1.02/\sqrt{1+\eta^2}$, $\widetilde{b}_{1,\eta} = 1.02\,\eta/\sqrt{1+\eta^2}$.

In Fig. 13.5 some less expected features can be seen. The black continuous plot is that of the function $\widetilde{R}_{0,\eta}$, which is the critical Reynolds number of a base flow that is Couette along the streamwise $\mathbf{i}$ direction and has an increasingly strong (with η) Poiseuille flow along the spanwise $\mathbf{j}$ direction. The other two gray plots in the figure are those of $\widetilde{R}_{1,\eta}$ and of $\widetilde{R}_{\eta}$, that corresponds to the Reynolds number of a

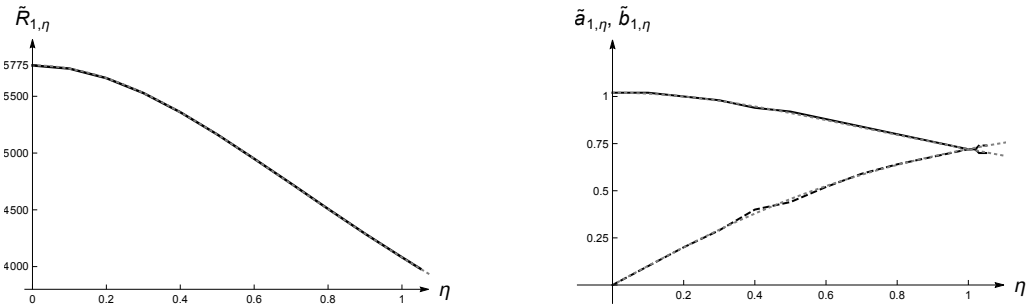

FIGURE 13.4: In the two panes the plots of $\widetilde{R}_{1,\eta}$, $\widetilde{a}_{1,\eta}$ (continuous black line) and of $\widetilde{b}_{1,\eta}$ (dashed black line) for η in the interval $[0, 1.1]$. The dotted grey graphs are their theoretical values, $\widetilde{R}_{1,\eta} = 5772/\sqrt{1+\eta^2}$, $\widetilde{a}_{1,\eta} = 1.02/\sqrt{1+\eta^2}$, $\widetilde{b}_{1,\eta} = 1.02\eta/\sqrt{1+\eta^2}$. When $\eta = 1$ the Poiseuille flow is precisely along the diagonal, and the two wave numbers become equal.

Poiseuille base flow nondimensionalised so that the maximal velocity of the fluid is η.

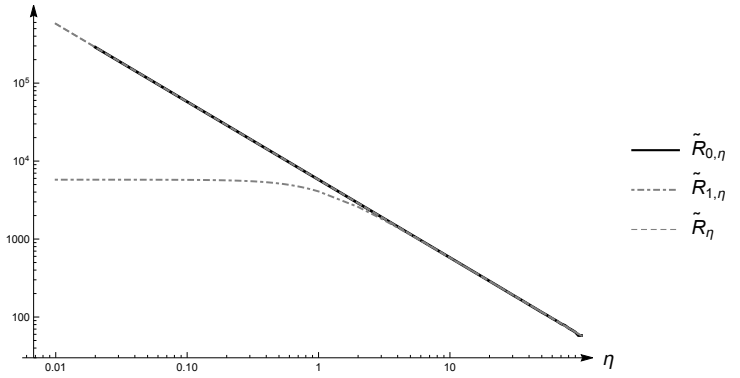

FIGURE 13.5: In black, the log-log-plot of $\widetilde{R}_{0,\eta}$ as η moves from 0 to 100. The grey dotdashed graph is the log-log-plot of the function $5772/\sqrt{1+\eta^2}$, that is the theoretical critical value of $\widetilde{R}_{1,\eta}$ already plotted in Fig. 13.4 left pane. The gray dotted graph superimposed to the black plot is that of the function $\widetilde{R}_{\eta} = 5772/\eta$, the Reynolds number of a Poiseuille flow nondimensionalised to have maximal velocity η.

As expected, the asymptotic behaviour of all three graphs is the same as η grows, since the Poiseuille component is increasingly strong and hence becomes dominating. As η tends to zero the graph of $\widetilde{R}_{1,\eta}$ tends, as expected, to 5774. What is striking is that the asymptotic of $\widetilde{R}_{0,\eta}$ and that of $\widetilde{R}_{\eta}$ is the same. Observe that the first one is the critical Reynolds number of Couette flow plus an infinitesimal transversal Poiseuille flow, while the second one is simply an infinitesimal Poiseuille flow.

13.6 Discussion of the results

In this article we made a modal and a non-modal analysis of a base flow that is Couette-Poiseuille in the streamwise direction and Poiseuille in the (crossed) spanwise direction. We did analyse in detail the effects of the Poiseuille crossflow on the monotonicity of the energy and on the spectrum of the linearisation at the base flow. In particular we did investigate the dependence of critical Reynolds number and critical wave numbers depending on the combination of Couette-Poiseuille streamwise flow and on the intensity of the Poiseuille crossflow.
The most interesting result can be obtained investigating the energy-critical wave number, where smooth changes from stream ($a = 0$) to mixed (both $a, b \neq 0$) to span ($b = 0$) can be observed, together with more surprising discontinuous changes from streamwise to spanwise changes, that take place if the Poiseuille-type contribution to the base flow in the streamwise direction is weak enough. This abrupt changes also reflects into a discontinuity of the first derivative of the energy-critical Reynolds numbers.
The modal analysis requires a heavier computational load, and we mostly obtained either confirmations of known results by Potter and Hains, or results that could be computed theoretically by considering known spectrum-critical Reynolds and wave numbers for Poiseuille flow applied to a non-normalised Poiseuille flow along a transverse direction. A new result is the observation that, if the base flow is Couette (obviously along the streamwise direction) plus a weak contribution of spanwise Poiseuille, event that is most probable in nature and is typical if one considers a small perturbation of a dominating base flow, then the spectrum-critical Reynolds number tends to infinity as it would do simply with a weak Poiseuille flow (meaning computing the Reynolds number for a Poiseuille flow nondimensionalised so that its maximal velocity equals η and not 1).

Chapter 14

A possible proof of the validity of the conjecture and final comments

The conjecture (see Sec. 9) would seem to lean towards the validity of Orr's results but the study of the transient does not (see Sec. 12)
However in a recent article Mulone, 2024 proposes a proof of the conjecture. In this section we report the principal results of Mulone, 2024 and we provide a possible reason why the Joseph's computations and the ones related to the transient growth's lead to underestimate the critical Reynolds number.

We recall the energy equation (see eq. (9.4.1) in SubSec. 9.4)

$$\dot{E} = -(f'w, u) - \mathrm{Re}^{-1}[\|\nabla u\|^2 + \|\nabla v\|^2 + \|\nabla w\|^2]$$

and the divergence free condition

$$u_x + v_y + w_z = 0.$$

First of all Mulone, 2024 underlines the observations made by Lorentz, 1907, also reported in Lamb, 1924, p. 640: "One or two consequences of the energy equation may be noted. In the first place, the relative magnitude of the two terms on the right-hand side is unaffected if we reverse the signs of u, v, w, or if we multiply them by any constant factor. The stability of a given state of mean motion should not therefore depend on the scale of the disturbance. On the other hand, certain combinations of u, v, w, appear to be more favourable to stability than others".
Therefore, Mulone says "In the study of the following maximum problems we will always assume that this scale invariance property holds."

Secondly he distinguishes two cases. For perturbations with $-(f'w, u) \leq 0$ and $\|\nabla \mathbf{u}\| > 0$, then $\dot{E} < 0$.
Otherwise, if $-(f'w, u) > 0$, from the energy equation we have

$$\begin{aligned} \dot{E} &= \left(\frac{-(f'w, u)}{\|\nabla u\|^2 + \|\nabla v\|^2 + \|\nabla w\|^2} - \frac{1}{\mathrm{Re}} \right) \|\nabla \mathbf{u}\|^2 \leq \\ &\leq \left(m - \frac{1}{\mathrm{Re}} \right) \|\nabla \mathbf{u}\|^2, \end{aligned} \tag{14.0.1}$$

(see eq. (9.4.2) in SubSec. 9.4) where

$$\frac{1}{\mathrm{Re}_E} = m = \max_{\mathcal{S}} \frac{-(f'w, u)}{\|\nabla u\|^2 + \|\nabla v\|^2 + \|\nabla w\|^2}, \tag{14.0.2}$$

(see eq. (9.4.3) in SubSec. 9.4) and $\mathcal{S}$ is the space of the *kinematically admissible fields* (see eq. (9.4.4) in SubSec. 9.4)

$$\begin{aligned} \mathcal{S} = \{u, v, w \in H^1(\Omega),\ u = v = w = w_z = 0 \text{ on the boundaries,} \\ \text{periodic in } x, \text{ and } y, \quad u_x + v_y + w_z = 0, \quad \|\nabla \mathbf{u}\| > 0\}. \end{aligned} \tag{14.0.3}$$

$H^1(\Omega)$ is the Sobolev space of the functions which are in $L_2(\Omega)$ together with their first generalized derivatives.

Now, consider the functional ratio

$$\mathcal{F}(u, v, w) = \frac{-(f'w, u)}{\|u_x\|^2 + \|u_y\|^2 + \|u_z\|^2 + \|v_x\|^2 + \|v_y\|^2 + \|v_z\|^2 + \|w_x\|^2 + \|w_y\|^2 + \|w_z\|^2} \tag{14.0.4}$$

in $\mathcal{S}$.
We have

Proposition 14.0.1. *There exists the maximum of $\mathcal{F}(u, v, w)$ in $\mathcal{S}$ (Rionero, 1968a) and the maximum is a non-negative value.*

Proposition 14.0.2. *The maximum of $\mathcal{F}(u, v, w)$ in $\mathcal{S}$ is equal to the maximum of the ratio $\mathcal{F}(u, v, w)$ where now $v_y = 0$.*

The idea is to prove that the maximum of $\mathcal{F}$ is less than or equal to the maximum of the ratio with $(u, v, w) \in \mathcal{S}$ such that $v_y = -(u_x + w_z) = 0$. To do this, define

$$\mathcal{F}_x(u, v, w) = \frac{-(f'w, u)}{\|u_x\|^2 + \|u_y\|^2 + \|u_z\|^2 + \|v_x\|^2 + \|v_z\|^2 + \|w_x\|^2 + \|w_y\|^2 + \|w_z\|^2} \tag{14.0.5}$$

and observe that for any fixed $(u_1, v_1, w_1) \in \mathcal{S}$ we have

$$\mathcal{F}(u_1, v_1, w_1) \leq \mathcal{F}_x(u_1, v_1, w_1).$$

Moreover,

$$\mathcal{F}_x(u_1, v_1, w_1) \leq \max \mathcal{F}_x(u, v, w),$$

where the maximum is sought among all fields $(u, v, w) \in \mathcal{S}$ with $v_y = 0$. Suppose that this maximum is obtained in $(\hat{u}, \hat{v}, \hat{w}) \in \mathcal{S}$ with $\hat{v}_y = 0$. We therefore have

$$\mathcal{F}(u_1, v_1, w_1) \leq \mathcal{F}_x(\hat{u}, \hat{v}, \hat{w}), \quad \text{for any} \quad (u_1, v_1, w_1) \in \mathcal{S}.$$

From this it follows that $\mathcal{F}_x(\hat{u}, \hat{v}, \hat{w})$ is an upper bound for the numerical set described by $\mathcal{F}(u_1, v_1, w_1)$ as (u_1, v_1, w_1) varies in $\mathcal{S}$. Consequently, for the maximum of $\mathcal{F}(u_1, v_1, w_1)$ in $\mathcal{S}$, which is the least upper bound (and maximum), we have

$$\max_{\mathcal{S}} \mathcal{F}(u_1, v_1, w_1) \leq \max \mathcal{F}_x(u, v, w) = \mathcal{F}_x(\hat{u}, \hat{v}, \hat{w}).$$

Obviously, in the previous inequality the equal sign holds because the set of elements (u, v, w) of $\mathcal{S}$ with $v_y = 0$ is a subset of $\mathcal{S}$. □

Proposition 14.0.3. *The maximum of $F_x(u, v, w)$ in $\mathcal{S}$ is obtained at a vector field $(u(x, z), 0, w(x, z))$. It coincides with the maximum of $F(u, v, w)$ assumed at two-dimensional spanwise perturbations, as Orr has supposed.*

First we prove that the maximum of $F_x(u, v, w)$ is obtained at a vector $(u(x, y, z), 0, w(x, y, z))$ of $\mathcal{S}$ such that $u_x + w_z = 0$. To see this, we write the Euler-Lagrange equations of this maximum (let us call this maximum with the same symbol m as before, in fact we will prove that it coincides with the maximum (14.0.2))

$$\frac{1}{\mathrm{Re}_E} = m = \max_{\mathcal{S}} \frac{-(f'w, u)}{\|\nabla u\|^2 + \|v_x\|^2 + \|v_z\|^2 + \|\nabla w\|^2}. \tag{14.0.6}$$

They are

$$(-f'w + 2m\Delta u)\mathbf{i} + 2m(v_{xx} + v_{zz})\mathbf{j} + (-f'u + 2m\Delta w)\mathbf{k} = \nabla\lambda, \tag{14.0.7}$$

where $\lambda(x, y, z)$ is a Lagrange multiplier.

Secondly we again consider the Euler-Lagrange equations, in particular we consider the system given by the first and the third component of the Euler-Lagrange equations. We adopt plane-form perturbations as usual with a and b wave numbers in the x and y directions respectively. From the first equation of the system we distinguish two cases: $b = 0$ and $b \neq 0$. The first case gives the Orr's equation. Otherwise, the second case leads to $\|\nabla \mathbf{u}\| = 0$ that has been excluded.
Therefore the only possibility is that the derivatives of u and w with respect to y are zero.

Proposition 14.0.4. *The critical Reynolds number Re_E is given by the Orr's equation*

$$\mathrm{Re}_E(f''w_x + 2f'w_{xz}) + 2\Delta\Delta w = 0, \tag{14.0.8}$$

with b.c. $w = w' = 0$. □

Finally, we have the proposition:

Proposition 14.0.5. *On the streamwise perturbations (those which satisfy the condition $\frac{\partial}{\partial x} \equiv 0$) the scalar product $(-f'u, w) \leq 0$.* □

This proposition is in agreement with Theorem 9.4.1 (See Sec. 9).
This fact can be proved here in a different way. Indeed the energy identity holds for both linear and nonlinear systems, see for instance what Schmid and Henningson, 2001a, p. 189, observe: "the terms stemming from the nonlinear terms of the Navier-Stokes equations are not present in the final evolution equation for the energy. We therefore conclude that the nonlinear terms of the Navier-Stokes equation preserve energy". Now, if we consider the spectral problem in the linear system, in the case of streamwise perturbations, it is well known that the eigenvalues are all real, negative, and distinct numbers (see for instance Schmid and Henningson, 2001a, Chap. 3). Therefore, for streamwise perturbations, as Mulone suggest in

2024, it can be proved that any finite linear combination of eigenvectors has the time derivative of the energy which is a negative-definite quadratic form for every Reynolds number.

Indeed, consider the system 9.3.1 without the non linear therms and suppose that $\frac{\partial}{\partial x} \equiv 0$. If (u, v, w) is an eigenvector of the resulting system associated to the eigenvalue σ, the system becomes:

$$\begin{cases} u_t = \mathrm{Re}^{-1}\Delta u - f'w \\ v_t = \mathrm{Re}^{-1}\Delta v - p_y \\ w_t = \mathrm{Re}^{-1}\Delta w - p_z. \end{cases} \tag{14.0.9}$$

Now if we multiply the first equation of the system by u, the second one by v and the third one by w we obtain:

$$\begin{cases} \sigma\|u\|^2 = -\mathrm{Re}\|\nabla u\|^2 - (f'w, u) \\ \sigma\|v\|^2 = -\mathrm{Re}\|\nabla v\|^2 - (p_y, v) \\ \sigma\|w\|^2 = -\mathrm{Re}\|\nabla w\|^2 - (p_z, w). \end{cases} \tag{14.0.10}$$

By adding the second and the third equation of the previous system and remembering that $v_y + w_z = 0$ we have

$$\sigma(\|u\|^2 + \|v\|^2) = -\mathrm{Re}(\|\nabla u\|^2 + \|\nabla v\|^2),$$

and this implies that σ is real and negative. This fact, that here is deduced analytically, is confirmed by the numerical results.

By adding the three equations we have

$$\sigma(\|u\|^2 + \|v\|^2 + \|w\|^2) = -\mathrm{Re}(\|\nabla u\|^2 + \|\nabla v\|^2 + \|\nabla w\|^2) - (f'w, u).$$

As $\sigma < 0$, from the last equation it follows that $-(f'w, u) < 0$.

Now we consider a combination of two eigenvectors $\mathbf{u}_1$ and $\mathbf{u}_2$, that is $a_1(u_1, v_1, w_1) + a_2(u_2, v_2, w_2)$, associated respectively to the eigenvalues σ_1 and σ_2 and we evaluate the system on this combination of eigenvectors:

$$\begin{cases} (a_1u_1 + a_2u_2)_t = \mathrm{Re}^{-1}\Delta(a_1u_1 + a_2u_2) - f'(a_1w_1 + a_2w_2) \\ (a_1v_1 + a_2v_2)_t = \mathrm{Re}^{-1}\Delta(a_1v_1 + a_2v_2) - p_y \\ (a_1w_1 + a_2w_2)_t = \mathrm{Re}^{-1}\Delta(a_1w_1 + a_2w_2) - p_z. \end{cases} \tag{14.0.11}$$

Now we multiply the first equation by $a_1u_1 + a_2u_2$, the second one by $a_1v_1 + a_2v_2$ and the third one by $a_1w_1 + a_2w_2$, and we obtain:

$$\begin{cases} {a_1}^2\sigma_1\|u_1\|^2 + 2a_1a_2(u_1, u_2)(\sigma_1 + \sigma_2) + \sigma_2{a_2}^2\|u_2\|^2 = -\mathrm{Re}^{-1}\|\nabla(a_1u_1 + a_2u_2)\|^2 + \\ \qquad\qquad - (f'(a_1w_1 + a_2w_2), a_1u_1 + a_2u_2) \\ {a_1}^2\sigma_1\|v_1\|^2 + 2a_1a_2(v_1, v_2)(\sigma_1 + \sigma_2) + \sigma_2{a_2}^2\|v_2\|^2 = -\mathrm{Re}^{-1}\|\nabla(a_1v_1 + a_2v_2)\|^2 - (p_y, a_1v_1 + a_2v_2) \\ {a_1}^2\sigma_1\|w_1\|^2 + 2a_1a_2(w_1, w_2) + {a_2}^2\|w_2\|^2 = -\mathrm{Re}^{-1}\|\nabla(a_1w_1 + a_2w_2)\|^2 - (p_z, a_1w_1 + a_2w_2). \end{cases} \tag{14.0.12}$$

As we did before we take into account the fact that both σ_1 and σ_2 are real negative. Furthermore from the numerical calculations we know that they are all distinct.

These three facts imply that the eigenvectors are orthogonal, i.e. $(\mathbf{u}_1, \mathbf{u}_2) = 0$. Therefore, also in this case, by adding the three equations we can deduce that $-(f'(a_1w_1 + a_2w_2), a_1u_1 + a_2u_2) < 0$.
It can be proved by induction that $-(f'w, u)$ is negative on the streamwise perturbations for a combination of n eigenvectors.
After proving that that the maximum of $\mathcal{F}(u, v, w)$ is assumed at two dimensional perturbations, according to the results of Orr, we highlight the problems that arises from the equation studied by Joseph and give a possible explanation of the reason why he underestimates the critical Reynolds number.

We first observe that the Euler-Lagrange equations of the maximum (14.0.2) are

$$\begin{cases} f'(\zeta_y + 2w_{xz}) + f''w_x + 2m\Delta\Delta w = 0 \\ f'w_y + 2m\Delta\zeta = 0, \end{cases} \tag{14.0.13}$$

where $\zeta = v_x - u_y$ is the third component of vorticity. Such equations, in the streamwise case, that is $\frac{\partial}{\partial x} \equiv 0$ reduce to the system

$$\begin{cases} f'\zeta_y + 2m\Delta\Delta w = 0 \\ f'w_y + 2m\Delta\zeta = 0, \end{cases} \tag{14.0.14}$$

where now $\Delta h = h_{yy} + h_{zz}$, $h = w$ or $h = \zeta$. This system, eliminating ζ, reduces (for simplicity consider the case of Couette, i.e. $f' = 1$) to the equation (used by Joseph)

$$4m^2\Delta\Delta\Delta w - w_{yy} = 0 \tag{14.0.15}$$

and this equation is a quadratic equation in m.

We do the following remarks:

1. Observe the often disregarded fact that if there exists an m such that the Euler-Lagrange equations admit a non-zero solution $(\bar{u}_m, \bar{v}_m, \bar{w}_m)$, then m is a critical value for $\mathcal{F}$ and $(\bar{u}_m, \bar{v}_m, \bar{w}_m)$ is a critical point only if also $\mathcal{F}(\bar{u}_m, \bar{v}_m, \bar{w}_m) = m$ holds.
   Indeed we must compute the maximum of $\mathcal{F}(u, v, w)$ in $\mathcal{S}$ and, if we denote the numerator and the denominator of $\mathcal{F}(u, v, w)$ respectively with $N_\mathcal{F}$ and $D_\mathcal{F}$, this implies to find $(\bar{u}_m, \bar{v}_m, \bar{w}_m)$ such that the derivatives of the function with respect to u, v and w are zero:

$$\begin{cases} \dfrac{\frac{\partial N_\mathcal{F}}{\partial u}D_\mathcal{F} - N_\mathcal{F}\frac{\partial D_\mathcal{F}}{\partial u}}{D_\mathcal{F}^2} = 0 \\ \dfrac{\frac{\partial N_\mathcal{F}}{\partial v}D_\mathcal{F} - N_\mathcal{F}\frac{\partial D_\mathcal{F}}{\partial v}}{D_\mathcal{F}^2} = 0 \\ \dfrac{\frac{\partial N_\mathcal{F}}{\partial w}D_\mathcal{F} - N_\mathcal{F}\frac{\partial D_\mathcal{F}}{\partial w}}{D_\mathcal{F}^2} = 0 \end{cases} \Leftrightarrow \begin{cases} \dfrac{\frac{\partial N_\mathcal{F}}{\partial u}}{D_\mathcal{F}} - \dfrac{N_\mathcal{F}}{G_\mathcal{F}}\dfrac{\frac{\partial D_\mathcal{F}}{\partial u}}{D_\mathcal{F}} = 0 \\ \dfrac{\frac{\partial N_\mathcal{F}}{\partial v}}{D_\mathcal{F}} - \dfrac{N_\mathcal{F}}{G_\mathcal{F}}\dfrac{\frac{\partial D_\mathcal{F}}{\partial v}}{D_\mathcal{F}} = 0 \\ \dfrac{\frac{\partial N_\mathcal{F}}{\partial w}}{D_\mathcal{F}} - \dfrac{N_\mathcal{F}}{G_\mathcal{F}}\dfrac{\frac{\partial D_\mathcal{F}}{\partial w}}{D_\mathcal{F}} = 0 \end{cases} \Leftrightarrow \begin{cases} \dfrac{N_\mathcal{F}}{\partial u} - m\dfrac{D_\mathcal{F}}{\partial u} = 0 \\ \dfrac{N_\mathcal{F}}{\partial v} - m\dfrac{D_\mathcal{F}}{\partial v} = 0 \\ \dfrac{N_\mathcal{F}}{\partial w} - m\dfrac{D_\mathcal{F}}{\partial w} = 0 \end{cases} \tag{14.0.16}$$

   where the last implication is true only if $\dfrac{N_\mathcal{F}}{D_\mathcal{F}} = m$.
   When we compute the Euler-Lagrange equations actually we are solving the last system of (14.0.16) and not the first one as we should. Therefore,

after finding $(\bar{u}_m, \bar{v}_m, \bar{w}_m)$ from (12.5.1), we should check if $\mathcal{F}(\bar{u}_m, \bar{v}_m, \bar{w}_m) = m$.

2. Eq. (14.0.14) depends only on m^2, but a solution $\bar{w}$ corresponds only to one possible choice, the positive m or the negative m whose square is m^2. It is not difficult to observe that every time there exists a non-zero $\bar{w}_m$ yielding a perturbation velocity field on which $\mathcal{F}$ evaluates to a positive m, then there exists another non-zero $\bar{w}_{-m}$ yielding a perturbation velocity field on which $\mathcal{F}$ evaluates to $-m$. Indeed if $\mathcal{F}$ evaluates to m on $(\bar{u}_m, \bar{v}_m, \bar{w}_m)$, then $\mathcal{F}$ evaluates to $-m$ on $(-\bar{u}_m, \bar{v}_m, \bar{w}_m)$ (note that $(-\bar{u}_m, \bar{v}_m, \bar{w}_m)$ satisfies the zero-divergence condition that is $v_y + w_z = 0$ on the streamwise.)

3. As Mulone observes in 2024 "due to the scale invariance of the energy identity, the term in the numerator of the ratio (14.0.2) does not need to change sign if we exchange u in $-u$ and w in $-w$. Instead, it changes sign if the sign of only one of the two fields u or w is swapped and the sign of the other is not changed. As the velocity vector u is solenoidal ($u_x + v_y + w_z = 0$), in the streamwise case, since $u_x = 0$, by exchanging the sign of u the zero-divergence condition is maintained. So both (u, v, w) and $(-u, v, w)$ are solenoidal. However, in correspondence to these fields the numerator changes sign. If we consider linear streamwise perturbations (see the linear equation obtained by $(9.3.1)_1$, with $\frac{\partial}{\partial x} \equiv 0$), it is easy to check that the change of sign of u implies the change of sign of w. Therefore, the (linear) streamwise perturbations cannot change the sign of the numerator of ratio (14.0.2). However, this happens if we consider the maximum problem whose Euler-Lagrange equations are those obtained by Joseph (14.0.14) (in this case $\zeta = -u_y$). In conclusion, the scale invariance limits the arbitrariness of the solenoid fields that can be considered in the search for the maximum of the functional ratio (14.0.2)."

Once we have highlighted all the critical issues related to the Joseph's equation we provide a possible explanation of his results. The error in the articles by Joseph, Busse and in many numerical works where the critical Reynolds values are found with streamwise perturbations is the following: from equation (14.0.15) they find two values $\pm m$.
The negative value obtained (in Couette's case $m = -1/20.6$) is the minimum value of the functional ratio. Joseph considers the absolute value of this minimum and confuses this value with the maximum of the functional ratio. This could be the reason why he underestimates the critical value of the Reynolds number.
This explanation is consistent with the proof of the conjecture and with the proof that the streamwise perturbations are always stabilizing (see SubSec. 9.4.1 and Prop. 14.0.5).

How do we justify the transient results obtained in correspondence to Joseph's critical wave numbers (see Fig. 12.3) that contradict the proof of the conjecture?
Actually, these results are not related to the Joseph's equation (14.0.15), but they are based on system (12.3.2) and, as we have highlighted in the point 3 of the latter list, in correspondance to the streamwise perturbations the eq. $(12.3.2)_1$ changes if we change only the sign of u by leaving the sign of w the same and this is in contrast with the invariance property we require. This could be a possible explanation of the results reported in Fig. 12.3.

Finally, we list some open problems:

- to complete the proof suggested by Mulone in 2024 (see also Mulone, 2024, to appear(b) and 2024, to appear(a)), whose principal results have been reported in this section, it would be necessary to prove that the maximum exists when we restrict to the space in which $-(f'u, w) > 0$;
- a deeper explanation about the results of Fig. 12.3 related to the transient growth should be provided;
- all the results reported in this thesis could be generalised to non-Newtonian fluids.

To conclude, in this thesis we have studied the stability/instability of laminar flows (Couette and Poiseuille), giving more attention to the non linear analysis. In particular, by doing this type of analysis we have found results that contradict the Joseph's ones. We realised that the equation he used for the computations has some criticalities and we explained the reason why he probably made a mistake. This explanation is in agreement with our results.
Furthermore, we think that an analysis with different Lyapunov functions should be done since the non linear terms of the Navier-Stokes equations disappear in the energy equation and probably the non linear terms are the ones responsible for the instability of the flow.

Bibliography

Alboussière, T. and R. J. Lingwood (2000). "A model for the turbulent Hartmann layer". In: *Physics of Fluids* 12.6, pp. 1535–1543.

Alexakis, A. et al. (2003). "Bounds on dissipation in magnetohydrodynamic Couette and Hartmann shear flows". In: *Physics of Plasmas* 10.11, pp. 4324–4334. DOI: 10.1063/1.1613962.

Balakumar, P. (1997). "Finite-amplitude equilibrium solutions for plane Poiseuille-Couette flow". In: *Theoretical and computational fluid dynamics* 9, pp. 103–119.

Barkley, D. and L. S. Tuckerman (1999). "Stability analysis of perturbed plane Couette flow". In: *Physics of Fluids* 11, pp. 1187–1195.

— (2007). "Mean flow of turbulent-laminar patterns in plane Couette flow". In: *Journal of Fluid Mechanics* 576, pp. 109–137.

Barkley, D. and L.S. Tuckerman (2005). "Computational study of turbulent laminar patterns in Couette flow". In: *Physical review letters* 94.1, p. 014502.

Bergström, Lars B. (2005). "Nonmodal growth of three-dimensional disturbances on plane Couette-Poiseuille flows". In: *Physics of fluids* 17.1.

Blasio, F.V. De (2011). *Introduction to the physics of landslides: lecture notes on the dynamics of mass wasting*. Springer Science.

Boor, C. De and B. Swartz (1973). "Collocation at Gaussian points". In: *SIAM Journal on numerical analysis* 10.4, pp. 582–606.

Busse, F. H . (1972). "A Property of the energy stability limit for plane parallel shear flow". In: *Archive for Rational Mechanics and Analysis* 47, pp. 28–35.

Cerquaglia, M.L. et al. (2017). "Free-slip boundary conditions for simulating free-surface incompressible flows through the particle finite element method". In: *International Journal for numerical methods in engineering* 110.10, pp. 921–946.

Chandrasekhar, S. (1961). *Hydrodynamic and hydromagnetic stability*. Oxford, Clarendon Press: Oxford University Press.

— (1981). *Hydrodynamic and hydromagnetic stability*. Dover Pub. Inc.

Couette, M. (1890). "Études sur le frottement des liquides". In: *Annales de Chimie et de Physique* 21, pp. 433–510.

Cowley, S.J. and F.T. Smith (1985). "On the stability of Poiseuille-Couette flow: a bifurcation from infinity". In: *Journal of Fluid Mechanics* 156.

Davidson, P. A. (2001). *An introduction to magnetohydrodynamics (Cambridge texts in applied mathematics)*. Cambridge: Cambridge University Press.

Drazin, P. G. and W. H. Reid (2004). *Hydrodynamic stability*. Cambridge University Press, 2nd Ed.

Eckhardt, B. et al. (2007). "Turbulence transition in pipe flow". In: *Annu. Rev. Fluid Mech.* 39, pp. 447–468.

Falsaperla, P., A. Giacobbe, and G. Mulone (2019a). "Inclined convection in a porous Brinkman layer: linear instability and nonlinear stability". In: *Proceedings of the Royal Society A* 475.2223, p. 20180614.

— (2019b). "Nonlinear stability results for plane Couette and Poiseuille flows". In: *Physical Review E* 100.1. DOI: 10.1103/PhysRevE.100.013113.

Falsaperla, P., A. Giacobbe, and G. Mulone (2020a). "Linear and nonlinear stability of magnetohydrodynamic Couette and Hartmann shear flows". In: *International Journal of Non-Linear Mechanics* 123. DOI: 10.1016/j.ijnonlinmec.2020.103490.

— (2020b). "Stability of laminar flows in an inclined open channel". In: *Ricerche di Matematica*.

Falsaperla, P., G. Mulone, and C. Perrone (2022a). "Energy stability of plane Couette and Poiseuille flows: a conjecture". In: *European Journal of Mechanics-B/Fluids* 93, pp. 93–100.

— (2022b). "Nonlinear energy stability of magnetohydrodynamics Couette and Hartmann shear flows: a contradiction and a conjecture". In: *International Journal of Non-Linear Mechanics* 138, p. 103835.

— (2022c). "Stability of Hartmann shear flows in an open inclined channel". In: *Nonlinear Analysis: Real World Applications* 64. DOI: 10.1016/j.nonrwa.2021.103446.

— (2022d). "Stability of plane shear flows in a layer with rigid and stress-free boundary conditions". In: *Ricerche di Matematica*.

Falsaperla, P., G. Mulone, and B. Straughan (2016). "Bidispersive-inclined convection". In: *Proceedings of the Royal Society A* 472.2192, p. 20160480.

Falsaperla, P. et al. (2016). "Laminar hydromagnetic flows in an inclined heated layer". In: *Atti della Accademia Peloritana dei Pericolanti-Classe di Scienze Fisiche, Matematiche e Naturali* 94.1, p. 5.

— (2017). "Laminar hydromagnetic flows in an inclined heated layer". In: *Ricerche di matematica* 66.1, pp. 125–140.

Falsaperla, Paolo, Andrea Giacobbe, and Giuseppe Mulone (2017). "On the hydrodynamic and magnetohydrodynamic stability of an inclined layer heated from below". In: *Rendiconti Lincei-Matematica e Applicazioni* 28.3, pp. 515–534.

Faraday, M. (1839). *Experimental researches in electricity*. Vol. 1. London, R. and J. E. Taylor Eds.

Fériet, J. Kampé de (1948). "Harmonic analysis of the two-dimensional flow on an incompressible viscous fluid". In: *Quarterly of Applied Mathematics* 6.1, pp. 1–13.

Ferraro, V. C. A. and C. Plumpton (1961). "An Introduction to Magneto-fluid Mechanics". In.

G. Galdi, P and M. Padula (1990). "A new approach to energy theory in the stability of fluid motion". In: *Archive for rational mechanics and analysis* 110, pp. 187–286.

Galdi, G. P. and S. Rionero (1985). *Weighted energy methods in fluid dynamics and elasticity*. Vol. 1134. Springer-Verlag, Berlin Heidelbergh.

Ghosh, D. and P.K. Das (2019). "Control of flow and suppression of separation for Couette-Poiseuille hydrodynamics of ferrofluids using tunable magnetic fields". In: *Physics of Fluids* 31.8.

Giacobbe, A., G. Mulone, and C. Perrone (2022). "Monotonic energy stability for inclined laminar flows". In: *Mechanics Research Communications* 125, p. 103987.

Giacobbe, A. and C. Perrone (2023). "Spectral and Energy-Lyapunov stability of streamwise Couette-Poiseuille and spanwise Poiseuille base flows". In: *Ricerche di Matematica*, pp. 1–15.

Guha, A. and I.A. Frigaard (2010). "On the stability of plane Couette-Poiseuille flow with uniform crossflow". In: *Journal of Fluid Mechanics* 656, pp. 417–447.

Hains, F.D. (1967). "Stability of plane Couette-Poiseuille flow". In: *Physics of Fluids* 10.9, 2079 – 2080.

— (1971). "Stability of plane Couette-Poiseuille Flow with Uniform Crossflow". In: *The Physics of Fluids* 14.8, pp. 1620–1623.

Hartmann, J. (1937). "Hg-dynamics I: Theory of laminar flow of electrically conductive Liquids in a Homogeneous Magnetic Field". In: *K. Dan. Vidensk. Selsk. Mat. Fys. Medd.* 15.6, pp. 1–28.

Höink, T. and A. Lenardic (2010). "Long wavelength convection, Poiseuille-Couette flow in the low-viscosity hasthenosphere and the strength of plate margins". In: *Geophysical Journal International* 180, pp. 23–33.

Hunt, J. C. R. (1966). "On the stability of parallel flows with parallel magnetic fields". In: *Proceedings of the Royal Society of London. Series A.* 293, pp. 342–358.

Ira M. Cohen, Pijush K. Kundu (2007). *Fluid Mechanics*. Academic Press, 4th Ed.

Jédidi, M. et al. (2005). "Effet d'un champ magnétique transversal sur la stabilité de l'écoulement de Hartmann: les modes tridimensionnels". In: *Comptes Rendus Mécanique* 333.5, pp. 447–451.

Joseph, D. D. (1968). "Eigenvalue bounds for the Orr-Sommerfeld equation". In: *Journal of Fluid Mechanics* 33.3, pp. 617–621.

— (1976). *Stability of fluid motions*. Vol. 1. Berlin, Germany: Springer.

Joseph, D. D. and S. Carmi (1969). "Stability of Poiseuille flow in pipes, annuli, and channels". In: *Quarterly of applied Mathematics* 26.4, pp. 575–599.

Kaiser, R. and G. Mulone (2005). "A note on nonlinear stability of plane parallel shear flows". In: *Journal of mathematical analysis and applications* 302.2, pp. 543–556.

Kaiser, R., A. Tilgner, and W. von Wahl (2005). "A generalized energy functional for plane Couette flow". In: *SIAM journal on mathematical analysis* 37.2, pp. 438–454.

Kaiser, R. and LX Xu (1998). "Nonlinear stability of the rotating Bénard problem, the case Pr= 1". In: *Nonlinear Differential Equations and Applications NoDEA* 5.3, pp. 283–307.

Kakutani, T. (1964). "The hydromagnetic stability of the modified plane Couette flow in the presence of a transverse magnetic field". In: *Journal of the Physical Society of Japan* 19.6, pp. 1041–1057.

Khaled, A.-R. A. and K. Vafai (2004). "The effect of the slip condition on Stokes and Couette flows due to an oscillating wall: exact solutions". In: *International Journal of Non-Linear Mechanics* 39, pp. 795–809.

Kloeden, P. and R. Wells (1983). "An Explicit Example of Hopf Bifurcation in Fluid Mechanics". In: *Proceedings of the Royal Society of London. Series A, Mathematical and Physical Sciences* 390.1799, pp. 293–320.

Klotz, L. and J.E. Wesfreid (2017). "Experiments on transient growth of turbulent spots". In: *Journal of Fluid Mechanics* 829, pp. 1–13.

Klotz, L. et al. (2017). "Couette-Poiseuille flow experiment with zero mean advection velocity: subcritical transition to turbulence". In: *Physical Review Fluids* 2.4, pp. 1–19.

K.M. Butler, B.F. Farrell (1992). "Nonlinear equilibration of two-dimensional optimal perturbations in viscous shear flow". In: *Physics of Fluids* 6, pp. 2011–2020.

Lamb, H. (1924). *Hydrodynamics, fth ed.* Cambridge Univ. Press.

Lilley, G.M. (1959). "On a generalized porous-wall " Couette-type" flow". In: *Journal of the Aerospace Sciences* 26.10, pp. 685–686.

Lorentz, H. (1907). "Ueber die Entstehung turbulenter Flüssigkeitschewegungen und über den Einuss dieser Bewegungen bei der Strömung durch Röhren". In: *Abhandlungen über theoretische Physik*. Leipzig. Chap. i, 43.

Moffatt, K. (1990). "Fixed points of turbulent dynamical systems and suppression of nonlinearity". In: *Whither Turbulence, J. Lumley (ed), Springer,* pp. 250–257.

Moresco, P. and T. Alboussiere (2004). "Experimental study of the instability of the Hartmann layer". In: *Journal of Fluid Mechanics* 504, pp. 167–181.

Mulone, G. (2024). "Nonlinear monotone energy stability of plane shear flows: Joseph or Orr critical thresholds?" In: *SIAM Appl. Math, in press*.

— (2024, to appear[a]). "Monotone energy stability for Poiseuille flow in a porous medium". In: *Riv. Mat. Univ. Parma*. DOI: 10.48550/arXiv.2304.11545.

— (2024, to appear[b]). "Monotone energy stability of magnetohydrodynamics Couette and Hartmann flows". In: *Ricerche di Matematica*.

Mulone, G. and S. Rionero (2003). "Necessary and sufficient conditions for nonlinear stability in the magnetic Bénard problem". In: *Archive for rational mechanics and analysis* 166.3, pp. 197–218.

Orr, W. M'F. (1907). "The stability or instability of the steady Motions of a perfect liquid and of a viscous liquid". In: *Proceedings of the Royal Irish Academy* 27, 9–68 and 69–138.

Orszag, S.A. (1971). "Accurate solution of the Orr-Sommerfeld stability equation". In: *Journal of Fluid Mechanics* 50, pp. 689–703.

Poiseuille, J.L.M. (1843). "Experimentelle untersuchungen über die bewegung der flüssigkeiten in röhren von sehr kleinen durchmessern". In: *Annalen der Physik* 134.3, pp. 424–448.

Potter, M.C. (1966). "Stability of plane Couette-Poiseuille flow". In: *Journal of Fluid Mechanics* 24.3, pp. 609–619.

Prigent, A. et al. (2003). "Long-wavelength modulation of turbulent shear flows". In: *Physica D: Nonlinear Phenomena* 174.1-4, pp. 100–113.

Rao, I.J. and K.R. Rajagopal (1999). "The effect of the slip boundary condition on the flow of fluids in a channel". In: *Acta Mechanica* 135.3-4, pp. 113–126.

Reddy, S.C. and D.S. Henningson (1993). "Energy Growth in Viscous Channel Flows". In: *Journal of Fluid Mechanics* 252, pp. 209–238.

Reddy, S.C. et al. (1998). "On stability of streamwise streaks and transition thresholds in plane channel flows". In: *Journal of Fluid Mechanics* 365, pp. 269–303.

Reynolds, O. (1883). "An experimental investigation of the circumstances which determine whether the motion of water shall be direct or sinuous, and of the law of resistance in parallel channels". In: *Proceedings of the Royal society of London* 35, pp. 84–99.

— (1895a). "On the Dynamical Theory of Incompressible Viscous Fluids and the Determination of the Criterion". In: *Philosofical transactions of of the Royal Society A* 186, pp. 123–164.

— (1895b). "On the Dynamical Theory of Incompressible Viscous Fluids and the Determination of the Criterion". In: 186, pp. 123–164.

Rionero, S. (1967). "Sulla stabilità asintotica in media in magnetoidrodinamica". In: *Ricerche di Matematica* 16, pp. 250–263.

— (1968a). "Metodi variazionali per la stabilità asintotica in media in magnetoidrodinamica". In: *Ann. Mat. Pura Appl* 78, pp. 339–364.

— (1968b). "Sulla stabilità magnetoidrodinamica in media con vari tipi di condizioni al contorno". In: *Ricerche di Matematica* 17, pp. 64–78.

— (2000). *Elementi di Meccanica razionale*. Second Ed. Liguori.

Rionero, S. and G. Mulone (1991). "On the non-linear stability of parallel shear flows". In: *Continuum Mechanics and Thermodynamics* 3, pp. 1–11.

Romanov, V. (1973). "Stability of plane-parallel Couette flow". In: *Functional analysis and its applications* 7, pp. 137–146.

Samanta, A. (2020). "Linear stability of a plane Couette-Poiseuille flow overlying a porous layer". In: *International Journal of Multiphase Flow* 123, p. 103160.

Schlatter, P. (2009). "Spectral Methods". In: *Lecture Notes KTH*.

Schmid, P.J. and D.S. Henningson (2001a). "Stability and transition in shear flows". In: *Applied Mathematical Sciences* 142.

— (2001b). "Stability and Transition in Shear Flows". In: *Applied Mathematical Sciences* 142.

Schmitt, B. and W. von Wahl (1992). "Decomposition of solenoidal fields into poloidal fields, toroidal fields and the mean flow. Applications to the Boussinesq-equations". In: vol. 1530, pp. 291–305.

Serrin, J. (1959). "Mathematical principles of classical fluid mechanics". In: pp. 125–263.

Sommerfeld, A. (1908). "Ein Beitrag zur hydrodynamische Erklärung der turbulenten Flüssigkeitsbewegungen". In: *Proceedings 4th International Congress of Mathematicians, Rome, vol III*, pp. 116–124.

Squire, H. B. (1933). "On the stability for three-dimensional disturbances of viscous fluid flow between parallel walls". In: *Proceedings of the Royal Society of London. Series A* 142, pp. 621–628.

Straughan, B. (2004). *The energy method, stability, and nonlinear convection*. Vol. 91. 2nd Ed., Springer-Verlag New York.

Takashima, M. (1996). "The stability of the modified plane Poiseuille flow in the presence of a transverse magnetic field". In: *Fluid dynamics research* 17.6, pp. 293–310.

— (1998). "The stability of the modified plane Couette flow in the presence of a transverse magnetic field". In: *Fluid dynamics research* 22.2, pp. 105–121.

Tan, H. (2018). "Applying the free-slip boundary condition with an adaptive Cartesian cut-cell method for complex geometries". In: *Numerical Heat Transfer, Part B: Fundamentals* 74.4, pp. 661–684.

Thomas, T.Y. (1943). "On the uniform convergence of the solutions of the Navier-Stokes equations". In: *Proceedings of the National Academy of Sciences* 29.8, pp. 243–246.

Trefethen, L. N. (2000). *Spectral Methods in MATLAB*. SIAM Publications Library.

Trefethen, L.N. et al. (1992). *A new direction in hydrodynamic stability: beyond eigenvalues*. Springer.

Wright, K. (1964). "Chebyshev collocation methods for ordinary differential equations". In: *The Computer Journal* 6.4, pp. 358–365.

Xu, L. (2020). "Nonlinear stability of laminar flows in an inclined heated layer with an imposed magnetic field". In: *Mathematical Methods in the Applied Sciences*, pp. 1–9.

Zikanov, O. et al. (2014). "Laminar-turbulent transition in magnetohydrodynamic duct, pipe, and channel flows". In: *Applied Mechanics Reviews* 66.3, p. 030802.